EFFECTS OF BIOMASS-GENERATED SYNGAS ON CELL-GROWTH, PRODUCT DISTRIBUTION AND ENZYME ACTIVITIES OF *CLOSTRIDIUM CARBOXIDIVORANS* $P7^T$

By

ASMA AHMED

Bachelor of Technology, Chemical Engineering

Osmania University

Hyderabad, India

2002

Submitted to the Faculty of the
Graduate College of
Oklahoma State University
in partial fulfillment of
the requirements for
the Degree of
DOCTOR OF PHILOSOPHY
December, 2006

EFFECTS OF BIOMASS-GENERATED SYNGAS ON CELL-GROWTH, PRODUCT DISTRIBUTION AND ENZYME ACTIVITIES OF *CLOSTRIDIUM CARBOXIDIVORANS* $P7^T$

Dissertation Approved:

Randy S. Lewis

Dissertation Adviser
Arland H. Johannes

Gary L. Foutch

Raymond L.Huhnke

Danielle Bellmer

A. Gordon Emslie

Dean of the Graduate College

ACKNOWLEDGEMENTS

First and foremost, I am very grateful for the opportunity to work with an advisor like Dr. Randy Lewis. I thank him for his guidance and direction, and for his constant encouragement throughout the course of my Ph.D. I have always admired the way Dr. Lewis works with his students. While providing guidance, he also allowed me to take initiative and explore directions in my research that interested me. I really hope I can continue my association with him.

I am grateful to my advisory committee members, Dr. Raymond Huhnke, Dr. A. H. Johannes, Dr. Gary Foutch, and Dr. Danielle Bellmer for their guidance, support and interest in my research. A special thanks to Dr. Huhnke for his help and encouragement during my Ph.D. I have really enjoyed working with him on this project.

I thank Dr. Ralph Tanner for providing the inoculum for all my studies and for all the information and advice regarding the bacterium. Thanks to my friend and colleague, Bruno Cateni for the syngas and all the help around the lab. I am also very thankful to Genny, Eileen and Carolyn at the Chemical Engineering office for all the help during these last four years. They have all been very pleasant, easy to talk to and always ready to help. I thank Robert for all the help with the analytical equipment as well as the timely ordering of chemicals.

I will always remember my colleagues and friends at the ATRC labs. I have really enjoyed the company of Rohit, Rustin, Hector, Kali, Kendall, Raghunath and Houssam

during my experiments and thank them for all the help and the good times we had.

I am deeply grateful to my parents, Ilyas Ahmed and Jyotsna Ilyas, for their unconditional love, support and encouragement throughout my life. They are two of the most wonderful people I have ever come across and I have learnt a lot from them. I am also thankful to my family and friends for all the encouragement I received. To Sarosh, my friend, companion and husband: Thank you for being with me during this important phase of life and for standing by me at all times.

TABLE OF CONTENTS

Chapter Page

LIST OF TABLES

LIST OF FIGURES

Figure Page

Figure Page

Figure Page

Figure Page

Figure Page

NOMENCLATURE

atm	Atmosphere (pressure unit)
bar	Bars (pressure unit)
Btu	British Thermal Unit
ºC	Degrees Celsius
CAA	Clean Air Act
CO	Carbon monoxide
CO_2	Carbon dioxide
CODH	Carbon monoxide dehydrogenase
D	Dilution rate, ratio of flow rate to volume in a chemostat (hr^{-1})
F	Liquid feed rate ($mlhr^{-1}$)
g	Gram
h	Number of interactive binding sites on an enzyme
hr	hour
hr^{-1}	per hour
H_2	Hydrogen
$[H_2]$	Concentration of hydrogen (µM)
H_2O	Water
K_m	Michaelis constant (µM)
K_{NO}	Inhibition constant for NO (µM)

l	Liter
mg	Milligram
ml	Milliliter
mol	Mole
MTBE	Methyl Tertiary Butyl Ether
N_2	Nitrogen
NO	Nitric oxide
[NO]	Concentration of nitric oxide (µM)
O_2	Oxygen
P	Product concentration (gl^{-1})
$P7^T$	Strain of *C. carboxidivorans*
ppm	Parts per million
psi	Pounds per square inch
q_p	product formation rate per cell mass (g (g cells) $^{-1}$ hr^{-1})
rpm	Rotations per minute
t	Time (hr)
U	Unit of specific enzyme activity ($\mu moles^{-1}min^{-1}$)
V	Liquid volume in reactor (ml)
v	velocity of reaction ($\mu moles\text{-}min^{-1}mg^{-1}$)
Vm	Maximum velocity ($\mu moles^{-1}min^{-1}mg^{-1}$)
X	Cell concentration (gl^{-1})
X_0	Initial cell concentration (gl^{-1})
µ	Specific growth rate (hr^{-1})

μm	Micron or micrometer
μM	Micromolar
μmoles	Micromoles

CHAPTER 1

INTRODUCTION

1.1 Ethanol as a Renewable Resource

Fast depleting fossil fuels, rapidly increasing air pollution and global warming have underscored the need for the development of renewable energy sources. Currently, more than 90% of the worldwide energy demand is met by non-renewable fuels like coal, oil and natural gas (Kosaric and Velikonja 1995). In the United States, the net oil imports currently exceed the domestic oil production and account for over 50% of the petroleum products supplied. Figure 1.1 shows the U.S oil production vs. imports. It has been projected that, assuming the demand for oil products continues to grow, the import share will reach almost 64% by the year 2020 (Geller 2001). Moreover, the global energy demand is projected to increase by 1.7% every year, reaching almost 15.3 billion tons of oil equivalent (btoe) by 2030 (Bilgen et al. 2004). At this rate, it may not be very long before the worldwide reserves of non-renewable energy are completely depleted. This has led to an increasing interest in alternative fuels such as ethanol. Ethanol is used as an additive to gasoline to enhance the fuel efficiency, as well as to reduce toxic emissions like CO, CO_2, NO_x and hydrocarbons (He et al. 2003; Hsieh et al. 2002; Yuksel and Yuksel 2004). The use of ethanol as a fuel additive can also help reduce the prices of gasoline by expanding gasoline supplies and reducing the need for importing oil.

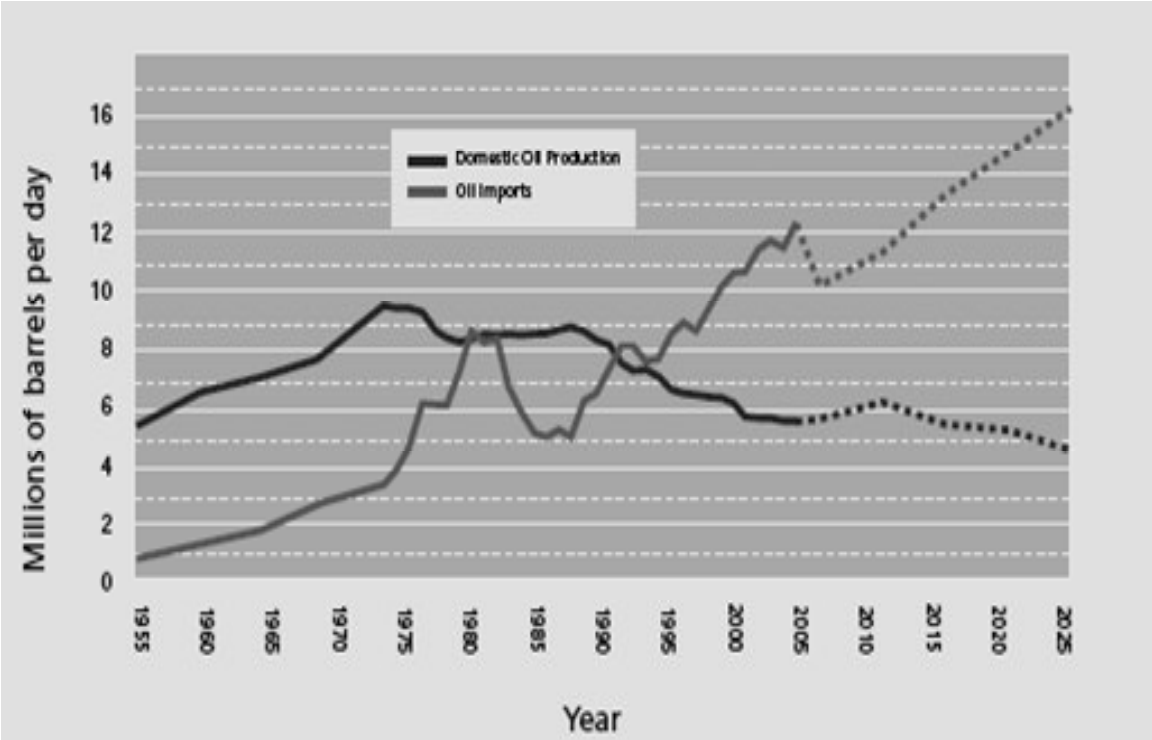

Figure 1.1 U.S Oil Production vs. Imports (U.S Energy Information Administration)

(Renewable Fuels Association. 2005)

Ethanol is currently blended with gasoline at 10% and 85% by volume (E10 and E85 respectively), and can also be used as a complete replacement for gasoline (Lynd 1996). Ethanol enables combustion engines to be run at a higher compression ratio, due to a higher octane rating than gasoline. This leads to a net performance gain of approximately 15% w/w, despite the fact that pure ethanol contains only about two-thirds of the calorific value of conventional gasoline (Wheals et al. 1999). Ethanol is also a promising alternative fuel due to its biodegradability and regenerative characteristics.

1.2 The Need for Ethanol Production

The oil embargoes of 1973 and 1979 provided the initial drive for fuel ethanol production, though the more recent impetus came from the Clean Air Act (CAA) Amendments of 1990. The CAA Amendments require gasoline to be oxygenated in order to reduce emissions of toxic gases like carbon monoxide and volatile organic compounds (VOCs) (Yacobucci 2000). This would have a two-fold effect as the oxygenation of gasoline also increases its octane number and hence the fuel efficiency. One of the major competitors of ethanol as an oxygenate has been Methyl Tertiary Butyl Ether (MTBE). MTBE is advantageous owing to its high octane number and low sulfur content. However, based on some laboratory studies, it has been found that MTBE is a potential carcinogen at high concentrations (Nadim et al. 2001). MTBE also contaminates groundwater due to its high water solubility and is much more resistant to biodegradability compared to the other components of gasoline (Nadim et al. 2001; Yacobucci 2000). Therefore, ethanol is being projected as a replacement for MTBE to avoid the adverse effects of MTBE on the environment and public health. Since oxygen

content by weight in an ethanol molecule is approximately twice that of MTBE, less ethanol is required to meet specified oxygen content in fuel (He et al. 2003).

There has been a tremendous growth in the ethanol industry over the last few years. In the United States alone, 81 ethanol plants located in 20 states produced 3.41 billion gallons in the year 2004. This amounts to a 21% increase from 2003 and a 109% increase from the year 2000 (Renewable Fuels Association. 2005). Figure 1.2 shows the historic fuel ethanol production in the United States over the last two decades. Ethanol is currently used as an additive to gasoline (E10, a 10% ethanol-90% gasoline blend) as well as an alternative fuel in the form of E85 (85% ethanol-15% gasoline). Small amounts of gasoline added to ethanol prevent corrosion of engine parts (Yacobucci 2000). However, even with the increased use of ethanol fuel in the last few years, it still remains more expensive than gasoline and diesel. Therefore, it is necessary to develop commercially viable processes for producing fuel ethanol from inexpensive feedstock to make it more price-competitive with gasoline.

1.3 Benefits of Fuel-Ethanol

Ethanol is a fully sustainable and renewable energy resource that has several advantages both as an additive and as an alternative fuel. Ethanol as a fuel has environmental, economic as well as social benefits as discussed in the following sections.

1.3.1 Environmental Benefits

One of the major advantages of using fuel ethanol is improved air quality. With

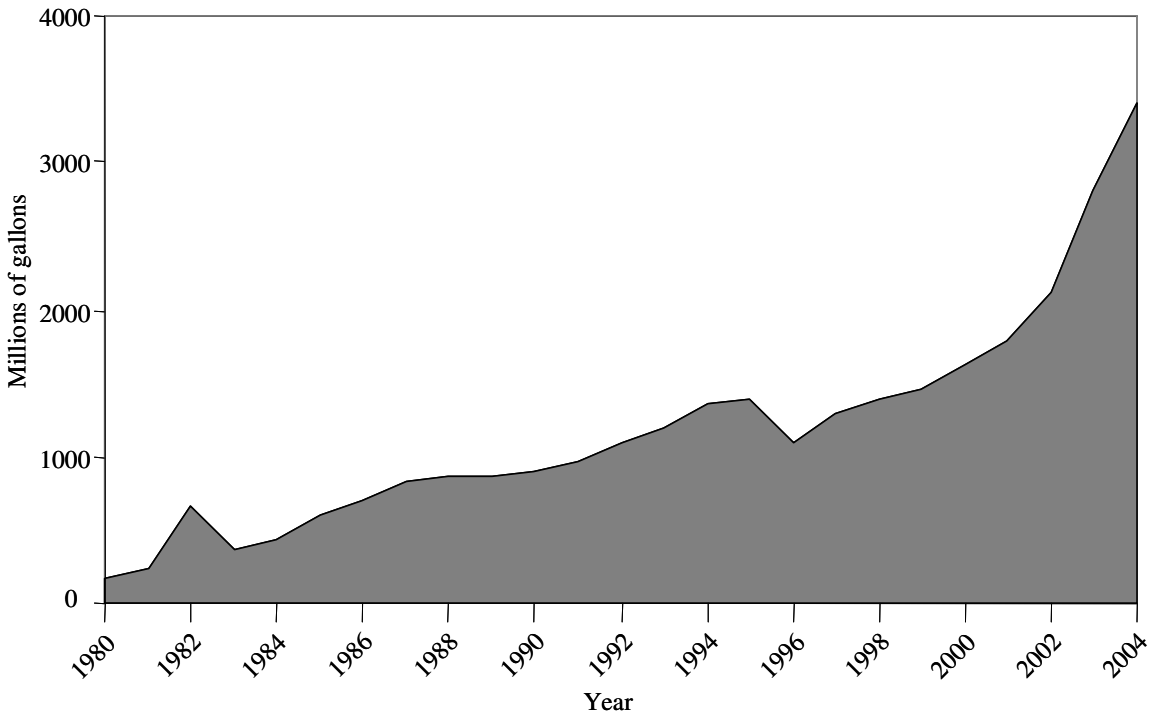

Figure 1.2 Historic U.S Ethanol Production. Adapted from Ethanol Industry Outlook 2005 (Renewable Fuels Association. 2005)

the growing population, the problem of air pollution caused by vehicles is also steadily increasing. The use of ethanol reduces tailpipe emissions of carbon monoxide and unburned hydrocarbons that form ground level ozone (Wyman 1999). The addition of ethanol increases the octane number and hence the efficiency of the fuel, thus replacing previously used oxygenates like tetraethyl lead or MTBE which are toxic and even carcinogenic in high concentrations. Ethanol is also biodegradable and water soluble, which gives ethanol an added advantage over MTBE which is not completely biodegradable and leads to groundwater contamination (Nadim et al. 2001).

Another important environmental benefit is that ethanol decreases global warming by reducing the greenhouse gas emissions. Greenhouse gases like carbon dioxide (CO_2), methane (CH_4) and nitrogen oxides (NO_x) contribute to global warming (Lashof and Ahuja 1990). The U.S transportation sector accounts for one-third of the total end-use sector CO_2 emissions currently, and is projected to rise to about 36% by 2020 (Greene 2003). When ethanol derived from crops is used as a transportation fuel, it merely releases the CO_2 that was fixed by the crops. This results in a carbon cycle, where the CO_2 released from the ethanol fuel can then be fixed by the new batch of biomass (Figure 1.3). That is, the CO_2 generated due to the production and use of ethanol is recaptured to grow new biomass to replace that which was harvested for ethanol production (Wyman 1999).

1.3.2 Socio-Economic Benefits

The use of ethanol as a renewable fuel not only has environmental benefits but also positively impacts the economy of the country. Ethanol reduces the need for

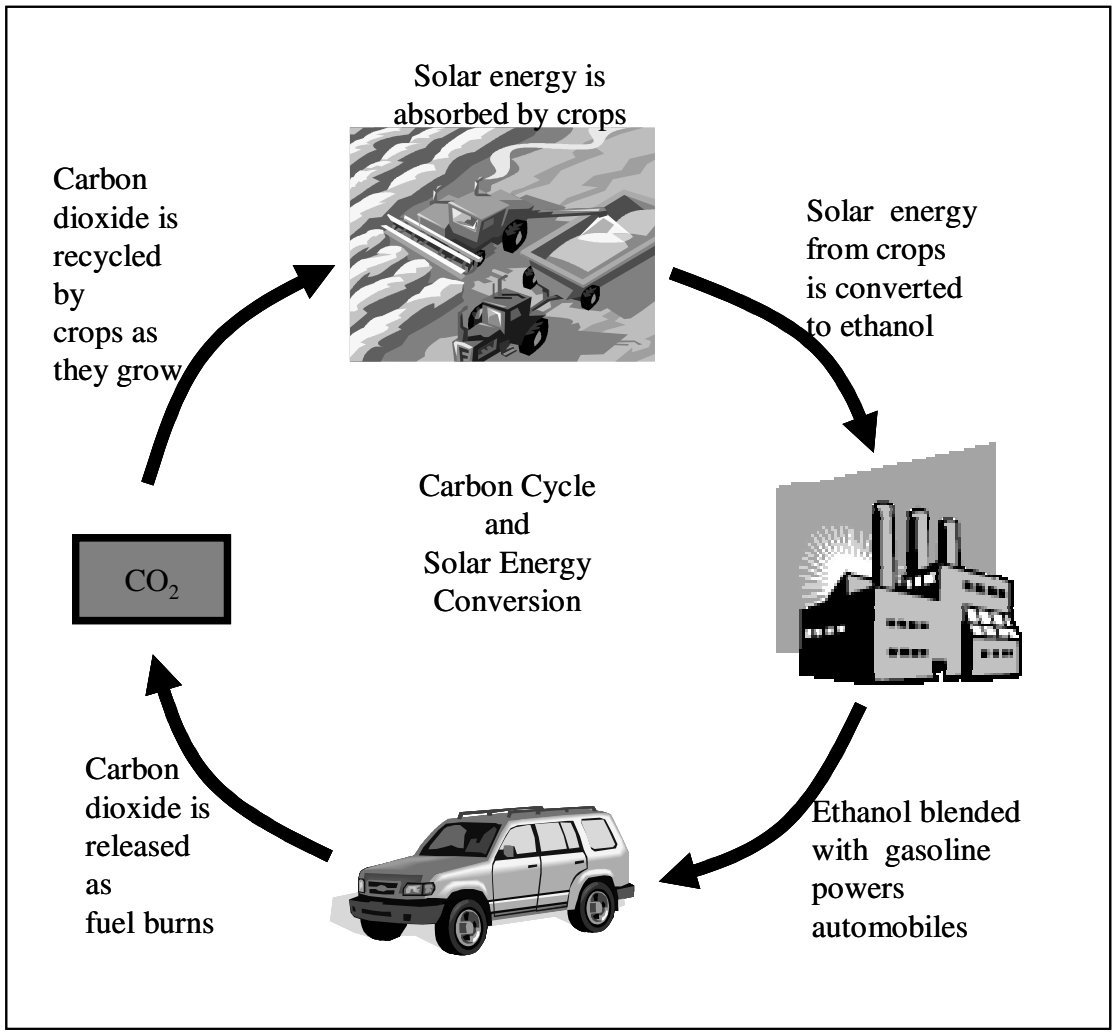

Figure 1.3 Carbon dioxide recycle. Adapted from (Renewable Fuels Association. 2005)

imported oil, thus decreasing the trade deficit of the country as well as creates new employment opportunities. In the year 2004, the ethanol industry reduced the U.S trade deficit by $5.1 billion by eliminating the need to import 143.3 million barrels of oil, supported the creation of 147,000 jobs in all sectors of the economy and added $1.3 billion of tax revenue for the Federal government and $1.2 billion for the State and Local governments (Renewable Fuels Association. 2005).

1.4 Drawbacks of Fuel Ethanol

Although ethanol has several advantages as a fuel, there have been a few arguments about the drawbacks of using fuel-ethanol. Some of the common disadvantages suggested in the literature are as follows (Rasskazchikova et al. 2004; Yacobucci 2000):

- Ethanol is highly corrosive and can damage rubber and plastic components of the vehicle.
- Fuel components containing ethanol have a tendency to separate in the presence of even small traces of water.
- Ethanol-blended fuels tend to increase aldehyde emissions which contribute to acid rain.
- The energy content of ethanol is lower than that of gasoline on a per gallon basis. Therefore, the vehicle would require more gallons of ethanol than gasoline to go the same distance.
- The cost of ethanol is too high for it to be used as an additive or replacement for gasoline. Ethanol fuel currently receives tax subsidies without which it cannot

compete with gasoline unless cheaper methods of production are used. However, this argument is not as strong with the current increase in gasoline prices.

These drawbacks have been or can be overcome in several ways. Though alcohols are corrosive, anti-corrosion agents can be added to the fuel to prevent corrosion of engine parts. For the problem of separation in the presence of water, several stabilizing agents like amines, ethers, ketones, etc. can be added (Rasskazchikova et al. 2004). The higher latent heat and combustion efficiency of ethanol compared to gasoline compensates for the fact that ethanol has a lower energy content than gasoline. The high cost of ethanol is currently a drawback to its use as a fuel, but research across the world shows promise that there will soon be commercially viable processes which can bring down the price of ethanol to make it competitive with gasoline.

1.5 Overview of Bio-ethanol Production

Fermentation of pre-treated biomass from sugar or starch based crops like corn is the current leading technology to produce ethanol in the U.S. However, use of food crops to produce ethanol has two limitations. First, the ethanol is produced at the cost of using these crops for food and second, food crops like corn can only be grown in selective regions. This has led to the geographic concentration of ethanol plants to only five states in the U.S. and subsequently higher costs related with transportation.

It is not surprising that there has been a recent focus on research to use lignocellulosic raw materials for ethanol production. Lignocellulosic materials offer advantages of abundant availability and low cost. Several processes such as (a) acid

hydrolysis, (b) enzymatic hydrolysis, (c) simultaneous gasification-fermentation, and (d) biomass gasification fermentation can be used to convert these materials to ethanol-fuel. These processes are discussed in detail in chapter 2. In this dissertation, gasification-fermentation of biomass has been studied. Biomass gasification-fermentation involves the partial oxidation of biomass to a gas mixture known as synthesis gas or syngas (containing CO, CO_2, H_2 and N_2) followed by the fermentation of this gas to ethanol and other co-products using a microbial catalyst. Anaerobic bacteria, such as *Clostridium ljungdahlii* and *Clostridium autoethanogenum*, have been shown to convert CO, CO_2 and H_2 to ethanol and acetic acid (Abrini et al. 1994; Vega et al. 1990).

1.6 Problem Statement and Research Objectives

The gasification-fermentation of biomass to ethanol is a relatively new technology and most of the research being conducted is still laboratory scale and makes use of synthetic syngas (mixed from commercial gases). However, biomass-generated syngas also contains other gases like methane, acetylene, ethylene, ethane and nitric oxide as well as gasification components like tars and ashes. Many of these "impurities" of syngas may have complex effects on the microbial catalyst being used. A thorough study of the effects of syngas constituents on the microorganism and its enzymes is required to (a) obtain a better understanding of the potential fermentation problems (b) develop gas clean-up methods and (c) improve the overall process and move it closer to commercialization.

The process being researched at Oklahoma State University is focused on the fermentation of biomass-syngas to ethanol, acetic acid and other valuable products.

Figure 1.4 shows a schematic of the overall process. Switchgrass, a warm-season perennial grass is used as the biomass and is gasified in a fluidized-bed gasifier to generate syngas. The microbial catalyst used in the fermentation is *Clostridium carboxidivorans* $P7^T$, an anaerobic bacterium that can ferment syngas. A typical experiment consists of growing the bacteria on synthetic syngas whose composition is matched to that of biomass-generated syngas. Once a steady cell-concentration is obtained, a continuous liquid feed and product removal is initiated, thus switching from a batch reactor mode to chemostat mode. After the cells stabilize in this mode, the feed gas is switched from the synthetic syngas to biomass-generated syngas. It was observed in previous studies (Datar 2003; Datar et al. 2004) that exposing the microbial catalyst to biomass-generated syngas resulted in the following:

1. After a delay of about 1.5 days, there was a cell-washout from the reactor in a chemostat mode. This implied that cells were switching over to a dormant mode with no growth, owing to one or more syngas impurities.
2. There was an immediate cessation of hydrogen consumption by the microbial catalyst. *C. carboxidivorans* $P7^T$ is an acetogen which consumes CO, CO_2 and H_2 for cell-growth and production of alcohols and acids. While carbon is obtained from CO and CO_2, the electrons are obtained from H_2. The enzyme 'hydrogenase' enables the bacterium to convert H_2 to electrons (Krasna 1979). If hydrogenase is inhibited, the bacterium would be unable to convert hydrogen to electrons and would need to obtain electrons from CO. This would limit the availability of CO for products and in turn decrease the efficiency of the overall process.

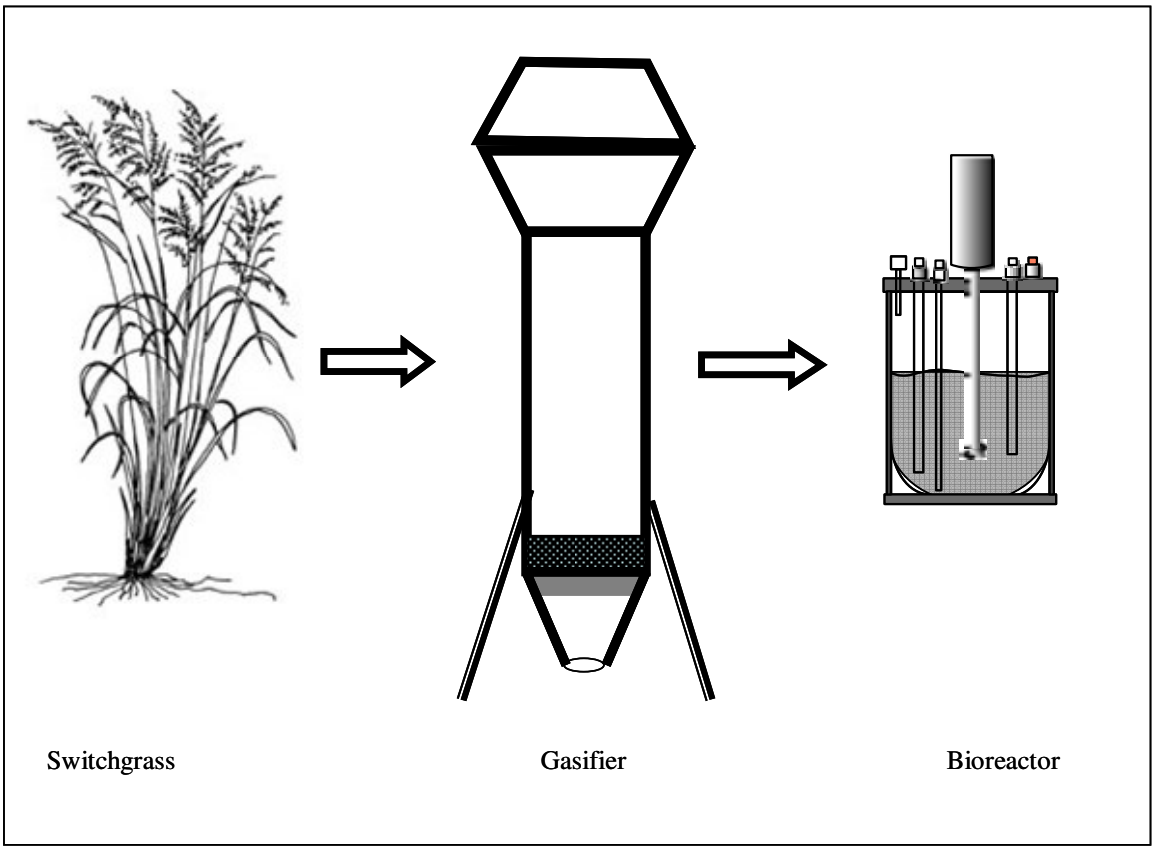

Figure 1.4 Schematic of the biomass gasification-fermentation process at Oklahoma State University.

3. There was an increase in ethanol concentration and a decrease in acetic acid concentration compared to when the cells were grown on the synthetic syngas.

These observations indicated gaps in our understanding of the effects of biomass-generated syngas on the microbial catalyst. It was considered important to determine the cause of cell dormancy, cessation of hydrogen consumption and the change in product distribution in order to improve the fermentation. The above critical issues were addressed in this dissertation, as outlined below.

Objective 1: Determine and eliminate the cause of cell-dormancy leading to cell-washout. The hypothesis was that one or more components of synthesis gas caused the cells to become dormant and inhibited growth, thereby leading to cell washout in a continuous reactor. The objective in this case was to identify and eliminate the component/s which were either gaseous impurities like ethylene, acetylene, ethane, methane etc. or solid materials from the gasifier like tars and ash (Baker 1987; Brown et al. 2000; Engelen et al. 2003; Zhang et al. 2004).

Objective 2: Determine the cause of hydrogenase inhibition and shutdown of hydrogen consumption. The hypothesis was that nitric oxide (NO) (a minor constituent in the synthesis gas) inhibited the hydrogenase enzyme of *C. carboxidivorans* $P7^T$ that was responsible for hydrogen uptake (Hyman MR 1988; Hyman MR 1991; Krasna 1954;

Tibelius and Knowles 1984), and that the removal of NO could increase the hydrogen consumption, which would in turn increase ethanol production by the microbial catalyst.

Objective 3: Increase ethanol production by *C. carboxidivorans* P7^T. The hypothesis was that ethanol production could be increased by regulating the metabolic pathway of the microbial catalyst towards solventogenesis (production of alcohol). Certain artificial electron carriers like methyl viologen, benzyl viologen and neutral red are known to initiate solventogenesis, resulting in an increased ethanol production by the bacteria (Girbal et al. 1995b; Guedon et al. 1999).

1.7 Dissertation Organization

In Chapter 2 of this dissertation a survey of the literature is presented, which reviews the methods of ethanol production from lignocellulosic feedstocks. Chapter 2 further describes the metabolic pathway of acetogens and some of the key enzymes involved. Chapter 3 addresses the effects of individual syngas impurities on cell-growth and product distribution of *C. carboxidivorans* P7^T, thereby identifying the cause of cell-dormancy in the presence of biomass-syngas. Chapter 4 describes the effect of cell-recycle on the fermentation of syngas. Chapter 5 addresses the cause of hydrogenase inhibition and presents a kinetic analysis of the inhibition. In chapter 6, a method of regulating the metabolic pathway of *C. carboxidivorans* P7^T is discussed, with emphasis on alcohol dehydrogenase which is an enzyme responsible for alcohol production. Chapter 7 presents conclusions to this work and discusses future recommendations.

CHAPTER 2

A LITERATURE REVIEW OF BIO-ETHANOL PRODUCTION AND MICROBIAL CATALYSTS

2.1 Methods of Bio-ethanol Production

2.1.1 Ethanol from Sugar and Starch-based Crops

There has been extensive research on the various processes used for ethanol production from biomass. Currently almost all of the commercial ethanol production is from corn and other starch-based crops. Processes utilizing sugar and starch based crops typically involve the following steps:

- Pre-treatment of the biomass by the dry milling (grinding) or wet milling (chemical treatment) process
- Enzymatic treatment of the biomass to convert starch into fermentable sugars
- Fermentations of biomass sugars into ethanol
- Distillation of the fermentation broth to obtain purified ethanol

Almost 90% of the ethanol production from corn in the United States occurs in five states, namely, Illinois, Iowa, Nebraska, Minnesota and Indiana. Due to transportation costs of the feedstock, these five top corn-producing states are also the top

five ethanol producers (Yacobucci 2000). The geographic concentration of ethanol plants has become disadvantageous to the use of ethanol in other regions as it increases the shipping costs of the fuel. Moreover, corn-ethanol competes with the use of corn as a food crop. Therefore, there has been a recent interest in finding alternative sources of biomass for ethanol production since biomass is abundant and generally inexpensive.

2.1.2 Ethanol from Lignocellulosic Feedstocks

Lignocellulosic materials such as prairie grasses, wood chips, paper wastes etc. are considered a favorable alternative feedstock owing to their abundance and competitive prices. Another important benefit of using these materials is that it leads to the utilization of marginal lands to cultivate grasses. Moreover, lignocellulosic materials "do not interfere with food security" (Kim and Dale 2004).

Lignocellulose is a mixture of 35-50% cellulose, 20-35% hemi-cellulose and 15-25% lignin (Wyman 1994). Cellulose and hemi-cellulose are long chain polymers of five and six carbon sugars. Hemi-cellulose is mostly a xylose polymer while cellulose is mostly a polymer of glucose. Most of the processes utilizing lignocellulosics as raw material for ethanol production are based on the disruption of the bonds (hydrolysis) linking these monomers together (Kaylen 2000). The breakage causes the raw material to be broken down to a form easily fermentable by microorganisms. However, lignin, the third constituent of lignocellulosic materials, is a complex polymer that cannot be broken down by these methods and leads to an incomplete conversion of the raw material to ethanol. Some of the basic approaches currently used for industrial hydrolysis are dilute acid hydrolysis, concentrated acid hydrolysis and enzymatic hydrolysis.

The dilute acid hydrolysis consists of two stages- first, dilute acid and steam convert the cellulose and hemi-cellulose to sugars, and then second the sugars are neutralized and fermented to produce ethanol. This process has the advantage of not requiring acid recovery but suffers from relatively low conversion efficiencies (50-60%) (Clausen 1988). Another disadvantage of this process is the degradation of sugars to form furfural and hydroxymethyl furfural, which in turn degrade to form tars and other undesirable by-products (Wyman 1994).

In the concentrated hydrolysis process, the feedstock is first dried, to avoid dilution of the acid due to the moisture content of the feedstock. Concentrated acids are then used to hydrolyze cellulose and hemi-cellulose at moderate temperatures. This prevents the degradation of sugars, resulting in higher yields. However, owing to the large quantities of acid required, and the high cost of acids, a substantial fraction of the acids must be recovered in order to make the process economically feasible. Therefore, the major challenge in this process is to achieve acid recovery at a cost which is significantly lower than the cost of the acid itself (Wyman 1994).

In enzymatic hydrolysis, the feedstock is pretreated so that its structure breaks down and allows the enzymes to penetrate the material and convert the cellulose to sugars and other co-products. During the fermentation, these sugars are then converted to ethanol. As the action of enzymes is highly specific, this process avoids the formation of unwanted by-products. Moreover, enzymatic reactions take place at relatively mild conditions and can achieve high product yields. However, this process has two main drawbacks: the process is slow and the enzymes are very expensive (Kaylen 2000).

Gasification-Fermentation of Biomass: Other than the hydrolysis processes, lignocellulosics can also be converted to ethanol by the gasification-fermentation process. This process involves the partial oxidation of biomass to a gas mixture known as synthesis gas or syngas (containing CO, CO_2, H_2 and N_2) followed by the fermentation of syngas to ethanol and other co-products. Anaerobic bacteria, such as *Clostridium ljungdahlii* and *Clostridium autoethanogenum*, have been shown to convert CO, CO_2 and H_2 to ethanol and acetic acid (Abrini et al. 1994; Vega et al. 1990). Unlike the hydrolysis processes, this process circumvents the problem of unconverted lignin, as the gasification of biomass converts all of the carbon to syngas (Reed et al. 1980). There is also no problem of solids handing in this process. Moreover, the gasification-fermentation process can utilize a wide variety of raw material such as prairie grasses, switchgrass, wood chips, solid municipal wastes and paper wastes. However, this process is known to be associated with issues like low ethanol productivity and gas mass transfer limitations (Worden et al. 1997).This necessitates a good bioreactor design and high cell-densities of the microorganism to make the process economically feasible.

Switchgrass (*Panicum virgatum*) is a sustainable herbaceous energy crop which can be used as biomass to produce synthesis gas. The Department of Energy chose Switchgrass as a model herbaceous crop species based on its high yields, high nutrient use efficiency, low water requirements and wide geographic distribution (McLaughlin and Walsh 1998). Switchgrass is a warm-season perennial grass which is found in most of the United States, and some parts of Canada and Central America. The use of perennial grasses for bio-ethanol production can have significant positive environmental effects compared to the use of row crops. Perennial grasses like Switchgrass can be

grown for several years without replanting, thus preventing soil erosion, reducing the use of pesticides and other agricultural chemicals and increase soil carbon, thus improving the soil texture (Sanderson et al. 1996b). The net energy gain of producing ethanol from Switchgrass has been estimated to be 334% as compared to the 21% gain in case of enzymatic hydrolysis of corn-grain to ethanol (McLaughlin and Walsh 1998).

2.2 Microbial Catalysts

Several anaerobic bacteria have been isolated that have the ability to ferment synthesis gas to ethanol, acetate and other useful end products. Known as acetogens, these microbes have the ability to reduce CO_2 to acetate in order to obtain energy and produce cell mass. Acetogenic bacteria are obligate anaerobes that utilize the acetyl-CoA pathway as their predominant mechanism for the reductive synthesis of acetyl-CoA from CO_2 (Drake 1994a). They may be Gram positive or Gram negative, rod-shaped or coccoid, and motile or non-motile. Being a versatile group of microorganisms, they can use gases like CO_2/H_2 and CO as well as sugars and other substrates (Drake 1994b; Wood et al. 1986b; Wood et al. 1986c).

Clostridium ljungdahlii, the first autotrophic microorganism known to ferment a mixture of CO, CO_2 and H_2 (synthesis gas) to ethanol was isolated in 1987, (Klasson et al. 1992). *C. ljungdahlii* is a gram-positive, rod-shaped anaerobe which is capable of fermenting sugars like xylose and fructose in addition to synthesis gas. Being an acetogen, this organism favors the production of acetate during its active growth phase while ethanol is produced primarily as a non-growth-related product (Klasson et al. 1992). An effect of pH on growth and product formation was also observed in this

organism. It was observed that the production of acetate was favored at a higher pH (5-7) whereas the production of ethanol was favored at lower values of pH (4-4.5).

Eubacterium limosum is an acetogen which has been isolated from various habitats like the human intestine, rumen, sewage and soil. It has a high growth rate under high CO concentrations and can ferment synthesis gas to produce acetate, ethanol, butyrate and isobutyrate (Chang et al. 1999; Chang et al. 2001; Chang et al. 1998).

Peptostreptococcus productus is a mesophilic, gram-positive anaerobic coccus, found in the human bowel and is capable of metabolizing CO_2/H_2 or CO to produce acetate (Lorowitz and Bryant 1984). Studies have shown that although acetate is one of the primary end-products of its metabolism, *P. productus* can also form additional products in response to CO_2 limitation (Misoph and Drake 1996).

Clostridium autoethanogenum is a strictly anaerobic, gram-positive, spore-forming, rod-like, motile bacterium which metabolizes CO to form ethanol, acetate and CO_2 as end products. It is also capable of using CO_2 and H_2, pyruvate, xylose, arabinose, fructose, rhamnose and L-glutamate as substrates (Abrini et al. 1994).

Clostridium carboxidivorans $P7^T$ is a novel solvent-producing anaerobic microbial catalyst, which was isolated from the sediment of an agricultural settling lagoon. It is motile, gram-positive, spore-forming and primarily acetogenic, forming acetate, ethanol, butyrate, and butanol as end-products (Liou et al. 2005).The optimum pH range for this strain is 5.0-7.0 and the optimum temperature range is 37-40 ºC. An examination of the metabolic end-products showed that strain $P7^T$ converted 600mmol CO into 264 mmol CO_2 , 96 mmol ethanol, 12 mmol acetate and 24 mmol butanol (Liou et al. 2005).

2.3 Acetogens and the Acetyl-CoA Pathway

"Acetogens are obligately anaerobic bacteria that can use the acetyl-CoA pathway as their predominant (i) mechanism for the reductive synthesis of acetyl-CoA from CO_2, (ii) terminal electron-accepting, energy-conserving process, and (iii) mechanism for the synthesis of cell carbon from CO_2" (Drake 1994b). The acetyl-CoA pathway, also known as the Wood-Ljungdahl pathway in honor of its discoverers, Harland Wood and Lars Ljungdahl, is an autotrophic pathway of CO_2 fixation as shown in Figure 2.1. Like all other anaerobes, acetogens require a terminal electron acceptor other than oxygen. In the acetyl-CoA pathway, CO_2 serves as an electron acceptor and H_2 serves as the electron donor. The synthesis of acetyl-CoA from CO_2 and H_2 requires an eight-electron reduction of CO_2 and can be considered to consist of the following three steps (Wood et al. 1986a):

1. Formation of the carbonyl precursor of acetyl-CoA by the enzyme Carbon monoxide dehydrogenase (CODH)
2. Formation of the methyl precursor of acetyl-CoA
3. Condensation of the above two precursors to form acetyl-CoA. An acetyl intermediate is formed on CODH and CoA is added to it. The final steps of acetyl-CoA synthesis are catalyzed by CODH wherein the acetyl and CoA groups are condensed.

Unlike other autotrophic pathways like the Calvin cycle or the reverse citric acid cycle, the acetyl-CoA pathway is not a cycle, but a combination of two linear pathways – the formation of the two branches and the synthesis of acetyl-CoA (Madigan 2003). A

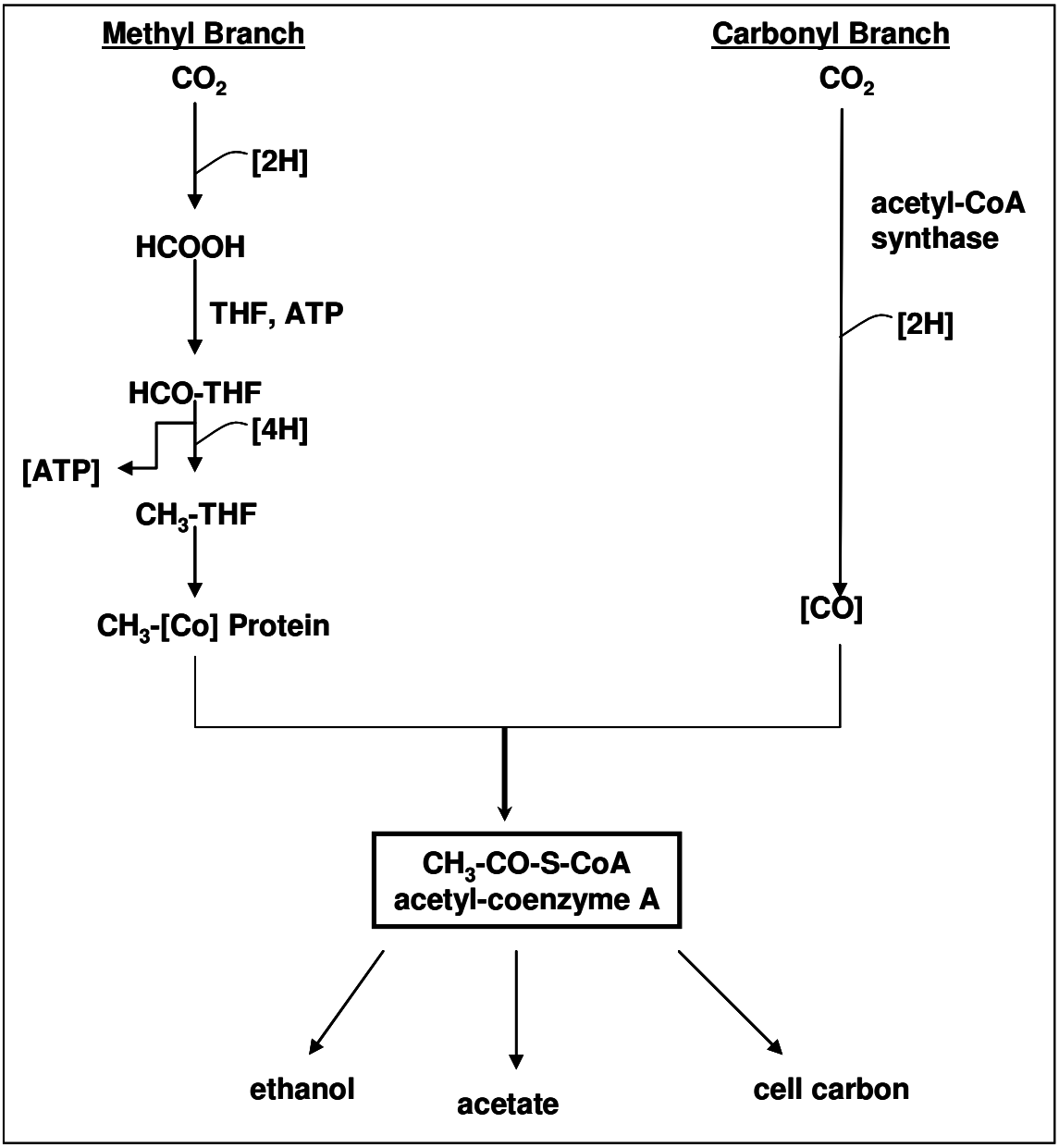

Figure 2.1. Simplified schematic of the acetyl-CoA or Wood-Ljungdahl pathway of acetogens. (THF-tetrahydrofolate, [Co] protein-corrinoid enzyme)(Drake 1994b) The methyl and carbonyl branches of the pathway are shown in the figure.

description of the pathway and the significance of some of the key enzymes involved are given in the following sections.

2.3.1 The Methyl Branch and its Key Enzymes

The methyl branch of the acetyl-CoA pathway is shown on the left in Figure 2.1. This part of the pathway results in the formation of the methyl-corrinoid protein, which then combines with the product of the carbonyl branch, to form acetyl-CoA. In the first step of this branch, CO_2 is reduced to formate ($HCOO^-$) as shown in the following equation:

$$CO_2 + 2[H] \Leftrightarrow HCOO^- + H^+ \quad (2.1)$$

Formate Dehydrogenase: The above reversible reaction is catalyzed by the enzyme formate dehydrogenase (FDH). This enzyme is difficult to isolate due to its high sensitivity to oxygen (Ljungdahl 1986). Though ferredoxin is the most commonly used electron acceptor, among acetogens, NADH often acts as the electron donor. For acetogens grown on CO, it has been suggested that CO must first be converted to CO_2 by the enzyme carbon monoxide dehydrogenase (CODH) and then reduced to formate by FDH (Ljungdahl 1986).

Tetrahydrofolate Enzymes: Formate is then activated with tetrahydrofolate (THF) to form 10-formyl-THF, as shown in the figure, by the enzyme formyl-THF synthetase. This is an ATP-dependent condensation. This bound formyl group is then reduced by a series of 3 enzymes to a bound methyl group (methyl-THF). In the final step of this

branch, the methyl group is transferred to a corrinoid containing protein, [Co]-E (Ragsdale 1991).

2.3.2 The Carbonyl Branch and Carbon Monoxide Dehydrogenase

The carbonyl branch of the acetyl-CoA pathway is shown on the right in Figure 2.1. This branch of the pathway results in the formation of a bound carbonyl group which is then merged with the bound methyl group formed in the methyl branch to form acetyl-CoA. Carbon monoxide dehydrogenase (CODH) plays a very important role in this branch of the pathway.

Carbon monoxide Dehydrogenase: This is considered one of the most important enzymes of the acetyl-CoA pathway due to its bi-functionality. It catalyzes the very first oxidation of CO to CO_2, the reduction of CO_2 to bound carbonyl and dominates the carbonyl branch of the pathway, finally mediating the synthesis of acetyl-CoA from the methyl and carbonyl groups. Due to this, CODH is also known as acetyl-CoA synthase and the pathway is often referred to as the carbon monoxide dehydrogenase pathway (Diekert and Wohlfarth 1994). In the carbonyl branch, CO_2 is first reduced to [CO] (indicating carbon monoxide in an enzyme bound form) as shown in equation 2.2 and then bound to CODH.

$$CO_2 + 2[H] \rightarrow [CO] + H_2O \qquad (2.2)$$

This bound carbonyl group is then merged with the bound methyl group from the methyl branch to form a bound acetyl-CODH moiety. In the final step, CODH condenses the bound acetyl with the free coenzyme A to form acetyl-CoA, as shown in equation 2.3.

$$E-[Co]-CH_3+[CO]+HS-CoA \rightarrow E-[Co]+Acetyl-CoA \quad (2.3)$$

Hydrogenase: Hydrogenase enzymes are expressed in organisms where their function is either hydrogen evolution, to dispose of electrons accumulated during fermentation or hydrogen uptake, where the oxidation of hydrogen is coupled to the energy yielding process (Lemon and Peters 1999) or hydrogen consumption. Studies have shown that CODH acts in combination with hydrogenase to form the carbonyl precursor of acetyl-CoA (Ljungdahl 1986; Wood et al. 1986b). Equation 2.4 shows the reversible reaction catalyzed by hydrogenase.

$$H_2 \Leftrightarrow 2e^- + 2H^+ \quad (2.4)$$

Hydrogenases are classified based on their metal content; depending on whether they contain nickel, iron, selenium or none of these and also what combination of metals they contain. Usually, the Ni containing hydrogenases are associated with hydrogen uptake and those containing Fe are associated with hydrogen evolution (Hyman MR 1991). Often microorganisms contain several different hydrogenases, and in many cases the functions of these enzymes are difficult to determine. The catalytic activity of hydrogenase can be determined by assaying the enzyme by a method which measures its interaction with hydrogen (Krasna 1979). One of the most popular assays is the reduction of an artificial electron acceptor by hydrogen. Dyes like methylene blue, methyl

viologen, benzyl viologen etc., or other compounds like nitrate, nitrite, cytochromes, ferredoxin, hydroxylamine, sulfate, sulfite and NAD are some of the commonly used electron acceptors (Krasna 1979).

Inhibition of hydrogenase has been of particular interest due to the fact that it results in a change in the metabolic pathway of the microorganism. Gases like O2 (Seefeldt and Arp 1989), acetylene, CO, and nitric oxide (NO) are known inhibitors of hydrogenase (Acosta et al. 2003; Byung Hong Kim 1984; Krasna 1954; Tibelius and Knowles 1984). The inhibition of hydrogenase by NO will be further discussed in section 2.5.1.

2.4 Fate of Acetyl-CoA

Acetyl-CoA is a versatile intermediate in the metabolic pathway of acetogens as it is a precursor of lipids, amino acids, nucleotides and carbohydrates (Ljungdahl 1986). It is the source for cellular carbon as well as cellular energy. Cellular material is formed via the anabolic pathway, in which acetyl-CoA is reductively carboxylated into pyruvate by the enzyme pyruvate synthase (Diekert and Wohlfarth 1994; Schlegel and Bowien 1989). Pyruvate is then converted to phosophoenolpyruvate which is an intermediate in the conversion to cellular material. For the purpose of energy conservation, acetyl-CoA goes through the catabolic pathway in order to make ATP. This is the route by which acetyl-CoA is converted to acetate. Equations 2.5 and 2.6 describe the two steps of the acetate branch of the pathway.

$$Acetyl - CoA + P_i \rightarrow Acetyl - phosphate + P_i \tag{2.5}$$

$$Acetyl - phosphate + ADP \rightarrow Acetate + ATP \quad (2.6)$$

In the first reaction, the CoA unit is removed from the acetyl-CoA and a phosphate group is added, resulting in the formation of acetyl-phosphate. This reaction is catalyzed by the enzyme phosphotransacetylase. In the second reaction, shown by equation 2.6, the acetyl phosphate is converted to acetate while a molecule of adenosine diphosphate (ADP) is phosphorylated to form ATP. This branch of the pathway is usually favored by the bacterium over the alcohol forming branch (described below) during its exponential growth phase as it provides the cell with energy in the form of ATP. This is often known as the acidogenic phase of the metabolism, which also results in a decrease in pH of the medium due to acid production (Rao and Mutharasan 1989). The second phase of the fermentation is the solventogenic phase, in which ethanol is produced. This is characterized by slower growth, as there is no evolution of ATP in this case. Equations 2.7 and 2.8 describe the solventogenic branch of this pathway in which ethanol is produced.

$$Acetyl - CoA + NADH + H^+ \rightarrow acetaldehyde + NAD^+ + CoA - SH \quad (2.7)$$

$$Acetaldehyde + NADH + H^+ \rightarrow Ethanol + NAD^+ \quad (2.8)$$

In the solventogenic branch of the pathway, the organism utilizes the reducing potential available, in the form of NADH, to first form acetaldehyde by the enzyme acetaldehyde dehydrogenase, and then finally form ethanol by the enzyme alcohol dehydrogenase.

Many acetogens also produce four-carbon products like butanol and butyric acid by combining two molecules of acetyl-CoA to form acetoacetyl-CoA. This intermediate is then converted to butyryl-CoA which serves a purpose similar to acetyl-CoA. The reactions involved in the formation of butyric acid and butanol from butyryl-CoA are analogous to those seen above (2.9-2.12). The formation of butyric acid produces ATP while the formation of butanol results in the consumption of reducing equivalents. The corresponding equations are given below:

$$Butyryl - CoA + P_i \rightarrow Butyryl - phosphate + P_i \quad (2.9)$$

$$Butyryl - phosphate + ADP \rightarrow Butyrate + ATP \quad (2.10)$$

$$Butyryl - CoA + NADH + H^+ \rightarrow Butyraldehyde + NAD^+ + CoA - SH \quad (2.11)$$

$$Butyraldehyde + NADH + H^+ \rightarrow Butanol + NAD^+ \quad (2.12)$$

Figure 2.2 shows the pathway of C. acetobutylicum which is a well-researched acetogen, and represents the metabolism of most acetogens using the acetyl-CoA pathway. The enzymes responsible for the metabolism are shown.

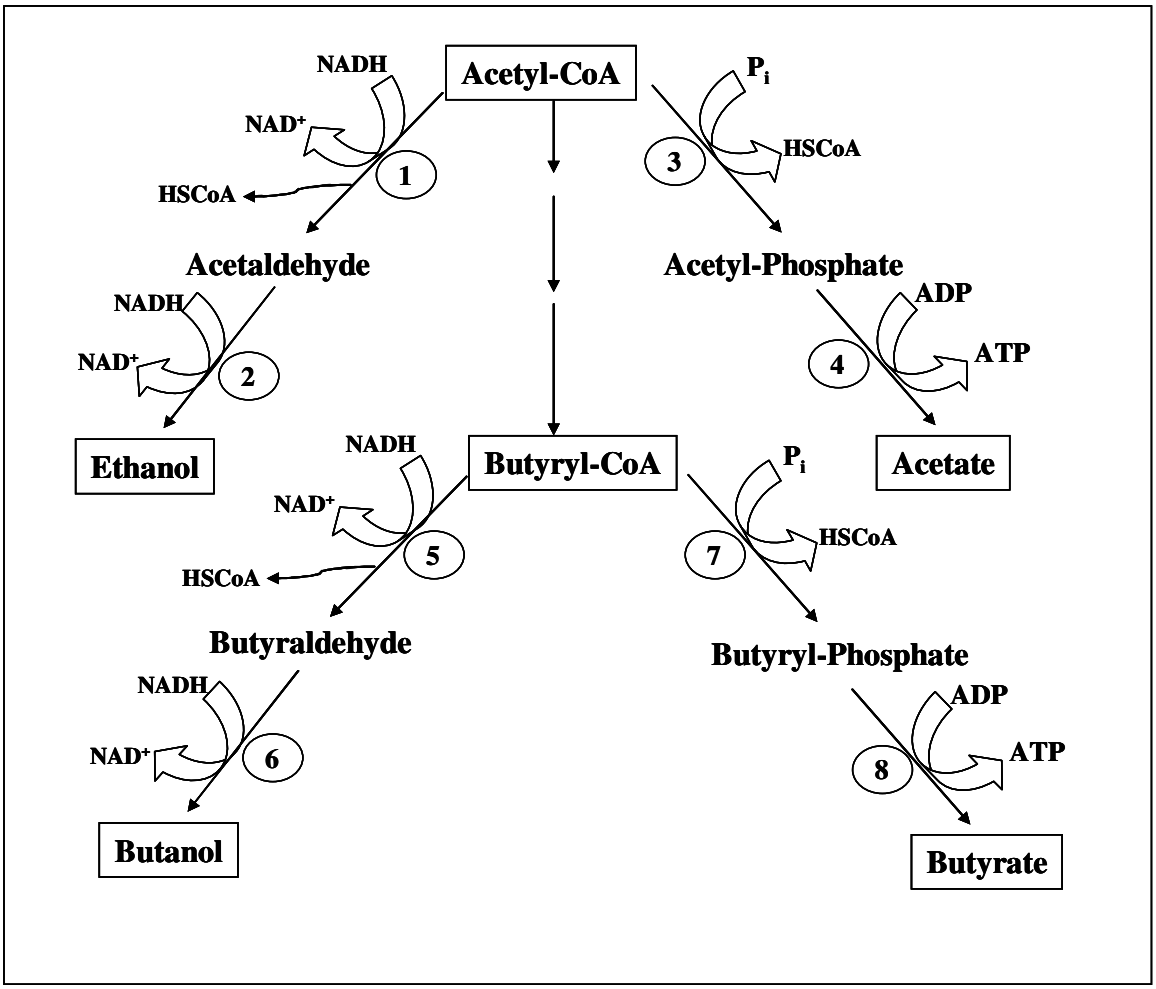

Figure 2.2. Fate of acetyl-CoA in *Clostridium acetobutylicum* adapted from (Vasconcelos et al. 1994). 1-acetaldehyde dehydrogenase, 2-alcohol dehydrogenase, 3-phosphotransacetylase, 4-acetate kinase, 5-butyraldedyde dehydrogenase, 6-butanol dehydrogenase, 7-phosphotransbutyrylase, 8-butyrate kinase

2.5 Acetogenesis vs. Solventogenesis

The complex metabolism of acetogens like *C. acetobutylicum* has generated considerable interest among researchers, leading to several studies conducted to determine the factors involved in the transition between acetogenesis (or acidogenesis) and solventogenesis. Studies have shown that these bacteria usually show a "biphasic batch fermentation pattern" (Girbal et al. 1995b). They produce acids like acetate and butyrate during their exponential growth phase and then switch to alcohol production when the growth slows down before they enter the stationary phase. Several factors have been found to affect this switch from acidogenesis to solventogenesis, such as pH, ATP demand, availability of nutrients, availability of reducing equivalents, enzyme activities etc. In fermentations where many different products are possible, the amount of ATP produced per mole of substrate consumed depends on the product distribution (Meyer and Papoutsakis 1989). For instance, in the acetyl-CoA pathway, the production of acetic acid results in ATP formation. Therefore, if the ATP demand of the cell is high, the pathway would preferably go towards acid production. On the other hand, if there is an excess availability of energy within the cell, the pathway would tend towards alcohol production so that the excess energy may be consumed.

Fermentation conditions and the state of the inoculum used have also been found to influence whether the microbial culture produces high levels of solvents. Grube et al. (2002) demonstrated that under strictly anaerobic conditions, using a spore inoculum led to almost three times the ethanol produced as compared to when a vegetative inoculum was used (Grube et al. 2002). It has also been seen that in some cases, an "acid crash"

occurs wherein high amounts of acid may be produced and the culture then loses the ability to switch to solventogenesis. Clostridial strains are known to "degenerate" if, at the end of the exponential phase, they do not switch to solventogenesis. Degeneration has typically been observed when the inoculum is repeatedly derived from cells in their exponential stage (Kashket and Zhi-Yi Cao 1995; Kutzenok and Aschner 1952).

Due to the uncertainty in the switch from acidogenesis to solventogenesis, several research teams have studied methods of inducing solventogenesis in acetogens. The addition of acetate and butyrate to batch cultures was found to shorten the acidogenic phase and induce solventogenesis (Gottschal and Morris 1981). It was proposed by Gottschal and Morris that this was due to the dissipation of the pH gradient (Δ pH) by acetate and butyrate as the intracellular pH could achieve the same low value as the culture medium. Klasson et al. (1992) showed that yeast extract, a component of the culture medium, also has an effect on the product ratio. They demonstrated that by decreasing the amount of yeast extract in the medium, a higher concentration of solvents can be achieved. Their studies also confirmed that solvent production was non-growth related, as the growth rate seemed to decrease with a decrease in yeast extract concentration. Klasson et al. also proposed that the addition of reducing agents can initiate solventogenesis, as the electrons can reduce NAD^+ to NADH, which provides reducing potential to form acetaldehyde and then ethanol in the alcohol pathway.

Meyer et al. demonstrated that reduced nitrogen-source availability in cultures of *C. acetobutylicum* induced solvent production. On the other hand, glucose-limited conditions caused high amounts of acids to be produced (Meyer et al. 1985). An excess availability of reducing equivalents has also been found to initiate solventogenesis

(Girbal et al. 1995b; Meyer et al. 1985). CO gassing and conditions of iron limitation are also known to increase alcohol production (Byung Hong Kim 1984). Artificial electron carriers like methyl viologen, benzyl viologen and neutral red are known to alter the electron flow by forming NADH, which in turn promotes alcohol production (Girbal et al. 1995a; Girbal et al. 1995b; Klasson et al. 1992). Girbal et al. (1995) demonstrated that adding 1mM neutral red to an acidogenic culture causes a deviation in the electron flow towards NADH production. This pool of NADH generated might be responsible for the change in the metabolism of the bacteria towards solventogenesis. Girbal et al. reported a 3-fold increase in ethanol production on the addition of 1mM neutral red to *C. acetobutylicum* cultures (Girbal et al. 1995a; Girbal et al. 1995b).

2.5.1 Hydrogenase Inhibition

In another study, Girbal et al. (Girbal et al. 1995a) reported that under solventogenic conditions, the *in vitro* hydrogenase activities of the culture were lower than those under acidogenic conditions. Studies have also shown that when batch fermenters of *C. acetobutylicum*, grown on a glucose medium were sparged with carbon monoxide, the hydrogenase enzyme was inhibited and the alcohol production was enhanced (Byung Hong Kim 1984; Meyer et al. 1985; Meyer et al. 1986).

However, the inhibition of hydrogenase in autotrophic organisms results in the inability of the microorganism to consume hydrogen. This in turn leads to the utilization of carbon monoxide to form electrons, so that CO can only partially be utilized to make cell mass and products. Therefore, from the standpoint of a process to produce acids or alcohols, the inhibition of hydrogenase in autotrophic microorganisms is not very

efficient. This has led to an interest among researchers to identify and characterize the inhibitors of hydrogenase. Gases like O_2 (Seefeldt and Arp 1989), acetylene, CO, nitrite and nitric oxide (NO) are known inhibitors of hydrogenase (Acosta et al. 2003; Byung Hong Kim 1984; Krasna 1954; Tibelius and Knowles 1984). Studies have also shown NO to inhibit hydrogenase activity in *Azotobacter vinelandii* (Hyman MR 1991), *Proteus vulgaris* (Krasna 1954), *Alcaligenes eutrophus* (Hyman MR 1988) and *Azospirillum brasilense* (Tibelius and Knowles 1984).

2.5.2 Alcohol Dehydrogenase - Function and Regulation

In the acetyl-CoA pathway, alcohol dehydrogenase (ADH) plays an important role in the formation of ethanol. It catalyzes the conversion of acetaldehyde to ethanol using NADH as a reducing equivalent. Assays to determine the activity of alcohol dehydrogenase can indicate whether the acetogen is in the solventogenic phase of ethanol production. ADH assays often use NADH as the reducing equivalent and acetaldehyde as the substrate. Studies have shown that the ADH activities of alcohologenic cultures are higher than those of acetogenic cultures. The addition of artificial electron carriers has been shown to increase ADH activity, which in turn results in an increase in alcohol production. Girbal et al. demonstrated that the addition of 1mM neutral red led to a 3-fold increase in ethanol production and a 6.6-fold increase in ADH activity of *C. acetobutylicum* cultures (Girbal et al. 1995b).

2.6 Discussion

A review of the literature points to several key areas that need to be explored in the field of gasification-fermentation of biomass to ethanol. Using biological catalysts for the conversion of biomass to ethanol poses several challenges as certain constituents of the biomass or the synthesis gas can be extremely toxic to the microorganisms thus preventing a successful fermentation. As discussed in Chapter 1, biomass-generated synthesis gas has three distinct effects on the microbial catalyst. Exposure to this gas leads to cell dormancy, cessation of hydrogen utilization and a change in the product distribution. The work reported in this dissertation aims at getting a better understanding of these effects and how some of the current problems may be overcome to improve the fermentation process. Three main hypotheses were tested in this work:

Hypothesis 1: Cell-dormancy is caused by one or more impurities of biomass-syngas and can be eliminated by removing the impurity from the gas. Chapter 3 describes the effects of individual impurities of biomass-syngas on cell-growth and product distribution. Chapter 3 also identifies the cause of cell-dormancy and suggests one method to overcome it. Chapter 4 describes studies conducted to determine the effect of cell-recycle on syngas-fermentation, proposing another way to overcome cell-dormancy.

Hypothesis 2: Hydrogenase inhibition is caused by nitric oxide in the biomass-syngas. In Chapter 5, studies conducted with nitric oxide are described and a kinetic analysis of the hydrogenase inhibition is presented.

Hypothesis 3: Addition of artificial electron carriers like neutral red can regulate the metabolic pathway of the organism towards ethanol production. Chapter 6 explores the effect of adding an artificial electron carrier on the product distribution during syngas fermentation.

CHAPTER 3

EFFECTS OF BIOMASS-GENERATED SYNGAS CONSTITUENTS ON CELL-GROWTH AND PRODUCT DISTRIBUTION

3.1 Introduction

In previous studies, certain effects of syngas fermentation were observed (Datar et al. 2004). The process involved growing cells in a batch system under continuous flow of synthetic syngas, following which the system was changed to a continuous liquid flow in which fresh media was added and products/cells were removed with no cell recycle. The term "synthetic syngas" refers to a mixture of purchased compressed gases with a similar CO, CO_2, and H_2 composition as the biomass-syngas. After the cells reached a steady concentration, the synthetic syngas was replaced with the biomass syngas (generated from gasification of Switchgrass) that had been cleaned with two cyclone separators followed by two 10%-acetone scrubbers, all in series. Following the biomass syngas introduction, the cells stopped consuming H_2 almost immediately and the cells stopped growing after a delay of approximately 1.5 days. The cessation in cell growth led to cell washout from the reactor as a result of the continuous operation. In addition, an increase in ethanol production and a decrease in acetic acid production were also observed.

Syngas via gasification typically contains tars, ash, and certain gaseous components (Devi et al. 2003; Engelen et al. 2003; Zhang et al. 2004). It was hypothesized that one or more of these potential "contaminants" induced cell dormancy, stopped H_2 utilization, and affected product distribution. Cleaning of syngas using filters was assessed in chemostat experiments to determine if any of the conditions could be eliminated. A detailed analysis for one chemostat experiment is described below in the results and discussion. Results of two other similar chemostat experiments are given in Appendix A. In addition, batch experiments were performed to assess whether gaseous impurities like ethane, ethylene and acetylene or particulate impurities like tars, and/or ash contributed to the cell-dormancy.

3.2 Materials and Methods

3.2.1 Biomass and Syngas

Biomass syngas was obtained by gasification of switchgrass. Switchgrass is a sustainable perennial herbaceous crop (Sanderson et al. 1996a) which is advantageous owing to its high yields, low nutrient requirements, and geographically-wide distribution (McLaughlin and Walsh 1998). The switchgrass was harvested, baled, chopped and then gasified in a fluidized-bed reactor (Datar et al. 2004). The exiting gas was passed through two cyclone separators in series to remove particulates (such as ash) and then through two scrubbers in series. Each 4-foot scrubber was packed with stainless steel pall rings containing a mixture of 90% water and 10% acetone at 20 ºC that was continuously circulated through the scrubbers. The average residence time of the syngas in each scrubber was 4 minutes. The syngas was then compressed and stored at

approximately 860 kPa in storage vessels. The syngas analysis showed approximately 16.5% CO, 15.5 % CO_2, 5 % H_2, and 56 % N_2 along with 4.5% CH_4, 0.1% C_2H_2, 0.35% C_2H_6, 1.4 % C_2H_4 and 150 ppm nitric oxide (compositions based on measured species).

3.2.2 Microbial Catalyst and Culture Medium

Clostridium carboxidivorans $P7^T$ was provided by Dr. Ralph Tanner, University of Oklahoma. This bacterium is capable of fermenting syngas, as well as sugars, to produce alcohols and acids. The bacterium was grown under strictly anaerobic conditions in a medium containing (per liter) 30 ml mineral stock solution, 10 ml trace metal stock solution, 10 ml vitamin stock solution and 10 ml of 4% cysteine-sulfide solution. For the batch experiments, 1 g yeast extract and 10 g morpholinoethanesulfonic acid (MES) were added to the medium, while for the chemostat experiments, 0.5 g yeast extract and 5 g MES were added. Resazurin solution (0.1%) was added as a redox indicator in all experiments. The mineral stock solution contained (per liter) 80 g sodium chloride, 100 g ammonium chloride, 10 g potassium chloride, 10 g potassium monophosphate, 20 g magnesium sulfate, and 4 g calcium chloride. The vitamin stock solution contained (per liter) 0.01g pyridoxine, 0.005g thiamine, 0.005g riboflavin, 0.005g calcium pantothenate, 0.005g thioctic acid, 0.005g amino benzoic acid, 0.005g nicotinic acid, 0.005g vitamin B12, 0.002g biotin, 0.002g folic acid, and 0.01g 2-mercaptoethanesulfonic acid sodium salt (MESNA). The stock solution of trace metals contained (per liter) 2g nitrilotriacetic acid, 1g manganese sulfate, 0.8g ferrous ammonium sulfate, 0.2g cobalt chloride, 0.2g zinc sulfate, 0.02g copper chloride,

0.02g nickel chloride, 0.02g sodium molybdate, 0.02g sodium selenate, and 0.02g sodium tungstate.

3.2.3 Batch Studies – Effects of Gaseous Contaminants

Batch experiments were conducted in 250-ml serum bottles with 100 ml of liquid media to assess the effects of ethane, ethylene and acetylene on cell growth and pH. As there was no external pH control in the batch studies, a higher amount of MES buffer was used in batch than in chemostat studies. The media was boiled and purged with nitrogen for five minutes to remove oxygen and then sterilized in an autoclave (Primus Sterilizer Co. Inc.) at 121°C for 20 minutes. The bottles were allowed to cool and the headspace was again purged with N_2 for approximately one minute. Cysteine sulfide (1 ml) was added to scavenge any remaining dissolved oxygen and the reactors were pressurized with a mixture of 80% CO and 20% CO_2 at 10 psig. The contaminant being tested was then added to the headspace of the reactors using a 1-ml gas-tight syringe (VICI Precision Sampling, Inc., Baton Rouge, Los Angeles). Approximately 1.4% ethane, 0.35 % ethylene and 0.1 % acetylene were assessed in each study. The reactors were then inoculated and placed at 37°C in a shaker (Innova 2100, New Brunswick Scientific). All studies were performed in triplicate. Cell concentration and pH were measured at regular time intervals for all the reactors.

3.2.4 Chemostat Studies

A BioFlo 110 Benchtop Fermentor (New Brunswick Scientific, Brunswick, NJ) with a 3-liter working volume was used for the fermentation studies involving continuous liquid feed and product removal (i.e. chemostat mode). The reactor consisted of an agitator, sparger, pH probe, dissolved oxygen probe, ports for liquid inlet and outlet, jacket for temperature control and pumps for feed, product removal and pH control. The experimental setup is shown in Figure 3.1. Media was autoclaved in the bioreactor and then sparged with nitrogen to remove the dissolved oxygen. Once the dissolved oxygen probe indicated an anaerobic environment in the bioreactor, synthetic gas mixture was introduced in the gas feed-line. Cysteine-sulfide was then added to the media to remove any residual dissolved oxygen.

As shown, a 4-way valve was used to introduce gas feed by switching between syngas and synthetic syngas. Gas was introduced through a sparger. Two liquid feed tanks were used to introduce sterile media into the bioreactor during chemostat operation. Liquid feed tanks were continuously purged with nitrogen to maintain anoxic conditions.

Although the pH of the reactor was controlled using a pH controller, MES was added as a buffer to prevent excessive fluctuations in pH during the course of the experiment. Prior to inoculation, the bioreactor was filled with three liters of liquid media (without the vitamins) at pH 5.85 and autoclaved at 121°C for 20 minutes. After cooling, media was purged with nitrogen to provide an anaerobic environment and filter-sterilized vitamin stock solution (10 ml per liter) was added to the media to avoid the inactivation of vitamins during steam sterilization. Cysteine-sulfide (30 ml) was added to scavenge any remaining dissolved oxygen.

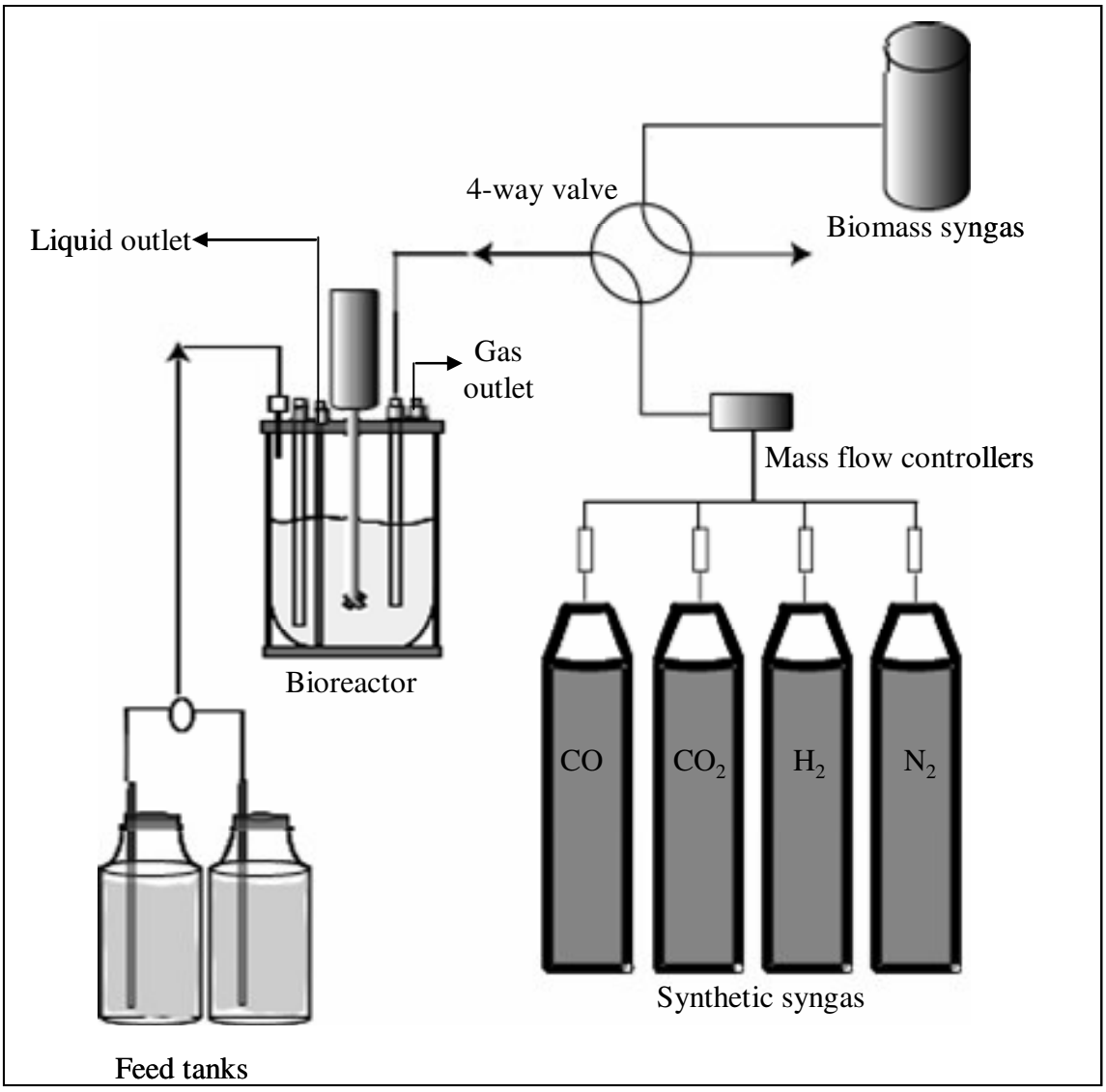

Figure 3.1. Schematic of 3-liter chemostat experiment. A mass flow controller was used to mix the synthetic gases. A 4-way valve was used to switch the gas supply between synthetic gas mixture and syngas obtained from gasified switchgrass.

Once the anaerobic environment was obtained, the gas feed was changed from N_2 to synthetic syngas (approximately 17% CO, 15% CO_2, 5% H_2, and balance N_2) flowing at 160 cm^3 min^{-1} at 25°C and 137 kPa. A mass flow controller was used to mix bottled gases in the same composition as the CO, CO_2, and H_2 in the syngas to obtain the synthetic syngas. The impellor agitation was 400 rpm and the temperature was 37°C.

The bioreactor operation was divided into four stages. In all stages, the gas flow was continuous. In the first stage, the liquid was maintained in batch mode and the synthetic syngas was fed to the bioreactor. The bioreactor was inoculated and the cells were allowed to grow until the cell concentration started to level off. The pH was allowed to drop from an initial value of 5.85 to the lower pH setpoint of 5.25 in increments of 0.2 during the first stage. A deadband of 0.2 was used to avoid too much addition of acid or base by the pH controller. During the second stage, continuous liquid feed and removal was initiated at 0.36 ml min^{-1}. This flow rate was based on the growth rate of the cells in the batch mode. Once the cell concentration stabilized with continuous liquid feed, the third stage was initiated by switching the gas feed from synthetic syngas to syngas. The syngas was additionally cleaned with a 0.025-µm filter (Millipore). In the fourth stage, the gas filter was replaced by a 0.2-µm filter with the syngas continuing as the feed. In all stages, the cell concentration, pH, product concentration, and inlet/outlet gas compositions were analyzed.

3.2.5 Batch Studies – Effects of Tar

Batch studies were performed to assess the effects of tar on cell-growth and product distribution. The experimental method was similar to that described in Section

3.2.3, except that in these studies, the 10% acetone solution used to scrub the syngas was added to the reactors (1 ml). Acetone was used for tar removal because tars dissolve in acetone. The first study contained two sets of reactors. One set was used as a control, containing the regular media described above. To the other set, the 10% acetone solution containing tars was added. A second study was performed similar to the first. In this case, for controls, one study had no additional components added and one study involved the addition of a 10% acetone solution (1 ml) that had not been used for scrubbing syngas. The cell concentration, pH, and product concentrations were measured at regular time intervals.

3.2.6 Analytical Methods

The optical density (OD), which is proportional to the cell concentration (~ 0.43 g L^{-1} per OD unit (Datar 2003)), was determined using a UV-Vis spectrophotometer. Cell samples were collected in 4-ml cuvettes from the bioreactor and the OD was measured at 660 nm. A standard calibration chart was used within a linear range of 0 to 0.4 OD units to estimate the cell concentration. Samples with an OD greater than 0.4 units were diluted so that the OD was within the linear range of calibration. Gas samples were taken from the outlet and inlet lines of the bioreactor in gas tight syringes. Gas compositions for the chemostat were determined using a gas chromatograph (3800 series, Varian Co., CA) with a Hayesep-DB column (Hayes Separations Inc, Bandera, TX) connected to a thermal conductivity detector (TCD) with argon as the carrier gas. The TCD was run at 40 ºC for 6 minutes, after which the temperature was ramped up to 140 ºC at 100 ºC min^{-1} for 20 minutes.

The liquid samples were centrifuged at 1,300 x *g* for 30 minutes. The cell-free supernatant was collected and then frozen at -18 ºC until further analysis. The liquid products were analyzed for ethanol and acetic acid using a 6890 Gas Chromatograph (Agilent Technologies, Wilmington, DE), equipped with a flame ionization detector and an 8-ft Porapak QS 80/100 column (Alltech, Deerfield, IL).

3.3 Results and Discussion

3.3.1 Batch Studies – Effects of Gaseous Contaminants

Figures 3.2, 3.3 and 3.4 show the cell concentration and pH profiles in the presence of 0.35% C_2H_6, 1.4 % C_2H_4 and 0.1% C_2H_2 respectively. The controls had no contaminant present in the headspace. As shown in Figure 3.2, the cell concentration of the controls as well as the reactors containing 0.35 % ethane in the headspace showed similar profiles. Cells began to grow in both cases within the first day, and cell concentration reached a maximum value of about 0.15 g/l after which it remained nearly constant. This showed that ethane did not cause any delay or inhibition in cell-growth. The similar pH profiles, represented on the right y-axis, further indicated that the addition of ethane did not have any effect on the fermentation. The pH at the beginning of the fermentation was about 6.0, and dropped to about 5.7 in both sets of reactors. Figures 3.3 and 3.4 show the effects of 1.4 % ethylene and 0.1 % acetylene on the cell-growth and pH profile of the cells. Once again, the cell concentration and pH profiles followed very similar trends for the controls as well as the reactors containing ethylene and acetylene.

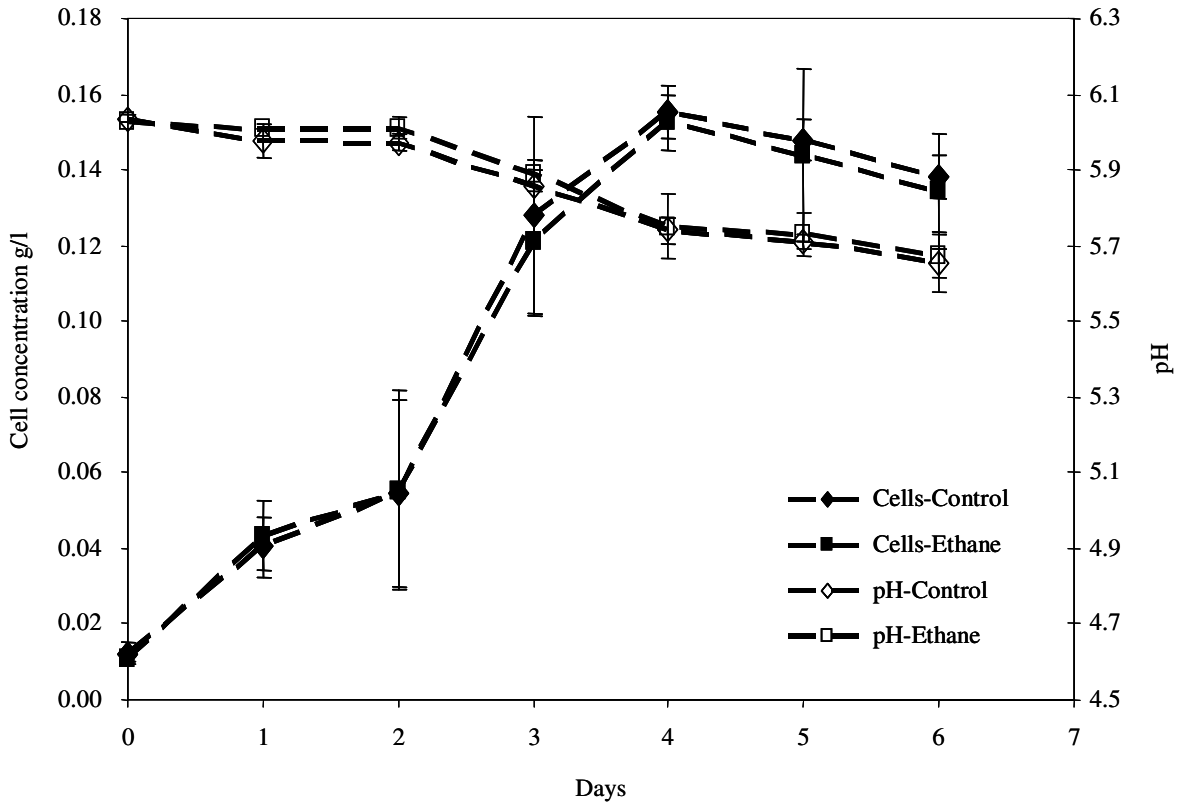

Figure 3.2 Effect of 0.35 % ethane on cell growth and pH profiles of *C. carboxidivorans* $P7^T$. The error bars represent the standard error (n=3). The overlapping error bars indicated that ethane had no effect on cell-growth or pH.

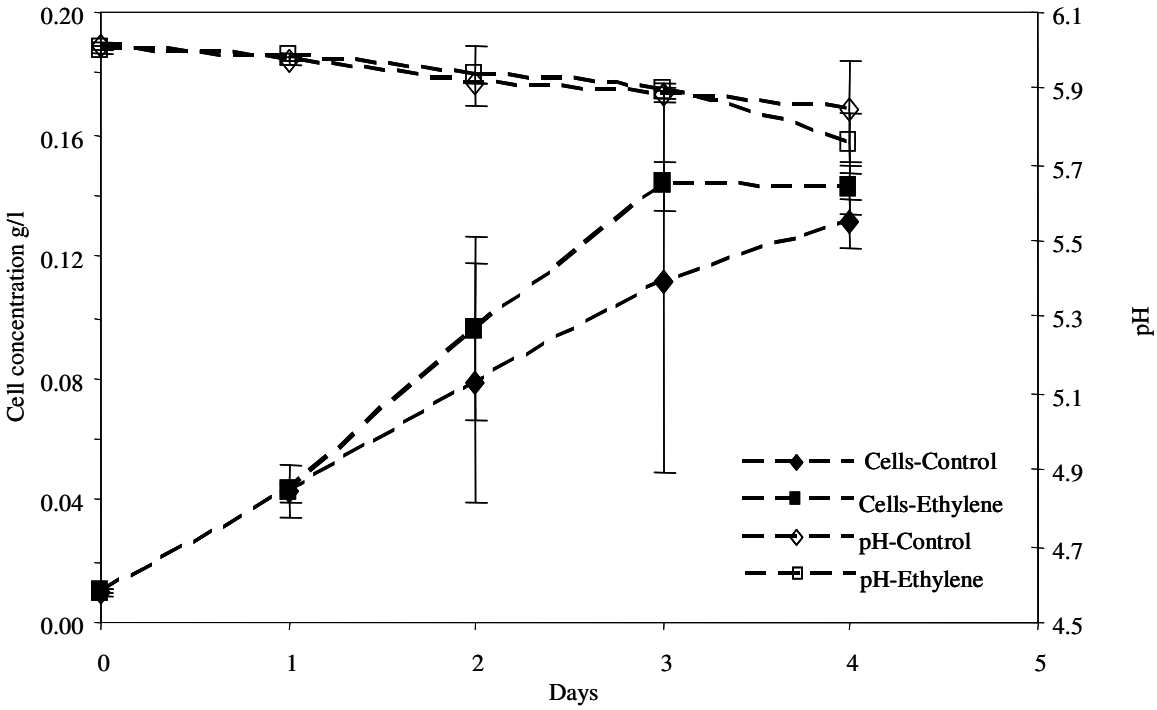

Figure 3.3 Effect of 1.4 % ethylene on cell-growth and pH profiles of *C. carboxidivorans* $P7^T$. The error bars represent the standard error (n=3). The overlapping error bars indicated that ethane had no effect on cell-growth or pH.

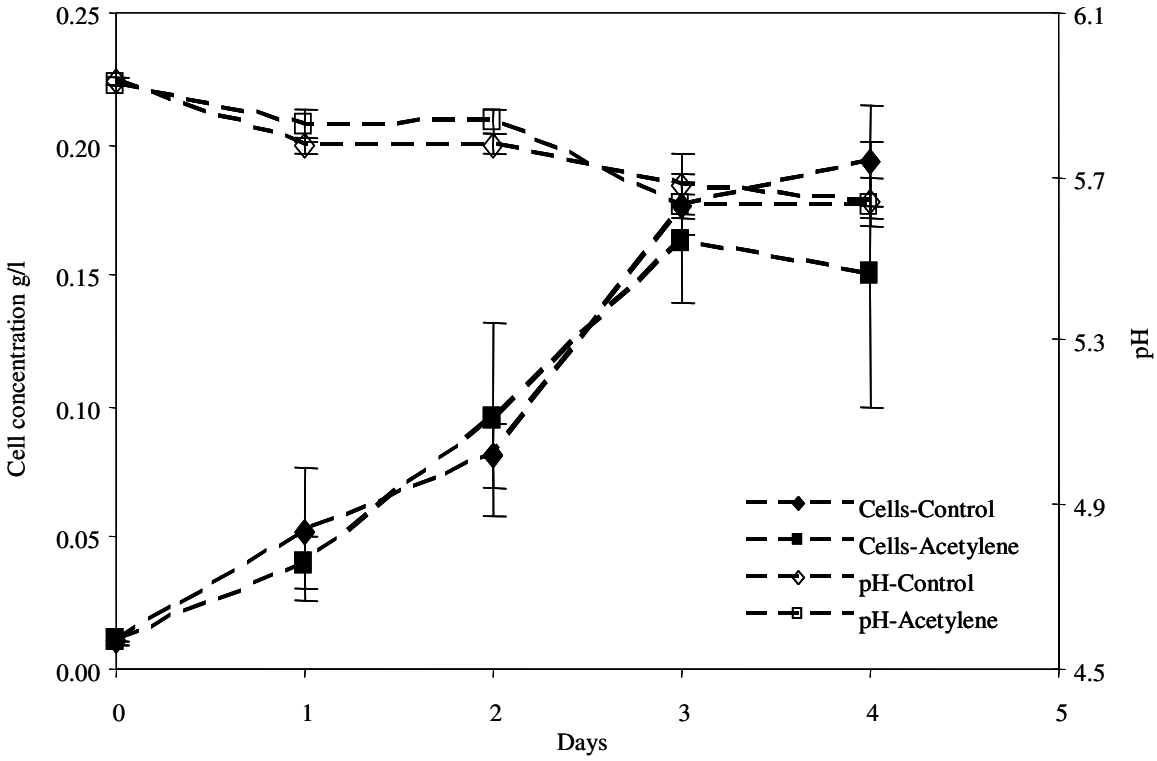

Figure 3.4 Effect of 0.1 % acetylene on cell-growth and pH profiles of *C. carboxidivorans* $P7^T$. The error bars represent the standard error (n=3). The overlapping error bars indicated that ethane had no effect on cell-growth or pH.

All reactors showed a final cell concentration very close to 0.15 g/l and a pH drop from about 6.0 to 5.7. It was previously seen that adding 4.5 % methane to a chemostat had no effect on cell-growth (Datar 2003). These results indicated that none of the gaseous syngas contaminants were the cause of cell-dormancy.

3.3.2 Chemostat Studies- Cell Growth

Since it was concluded that gaseous contaminants like methane, ethane, ethylene and acetylene were not the cause of cell-dormancy, it was necessary to determine whether additional cleaning of the gas using a 0.025-µm filter could prevent cell dormancy in a chemostat mode. The cell concentration profile for one chemostat study is shown in Figure 3.5. In the first stage, cells grew and cell concentration began leveling off on Day 8. Following the initiation of continuous liquid flow on Day 8 (stage 2), cell concentration remained essentially constant. There was little change in the cell concentration during the third stage following the introduction of syngas. The 0.025-µm filter negated the previously observed decline in cell concentration observed with syngas introduction using a 0.2-µm filter (Datar et al. 2004). However, upon switching to the 0.2-µm filter (stage 4), the cell concentration declined after approximately 1.5 days.

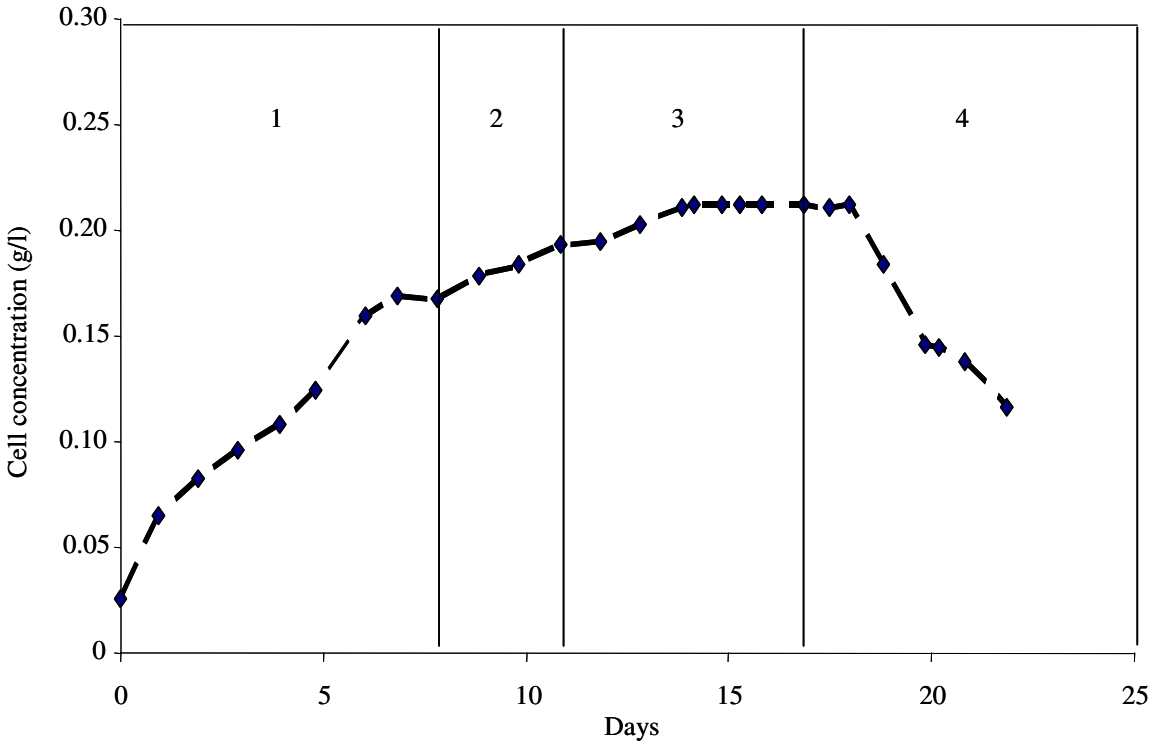

Figure 3.5 Cell concentration profile in chemostat. In stage 1, the liquid phase was batch and cells were grown on synthetic syngas. In stage 2, the liquid phase was changed to continuous. In stage 3, the gas supply was changed to filtered (0.025-µm) syngas. In stage 4, the syngas was cleaned with a 0.2-µm filter. The gas phase was continuous in all stages.

The chemostat material balance for cells, neglecting death, is represented by Equation 3.1.

$$\frac{dX}{dt} = \mu X - DX \qquad (3.1)$$

where X is the cell concentration, D is the dilution rate defined as the ratio of the liquid feed rate (F) to the liquid volume (V), and μ is the cell growth rate. The cell balance is important for understanding the experimental observations. During batch growth (stage 1), D=0 and integration of Equation 3.1 yields a slope of μ when $\ln(X/X_0)$ is plotted versus time. X_0 is the initial cell concentration. For this study, μ was 0.0074 hr^{-1} during stage 1. For stage 2, when the cell concentration was nearly constant (dX/dt=0), μ = D. Thus, a liquid flow rate of F = 0.36 ml min^{-1} was chosen to maintain D just below 0.0074 hr^{-1} (D = 0.0069 hr^{-1}).

On Day 11, the gas was switched from the synthetic syngas to syngas that had passed through a 0.025-μm filter. The cell concentration remained independent of time, thus the cells were still growing in the presence of the 0.025-μm filtered syngas since μ=D. This result was confirmed in two additional chemostat experiments, shown in Appendix A. Upon replacing the 0.025-μm filter with a 0.2-μm filter, the cell concentration began declining after approximately 1.5 days. Assuming μ=0 (i.e. no cell growth) in Equation 3.1, when the cell concentration begins to decline, integration yields Equation 3.2.

$$\ln(X / X_0) = -D * t \qquad (3.2)$$

In Equation 3.2, X_0 represents the cell concentration just as the decline begins. Using the cell concentration data in stage 4 (the declining portion), a plot of $\ln(X/X_0)$ versus time with Equation 3.2 yielded D= 0.0068 hr^{-1}, which is in agreement with the value of D used in the experiment. This agreement demonstrated that cells were not dying, but rather were remaining in a non-growth state and were washing out of the reactor. Figure 3.6 shows the comparison between the data and the washout model starting from the time when the cell concentration began to decay. This was also observed in previous studies with the use of a 0.2 µm filter (Datar et al. 2004). As noted below in the product formation section, acetic acid was still being produced in stage 4 providing evidence that the cells were not dead.

Regarding cell dormancy, studies with similar concentrations of ethylene, acetylene, or ethane added to batch cultures grown under "clean" CO/CO_2 gases showed no difference in growth characteristics, as described in Section 3.3.1. During the chemostat run, the filter inlet and outlet compositions of ethylene, acetylene and ethane in the syngas were measured and it was found that there was no detectable change in the compositions - again suggesting that these gases do not contribute to cell dormancy.

3.3.3 Chemostat Studies- pH Changes

The pH profile is shown in Figure 3.7. The pH of the medium was initially adjusted to 5.85 before inoculation. Once the cells started growing, pH started to drop due to the production of acids. The pH was allowed to drop during stage 1, but the pH setpoint was adjusted from 5.85 to 5.25 over the first three days to minimize a rapid drop in pH. Once the pH was 5.25, the setpoint was maintained at 5.25 during stage 2 with a

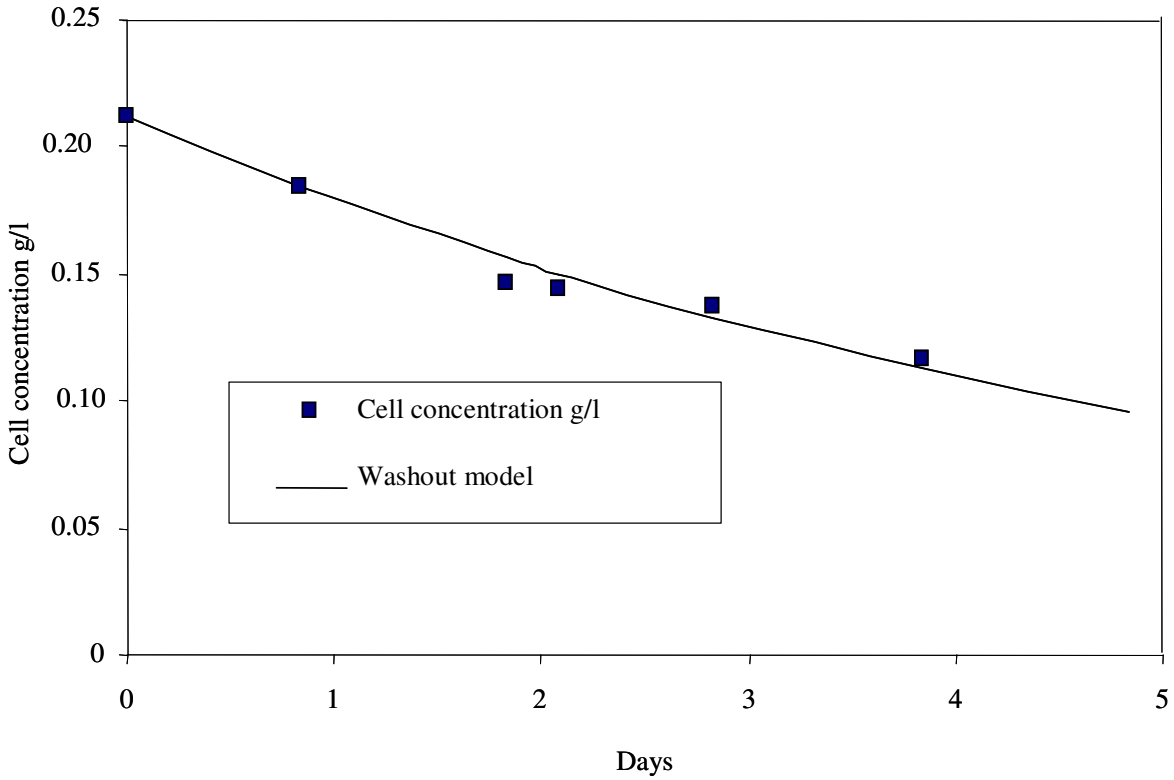

Figure 3.6. Cell washout on exposure to biomass syngas using the 0.2-µm filter. Day 0 represents the beginning of the cell washout. The solid line represents the cell-washout model as described by Equation 3.2.

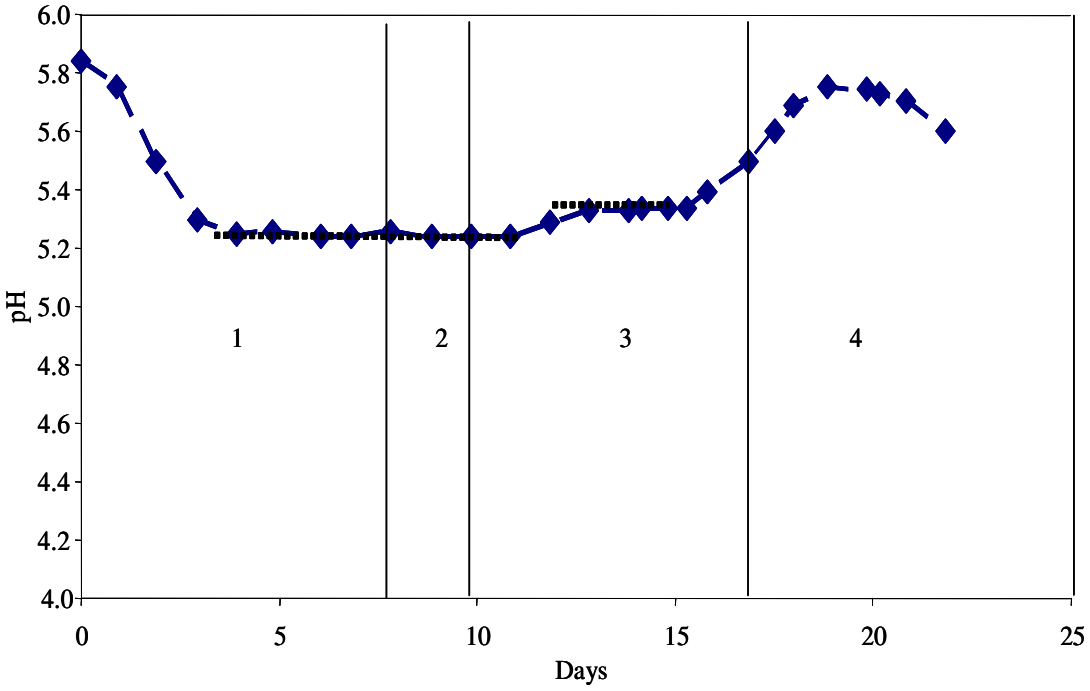

Figure 3.7. pH profile in chemostat. The stages are as described in Figure 3.5. The horizontal dotted lines show the pH control set-point.

dead band of 0.2. After the introduction of syngas (stage 3), pH began to rise (as previously observed) and was controlled at a value of 5.35. After about 4 days, pH was allowed to rise. The pH reached a value of 5.75 and then started to decrease as the cells washed out of the reactor in stage 4.

3.3.4 Chemostat Studies - Substrate Utilization

In the presence of synthetic syngas, cells consumed CO and H_2 and produced CO_2. The inlet gas contained 0.165 moles/min of CO and 0.15 moles/min of CO_2, while the outlet gas contained 0.14 moles/min of CO and 0.16 moles/min of CO_2. An overall carbon balance showed that more than 97% of the utilized carbon was accounted for in the production of CO_2, ethanol, acetic acid, and cell mass. Upon switching from synthetic syngas to biomass-generated syngas, H_2 consumption immediately ceased, irrespective of the filter size.

3.3.5 Chemostat Studies- Product Formation

Figure 3.8 shows the change in the ratio of the product concentration (P) to the cell concentration (X) with time for both ethanol and acetic acid. The transient mass balance for P (g L^{-1}) in a well-mixed chemostat is:

$$\frac{dP}{dt} = q_P X - DP \tag{3.3}$$

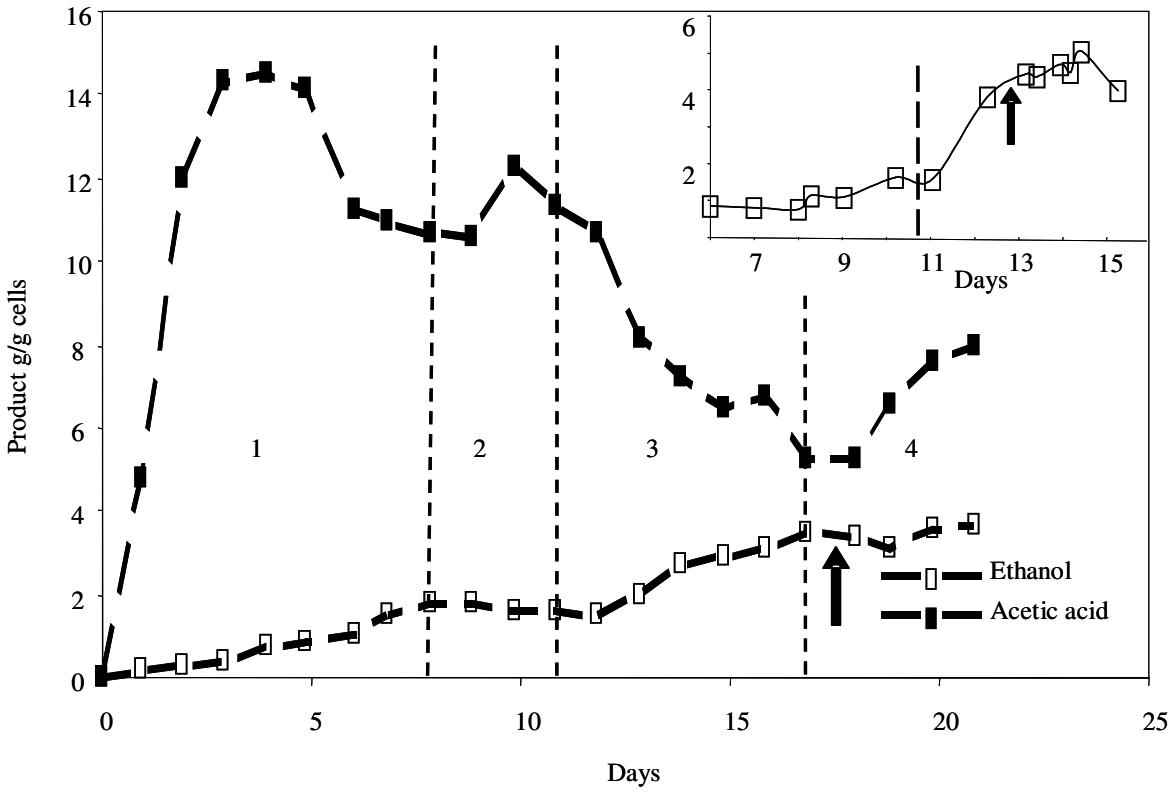

Figure 3.8 Ethanol and acetic acid profile in chemostat. The stages are the same as described in Figure 3.5. The inset is from a previously published experiment (Datar et al. 2004). Arrows indicate the beginning of cell washout in both experiments.

where q_p is the product formation rate per cell mass [g (g cells)$^{-1}$ time^{-1}] and D is the dilution rate [time^{-1}]. Since (P/X) is shown in Figure 3.8, time differentiation of (P/X) shows

$$\frac{d(P/X)}{dt} = \frac{X\frac{dP}{dt} - P\frac{dX}{dt}}{X^2} \tag{3.4}$$

Substitution of Equation 3.3 into Equation 3.4, with some re-arrangement, gives Equation 3.5 that is useful for understanding the results shown in Figure 3.8.

$$q_P = \frac{d(P/X)}{dt} + \frac{P}{X^2}\frac{dX}{dt} + D\left(\frac{P}{X}\right) \tag{3.5}$$

During stage 2, both X (Figure 3.5) and (P/X) (Figure 3.8 for both ethanol and acetic acid) were relatively constant such that the derivatives in Equation 3.5 are small compared to the last term. Thus, $q_p \approx D(P/X)$ and q_p for acetic acid is approximately six times that of ethanol during the fermentation of synthetic syngas. It is noted that (P/X) for acetic acid may be slightly increasing during stage 2 such that q_p would be slightly greater than D(P/X). Nevertheless, q_p for acetic acid is still much greater than for ethanol.

This observation that q_p for acetic acid is much greater than for ethanol is contrary to what was previously observed (Rajagopalan et al. 2002) in which more ethanol was produced than acetic acid. *C. carboxidivorans* is an acetogen that produces primarily acetic acid during the growth phase. A switch to solventogenesis (ethanol production) occurs when the medium conditions are no longer favorable for growth. In many cases, initiation of solventogenesis in clostridium bacteria is associated with the onset of

sporulation (Grube et al. 2002; Kashket and Zhi-Yi Cao 1995; Long 1984). It is feasible that the initial inoculum in the previous experiments contained a mix of cells that were both acid and ethanol producing. Therefore, this discrepancy in the product ratio may be explained by the fact that the inoculum used in both cases may have been in different states.

When syngas was introduced through a 0.025-µm filter in stage 3, (P/X) for ethanol nearly doubled and approached a steady value (where $q_p \approx D(P/X)$). Thus, in comparison with stage 2, q_p for ethanol approximately doubled. On the other hand, (P/X) for acetic acid decreased from 11.3 to 5.1 grams per gram of cells over six days. Initially, $d(P/X)/dt \approx -1$ g g^{-1} day^{-1} but then began leveling off towards zero. Since X remained essentially constant (i.e. dX/dt is small) and D(P/X) initially began at 1.85 but leveled off at 0.85 g g^{-1} day^{-1} (with D=0.007 h^{-1}), Equation 3.5 shows that q_p for acetic acid decreased compared to stage 2 but still remained positive. Even if the net value of q_p is positive, acetic acid could be both produced and then consumed to make ethanol. Additional experiments must be performed to determine if the increase in ethanol is due to the consumption of acetic acid rather than from direct conversion of CO to ethanol. However, this increase in ethanol production by the cells suggests that some constituent of the syngas could be making the cells more solventogenic as compared to the synthetic syngas.

In stage 4, the filter was changed to 0.2-µm and washout of the cells began after about 1.5 days. The arrow in Figure 3.8 indicates the time at which washout of the cells began. Prior to washout, $q_p \approx D(P/X)$ as previously explained in stage 3. However, at the onset of cell dormancy in which washout occurs, $dX/dt \approx -DX$ as described in the cell

growth section. Thus, substitution into Equation 3.5 shows that $q_p \approx d(P/X)/dt$ during cell dormancy. Therefore, prior to washout, q_p for ethanol and acetic acid were positive. Throughout cell dormancy, q_p for ethanol was negligible since (P/X) remained essentially constant, although q_p for acetic acid increased.

Due to some problems with the GC analysis, a product profile could not be obtained for the studies shown in Appendix A. However, similar results were observed in previous studies in which syngas was cleaned with a 0.2-µm filter (Datar et al. 2004). When syngas was introduced, an increase in the ethanol concentration was observed for about 1.5 days while the cell concentration remained relatively stable. Thus, q_p for ethanol increased. After cell dormancy (washout) began, (P/X) for ethanol (plotted using the reported data of P and X and shown as the inset in Figure 3.8) was essentially constant. Since $q_p \approx d(P/X)/dt$ during washout, q_p for ethanol was negligible.

3.3.6 Filter Analysis

As it was conclusively shown that the filter size affected cell dormancy and q_p for ethanol and acetic acid, an analysis of the filter was performed. Particulates trapped by the filter could include ash and tar generated during the gasification process. The 0.025-µm filter was evaluated using a scanning electron microscope (JEOL JSM 6360). Figure 3.9 (A) shows the filter used to clean the syngas. The particle shown was one of the larger agglomerates seen on the filter. There were also several smaller particles of similar appearance spread over the filter. The trapped particulates differ from ash shown in Figure 3.9 (B). Thus, ash was not the culprit leading to cell dormancy, but tar particulates were the likely candidates.

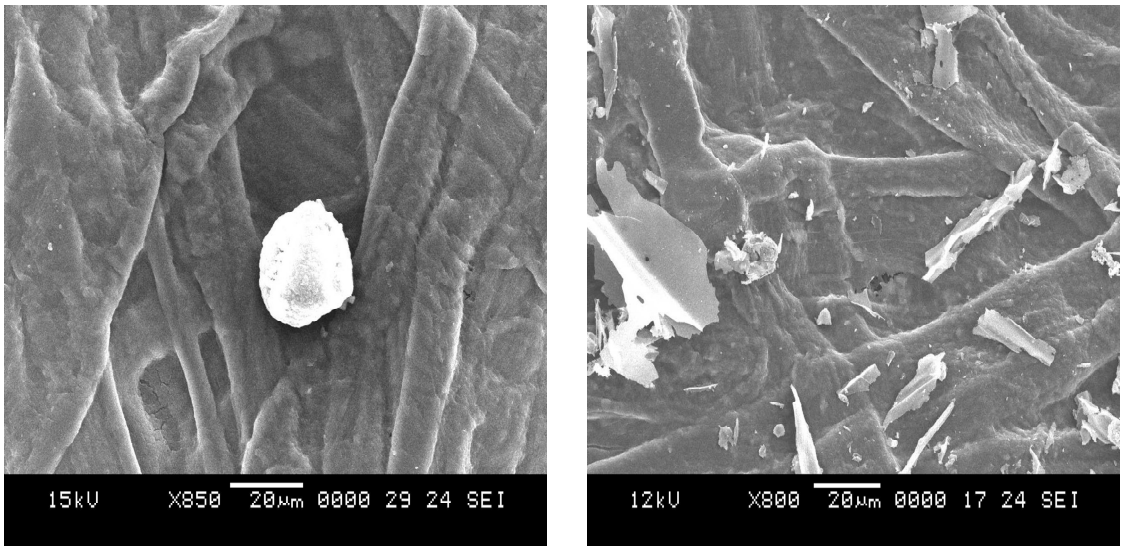

a b

Figure 3.9 Scanning electron microscope analysis of (A) 0.025-µm filter used in chemostat studies and (B) 0.025-µm filter exposed to ash from gasifier.

3.3.7 Batch studies – Effects of Tar

To assess the effects of tars on cell growth and product distribution, batch experiments were performed. Figures 3.10-3.12 show the cell growth, ethanol formation and acetic acid formation in the presence of media and media supplemented with the 10% acetone solution from the scrubbers. The stored syngas was bubbled through a 10% acetone solution to identify potential tar species in the gas. A GCMS analysis of the acetone solution identified benzene (327 µg/ml), toluene (117 µg/ml), ethylbenzene (131 µg/ml) and p-xylene (92 µg/ml), in addition to less abundant species like o-xylene and naphthalene. A significant delay in cell growth was observed in the presence of tar in the reactors. Product redistribution, resulting in higher amounts of ethanol and lower amounts of acetic acid compared to the controls, was also observed. In order to ensure that these effects were due to tars and not acetone, another similar experiment was conducted in which a third set of reactors were tested, containing "clean" acetone in the media. Figures 3.13-3.15 show the cell growth, ethanol formation and acetic acid formation in the presence of media, media supplemented with "clean" 10% acetone, and media supplemented with the 10% acetone solution from the scrubbers. The "clean" acetone studies showed no difference with the studies containing media alone. However, the presence of tars in the scrubbed acetone solution once again showed a significant delay in cell growth. The delay was much longer than the washout period shown in Figure 3.5. For the studies with tars, the results are shown separately for two of the three studies since the onset of growth varied. The third study is not shown since growth was not observed. A likely scenario is that the tars initially inhibit growth (but do not cause death), which is consistent with the washout of cells in the chemostat. After a long

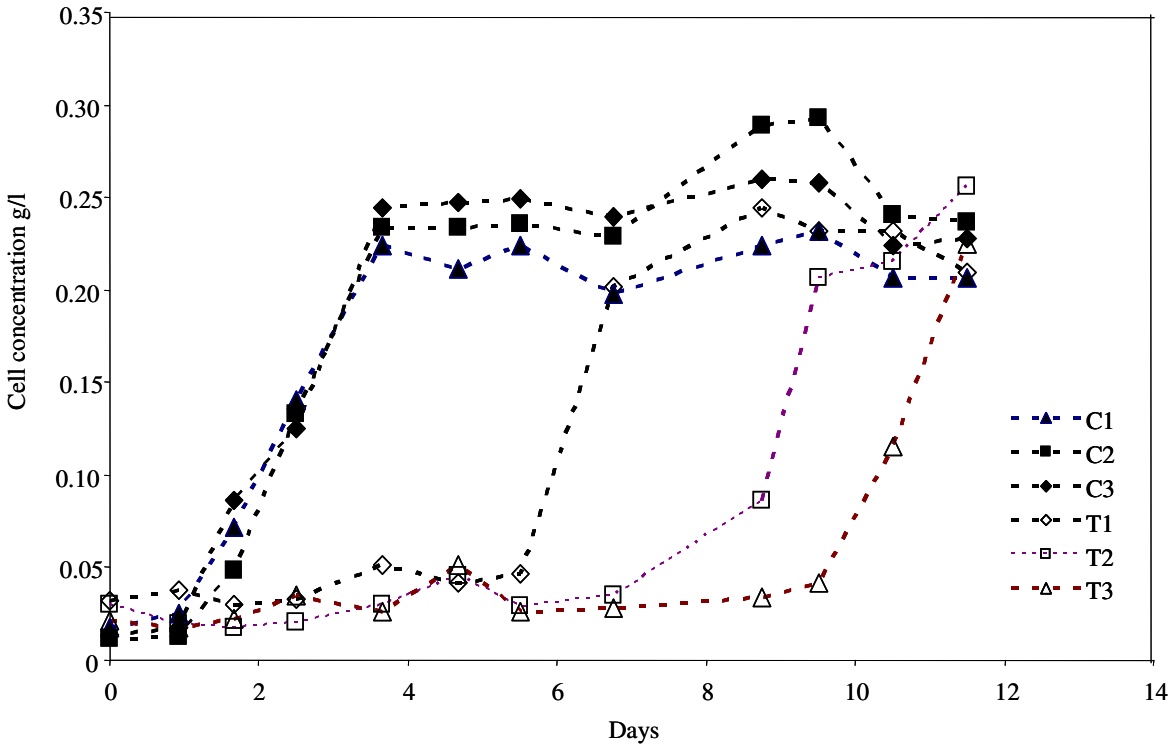

Figure 3.10 Cell concentration profile for batch study. C1, C2, C3 are the controls with regular media. T1, T2, T3 contained the acetone solution from the scrubbers with tar. There was a significant delay in cell-growth in the presence of tar.

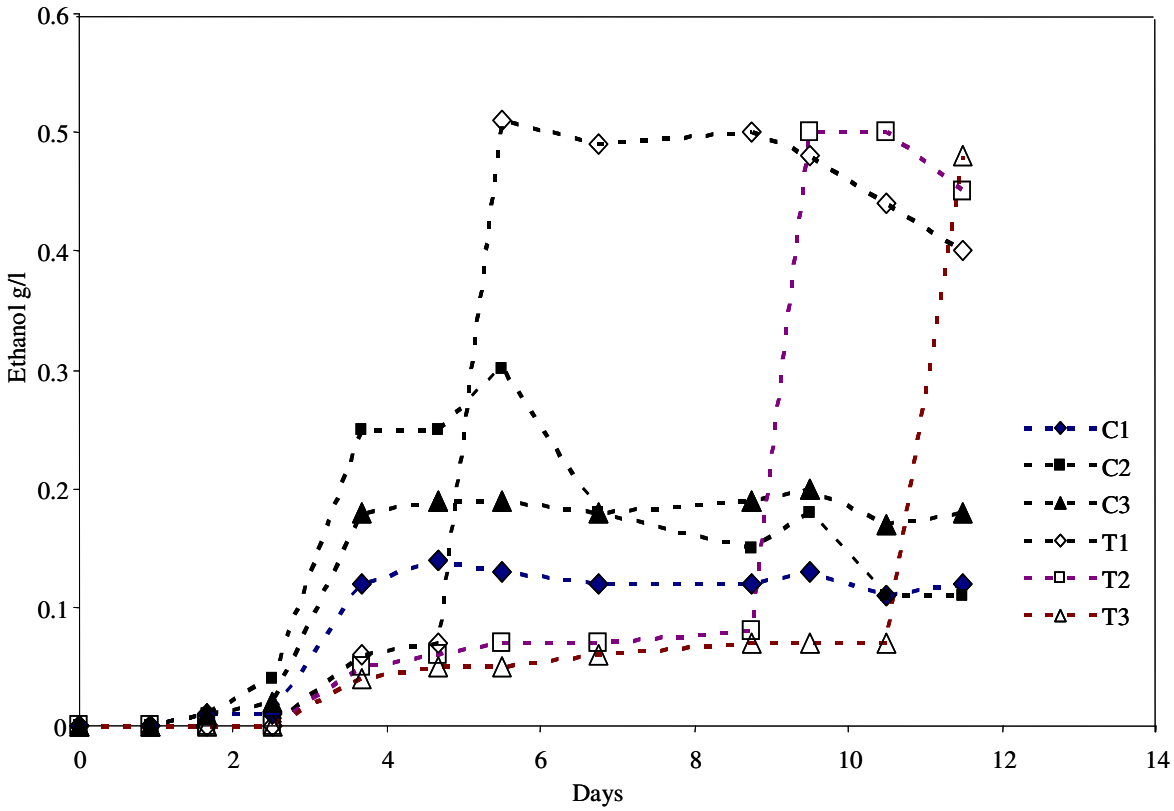

Figure 3.11 Ethanol profile for batch study. C1, C2, C3 are the controls with regular media. T1, T2, T3 contained the acetone solution from the scrubbers with tar. The cells produced more ethanol in the presence of tar.

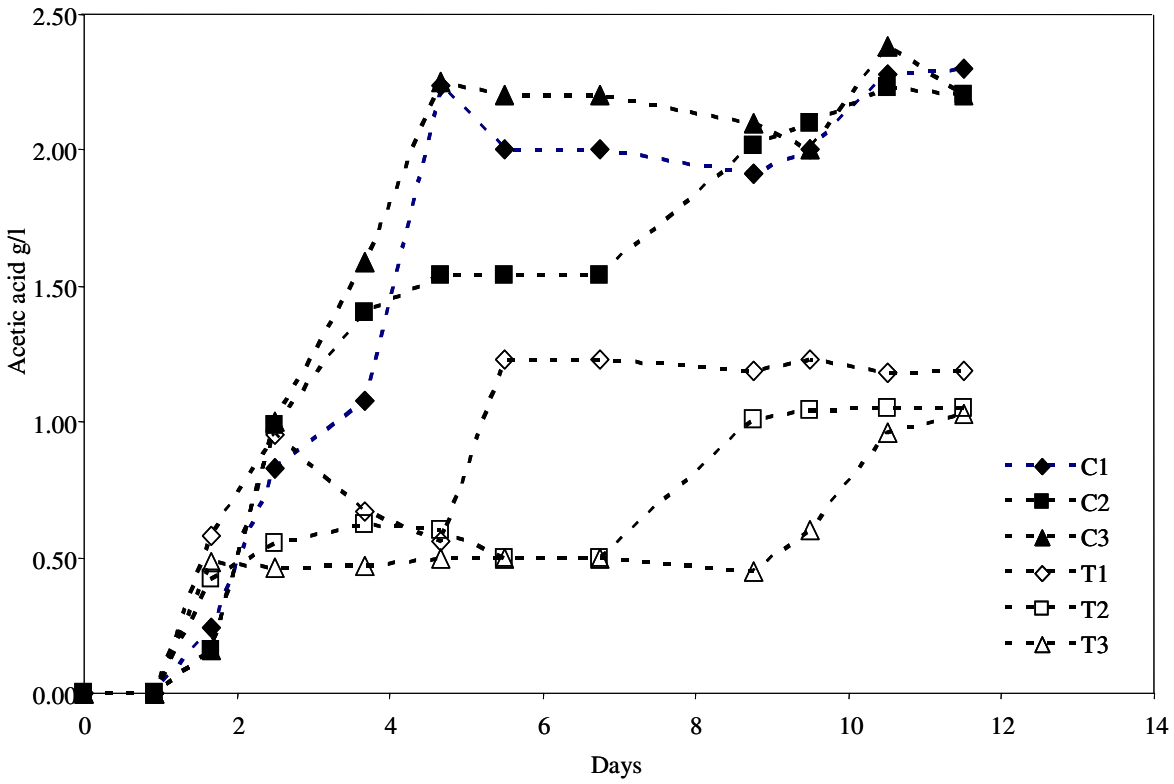

Figure 3.12 Acetic acid profile for batch study. C1, C2, C3 are the controls with regular media. T1, T2, T3 contained the acetone solution from the scrubbers with tar. In the presence of tar, the acetic acid produced by the cells was lower than that of the controls.

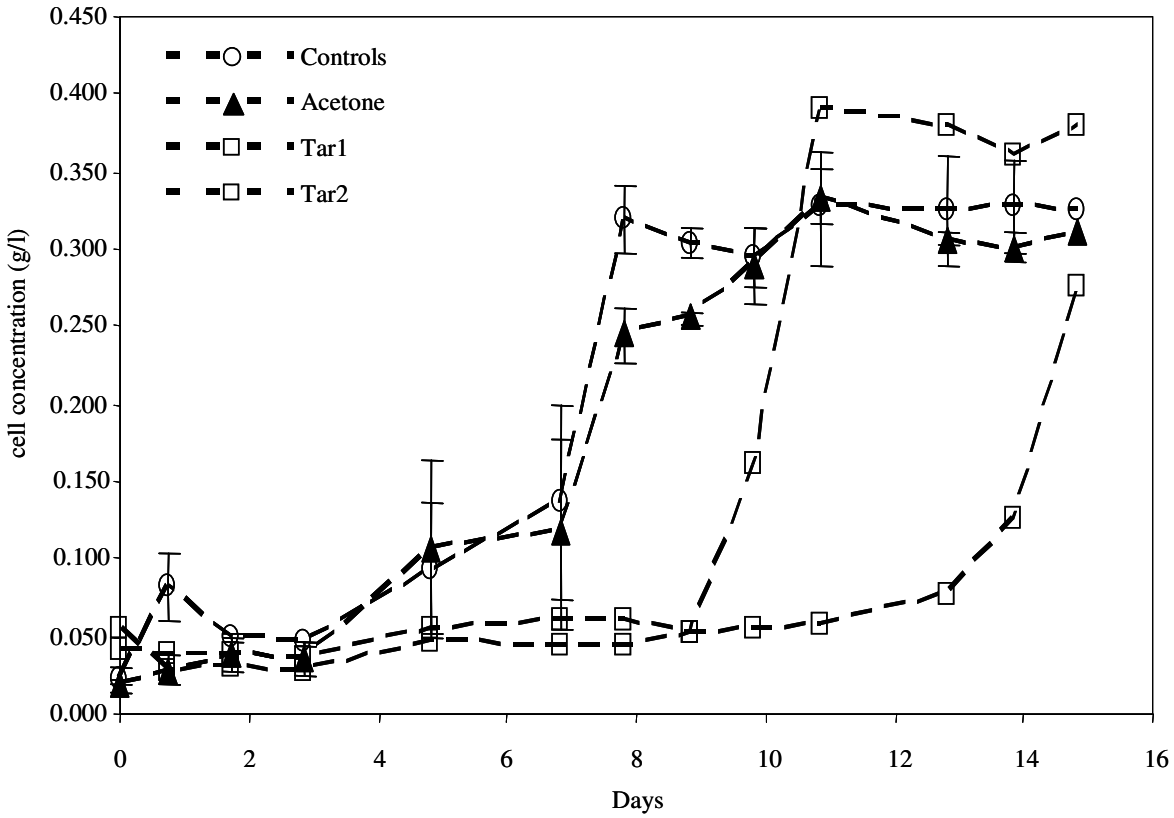

Figure 3.13 Cell concentrations in 100-ml batch studies. The control study contained media. The acetone study contained media supplemented with 1 ml of acetone. The error bars represent the standard error (n=3). The two tar studies contained media supplemented with 1 ml of acetone scrubbing solution used to clean the syngas. As the onset of growth varied upon exposure to the acetone scrubbing solution (tar experiments), the results are shown separately.

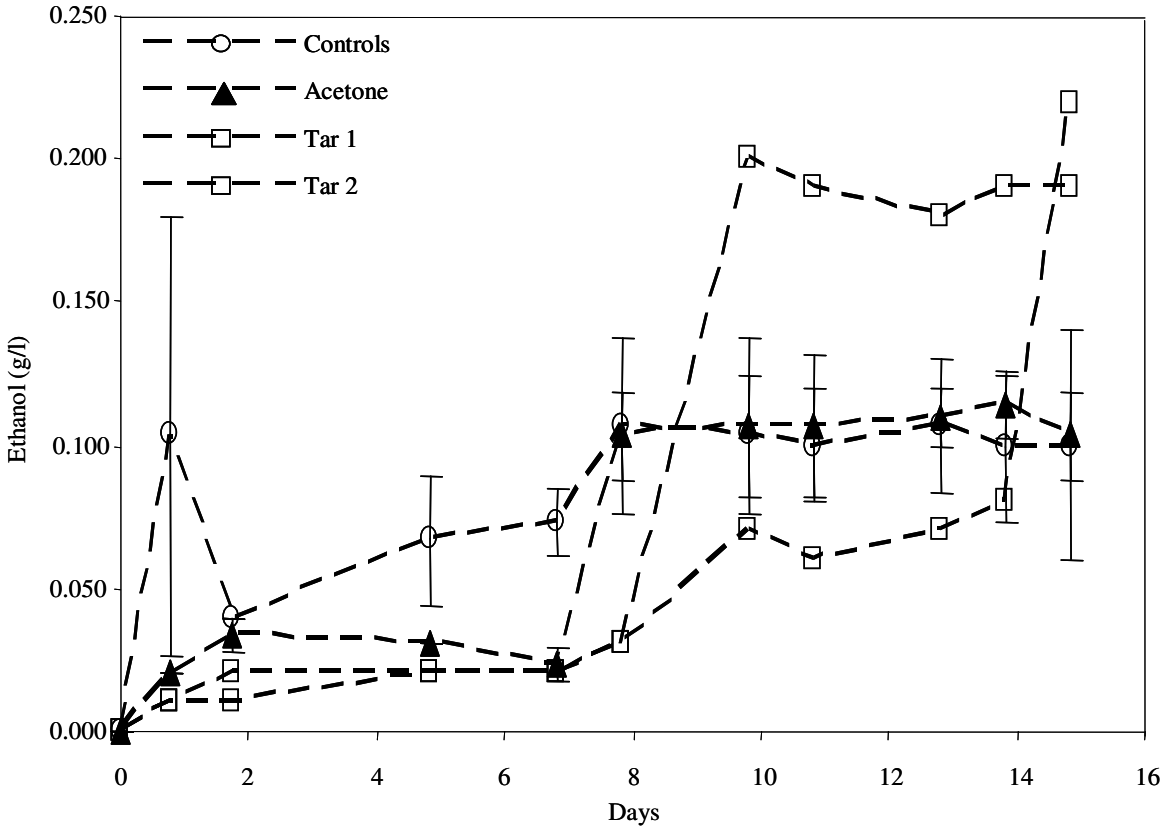

Figure 3.14 Effect of tar on ethanol concentration. The studies are described in Figure 3.13. The error bars represent the standard error (n=3).

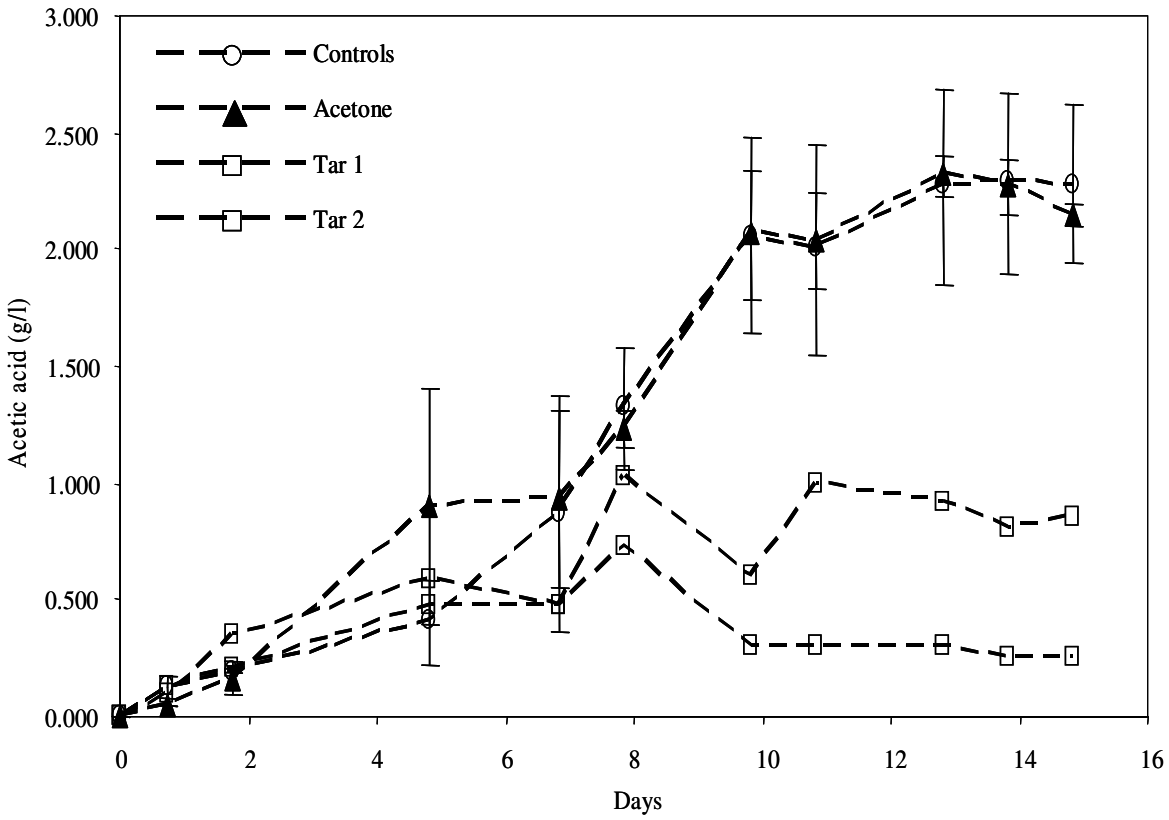

Figure 3.15 Effect of tar on acetic acid concentration. The studies are described in Figure 3.13. The error bars represent the standard error (n=3).

period of time, the cells could adapt to the tars and begin to grow (as observed in batch studies). The adapted growth would not be observable in the chemostat since the washout of cells would occur before the cells had time to adapt.

The cells in the presence of tar produced much lower quantities of acetic acid and much higher amounts of ethanol than the controls once the cells starting growing following adaptation. Thus, there was a change in the product distribution, although these results appear contrary to the results of Figure 3.8 in which the 0.2-µm filter resulted in a decrease in ethanol production and an increase in acetic acid production. However, the cells in the batch studies had a chance to adapt to the tars, unlike the cells in the chemostat studies in which the cells washed out before adaptation. Therefore, the key point is that the tars appear to affect the cell dormancy and product distribution.

3.4 Conclusions

From the batch and chemostat studies conducted, the following results were obtained, which provided insight into the effects of biomass syngas on cell-growth and product distribution of *C. carboxidivorans* $P7^T$:

- Gaseous impurities like ethane, ethylene and acetylene had no effect on cell-growth.
- Additional cleaning of syngas using a 0.025-µm filter prevented growth inhibition although the filter cleaning did not eliminate the hydrogenase inhibition.
- Analysis of the 0.025-µm filter paper indicated that the contaminant causing cell-dormancy was most likely particulate tar.

- Batch studies further confirmed that tars induced cell dormancy. However, cells could adapt and grow in the presence of tars following prolonged exposure.
- Once the cells adapted to and grew in the presence of tar, a redistribution of ethanol and acetic acid production occurred. Cells produced more ethanol and less acetic acid compared to controls.

The extent of gas cleanup is a critical issue when applied to syngas fermentation. Cells are sensitive to many chemical species and the potential for numerous species to be generated during biomass gasification is high. These studies showed that cleaning the syngas with a series of cyclone separators, 10% acetone scrubbing bath, and a 0.025-µm filter enabled the cells to remain viable and produce ethanol and acetic acid. Gas clean-up issues will likely vary depending upon the biomass since some feedstocks contain species, such as sulfur compounds, that may affect cell function in fermentation. Nevertheless, this work identified some key gas clean-up issues (tar removal) for the fermentation of syngas to ethanol and acetic acid.

CHAPTER 4

EFFECT OF CELL-RECYCLE ON SYNGAS FERMENTATION

4.1 Introduction

Previous studies with *C. carboxidivorans* $P7^T$ showed that biomass-generated syngas led to cell washout from a chemostat reactor after a delay of about 1.5 days (Datar et al. 2004). Chapter 3 described the effects of biomass syngas impurities on the microbial catalyst. It was observed that particulate impurities in the biomass syngas caused cell-dormancy, leading to cell-washout from the reactor. Results showed that using a 0.025-µm filter to clean the syngas could eliminate this problem of cell dormancy by removing the tar particles from the gas. Even though this result provided a clear understanding of the underlying cause of cell-dormancy, using a small filter may not be a very practical solution in larger reactor systems with high gas flow rates. Moreover, batch studies with tar showed that on prolonged exposure, cells could adapt and grow in the presence of tar. In a chemostat, cells could not grow on biomass-syngas as they washed out of the reactor before they had an opportunity to adapt. This led to the hypothesis that, if the cells were contained within a continuous system while being exposed to biomass-syngas, they would be able to adapt and grow. This could be done using a cell-recycle system, where the cells would be recycled to the reactor during a continuous bioreactor run. A cell-recycle system would serve several

purposes including the elimination of the 0.025-µm filter. Cell-recycle has been commonly used to increase cell-mass and to enhance product yields (Amartey 1999; Bull and Young 1981; Chang et al. 1994; Parekh and Cheryan 1994). Klasson et al. (1993) reported that the use of cell-recycle during the fermentation of syngas by *C. ljungdahlii* resulted in cell-concentrations of about 4g/l and ethanol concentrations as high as 48 g/l. These values were approximately 2.5 times higher than those without cell-recycle.

Using membrane filters for cell-recycle also has the advantage of a cell-free harvest solution that does not require any additional clarification before the final separation (van Reis and Zydney 2001). The work reported in this chapter describes the effects of using cell-recycle during the fermentation of biomass-syngas by *C. carboxidivorans* $P7^T$. The objective of the study was to test the hypothesis that the cells could adapt to biomass-syngas in a chemostat and that the cell-density in the reactor could be increased using a cell-recycle system.

4.2 Materials and Methods

4.2.1 Biomass and Syngas

Syngas was obtained by gasification of switchgrass, as discussed in Section 3.2.1. The biomass syngas used in the first study was generated by air-gasification of switchgrass, and consisted of approximately 16.9 % CO, 15.8 % CO_2, 5.1% H_2, and 55.2 % N_2 along with 4.2% CH_4, 0.16% C_2H_2, 0.46% C_2H_6, 1.9 % C_2H_4 and 140 ppm nitric oxide (compositions based on measured species). In the second study, the biomass syngas used in stage 3A was the same as that used in study 1. In stage 3B, a second batch of air-gasified biomass syngas was used, which consisted of approximately 16.3 % CO, 15.2 %

CO_2, 4.8 % H_2, and 57.8 % N_2 along with 3.7% CH_4, 0.12% C_2H_2, 0.2% C_2H_6, 1.7 % C_2H_4 and 150 ppm NO. In stage 3C, steam-gasified biomass syngas was used, which consisted of approximately 31 % CO, 19.8 % CO_2, 32.7 % H_2, and 1.04 % N_2 along with 4.2% CH_4, 0.15% C_2H_2, 0. 6% C_2H_6 and 3.5 % C_2H_4 and 140ppm NO

During the scrubbing of the second batch of air-gasified biomass syngas for tar removal, there was a mechanical failure in the scrubbing system causing the temperature in the scrubbers to increase, thereby preventing some of the lower boiling point compounds from condensing. At the end of the study, the gas was bubbled through acetone and the acetone was then tested on a Gas Chromatograph and Mass Spectrometer (GCMS) for tar. The concentration of tar in this batch of gas was approximately 0.33 g/Nm^3, while the tar in the third batch of biomass syngas (generated from steam gasification) was approximately 0.14 g/Nm^3. The gas clean-up was comparable for the first and third batches of biomass syngas, as the scrubbing system worked satisfactorily. The second batch of syngas contained higher tar levels compared to the third. The tar could not be measured in the first batch of biomass syngas as the gas was completely utilized by the bioreactor during the study.

4.2.2 Microbial Catalyst and Culture Medium

C. carboxidivorans $P7^T$ was used as the microbial catalyst for the fermentation of syngas. The bacterium was grown in a culture medium consisting of minerals, vitamins and trace metals, as described in Section 4.2.2.

4.2.3 Bioreactor and Cell-Recycle Set-up

A BioFlo 110 Benchtop Fermentor (New Brunswick Scientific, Brunswick, NJ) with a 3-l working volume was used for the fermentation studies involving continuous liquid feed and product removal (i.e. chemostat mode). The reactor and its components are described in Section 3.2.3. The experimental setup is shown in Figure 4.1. The bioreactor was connected to two 0.2-µm hollow fiber membrane filters with a surface area of 1200 cm^2 (CSP-2-E-5A, A/G Technology Corporation, 101 Hampton Ave, Needham MA) in parallel for cell-recycle. However, only one filter was used at a time. The other filter was in reserve in case the filter in use became clogged. The recycle filters consisted of a bundle of parallel polysulfone fibers within a plastic housing and operated in a cross-flow mode, which allowed for recirculation of the feed stream.

Before use, the recycle filters were soaked in 70% ethanol for 1 hour, rinsed with DI water and then 0.5N sodium hydroxide was circulated through them at 50 ºC for 1 hour. Finally, the recycle filters were once again rinsed with DI water. The recycle filters and the bioreactor were connected, filled with media, and then autoclaved at 121°C for 20 minutes. The reactor was then sparged with nitrogen to remove the dissolved oxygen, after which the gas feed was changed from N_2 to synthetic syngas flowing at 160 cm^3 min^{-1}, at 25°C and 137 kPa. A mass flow controller was used to mix bottled gases in the same composition as the CO, CO_2, and H_2 in the biomass-syngas to obtain the synthetic syngas. The impellor agitation was set to 400 rpm and the temperature was maintained at 37°C. Cysteine-sulfide was then added to the media to remove any residual dissolved oxygen. Once it was ensured that the media and bioreactor were anaerobic,

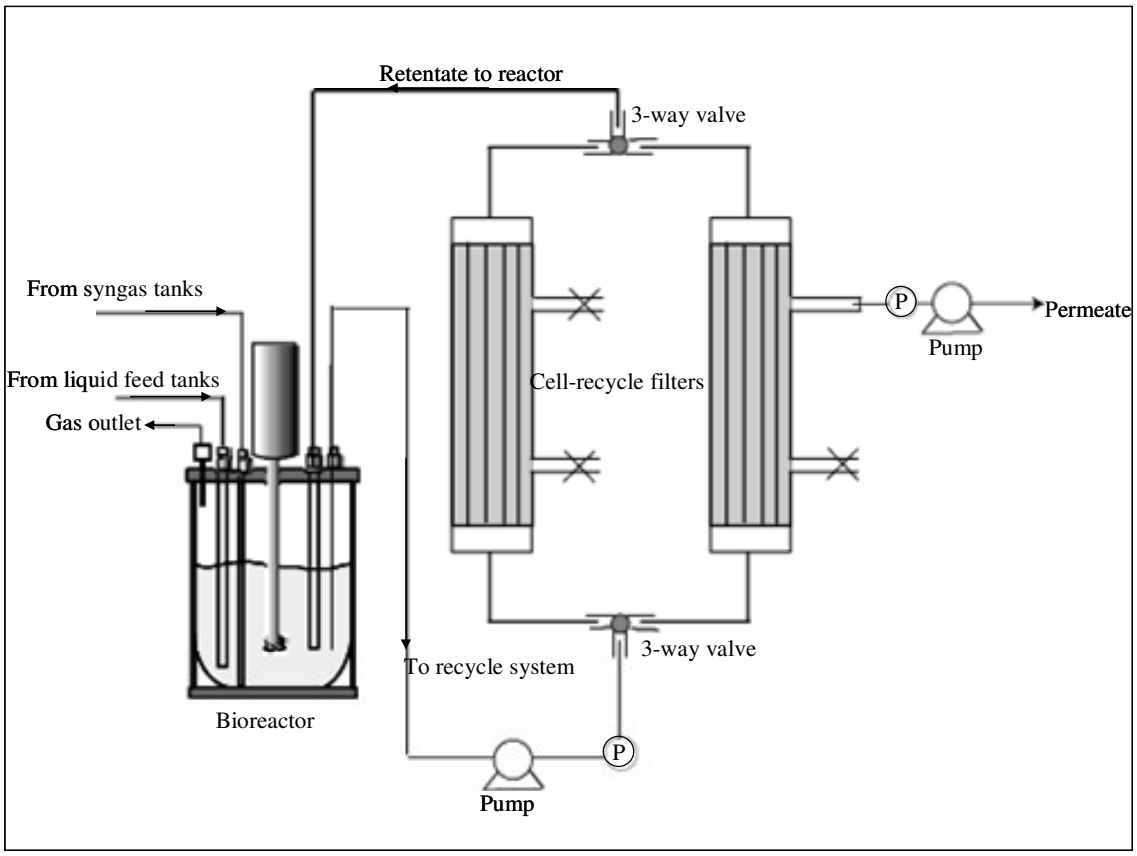

Figure 4.1 Schematic of the bioreactor set-up with cell-recycle. The gas and liquid feed sources are not shown in the figure, but were similar to those described in Chapter 3.

30 ml inoculum of *C. carboxidivorans* $P7^T$ was added to the reactor under sterile conditions.

The bioreactor was connected to two liquid feed tanks containing sterile media for chemostat operation. The liquid feed tanks were continuously purged with nitrogen to maintain anoxic conditions. A 4-way valve was used to introduce gas feed by switching between biomass-syngas and synthetic syngas (not shown in the figure). The gas was introduced through a sparger.

An external pump was used to circulate the reactor broth through the recycle filter at about 60 ml/min. A 3-way valve connected the two filters in parallel to allow for switching between them in case of clogging. This valve was also used as a sampling port to measure cell density when the recycle system was in operation. When the reactor broth was pumped through the filter, the retentate stream (containing cells) continued through the recirculation loop and returned to the reactor, while the permeate stream (without cells) was pumped at the same flow rate as the feed and collected in a reservoir. A pressure gauge at the inlet of the recycle filter and a vacuum gauge on the permeate line were used to monitor clogging. If the cells started to clog the recycle filter, it could either lead to a pressure build-up at the inlet (since a higher force would be required to pump the broth through) or a vacuum on the permeate line (to pull the permeate out of the recycle filter). Thus, the two gauges were closely monitored to ensure there was no such clogging in the recycle filter.

4.2.4 Bioreactor Operation

Two studies were performed to assess the effect of cell-recycle on syngas fermentation. In both studies, the bioreactor operation was divided into three stages. In all stages, the gas flow was continuous. In the first stage, the liquid was maintained in batch mode and the synthetic syngas was fed to the bioreactor (stage 1). As soon as cell-growth commenced, continuous feed and product removal with cell-recycle were initiated (stage 2). Before connecting the bioreactor to the cell-recycle, the filter was purged with sterile, anaerobic media for a few minutes. Stage 3 was initiated when the cells reached the stationary growth phase, and the gas feed was switched from synthetic syngas to biomass syngas.

In the second study, the first two stages were similar to the first study. Stage 2 was initiated on day 3.6. On day 9.5, air-gasified biomass syngas was introduced into the reactor (stage 3A). This gas was almost completely consumed in this stage and a fresh batch of air gasified biomass syngas was prepared and filled in the storage tanks. Stage 3B was initiated on day 25, when this new batch of biomass syngas was introduced into the reactor. On day 37.5, the gas source was switched once again, and steam-gasified biomass syngas was introduced into the reactor. This final stage is called stage 3C in the results and discussion.

4.2.5 Analytical Methods

The optical density (OD), which is proportional to the cell concentration (~ 0.43 g L^{-1} per OD unit (Datar 2003)), was determined using a UV-Vis spectrophotometer. Cell samples were collected in 4-ml cuvettes from the bioreactor and the OD was measured at

660 nm. A standard calibration chart was used within a linear range of 0 to 0.4 OD units to estimate the cell concentration. Samples with an OD greater than 0.4 units were diluted so that the OD was within the linear range of calibration. Gas samples were taken from the outlet and inlet lines of the bioreactor in gas tight syringes. Gas compositions for the chemostat were determined using a gas chromatograph (3800 series, Varian Co., CA) with a Hayesep-DB column (Hayes Separations Inc, Bandera, TX) connected to a thermal conductivity detector (TCD) with argon as the carrier gas. The TCD was run at 40 ºC for 6 minutes, after which the temperature was ramped up to 140 ºC at 100 ºC min^{-1} for 20 minutes.

The liquid samples were centrifuged at 1,300 x *g* for 30 minutes. The cell free supernatant was collected and then frozen at -18 ºC until further analysis. The liquid products were analyzed for ethanol and acetic acid using a 6890 Gas Chromatograph (Agilent Technologies, Wilmington, DE), equipped with a flame ionization detector and an AT-treated steel 8-ft Porapak QS 80/100 column (Alltech, Deerfield, IL).

4.3 Results and Discussion

4.3.1 Chemostat Study 1 – Cell Growth

Figure 4.2 shows the cell concentration profile from the first study. In the first stage, when the reactor was operated in a batch mode with synthetic syngas, cells began to grow after a delay of about 2.5 days. As soon as cell growth commenced, stage 2 was initiated as described in Section 4.2.4. In this stage, fresh media was introduced at a flow rate of 0.6 ml/min (i.e., dilution rate, D=0.012 hr^{-1}). The outlet

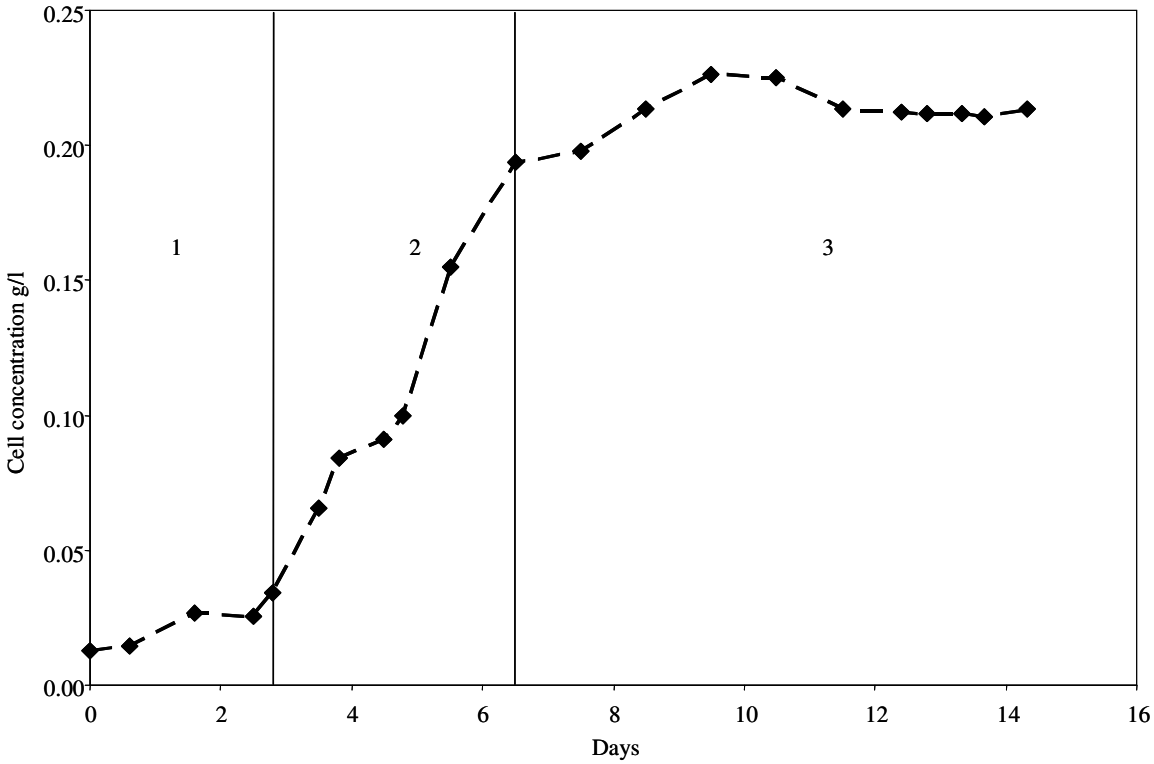

Figure 4.2 Cell-growth profile during syngas fermentation. Stage 1 represents batch liquid mode with synthetic syngas; stage 2 represents continuous liquid with recycle and synthetic syngas feed; stage 3 represents continuous liquid feed with recycle and biomass-syngas feed.

stream from the bioreactor was pumped through the filter such that the cells were recycled to the bioreactor. However, the filter had not been completely deoxygenated and this introduced oxygen into the reactor, which was indicated by the dissolved oxygen probe. At this point, in order to hasten the oxygen removal from the reactor, the liquid feed rate was increased to about 0.9 ml/min ($D = 0.018\ hr^{-1}$). The oxygen concentration in the reactor subsequently decreased to zero after approximately 0.5 day and the cells kept growing.

During stage 2, the cell concentration increased from 0.03 g/l to about 0.19 g/l, after which biomass-syngas was introduced to the reactor. At this point, the cell concentration remained steady at a value of approximately 0.22 g/l. Since this study involved cell-recycle, a steady cell-concentration indicated that there was no cell-growth or cell-death. These results are similar to the previous studies (without a 0.025-µm filter) when biomass-syngas caused the cells to stop growing after about 1.5 days (see Chapter 3, section 3.3.2).

4.3.2 Chemostat Study 1 – pH Changes

Figure 4.3 shows the pH profile. The pH of the media at the beginning of the fermentation was 5.96. The pH controller was set at 5.6 with a deadband of 0.4 such that the pH would be controlled between 5.2 and 6.0. The pH dropped to about 5.9 in stage 1, and then to about 5.2 in stage 2. After switching to biomass-syngas, the pH increased (as seen in previous studies) and reached a value of about 5.7 at the end of the experiment. The rise in pH was seen previously in the presence of biomass-syngas.

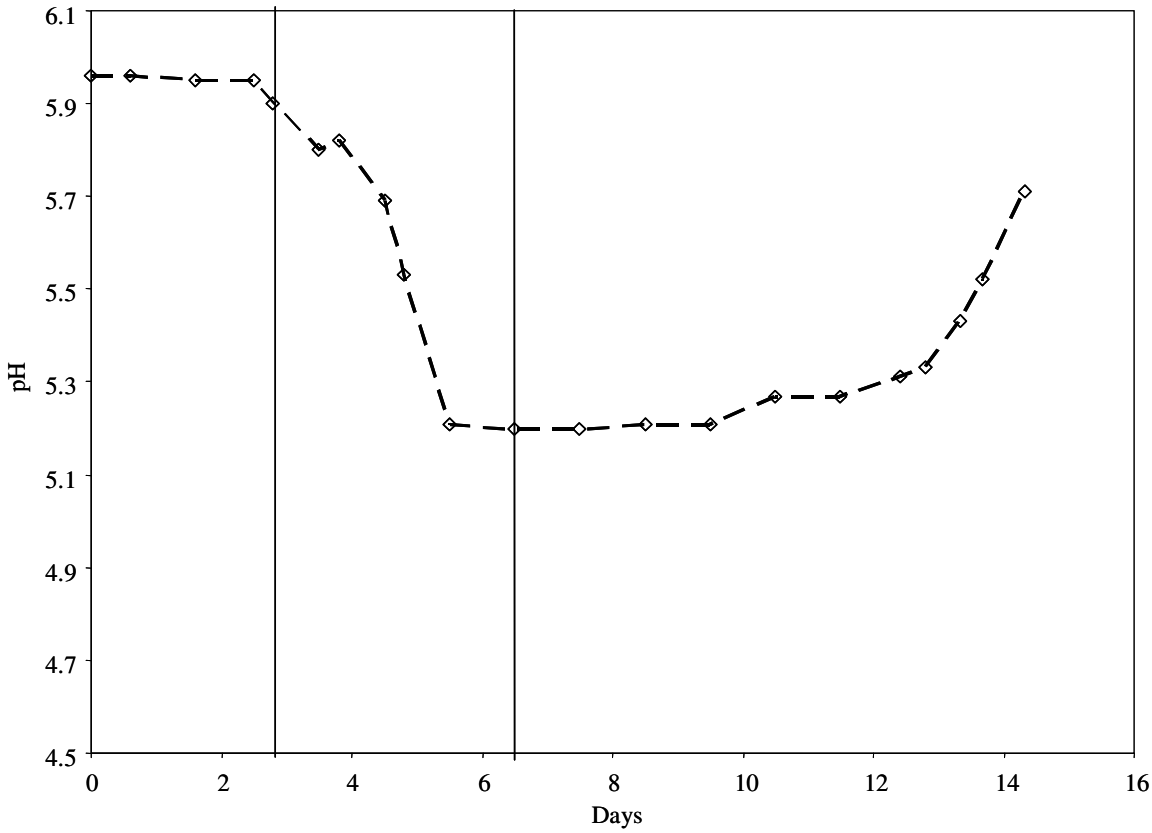

Figure 4.3 pH profile during syngas fermentation with cell-recycle. Stages 1, 2 and 3 are described in Figure 4.2.

4.3.3 Chemostat Study 1 – Product Profile

The ethanol and acetic acid profiles are shown in Figure 4.4. The ethanol and acetic acid concentrations were at a minimum in stage 1 as cell-growth had not commenced. In stage 2, the ethanol concentration increased to about 0.1 g/l, while acetic acid increased to about 1.16 g/l. Once the biomass-syngas was introduced, the ethanol concentration dropped slightly and reached a steady concentration of 0.09 g/l, while the acetic acid increased to approximately 2.2 g/l. This result was contrary to the previous results observed with biomass-syngas. In previous studies, switching to biomass-syngas increased the ethanol concentration and decreased the acetic acid concentration. However, the previous studies were conducted without the use of a cell-recycle and at lower dilution rates (D=F/V). In this study, due to the initial problems with oxygen, the dilution rate was set at a high value of 0.018 hr^{-1} (the growth rate μ was 0.014 hr^{-1}). Even though the dilution rate was higher than the maximum growth rate of cells, the cells remained within the reactor because of the cell-recycle. However, a high dilution rate implies a high media flow rate such that the cells were being supplied with fresh nutrients faster. This could have led to the increased acetic acid formation since these microorganisms are known to make acetic acid under favorable and ethanol under unfavorable conditions. Studies have shown that changes in the dilution rate can lead to a change in the product distribution (Amartey 1999; Qureshi et al. 2000). Qureshi et al. observed a similar effect of increased acid production at high dilution rates.

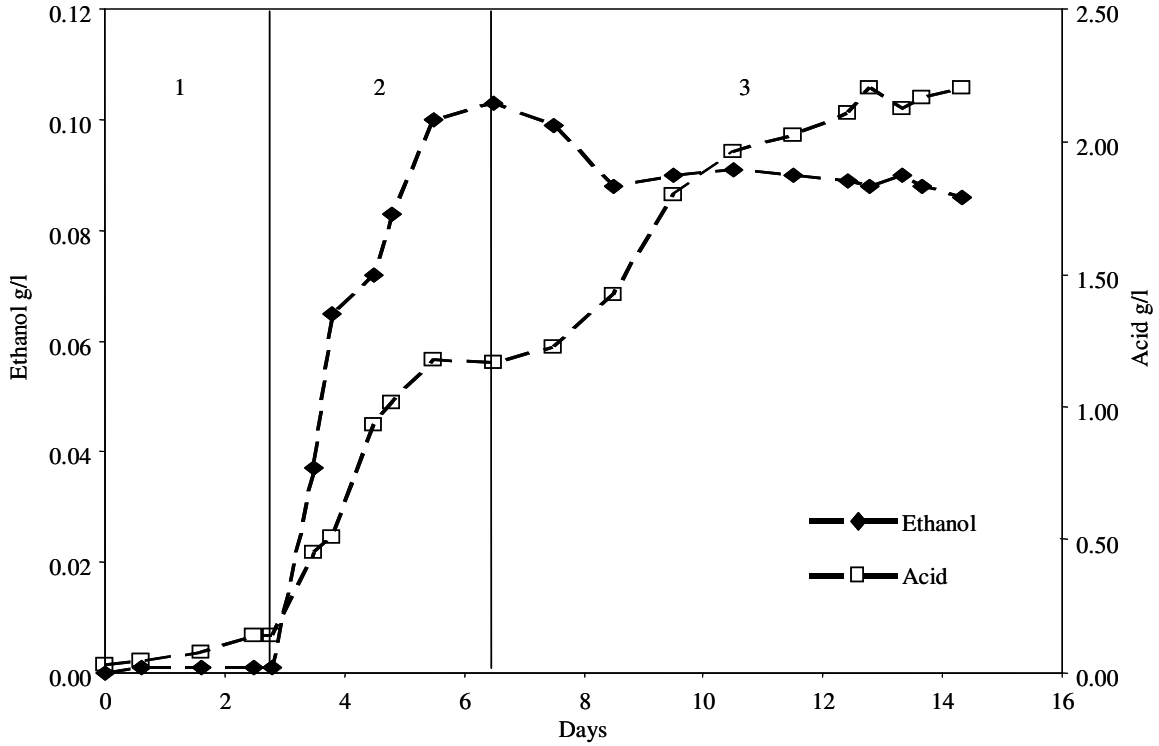

Figure 4.4 Product profile during syngas fermentation with cell-recycle. The stages 1, 2 and 3 are described in Figure 4.2.

4.3.4 Chemostat Study 2 – Cell Growth

A second study was conducted with cell-recycle. The cell-growth profile of this study is shown in Figure 4.5. Quantity of cells (g) is plotted at each time point in this figure to give an accurate measure of cell-growth and account for volume loss due to sampling for an extended period of time. In stage 1, the bioreactor was operated in batch liquid mode, with a continuous flow of synthetic syngas. The amount of cells in the reactor increased from 0.05 to 0.23 g in this stage. Once the cells started growing, stage 2 was initiated, which involved continuous feed and product removal with cell-recycle. A flow rate of 0.6 ml/min was used in this study. Unlike the previous study, recycle filter was flushed with anaerobic media thoroughly, eliminating the possible oxygen contamination. The cell mass increased to 0.54 g in this stage. On day 9.5, biomass-syngas was introduced into the reactor (stage 3A). As observed previously, the cells stopped growing at this point with cell concentration remaining steady. However, after about 7 days of this state of no-growth, the cells started to grow on biomass-syngas. This indicated that the cells had adapted to the gas since they were prevented from being washed out by the cell-recycle. On day 23.5, the cell mass in the reactor had reached approximately 0.8 g. At this point, the biomass-syngas was almost completely utilized and needed to be re-filled in the storage tanks. A new batch of biomass-syngas was then introduced into the reactor on day 25 (stage 3B). The cells continued to grow for another 3 days, but then stopped growing once again, reaching a steady value of about 1 g. After another 4 days, the cell mass started decreasing in the reactor indicating some cell-death. This effect could be attributed to the fact that the second batch of biomass-syngas had

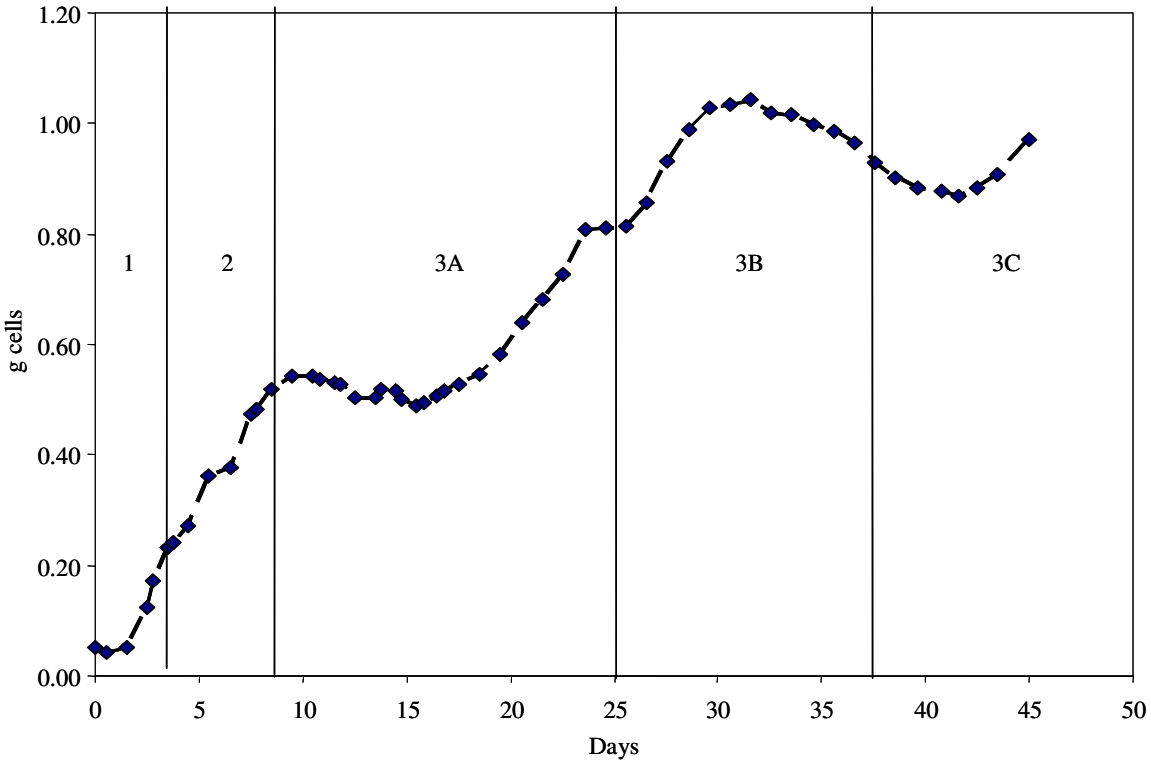

Figure 4.5 Cell-growth profile during syngas fermentation with cell-recycle. Cell mass (g) is shown in this figure. Stage 1 represents batch-liquid mode and synthetic syngas feed; stage 2 represents continuous liquid mode with cell-recycle and synthetic syngas feed; stage 3A represents continuous liquid mode with cell-recycle and biomass-syngas; stage 3B represents continuous liquid mode with cell-recycle and biomass-syngas (re-filled); stage 3C represents continuous liquid mode with cell-recycle and steam-gasified biomass-syngas.

higher amounts of tar than the first. As mentioned in Section 4.2.1, the second batch of air-gasified biomass syngas contained higher tar levels due to a problem during gas cleaning. Thus, the cells could have adapted to a certain amount of tar in the syngas in stage 3A, but when they were exposed to higher amounts of tar, cell-dormancy was induced once again. On day 37.5, the gas feed was again switched to biomass-syngas generated from steam-gasification of switchgrass (as opposed to air-gasification used previously), indicated by stage 3C. On day 41.5, the cells started growing again as shown in the figure.

These results indicated that cells could adapt and grow on biomass-syngas if exposed for an appropriate length of time. It is likely that if the syngas used in stage 3B had been similar to that used in stage 3A (in terms of tar concentrations), cell concentration could have increased significantly due to the use of cell-recycle. This was also indicated by the fact that cell-growth resumed in stage 3C when the gas source was changed to the steam-gasified biomass syngas with lower tar concentrations (less than half the tar concentrations of the syngas used in stage 3B, as reported in Section 4.2.1).

4.3.5 Chemostat Study 2 – pH Profile

Figure 4.6 shows the pH profile of the cells. The pH at the beginning of the experiment was about 5.9. In the first stage, the pH controller was set at 5.6 with a

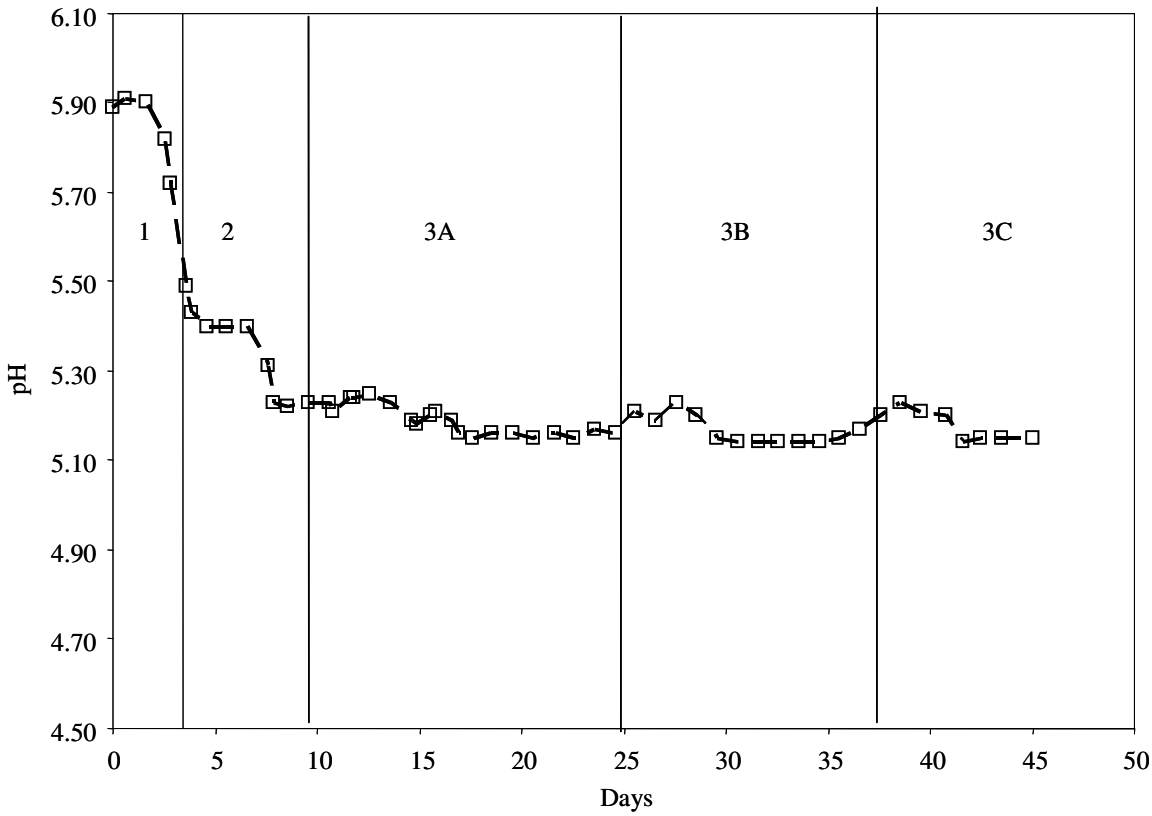

Figure 4.6 pH profile during syngas fermentation with cell-recycle. The stages are described in Figure 4.5.

deadband of 0.4 so that it would not increase above 6.0 or decrease below 5.2. The pH dropped to about 5.5 in the first stage and 5.22 in the second stage. After this stage, the pH was controlled at 5.2 (deadband of ±0.05) throughout the rest of the study.

4.3.6 Chemostat Study 2 – Product Profile

Figure 4.7 presents the product profile of the cells during syngas fermentation. To provide a better understanding of the rates of production of ethanol and acetic acid during the various stages of fermentation, the following analysis was performed, similar to that in Chapter 3. Equation 4.1 represents the transient mass balance for a product P (g L^{-1}) in a well-mixed chemostat:

$$\frac{dP}{dt} = q_P X - DP \tag{4.1}$$

where X is the cell concentration (g L^{-1}), q_p is the product formation rate per cell mass [g (g cells)$^{-1}$ time^{-1}] and D is the dilution rate [time^{-1}]. Time differentiation of (P/X) shows

$$\frac{d(P/X)}{dt} = \frac{X\frac{dP}{dt} - P\frac{dX}{dt}}{X^2} \tag{4.2}$$

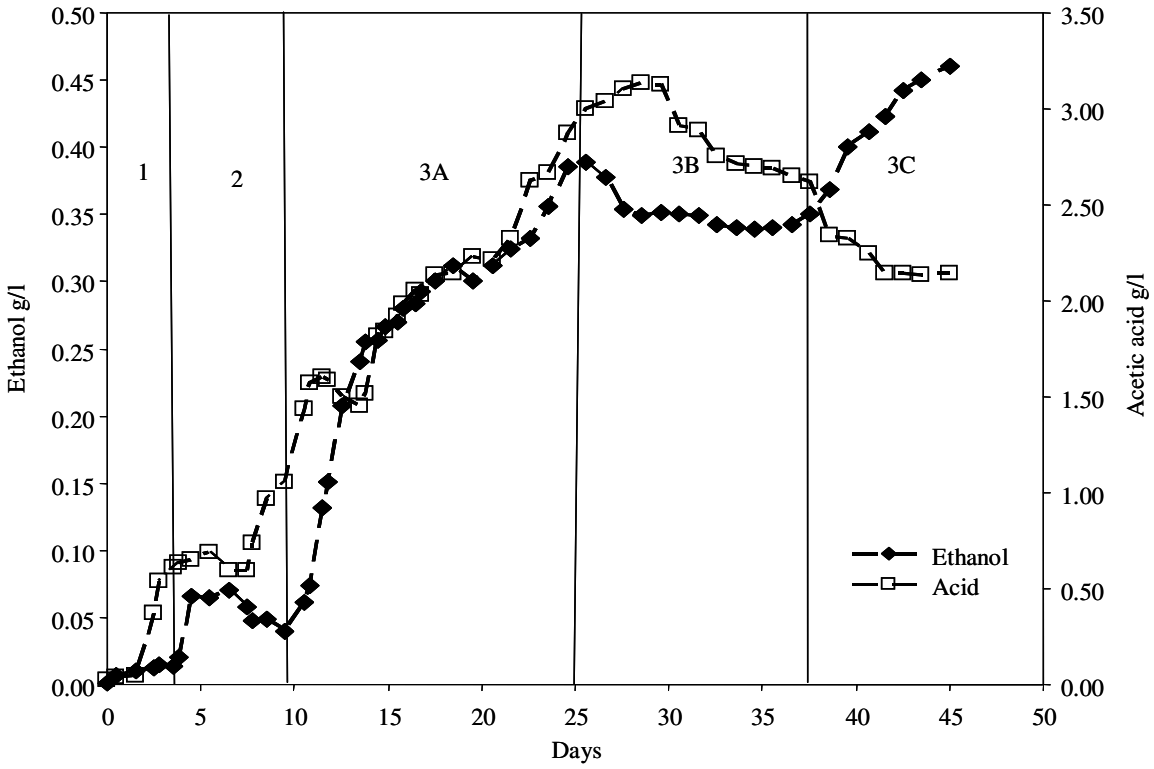

Figure 4.7 Product profile during syngas fermentation with cell-recycle. The stages are described in Figure 4.5.

Substitution of Equation 4.1 into Equation 4.2, with some re-arrangement, gives Equation 4.3

$$q_P = \frac{d(P/X)}{dt} + \frac{P}{X^2}\frac{dX}{dt} + D\left(\frac{P}{X}\right) \tag{4.3}$$

In the first stage, the ethanol concentration increased to about 0.015 g/l while the acetic acid increased to 0.6 g/l. When the continuous liquid mode was initiated, ethanol concentration increased to approximately 0.066 g/l and remained almost steady until dropping slightly to about 0.05 g/l towards the end of stage 2. On the other hand, in stage 2, the acetic acid increased further to 1 g/l, likely due to the fresh incoming media and product removal in this stage. In stage 2, q_p for ethanol was calculated from Equation 4.3 to be approximately 0.0015 g (g cells)$^{-1}$ hr^{-1}, while that for acetic acid was approximately 0.015 g (g cells)$^{-1}$ hr^{-1}.

On Day 9.5, biomass-syngas was introduced into the bioreactor. In this stage (3A), ethanol concentration increased significantly from 0.05 g/l to approximately 0.39 g/l. The q_p increased more than 10-fold to about 0.02 g (g cells)$^{-1}$ hr^{-1} during the non-growth phase. However, when the cells adapted to the biomass-syngas and resumed their growth, the rate of production of ethanol decreased to approximately 0.008 g (g cells)$^{-1}$ hr^{-1}. This is due to the bi-phasic metabolism of acetogens described in Chapter 2. Since ethanol is a non-growth related product, much more ethanol is produced when there is little or no cell-growth and high amounts of acetic acid are produced during the active growth phase of these cells.

The rate of acetic acid production increased from 0.015 g (g cells)$^{-1}$ hr^{-1} to approximately 0.02 g (g cells)$^{-1}$ hr^{-1} when the cells stopped growing in stage 3A, after

which it remained steady until cell-growth resumed. Acetic acid then increased further to about 0.035 g (g cells)$^{-1}$ hr^{-1} and then stabilized at 0.03 g (g cells)$^{-1}$ hr^{-1} at the end of this stage.

When the second batch of biomass-syngas was introduced on Day 25, the production rates of both ethanol and acetic acid dropped, along with the cessation of cell-growth. Even though the ethanol concentration seemed to remain constant at about 0.35 g/l, the rate of production, q_p decreased to 0.003 g (g cells)$^{-1}$ hr^{-1}. In this stage, the acetic acid concentration decreased to 2.65 g/l and the rate of acid production decreased to 0.02 g (g cells)$^{-1}$ hr^{-1}. These effects on cell-growth and product rates indicated that the levels of tar in the biomass-syngas were probably a lot higher than the tolerable levels for the bacteria.

In stage 3C, syngas obtained from the steam gasification of biomass was introduced into the reactor. In this stage, the ethanol concentration increased from 0.35 g/l to 0.46 g/l. The rate of production of ethanol increased slightly to about 0.005 g (g cells)$^{-1}$ hr^{-1}. The acetic acid concentration decreased further to about 2.2 g/l and the rate of acid production dropped to 0.015 g (g cells)$^{-1}$ hr^{-1} in this stage. The biomass-syngas used in this stage contained higher amounts of carbon monoxide and hydrogen. This could account for the increase in ethanol concentration, along with the fact that the gas-cleaning in this case was comparable to that of the gas used in stage 3A. However, the drop in the acetic acid concentration cannot be completely explained.

4.4 Conclusions

The studies described in this chapter showed that the fermentation of biomass-syngas can be successfully carried out using a cell-recycle system. This method also eliminates the need for additional cleaning of biomass syngas (like the use of a 0.025-µm filter) and allows the cells to adapt to biomass-syngas. Study 2 was the first chemostat experiment wherein cell-growth was observed in the presence of biomass-syngas. To summarize, the following effects were observed during the fermentation of syngas using a cell-recycle system.

- The cells could adapt and grow on biomass-syngas after prolonged exposure
- The use of cell-recycle increased the cell concentration significantly and allowed for longer fermentation times
- The rate of ethanol production was highest in the presence of biomass-syngas during the non-growth phase of the cells while the rate of acetic acid production was the highest during the active growth-phase of the cells.
- Dilution rates during the fermentation had an effect on product distribution. In the presence of biomass-syngas, lower dilution rates caused higher amounts of ethanol production compared to higher dilution rates.

CHAPTER 5

EFFECTS OF NITRIC OXIDE AND CARBON MONOXIDE ON CELL-GROWTH, HYDROGENASE ACTIVITY AND PRODUCT DISTRIBUTION

5.1 Introduction

Unlike synthetic syngas, biomass syngas can also contain additional constituents including methane, some higher hydrocarbons, tars, ash, and char particles as a result of the gasification process (Bridgwater 1994). An understanding of the potential contaminants on the fermentation process is essential for assessing the degree to which biomass-generated syngas must be cleaned. Recent work showed that syngas had certain effects on the fermentation process, including cell-dormancy, shutdown of hydrogen consumption, and product redistribution between ethanol and acetic acid (Datar et al. 2004). The studies described in chapter 3 showed that cell dormancy can be overcome by cleaning the biomass gas with a 0.025-µm filter, but not the traditional sterilization filter size of 0.2-µm. Filter analysis showed the capture of small particulates that appeared to be tars. Further analysis demonstrated that tars indeed delayed cell growth. However, use of the smaller filter did not prevent the shutdown of hydrogen consumption by the cells. The hypothesis was that a gaseous species permeating through the filter was responsible for the shutdown of hydrogen consumption. *C. carboxidivorans* $P7^T$ uses the Acetyl-CoA pathway to convert CO, CO_2 and H_2 into biomass, ethanol, acetic acid and

other products. Figure 5.1 shows a brief diagram of the Acetyl-CoA pathway in which CO and CO_2 are converted to acetyl-CoA (Ragsdale 1991). The electrons required for this conversion are obtained from H_2, via the hydrogenase enzyme, or from CO, via the carbon monoxide dehydrogenase (CODH) enzyme. If the hydrogenase enzyme is inhibited, cells cannot consume H_2 which means the electrons must come from CO. This scenario is inefficient for ethanol production since the CO is sacrificed for electrons rather than used for product formation. Therefore, it is important that the cause of the shutdown of hydrogen consumption, via hydrogenase inhibition, is assessed so that the fermentation process can be designed to utilize hydrogen from biomass-generated syngas.

Gases like O_2, acetylene, CO, and nitric oxide (NO) are known inhibitors of hydrogenase (Acosta et al. 2003; Byung Hong Kim 1984; Krasna 1954; Seefeldt and Arp 1989; Tibelius and Knowles 1984). Studies have shown NO to inhibit hydrogenase activity in *Azotobacter vinelandii*(Hyman and Arp 1991), *Proteus vulgaris* (Krasna 1954), *Alcaligenes eutrophus* (Hyman MR 1988) and *Azospirillum brasilense* (Tibelius and Knowles 1984). Hyman and Arp (1991) performed a kinetic analysis of the interaction of NO with hydrogenase in *A. eutrophus* although the studies were performed with NO concentrations above 1 µM. Moreover, a complete kinetic analysis on the interaction of NO with clostridial hydrogenase has not been performed. Approximately 140-150 ppm of NO was detected in the biomass-generated syngas using a chemiluminescence analyzer. Though pure gasification processes theoretically contain ammonia (Devi et al. 2003) rather than NO, the presence of NO in the syngas could be due to some pockets of combustion within the gasifier.

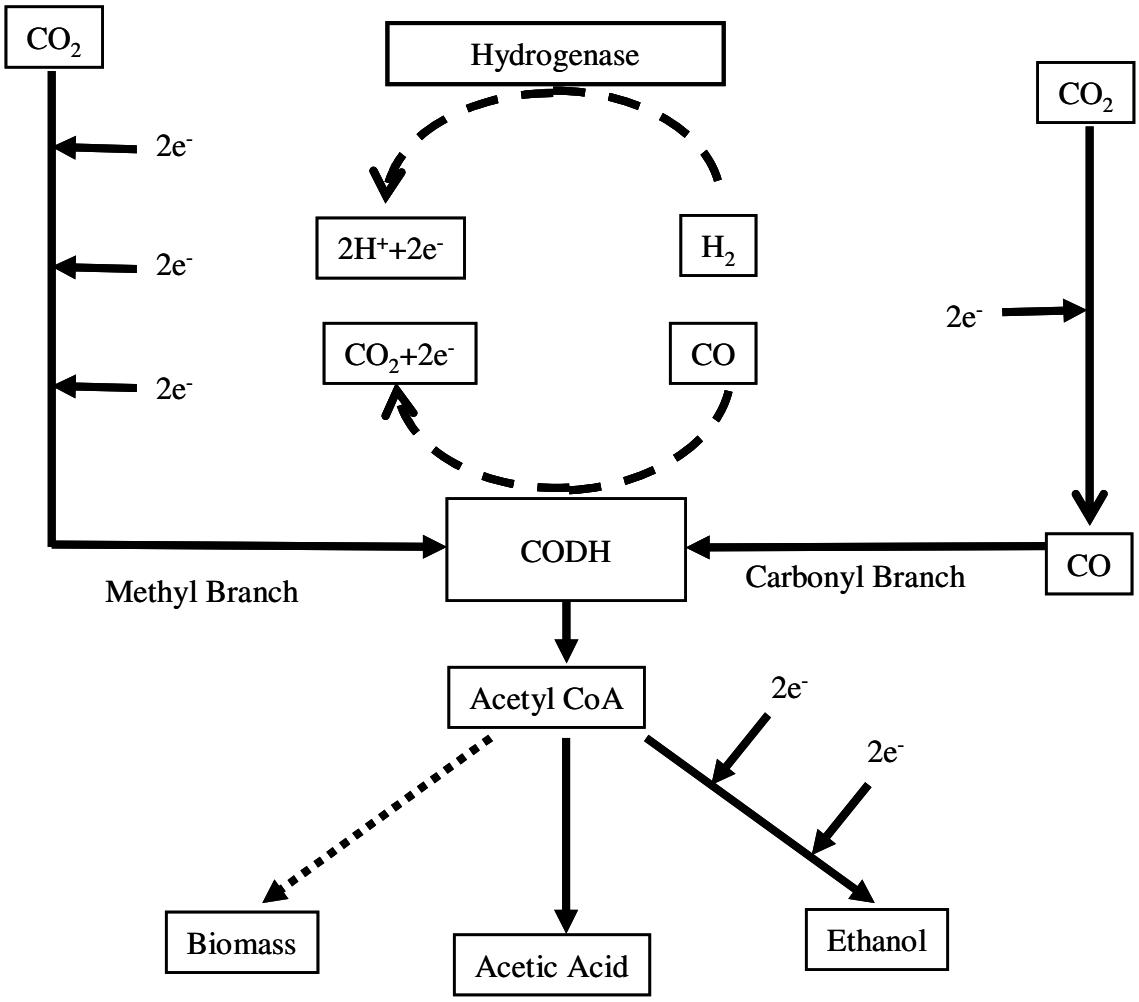

Figure 5.1 Schematic of the Acetyl-CoA pathway showing the utilization of CO, CO_2 and H_2 to ethanol, acetic acid, and biomass. The hydrogenase enzyme is utilized to produce electrons. CODH: carbon monoxide dehydrogenase enzyme. Adapted from (Ragsdale 1991).

Though CO is mainly used by microorganisms to produce cell mass and products, CO can also provide electrons during the metabolism of acetogens. Studies have shown that CO can also inhibit hydrogenase activity in cells, which means that the organism would need to obtain electrons from CO instead of H_2 as described above. Therefore, even though high partial pressures of CO can result in a high cell mass, CO may potentially inhibit the hydrogenase activity of the cells. This makes it necessary to understand the effects of CO partial pressures on the hydrogenase activity of the microbial catalyst, in order to predict the ideal quantity of CO in the feed gas. The studies described in this chapter investigated the effects of CO partial pressure on the hydrogenase activity, as well as the effect of NO on cell-growth, product distribution and hydrogenase activity of *C. carboxidivorans* $P7^T$.

5.2 Materials and Methods

5.2.1 Microbial Catalyst and Culture Medium

Clostridium carboxidivorans $P7^T$, provided by Dr. Ralph Tanner, University of Oklahoma, was utilized for the fermentation. The bacterium was grown under strictly anaerobic conditions in a medium containing (per liter) 30 ml mineral stock solution, 10 ml trace metal stock solution, 10 ml vitamin stock solution, 0.5 g yeast extract, 5 g morpholinoethanesulfonic acid (MES), and 10 ml of 4% cysteine-sulfide solution. Resazurin solution (0.1%) was added as a redox indicator. The composition of the mineral, vitamin and trace metal stock solutions was the same as that described in chapter 3.

5.2.2 Experimental Methods

The experimental set-up used for CO partial pressure studies has been previously described in detail (Hurst 2005) and has been summarized in this section to provide an understanding of the experiments. The set-up consisted of three 120-ml bioreactors, each of which had one top port and two side ports. Disposable stir-bars in each reactor were used in conjunction with a Thermolyne Cellgro 45600 five-position stir plate (Cole Parmer, Vernon Hills, Illinois), to provide continuous stirring. Clean bottled gas mixtures of either 80% CO and 20% CO_2 (Aeriform, Pasadena, Texas) or 25% CO, 15% CO_2 and 60% N_2 were bubbled through the reactors via the side ports using 22-guage stainless steel needles (Hamilton Company, Reno, Nevada). The top ports of the bioreactors were used as gas outlets via 22-guage syringe needles. Needle valves (Swagelok, Solon, Ohio) were used to control the flow rate of the exiting gas. The flow rates were measured using 65-mm flowmeters (Cole Parmer, Vernon Hills, Illinois). The entire assembly was placed in a 2.5-ft^3 Isotemp 600 Series incubator (Fisher Scientific, Pittsburg, Pennsylvania) with digital temperature control to maintain the cultures at 37 ºC. The incubator itself was placed in a fume hood due to the nature of the experiment involving continuous flow of gases. In order to maintain constant headspace pressure in the reactors, outlet needles were connected to a strain-gauge pressure system (constructed by Mike Veldman, Department of Biosystems and Agricultural Engineering, Oklahoma State University). This system contained pressure sensors (Omega Engineering, Inc., Stamford, Connecticut), which provided differential pressure measurements between 0 and 100 psig in reference to atmospheric pressure.

The media was prepared as described in Section 5.2 and 120 ml was transferred into each reactor. The ports of the reactors were sealed and covered with aluminum foil and then autoclaved at 121°C for 20 minutes. Once cooled, the reactors were transferred into an anaerobic chamber, where 1.2 ml Cysteine-Sulfide was added through a 0.2-µm filter to each reactor. About 1 ml of inoculum was then added to each bioreactor. Within the incubator, the reactor outlets were completely closed initially, until all the reactors reached the desired pressure. The needle valves were then opened to allow the gas to leave the reactors at a low flow rate. CO partial pressures of 0.35, 0.50, 0.70, 1.05, 1.35, and 2.0 atmospheres were used in the experiments.

For the experiments with NO, two 500-ml Cytostir® cell culture flasks (Kontes/Kimble Glass Inc., Vineland, NJ) were used. Each sampling arm contained a rubber stopper for inoculation, sampling, and gas sparging. One liter of media, excluding the cysteine-sulfide, was prepared and equally distributed into both reactors, which were then autoclaved at 121°C for 20 minutes. After cooling, the media was continuously purged with N_2 to provide an anaerobic environment. The reactors were then placed in a water bath maintained at 37°C. The water bath was a rectangular propylene tank fitted with a circulating thermostat unit (Model 1112, VWR International, West Chester, PA). The water bath was placed on magnetic stir plates to provide agitation. The water-bath level was always maintained such that the liquid level in the reactors was always below that of the water bath. Cysteine-sulfide (5 ml) was added to each reactor to scavenge any remaining dissolved oxygen.

Following the presence of an anaerobic environment, continuous gas sparging of the feed gases at 10 ml/min was initiated via the use of 18G luer needles for the inlet and

outlet. Reactor A (control) was initially sparged with a gas mixture containing 20% CO, 15% CO_2, 5% H_2 and balance N_2 (Air Liquide, Houston, TX). Reactor B was initially sparged with 20% CO and 15% CO_2, with the concentrations of NO and H_2 ranging between 0-160 ppm and 2.5-15% respectively. Combinations of gas cylinders containing CO, CO_2, H_2, N_2 and NO were mixed using mass flow controllers to obtain the appropriate concentrations. With gas flow initiated, 5 ml of inoculum was added to each reactor.

For all the experiments described above, samples (1.5 ml) were taken periodically from each reactor to measure the OD, pH, and product concentrations. Samples for hydrogenase activity (0.4-0.6 ml) and gas compositions (20 µl) were also obtained. In experiments with more than 80 ppm of NO in the gas stream, it was seen that the cells could not grow in the presence of NO (Reactor B) at the beginning of the run. In these experiments, the gas sources were switched once the cells in the Reactor A had reached a constant cell concentration. The gases were switched to determine the effects of NO on active cells and also to determine whether the inhibition of growth by NO was reversible. In some experiments, the gases were switched back again to their original compositions to once again determine the reversibility of the effects of NO on growth and hydrogenase activity.

5.2.3 Hydrogenase Assay

For the hydrogenase assay, benzyl viologen was used as the electron acceptor and a nonionic detergent, triton X-100 was used to permeabilize the cell membranes. The assay buffer contained 0.4 ml 1M Tris-HCl, 0.2 ml 0.04 M benzyl viologen, 0.1 ml 5%

v/v triton X-100, 0.2 ml 0.04 M dithiothreitol and 3 ml degassed DI water (Shenkman 2003). All the above reagents, except for dithiothreitol, were prepared and stored in an anaerobic glove box (Coy Laboratory Products Inc., Grass Lake, MI). Dithiothreitol was freshly prepared each day as it is unstable in water. Within the anaerobic chamber, the reagents were added in the above quantities to a 4.5 ml optical glass cuvette (Starna Cells Inc., Atascadero, CA) fitted with 10 mm screw caps (SCHOTT Corp., Yonkers, NY) and 13mm butyl rubber stoppers (Bellco Glass Inc., Vineland, NJ). The cuvette was then removed from the chamber and purged with 100% H_2 for approximately one minute, using a 23 G long stainless steel needle as the inlet and a short 22 G needle as the outlet. The cuvette was placed in a 30°C receptacle of a spectrophotometer (Varian Inc., Palo Alto, CA). A gas-tight syringe was used to transport approximately 0.5 ml of anoxic broth from the reactor to the cuvette, after which the cuvette was shaken vigorously, placed in the spectrophotometer, and the absorbance (Abs) recorded at 546 nm every 0.5 seconds.

The concentration (C_{BV}) of reduced benzyl viologen (following the acceptance of electrons from H_2 consumption) was obtained from $C_{BV}=Abs/(\varepsilon \cdot b)$, where b is the cuvette path length (1cm) and ϵ is the extinction coefficient for benzyl viologen (7.55 $mM^{-1}cm^{-1}$ at 546 nm). The maximum volumetric rate of benzyl viologen reduction (R_{BV}) was calculated from the linear slope of the initial portion of the curve following the short lag phase ($R_{BV}=\Delta C_{BV}/\Delta t$). Since two moles of benzyl viologen are reduced per mole of H_2 consumed, the volumetric rate of H_2 consumption (R_{H2}) was calculated as ½ R_{BV}. R_{H2} was finally divided by the measured cell density and converted into specific activity (U/mg) where U represents µmols of H_2 consumed per minute.

For the cell density, samples were collected in 4-ml cuvettes and the OD was measured at 660 nm using a UV-Vis spectrophotometer. OD is proportional to the cell density (~ 0.43 g/L per OD unit) as obtained from a standard calibration chart showing a linear range of cell density between 0 to 0.4 OD units. Samples with an OD greater than 0.4 units were diluted so that the OD was within the linear range of calibration.

5.2.4 Product and Gas Analysis

Once the cell density and pH were measured, the samples from the reactors were centrifuged at 14000 rpm for 10 minutes. The cell-free supernatant was then analyzed for ethanol and acetic acid using a 6890 Gas Chromatograph (Agilent Technologies, Wilmington, DE), with a flame ionization detector and an 8 ft Porapak QS 80/100 column (Alltech, Deerfield, IL).

Gas samples were taken periodically to measure the CO, CO_2, H_2 and NO concentrations in the inlet and outlet gas streams. Two 6890 Gas Chromatographs (Agilent Technologies, Wilmington, DE), each with a TCD, were used to measure CO, CO_2 and H_2. A Chemiluminescence analyzer (Sievers) was used to measure the NO concentration. To convert NO and H_2 to aqueous concentrations, aqueous solubilities of 1.8 mM/atm for NO and 0.78 mM/atm for H_2 were used. (Sander 1999).

5.3 Results and Discussion

5.3.1 Effect of Carbon Monoxide on Hydrogenase Activity

Table 5.1 shows the average hydrogenase activity with time at each partial pressure of CO studied. As the cells in these studies were not exposed to hydrogen, their hydrogenase activities were lower than the activities they would have had in the presence of hydrogen. It was observed that at partial pressures above 1 atm, the hydrogenase activity dropped as the experiment progressed, leveling off at a lower value. On the other hand, at partial pressures of 0.2 and 0.33 atm, the hydrogenase activity increased and then leveled off. The values after the initial decrease or increase (italicized in Table 5.1) were averaged and the average was taken to be the specific activity at each value of partial pressure. The drop in the activity could be a result of the inhibition due to the presence of high amounts of CO. The inoculum used in these studies was from a batch reactor containing very low partial pressures of CO. Therefore, the initial hydrogenase activity of the cells could have been higher than when they were exposed to high amounts of CO. At very low partial pressures, since there was little inhibition of hydrogenase, there was an increase in hydrogenase activity corresponding to cell-growth. In the study with 0.5 atm CO, the initial hydrogenase activity was not measured as the cells started growing faster than in the other studies. On day 0.7 when the first data point was collected, cell concentration was already very high and therefore the hydrogenase activity was approximately 1.5 U/mg.

Figure 5.2 shows the specific activity of hydrogenase (U/mg) as a function of the CO partial pressure in the headspace. The figure shows the rapid decrease in the hydrogenase activity over a very narrow range of CO partial pressure values, after which

2.7 atm CO		**1.88 atm CO**		**1.34 atm CO**		**1.05 atm CO**	
Days	**U/mg**	**Days**	**U/mg**	**Days**	**U/mg**	**Days**	**U/mg**
1.6	0.105	0.8	0.402	1.6	0.130	1.0	0.263
2.6	*0.056*	1.8	*0.078*	2.6	*0.050*	1.8	*0.081*
3.6	*0.054*	2.8	*0.075*	3.6	*0.045*	2.8	*0.079*
4.6	*0.053*	3.8	*0.036*	4.6	*0.044*	4.0	*0.066*
Average	0.054	Average	0.063	Average	0.067	Average	0.075

0.7 atm CO		**0.5 atm CO**		**0.33 atm CO**		**0.2 atm CO**	
Days	**U/mg**	**Days**	**U/mg**	**Days**	**U/mg**	**Days**	**U/mg**
1.0	*0.386*	0.7	*1.504*	0.9	0.353	0.8	0.529
1.8	*0.244*	1.0	*1.677*	1.6	*2.551*	1.2	1.233
2.8	*0.372*	1.6	*1.343*	2.8	*2.325*	1.8	*2.530*
3.8	*0.523*	2.0	*1.263*	3.6	*2.372*	2.2	*2.560*
Average	0.381	Average	1.447	Average	2.416	Average	2.545

Table 5.1 Hydrogenase specific activities with time at CO partial pressures ranging from 0.2 atm to 2.7 atm. The average reported in each column is the average of the italicized values.

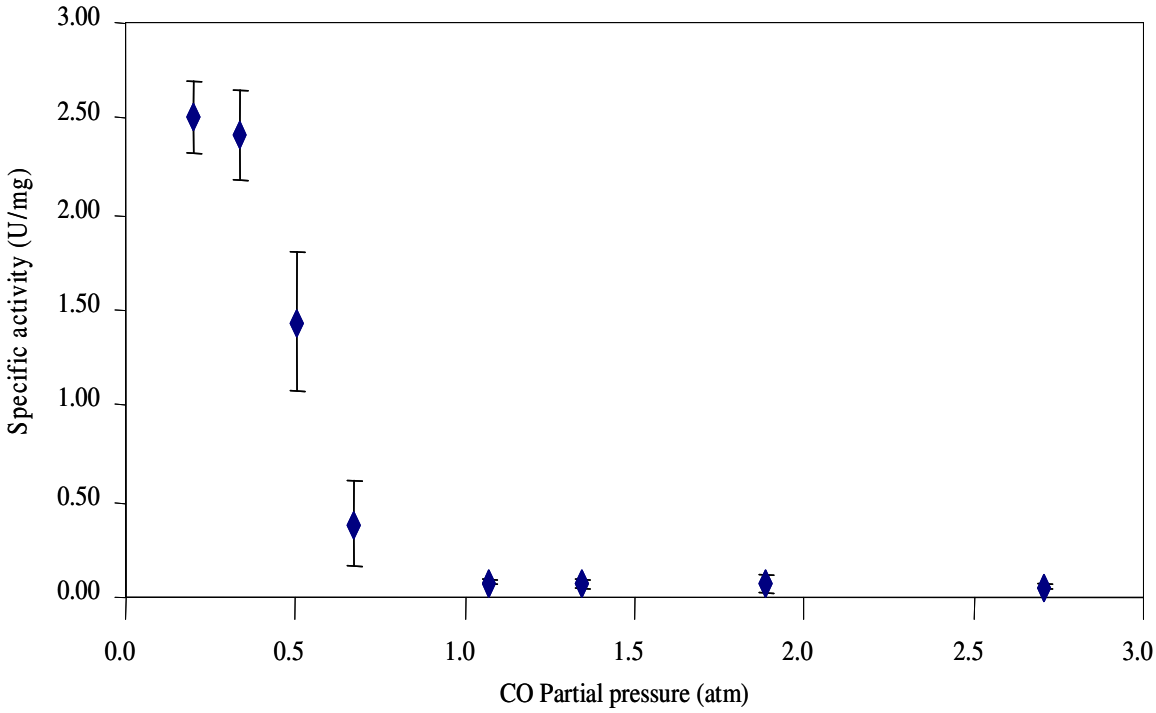

Figure 5.2 Effect of CO partial pressure on specific activity of hydrogenase. The average values shown in Table 5.1 are plotted versus the partial pressure of CO. The error bars represent the standard error (n=3).

it levels off at a value just above zero. The hydrogenase activity at a partial pressure of 0.2 atm was about 2.55 U/mg, whereas; at partial pressures of 1 atm and higher, the activity decreased by about 97%. This data indicates that the hydrogenase activity of the cells is sacrificed at high partial pressures of CO. Therefore, it may be necessary to select an optimal partial pressure of CO in the reactor, which can result in high cell mass without compromising the ability of the cells to consume hydrogen.

5.3.2 Effect of Nitric Oxide on Cell-Growth, Hydrogenase Activity and Product Distribution

Studies were conducted at varying concentrations of NO ranging from 40-200 ppm in the gas phase. Studies were also conducted at 2.5, 5, 10 and 15% H_2 to determine the effect of the substrate (H_2) on the enzyme activity. Figure 5.3 shows the effect of 40 ppm (0.072 μM) NO on cell growth and hydrogenase activity of *Clostridium carboxidivorans* $P7^T$. Reactor A was not exposed to any NO while Reactor B was exposed to 40 ppm NO on a continuous basis. At this level of NO concentration, there was no inhibition of cell growth or hydrogenase activity, as seen in Figure 5.3. On the other hand, the cells exposed to NO reached a higher concentration than the cells in Reactor A. Even though 40 ppm NO had no adverse effect on cell growth or hydrogenase activity, the presence of NO changed the product distribution of the cells, as shown in Figure 5.4. The cells in Reactor B which were exposed to NO produced much more ethanol compared to Reactor A. The ethanol concentration in Reactor B reached a value of about 0.23 g/l, while that in Reactor A was less than 0.05 g/l. The difference in the

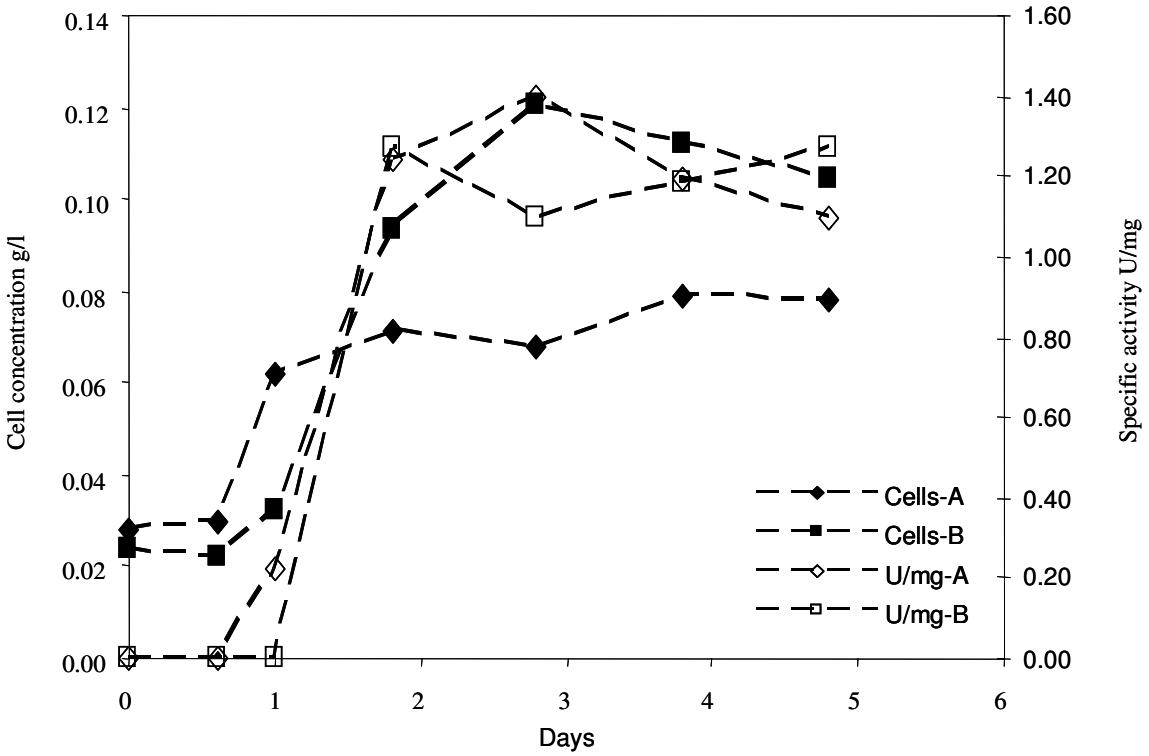

Figure 5.3 Effect of 40 ppm NO on cell concentration and specific activity of hydrogenase (U/mg). The cell concentration is represented by solid data points on the left y-axis and the specific activity is represented by open data points on the right y-axis. Reactor A was a control, which was not exposed to any NO and Reactor B was exposed to 40 ppm NO.

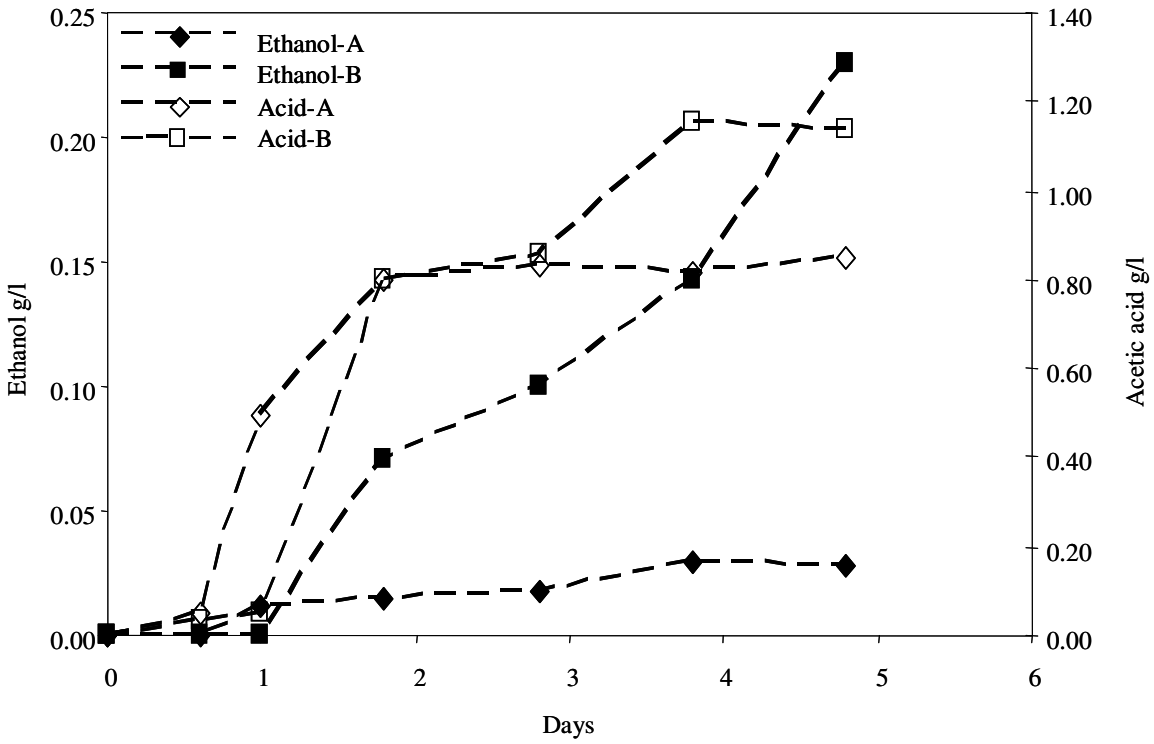

Figure 5.4 Effect of 40 ppm NO on ethanol and acetic acid concentrations. Reactor A was a control, which was not exposed to any NO and Reactor B was exposed to 40 ppm NO.

acetic acid concentrations was not as drastic, though the cells exposed to NO produced about 1.5 times the acid produced by those in Reactor A.

At concentrations above 40 ppm, NO had complex effects on the fermentation. In all the experiments above 40 ppm NO, an inhibition of initial cell-growth was observed in the presence of NO. During these experiments, the gas sources were switched at a later time such that NO was introduced to Reactor A (with no initial NO exposure) and removed from Reactor B (which was exposed to NO initially). The vertical line shown in each figure indicates the time when the gas sources were switched.

Figures 5.5 and 5.6 show the effects of 80 ppm NO on cell-growth, hydrogenase activity and product distribution. As shown in Figure 5.5, Reactor A (with no initial NO exposure) had cell-growth within the first day. On Day 2.6, 80 ppm NO was introduced into the feed gas stream entering Reactor A, after which the cell concentration increased from 0.13 g/l to 0.19 g/l. This indicates that once cells are growing, NO does not inhibit cell growth. In contrast, no cell growth was observed in Reactor B when the cells were initially exposed to a continuous stream of 80 ppm NO. However, once the NO was removed on Day 2.6, the cells began to grow indicating that the inhibition of cell growth was reversible. Similarly, the specific activity, which is the enzyme activity divided by the cell mass increased in Reactor A to a steady value of about 1.84 U/mg, but when the cells were exposed to 80 ppm NO, the activity dropped to about 1.48 U/mg. In Reactor B, the specific activity was initially zero, but when the NO was removed from the gas feed, the activity increased to a value of about 1.6 U/mg. This result indicated that the inhibition of hydrogenase activity by NO was also reversible. Figure 5.6 shows the effect of NO on the ethanol and acetic acid production. As seen in the previous study, NO

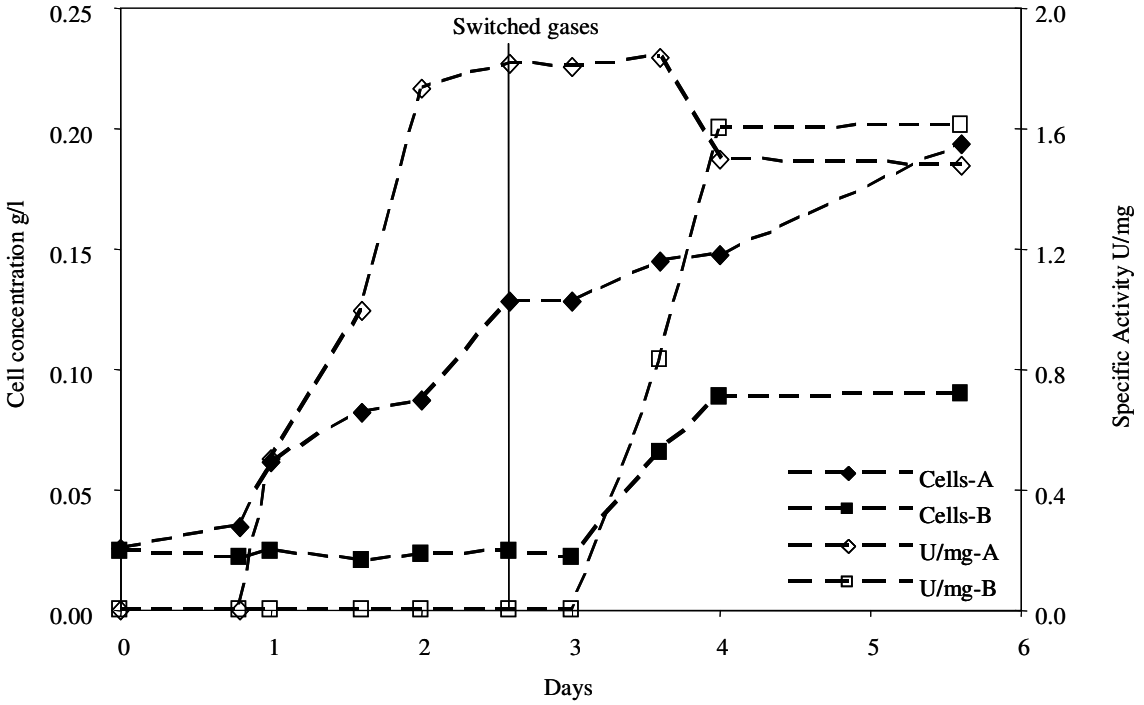

Figure 5.5 Effect of 80 ppm NO on the specific activity of hydrogenase (U/mg) and cell concentration (g/l). The cell concentration is represented by solid data points on the left y-axis and the specific activity is represented by open data points on the right y-axis. Reactor A was not exposed to NO initially but was switched to a gas containing 80 ppm NO, as shown by the vertical line. Reactor B was initially exposed to 80 ppm NO but the NO was removed from the gas feed on day 2.6.

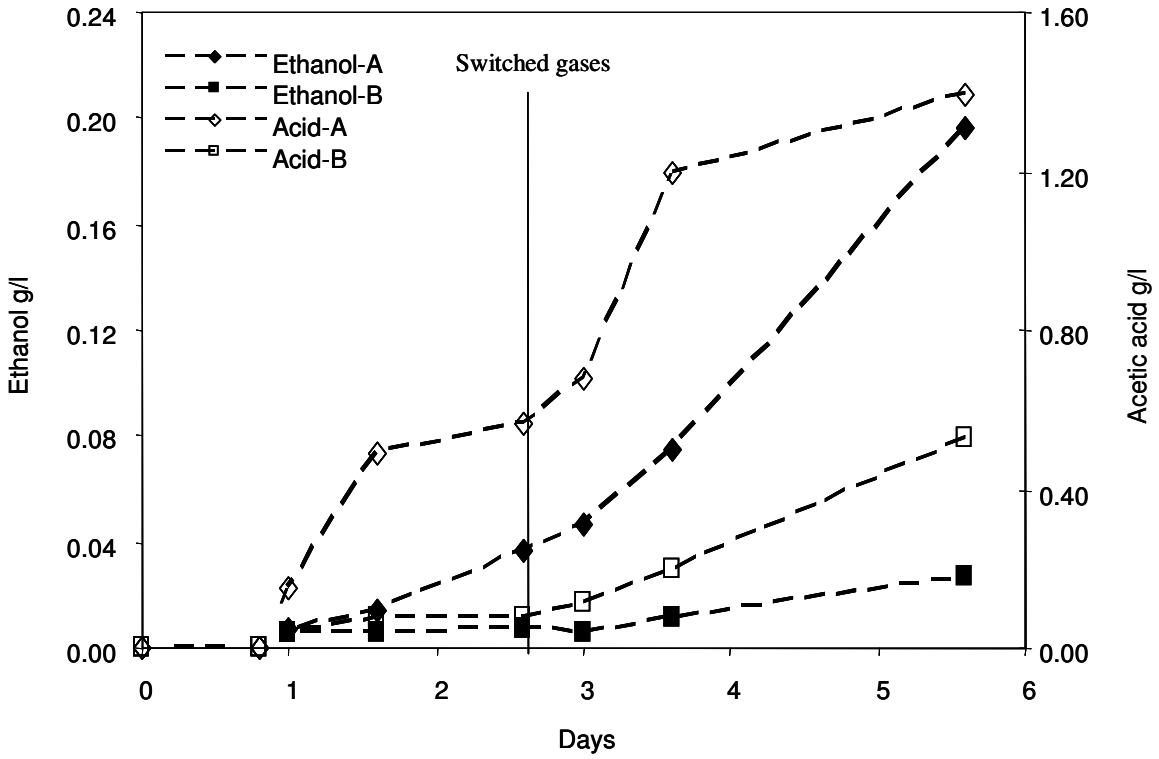

Figure 5.6 Effect of 80 ppm NO on the ethanol and acetic acid concentrations.

The reactors were set-up as described in Figure 5.5

increased the ethanol production by the cells. In the presence of NO, the ethanol concentration increased from about 0.04 g/l to about 0.2 g/l in Reactor A. On the other hand, when NO was removed from Reactor B, the cells began to grow and produced approximately the same amount of ethanol that was observed in Reactor A in the absence of NO. On switching Reactor A to NO, an increase in acetic acid was also observed, which could be associated with the cell-growth in the presence of NO.

In another study with 80 ppm NO, shown in Figures 5.7 and 5.8, similar effects were observed where there was an inhibition of initial cell-growth as well as hydrogenase activity presence of NO. The specific activity of hydrogenase decreased from about 3 U/mg in the absence of NO to approximately 2 U/mg in the presence of 80 ppm NO. In Reactor A, the cell concentration increased from 0.13 g/l to 0.18 g/l, while in Reactor B it inhibited initial cell-growth but the cells started to grow once NO was removed. The effect of product redistribution was also similar to that observed in the previous experiments. NO increased the ethanol concentration from 0.1 g/l to about 0.75 g/l and the acetic acid concentration from 1.2 g/l to approximately 1.4 g/l.

Figures 5.9 and 5.10 show the effect of 100 ppm NO on cell-growth, hydrogenase activity and product distribution. In this study, the acetic acid concentration decreased after the addition of NO to Reactor A. This result was not seen in any other study, as in other studies, NO led to an increase in acetic acid concentration. Figures 5.11 and 5.12 show another study with a 100 ppm NO. Both these studies also showed results similar to 80 ppm experiments.

Figures 5.13 and 5.14 present the effect of 100 ppm NO and 2.5% H_2 (instead of the 5% H_2 used in previous experiments) on cell concentration, hydrogenase activity and

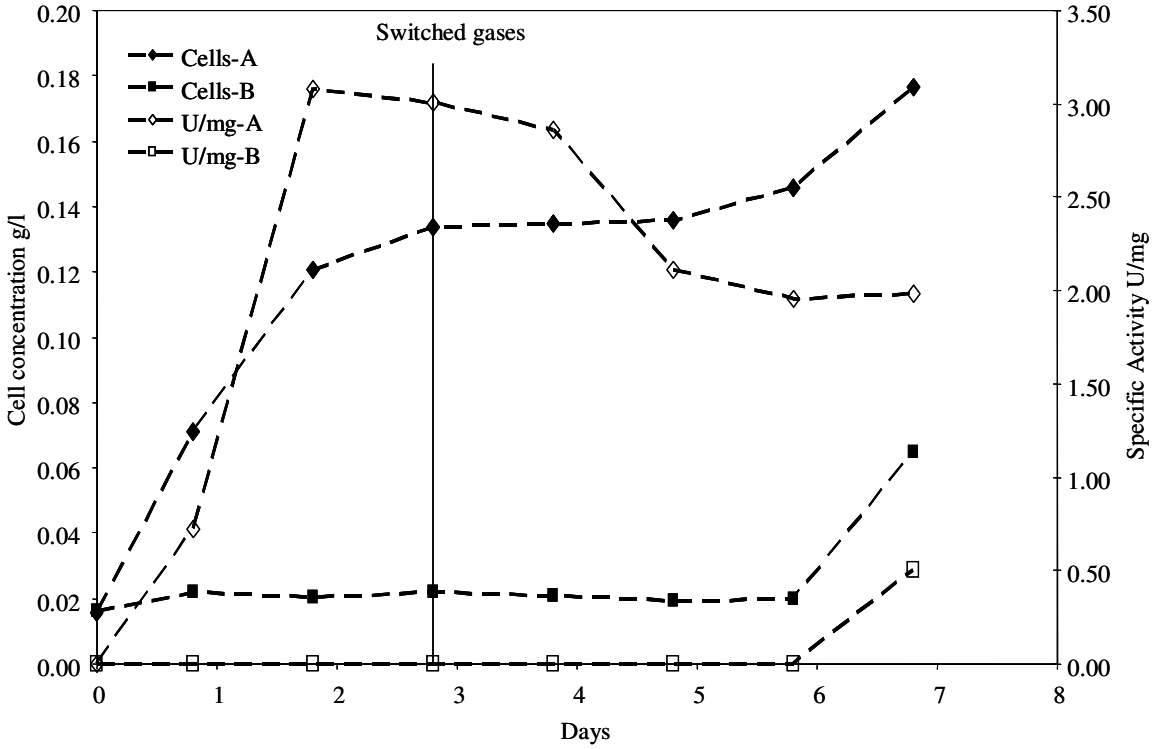

Figure 5.7 Study 2-effect of 80 ppm NO on the specific activity of hydrogenase (U/mg) and cell concentration (g/l). The cell concentration is represented by solid data points on the left y-axis and the specific activity is represented by open data points on the right y-axis. Reactor A was not exposed to NO initially but was switched to a gas containing 80 ppm NO, as shown by the vertical line. Reactor B was initially exposed to 80 ppm NO but the NO was removed from the gas feed on day 2.8.

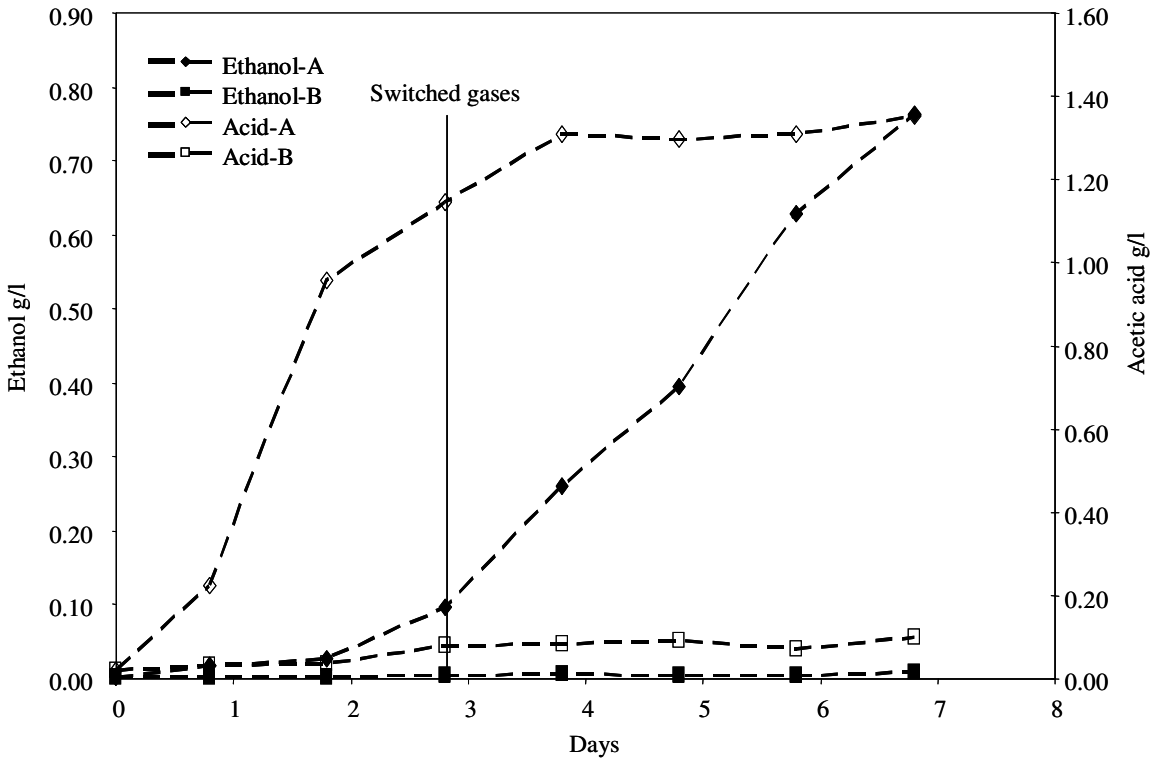

Figure 5.8 Effect of 80 ppm NO on the ethanol and acetic acid concentrations.

The reactors were set-up as described in Figure 5.7

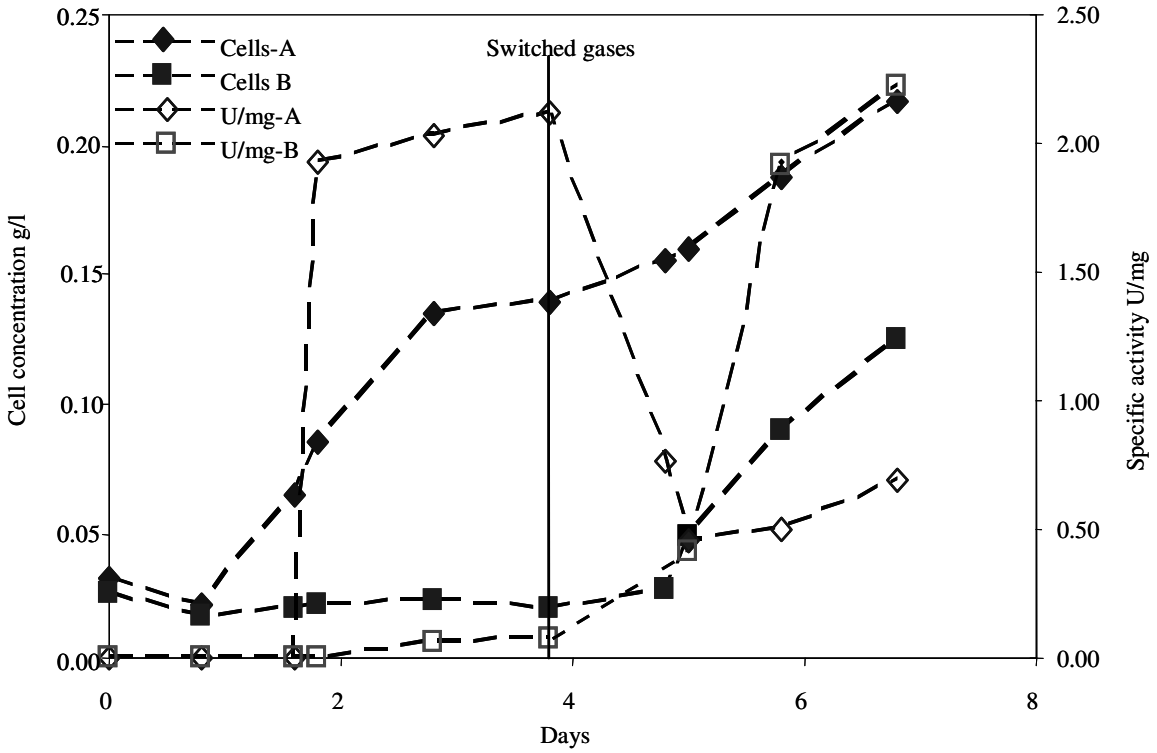

Figure 5.9 Effect of 100ppm NO on cell-concentration and specific hydrogenase activity. Gas sources were switched on Day 3.8.

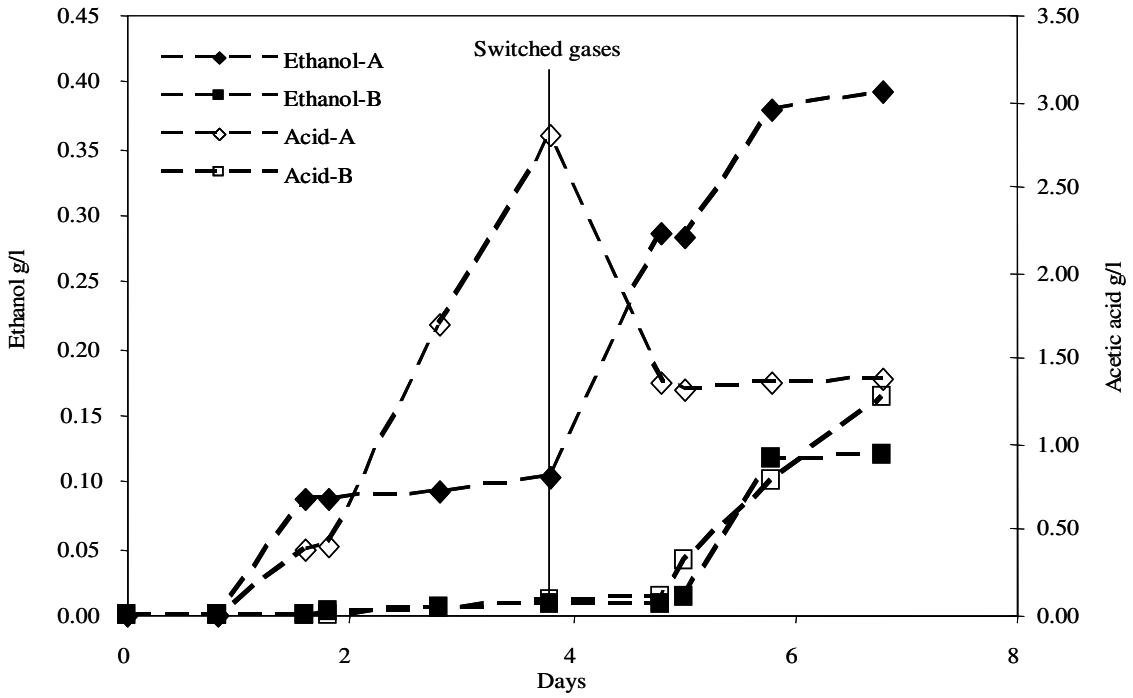

Figure 5.10 Effect of 100 ppm NO on ethanol and acetic acid concentrations. Gas sources were switched on Day 3.8.

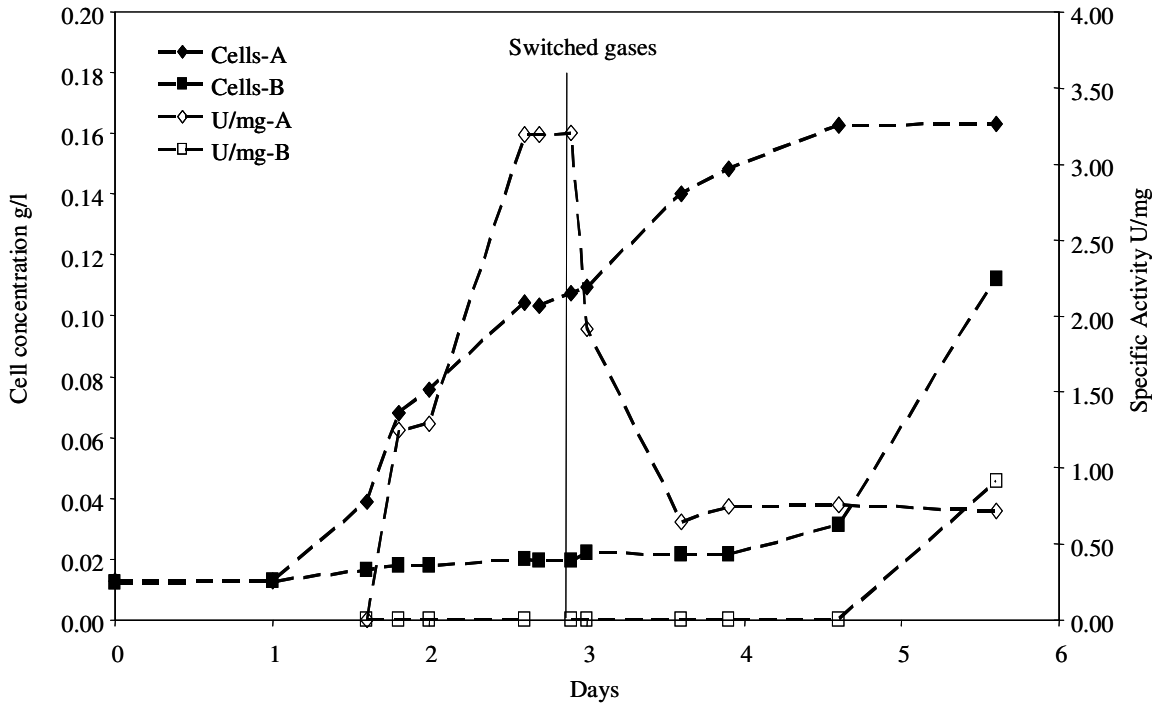

Figure 5.11 Study 2-effect of 100 ppm NO on cell concentration and specific hydrogenase activity. Gas sources were switched on Day 2.9.

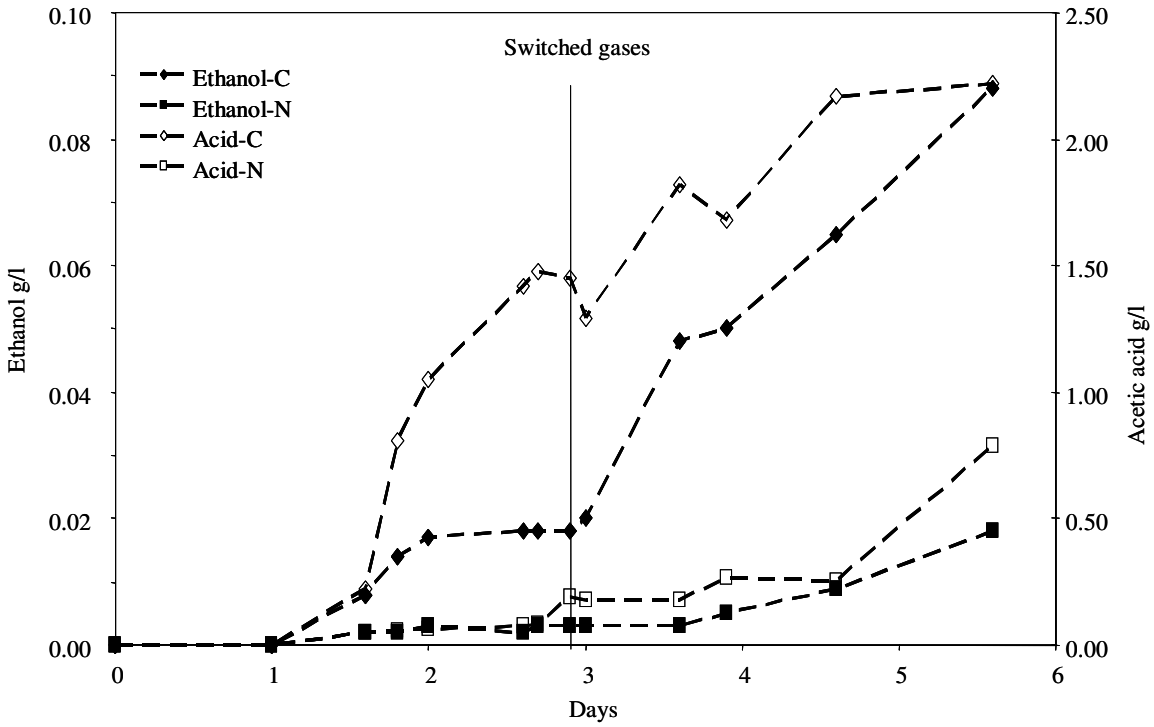

Figure 5.12 Study 2-effect of 100 ppm NO on ethanol and acetic acid concentrations. Gas sources were switched on Day 2.9.

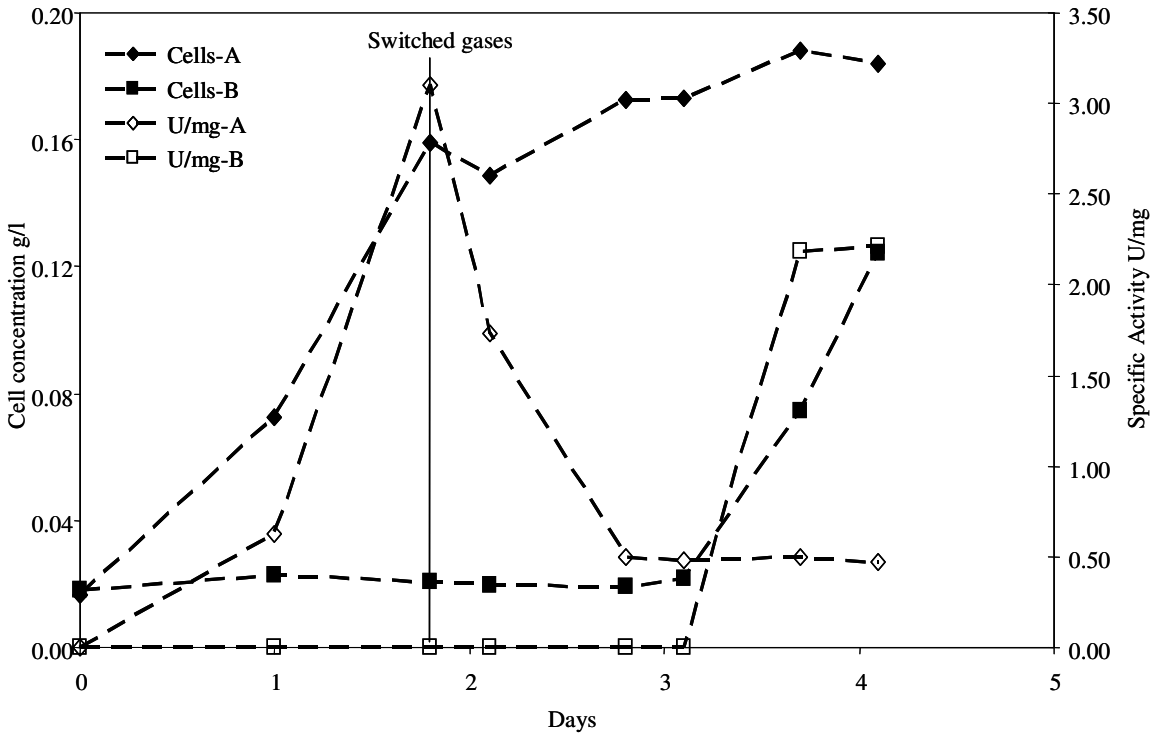

Figure 5.13 Effect of 100 ppm NO and 2.5 % H_2 on cell concentration and specific hydrogenase activity. Gas sources were switched on Day 1.8.

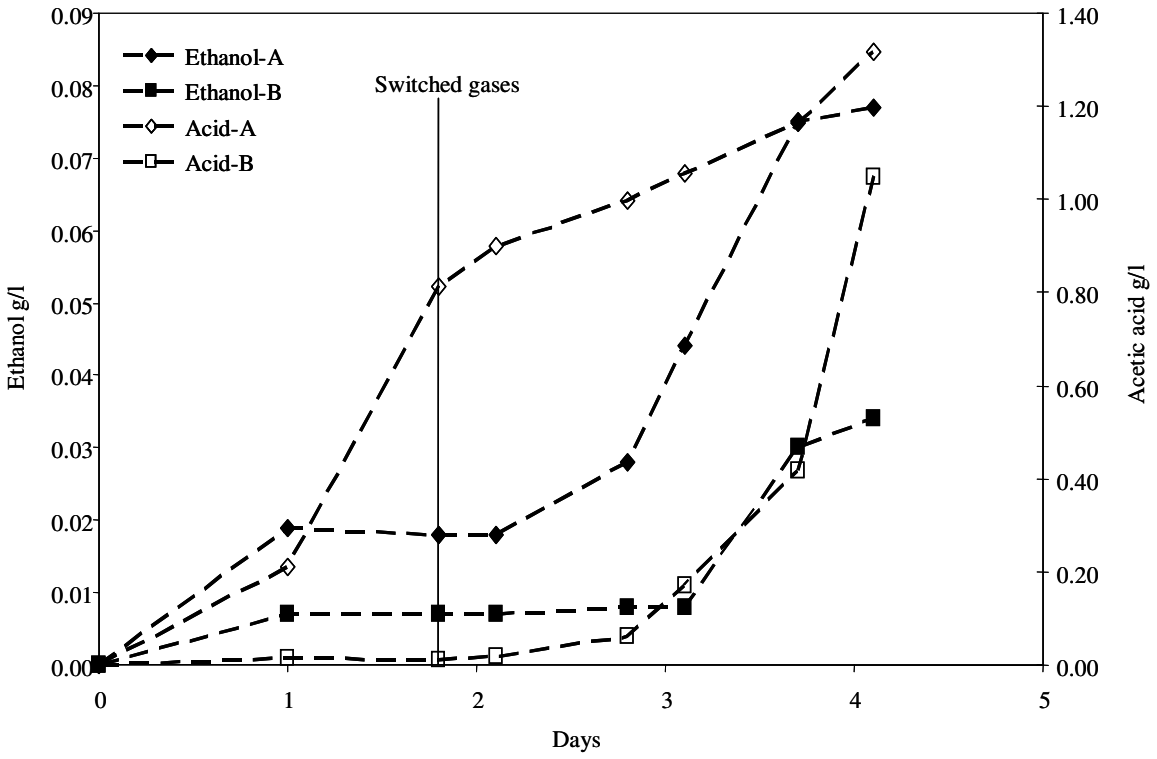

Figure 5.14 Effect of 100 ppm NO and 2.5 % H_2 on ethanol and acetic acid concentrations. Gas sources were switched on Day 1.8.

ethanol and acetic acid concentrations. The results followed a similar trend to the previous experiments. Introducing NO into the gas feed of Reactor A increased the cell concentration from 0.16 g/l to 0.18 g/l and decreased the hydrogenase activity from about 3.0 U/mg to 0.5 U/mg. As shown in Figure 5.14, the ethanol concentration increased from 0.02 g/l to about 0.08 g/l on switching to NO, while the acetic acid increased from 0.8 g/l to about 1.3 g/l. The inhibition of initial cell-growth and hydrogenase activity observed in Reactor B were reversible in nature as seen in previous studies.

Another study with 100 ppm NO and 7.5 % H_2 is shown in Figures 5.15 and 5.16. Introducing NO to Reactor A on day 2.8 led to an increase in cell concentration from 0.11 g/l to 0.15 g/l, a decrease in hydrogenase activity from 2.6 U/mg to 0.7 U/mg, and an increase in ethanol and acetic acid concentrations from 0.02 g/l to 0.1 g/l and 0.9 g/l to 1.4 g/l, respectively.

Figures 5.17 and 5.18 show the effect of 130 ppm NO at 5 % H_2 concentration. On switching gas sources as described above, the cell concentration in Reactor A increased from 0.09 g/l to 0.15 g/l and the hydrogenase activity decreased from 2.6 U/mg to about 0.1 U/mg. An increase in ethanol concentration from 0.08 g/l to 0.34 g/l and an increase in acid concentration from 0.96 g/l to 1.1 g/l were also observed.

Figures 5.19 and 5.20 represent a study conducted at 130 ppm NO and 3.25 % H_2. On introducing NO to Reactor A, the cell concentration increased from 0.13 g/l to 0.19 g/l and the hydrogenase activity decreased from 2.78 U/mg to about 0.09 U/mg. As seen in previous studies, the ethanol concentration increased from 0.02 g/l to 0.09 g/l and the acid concentration increased from 1.2 g/l to 1.8 g/l.

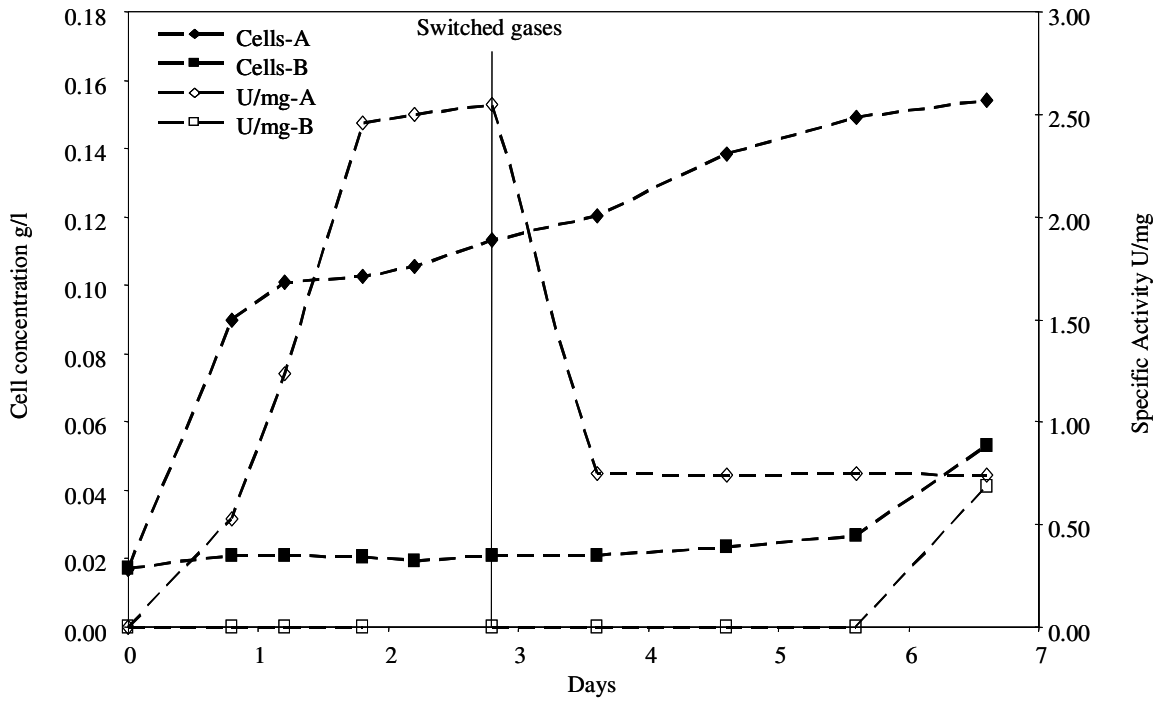

Figure 5.15 Effect of 100 ppm NO and 7.5 % H_2 on cell concentration and specific hydrogenase activity. Gas sources were switched on Day 2.8.

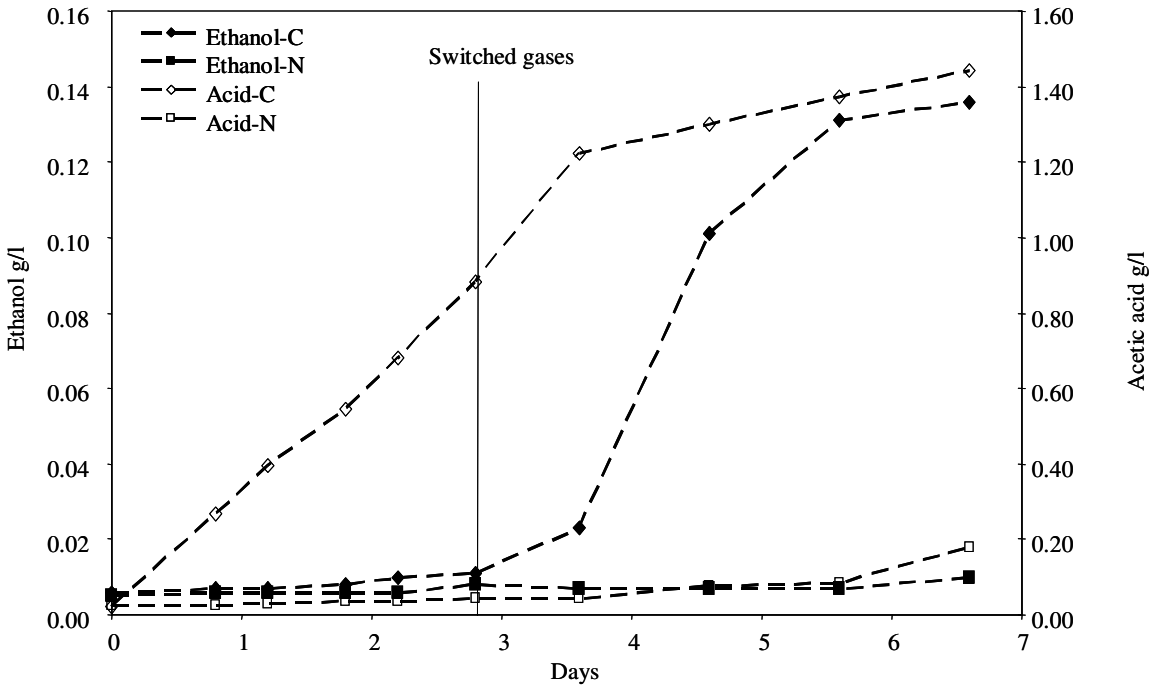

Figure 5.16 Effect of 100 ppm NO and 7.5 % H_2 on ethanol and acetic acid concentrations. Gas sources were switched on Day 2.8.

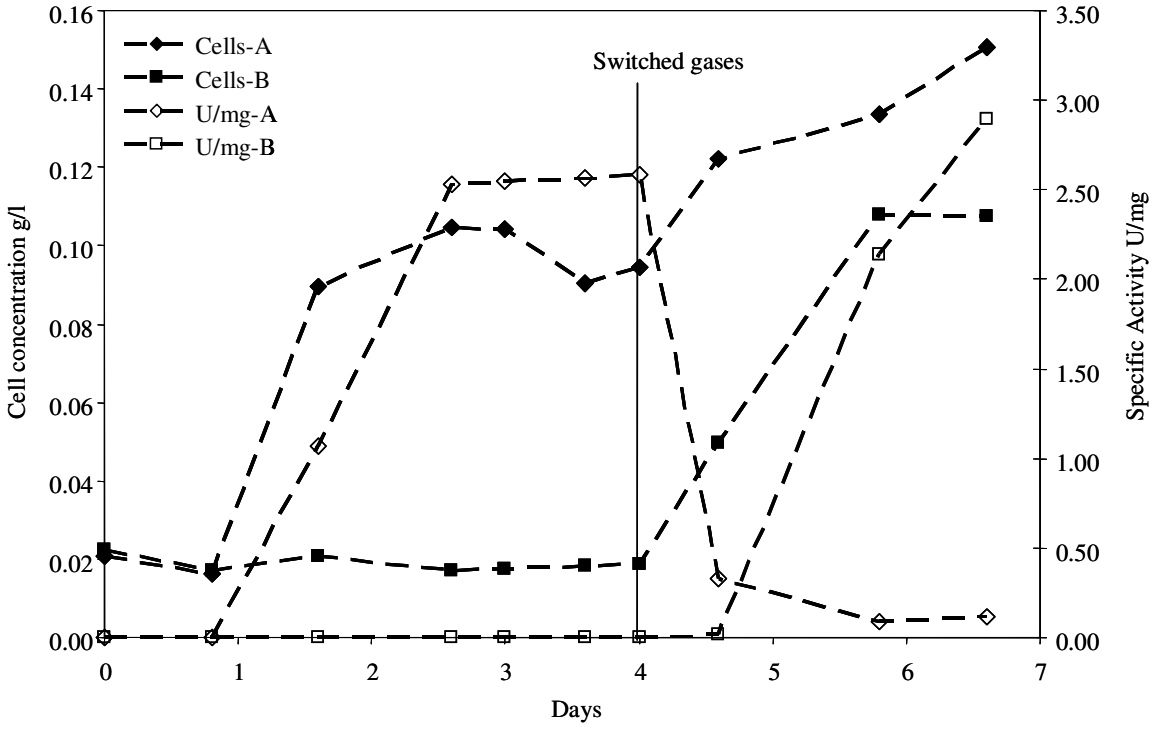

Figure 5.17 Effect of 130 ppm NO on cell concentration and specific hydrogenase activity. Gas sources were switched on Day 4.

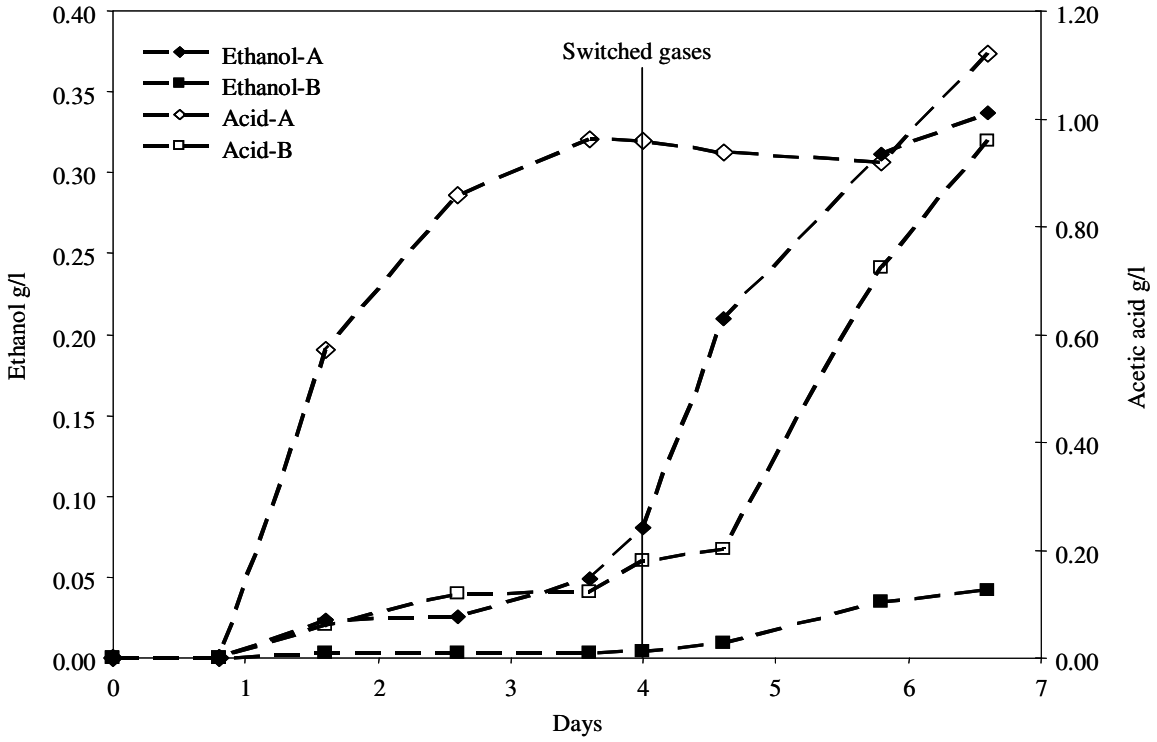

Figure 5.18 Effect of 130 ppm NO on ethanol and acetic acid concentrations. Gas sources were switched on Day 4.

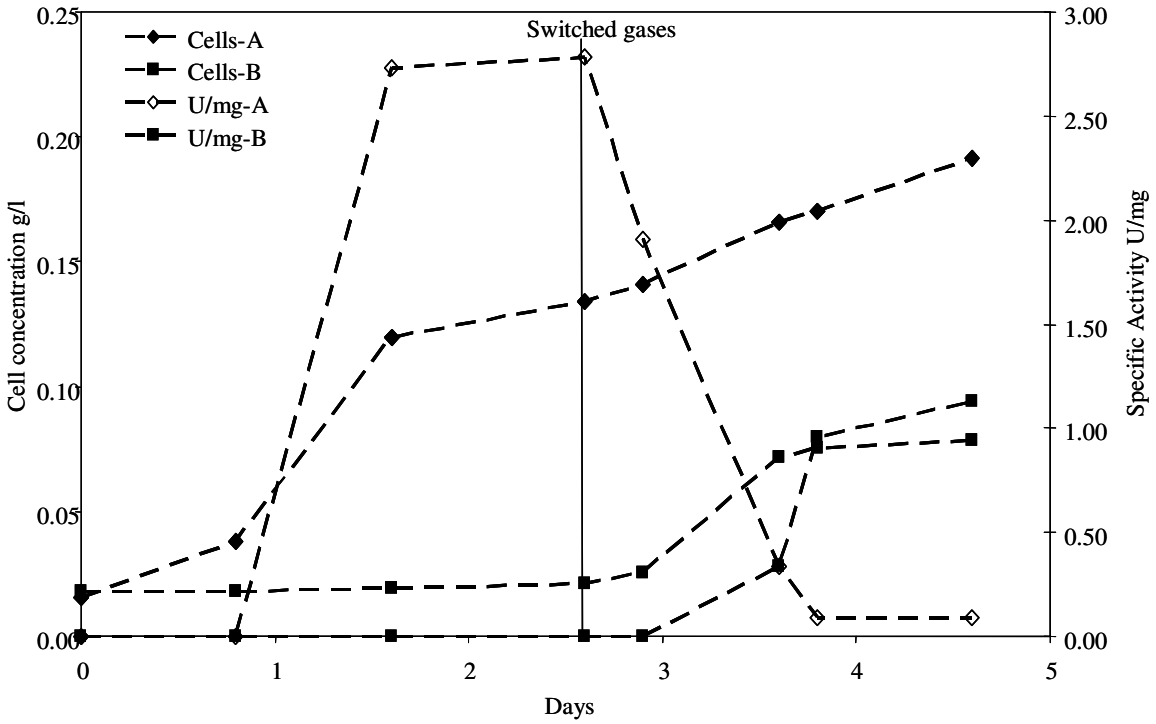

Figure 5.19 Effect of 130 ppm NO and 3.25 % H_2 on cell concentration and specific hydrogenase activity. Gas sources were switched on Day 2.6.

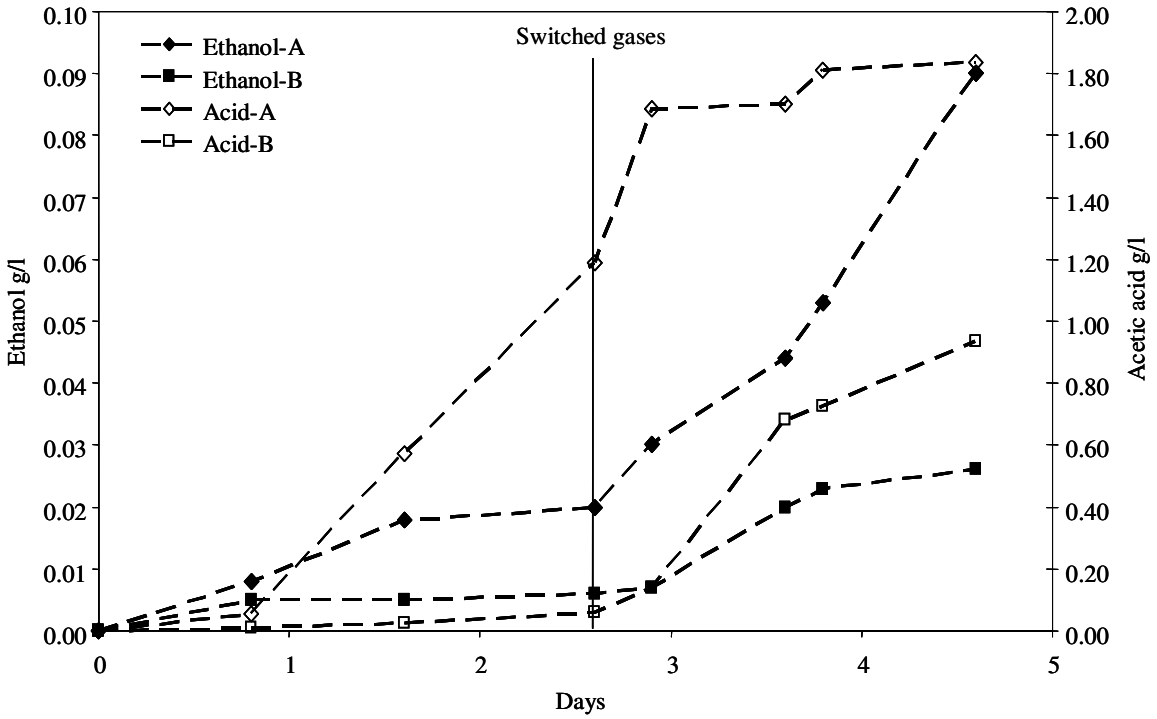

Figure 5.20 Effect of 130 ppm NO and 3.25 % H_2 on ethanol and acetic acid concentrations. Gas sources were switched on Day 2.6.

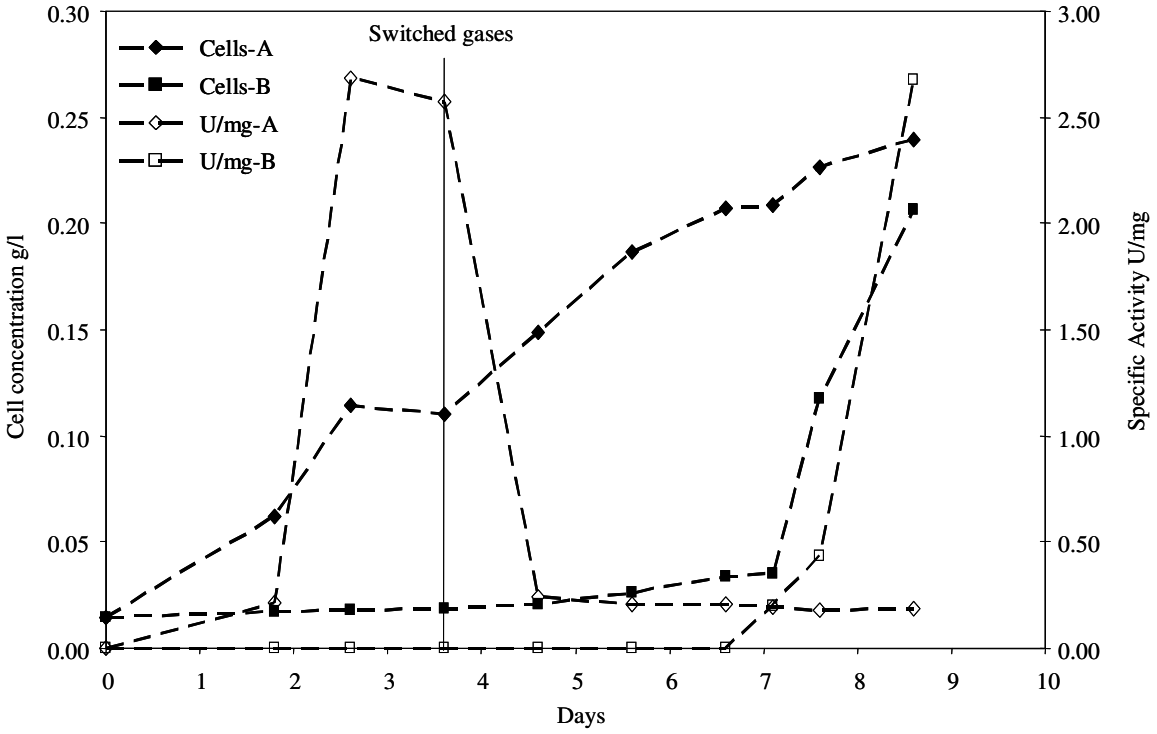

Figure 5.21 Effect of 130 ppm NO and 6.75 % H_2 on cell concentration and specific hydrogenase activity. Gas sources were switched on Day 3.6.

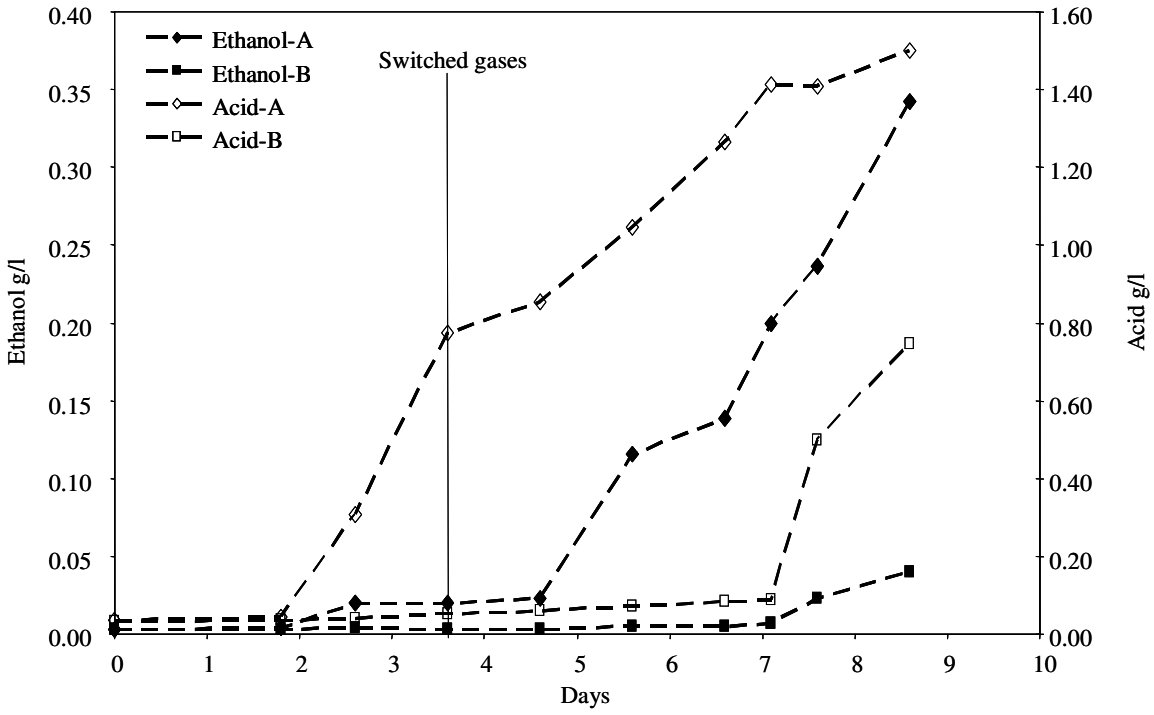

Figure 5.22 Effect of 130 ppm NO and 6.75 % H_2 on ethanol and acetic acid concentrations. Gas sources were switched on Day 3.6.

The effects of 130 ppm NO and 6.75% H_2 are shown in Figures 5.21 and 5.22. The cell concentration in Reactor A increased from 0.11 g/l to 0.24 g/l on introducing NO in the feed gas. The hydrogenase activity of these cells decreased from 2.7 U/mg to 0.18 U/mg due to inhibition by NO. The ethanol concentration increased from 0.02 g/l before the introduction of NO to about 0.34 g/l after almost 5 days of exposure to NO. The increase in ethanol concentration was higher than that observed in previous studies possibly due to the fact that this experiment was run longer. As the ethanol concentration in the previous studies had not stopped increasing, it is possible that the longer the cells are exposed to NO, the more ethanol they can produce. The increase in acetic acid in the presence of NO was from 0.8 g/l to about 1.5 g/l, which was also more than that observed in previous studies, perhaps due to the same reason.

Figures 5.23 and 5.24 show the effects of 160 ppm NO at 5% H_2 concentration. Gas sources were switched while the cells were still in the growth phase, compared to the other studies where the switch was made after the cells had reached a steady cell concentration. Therefore, the specific hydrogenase activity of the cells in Reactor A had not yet reached its maximum value and was still at 0.8 U/mg when NO was introduced. Immediately after the introduction of NO, the specific activity decreased to zero indicating that the enzyme was completely inhibited at 160 ppm NO. The cell concentration continued to increase even after the introduction of NO and reached a value of about 0.11 g/l at the end of the experiment. The cells in Reactor B showed no growth after switching the gases, possibly due to the fact that the experiment was not continued long enough to observe cell-growth. From the product profile shown in Figure 5.24, it can be seen that the ethanol and acid concentrations continued to increase after the

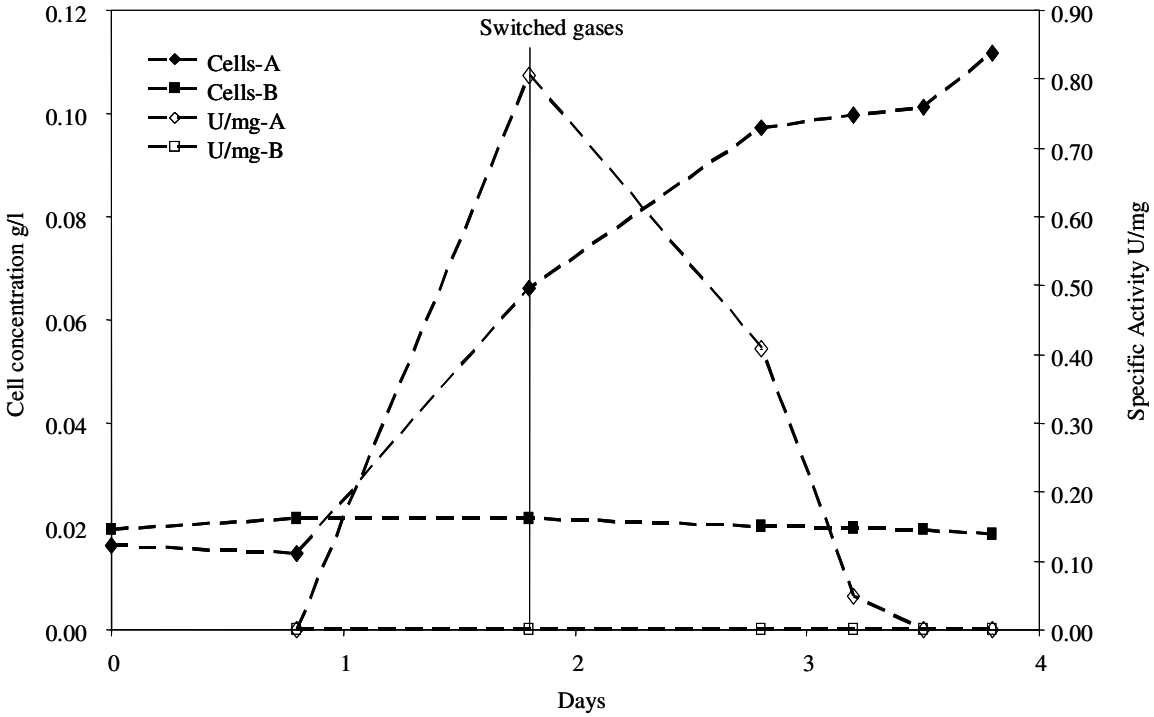

Figure 5.23 Effect of 160 ppm NO on cell concentration and specific hydrogenase activity. Gas sources were switched on Day 1.8.

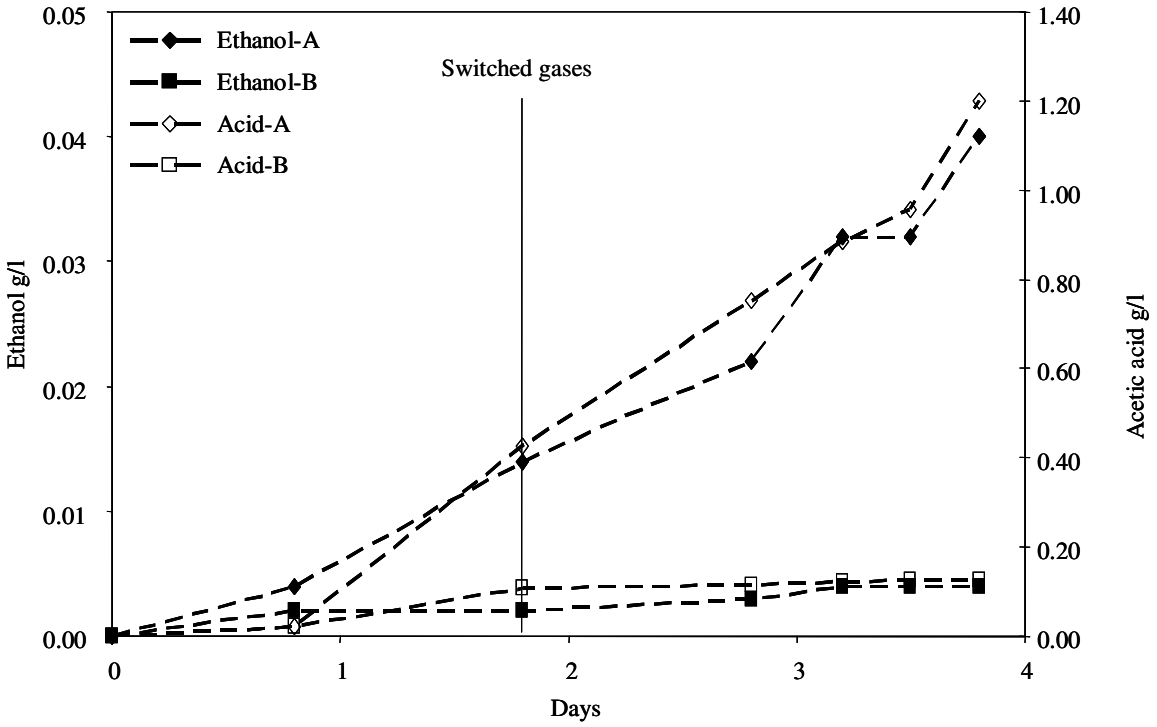

Figure 5.24 Effect of 160 ppm NO on ethanol and acetic acid concentrations. Gas sources were switched on Day 1.8.

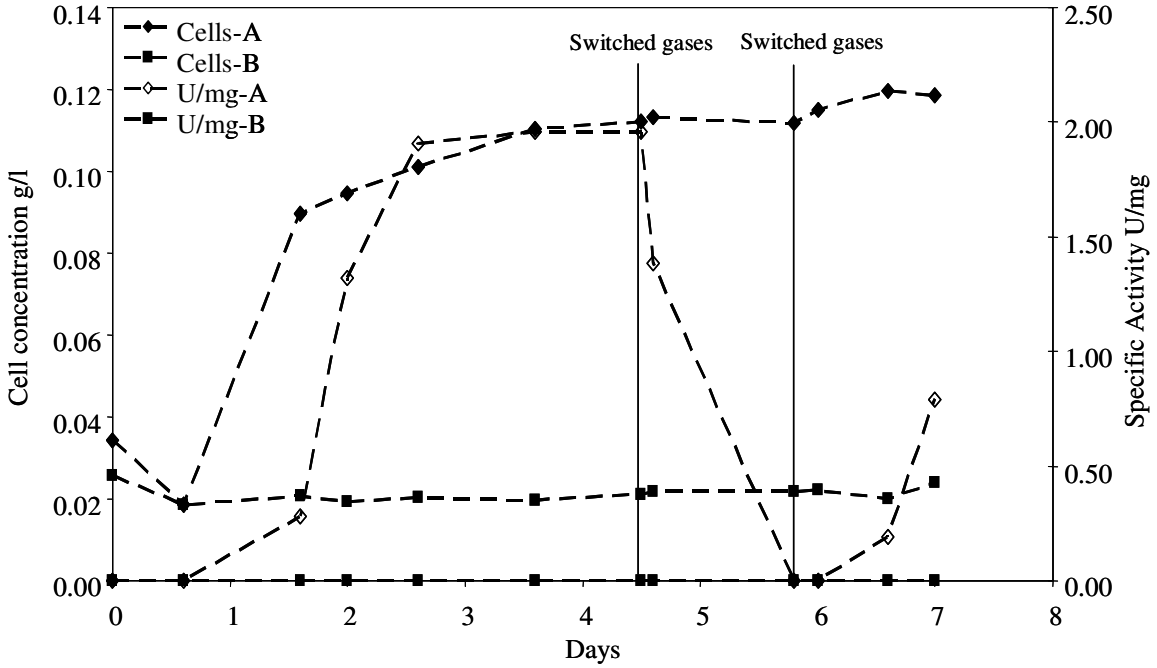

Figure 5.25 Effect of 160 ppm NO on cell concentration and specific hydrogenase activity. Gas sources were switched on Day 4.5 and then switched back on Day 5.8, as indicated by the two vertical lines.

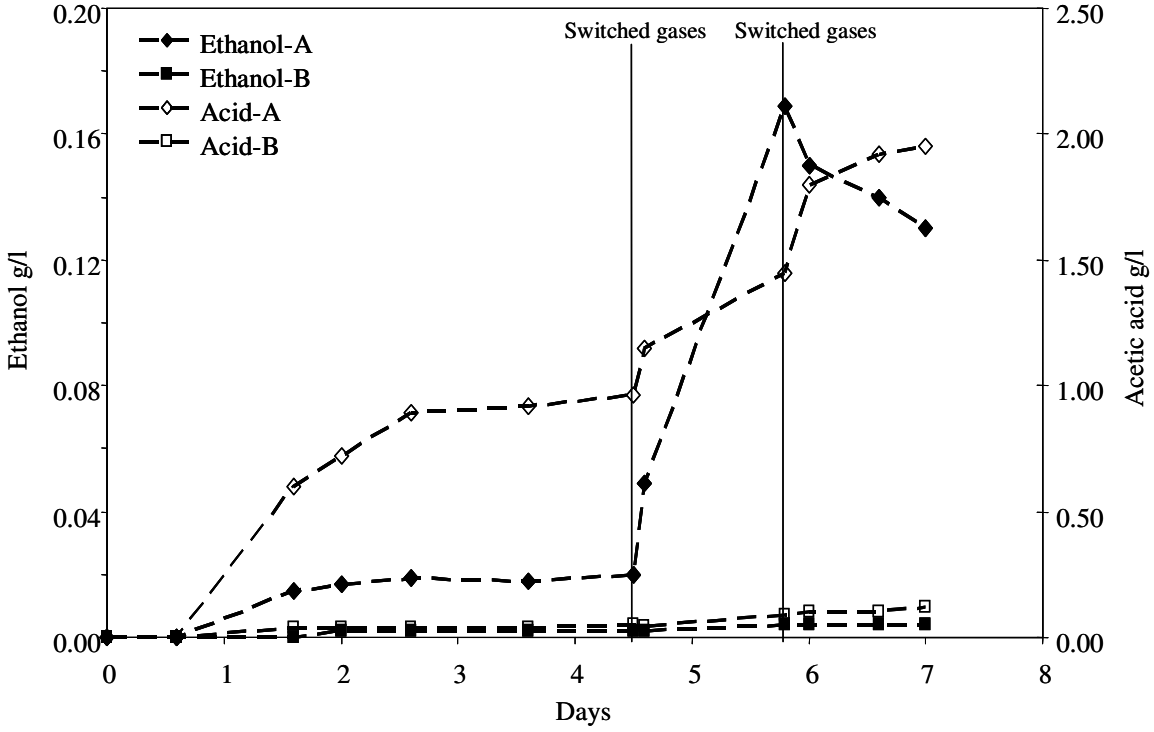

Figure 5.26 Effect of 160 ppm NO on ethanol and acetic acid concentrations. Gas sources were switched on Day 4.5 and then switched back on Day 5.8, as indicated by the two vertical lines.

addition of NO. Figures 5.25 and 5.26 show another study conducted at 160 ppm NO. In this study, gas sources were first switched on day 4.5. After this switch, the hydrogenase activity of the cells in Reactor A decreased to zero. The cell concentration did not increase significantly on exposure to NO in this case. However, the ethanol concentration increased from about 0.02 g/l to 0.16 g/l and acetic acid concentration increased from 0.92 g/l to about 1.1 g/l. Although the previous experiments in which NO was initially exposed to the cells showed that the up-regulation of hydrogenase occurred after the NO was removed, the reversibility of activity loss needed to be assessed. For this, the gases were switched back on Day 5.8 (indicated by the second vertical line), so that once again there was no NO being fed into Reactor A, while Reactor B was exposed to 160 ppm NO. After the second switch, the hydrogenase activity of the cells in Reactor A began to increase, indicating that the inhibition was reversible. On the other hand, ethanol concentration began to drop while the acid concentration continued to increase. Figures 5.27 and 5.28 show the effect of 200 ppm NO on cell-growth, hydrogenase activity and product concentrations. The gases were switched twice in this study, similar to the previous study with 160 ppm NO. There was a complete inhibition of hydrogenase activity due to NO, but when NO was removed, the activity started to increase indicating that the inhibition was reversible. In Reactor B, once the NO was removed, the cells began to grow, though they reached a lower final concentration compared to Reactor A. The hydrogenase activity in Reactor B increased slightly when NO was removed, but dropped to zero once the gases were switched back. In Reactor A, the ethanol concentration increased from 0.07 g/l to about 0.4 g/l when NO was introduced. However, when NO was removed, the ethanol stopped increasing and started to decrease

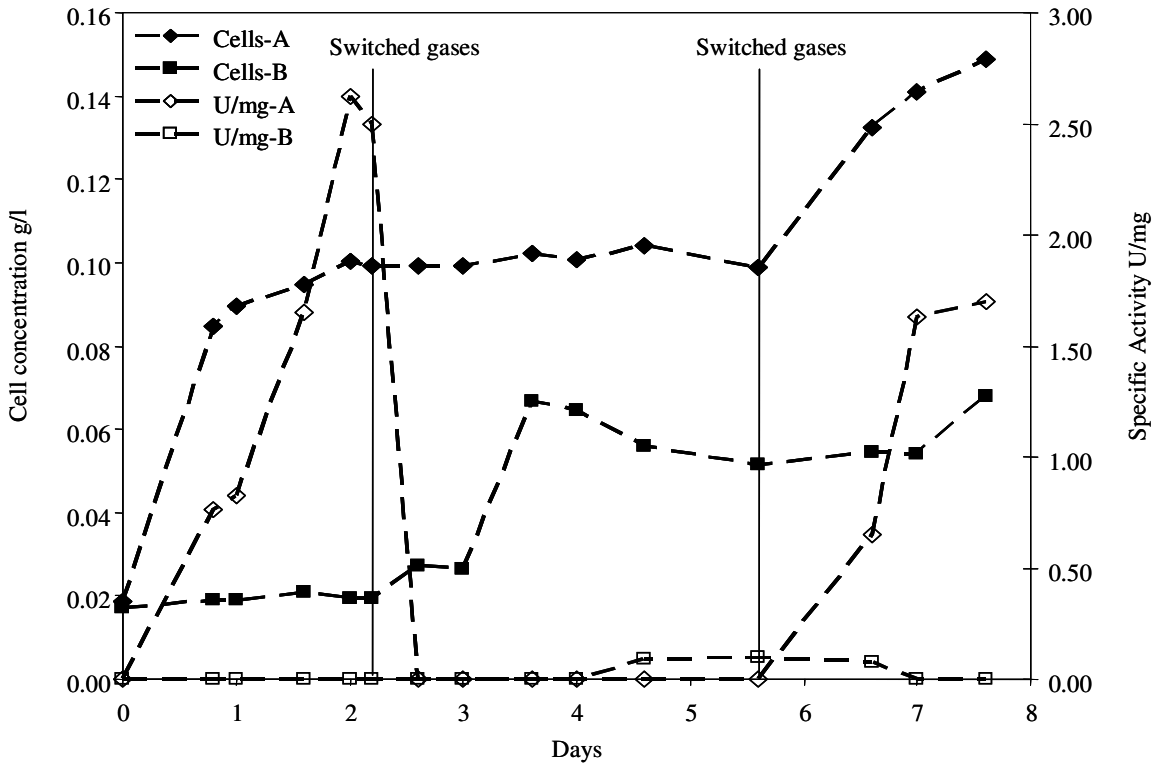

Figure 5.27 Effect of 200 ppm NO on cell concentration and specific hydrogenase activity. Gas sources were switched on Day 2.1 and then switched back on day 5.5.

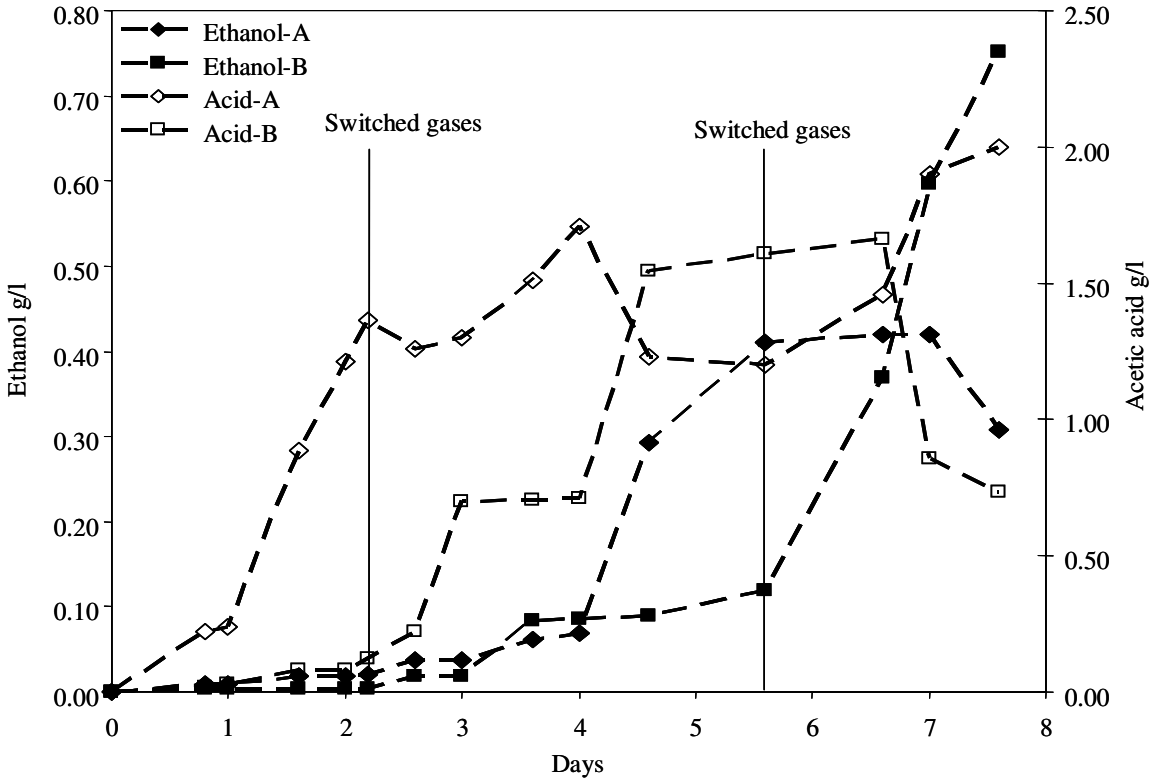

Figure 5.28 Effect of 200 ppm NO on ethanol and acetic acid concentrations. Gas sources were switched on Day 2.1 and then switched back on day 5.5

towards the end of the study. The acetic acid increased on exposure to NO from 1.4 g/l to 1.7 g/l, but then dropped to about 1.2 g/l. This decrease in acid was not observed in previous experiments. The acid started to increase once again when the NO was removed from Reactor A. In Reactor B the cells began to grow after NO was removed, making about 0.1 g/l ethanol. However, once NO was introduced again into Reactor B, the ethanol concentration increased to about 0.75 g/l. This was accompanied by a drop in the acid concentration from 1.6 g/l to about 0.7 g/l in the last stage of the experiment. This experiment demonstrated that up to a concentration of 200 ppm NO, the inhibition of initial cell-growth and hydrogenase activity are reversible.

5.3.3 Effect of Hydrogen on Hydrogenase Activity

Apart from varying the hydrogen concentration in the presence of the inhibitor (NO), two other studies were conducted at 10 % and 15 % H_2 in the absence of NO. These studies were carried out to assess the effect of the substrate on the enzyme and also to develop the kinetic model discussed in the next section. In these studies, Reactor A was used as a control and was sparged with the standard gas mixture containing 5% H_2, 20 % CO, 15 % CO_2 and balance N_2 as described in Section 2.2. Reactor B was sparged with the same composition of CO and CO_2 but with 10% and 15 % H_2 in each study. The results are shown in Table 5.2. It was observed that increasing the hydrogen concentration led to an increase in hydrogenase activity. Compared to the control (5% H_2), cells exposed to 10 % H_2 had 1.3 times the hydrogenase activity while cells exposed to 15 % H_2 had about twice the hydrogenase activity. The product distribution

10 % H_2

	Cells g/l		U/mg		Ethanol g/l		Acetic acid g/l	
Days	**A**	**B**	**A**	**B**	**A**	**B**	**A**	**B**
0.0	0.0052	0.0047	0.00	0.00	0.003	0.003	0.023	0.023
1.8	0.0730	0.0658	0.77	0.56	0.014	0.015	0.288	0.272
2.7	0.1068	0.0937	2.08	2.50	0.040	0.046	0.786	0.591
3.0	0.1137	0.0961	2.04	2.63	0.040	0.058	0.887	0.712
3.8	0.1401	0.1191	2.03	2.60	0.039	0.073	1.093	1.053

15 % H_2

	Cells g/l		U/mg		Ethanol g/l		Acetic acid g/l	
Days	**A**	**B**	**A**	**B**	**A**	**B**	**A**	**B**
0.0	0.0129	0.0129	0.00	0.00	0.002	0.002	0.023	0.020
0.8	0.0117	0.0108	0.00	0.00	0.003	0.003	0.040	0.030
1.8	0.0661	0.0095	0.00	0.00	0.004	0.002	0.194	0.034
2.2	0.0920	0.0142	0.50	0.00	0.007	0.002	0.210	0.052
2.8	0.0996	0.0843	0.92	1.34	0.009	0.013	0.629	0.381
3.8	0.1185	0.0956	1.57	2.58	0.023	0.025	0.795	0.523
4.8	0.1325	0.1006	1.30	2.53	0.031	0.067	1.146	0.853

Table 5.2 Effect of hydrogen concentrations on hydrogenase activity (U/mg) and product concentrations.

also changed with hydrogen concentration. The cells exposed to 10 and 15 % H_2 made more ethanol and less acetic acid than the cells exposed to 5 % H_2. This could be connected to the higher hydrogenase activities of the cells exposed to higher amounts of hydrogen.

5.3.4 Hydrogenase Kinetic Model – Inhibition by Nitric Oxide

To assess the hydrogenase kinetic model in the presence of NO, Figure 5.29 shows the double reciprocal plot of 1/v vs. 1/[H_2] where v is the hydrogenase activity (μmoles min^{-1} mg^{-1}). To appropriately compare the hydrogenase activity between experiments, activities plotted in Figure 5.29 were obtained by dividing the activity by the maximum activity observed in Reactor A in the absence of NO (e.g. Figure 5.19, the maximum activity is shown at 2.6 days for Reactor A) and then multiplying by the average of the maximum activities observed in Reactor A for all experiments. The plot is shown for NO concentrations of 0, 0.18 μM (100 ppm), and 0.234 μM (130 ppm) and aqueous H_2 concentrations varying from 18-110 μM (2.5-15% in the gas phase). The three lines converged on the negative x-axis, indicating a non-competitive inhibition of the enzyme.

Equation 5.1, which was derived by combining a typical model for allosteric enzymes (Shuler and Kargi 1992) with the non-competitive enzyme inhibition model (Roberts 1977), characterizes the hydrogenase activity in the presence of inhibition by NO:

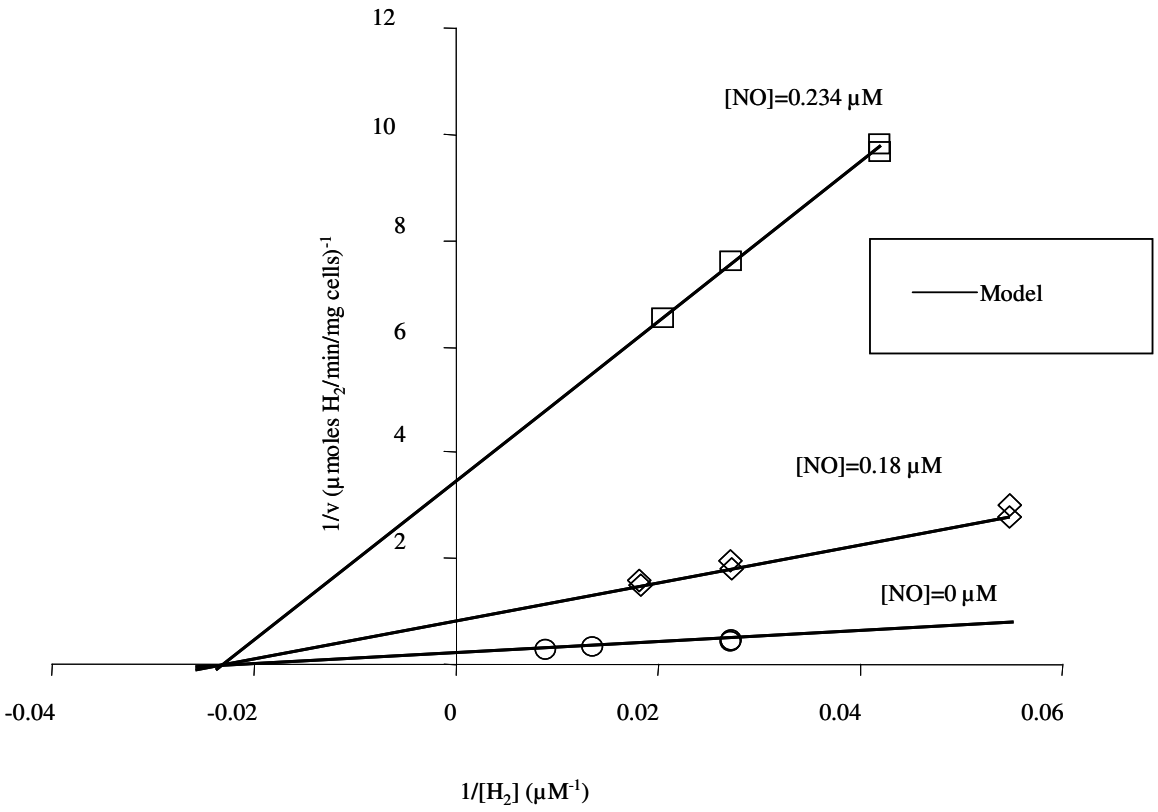

Figure 5.29 Double reciprocal plot of 1/v vs. 1/[H_2] where v is the hydrogenase activity (µmoles min^{-1} mg^{-1}). The studies conducted at 0, 100 ppm (0.18µM) and 130 ppm (0.234 µM) NO are shown here. The solid line represents the model discussed in equations 5.1 and 5.2.

$$v = \frac{V_m}{\left[1 + \frac{K_m}{[H_2]}\right]\left[1 + \left(\frac{[NO]}{K_{NO}}\right)^h\right]} \tag{5.1}$$

where V_m represents the maximum hydrogenase activity (under the experimental conditions of this study), K_m is the Michaelis constant for H_2, K_{NO} is the inhibition constant for NO, and h is a constant for allosteric enzymes that generally refers to the number of interactive binding sites with the inhibitor. Equation 5.1 is the model shown in Figure 5.29.

The double-reciprocal plot for Equation 5.1 is:

$$\frac{1}{v} = \frac{K_m}{V_m}\left[1 + \left(\frac{[NO]}{K_{NO}}\right)^h\right]\frac{1}{[H_2]} + \frac{1}{V_m}\left[1 + \left(\frac{[NO]}{K_{NO}}\right)^h\right] \tag{5.2}$$

Regression analysis of the data in Figure 5.29, as applied to Equation 5.2, resulted in K_m = 37.4 ± 2.3 µM, V_m = 4.8 ± 2.0 U/mg, h = 6.1 ± 0.25 and K_{NO} = 0.141 ± 0.001 µM (95% confidence intervals). Therefore, it appears that NO interacts with up to six sites on the enzyme if NO binds as a first-order reaction (Hyman MR 1988). NO can also interact with many species as a second-order reaction (Davis 2001) and thus the interaction sites would be ½ of h or three sites. The possibility of multiple sites of inhibitor-binding has been addressed by Hyman and Arp (Hyman MR 1991), who suggested that NO interacts with at least two distinct hydrogenase sites in *A. vinelandii*, possibly at the Fe-S centers. Other types of non-linear inhibition models include parabolic and hyperbolic inhibitions (Blanchard and Waldrop 1998; Roberts 1977). Further, it has also been observed that

certain hydrogenases, like the Fe-only hydrogenase of *Clostridium pasteurianum,* have up to five distinct [Fe-S] clusters (Peters et al. 1998). Therefore, numerous binding sites for NO are feasible although the details of hydrogenase binding domains for *Clostridium carboxidivorans* $P7^T$ have not been assessed. The K_m value of 37.4 μM for H_2 is similar to the literature value of 37 μM (Schneider K 1976) for a study conducted on the hydrogenase of *A .eutrophus* H16 in the absence of any inhibitor.

Figure 5.30 presents the percent inhibition of the hydrogenase enzyme with varying concentrations of NO and hydrogen. The solid line represents the model fit to Equation 5.1 in which % inhibition is the activity (v_{NO}) in the presence of NO divided by the specific activity in the absence of NO i.e., v_{NO}/v. The plot indicates that NO is a potent inhibitor of hydrogenase activity and that almost the entire inhibition occurs in a very narrow range of NO concentrations. Below 40 ppm NO, there was no inhibition of the hydrogenase, and above 160 ppm NO, there was almost complete inhibition.

5.4 Conclusions

The studies conducted with varying concentrations of NO and with varying partial pressures of CO showed certain pronounced effects of both gases on the microbial catalyst and the fermentation. These effects can be summarized as follows:

- Hydrogenase inhibition by CO: At partial pressures of more than 1 atm CO, the hydrogenase activity decreased by almost 97 % compared to that at lower partial

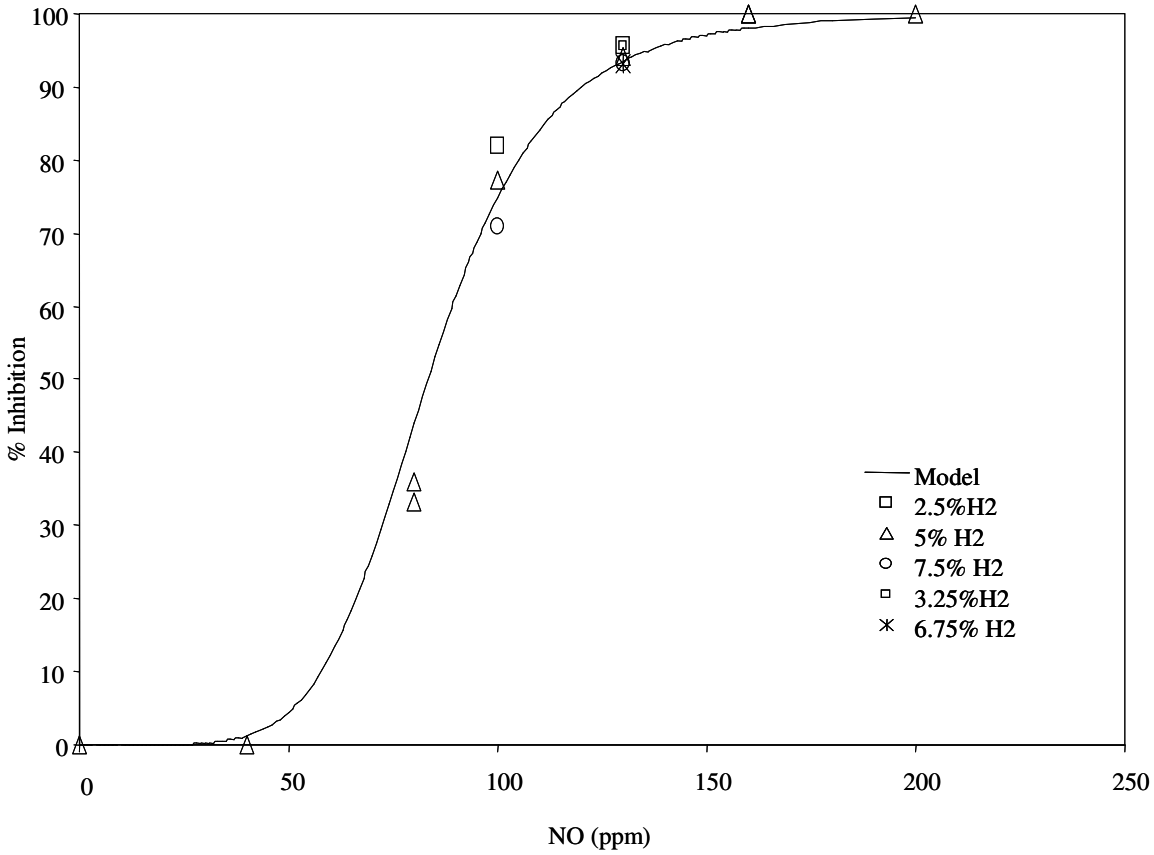

Figure 5.30 Percent inhibition of the hydrogenase enzyme with varying concentrations of NO and hydrogen. The solid line represents the model fit to Equation 5.1 in which % inhibition is the activity (v_{NO}) in the presence of NO divided by the specific activity in the absence of NO (v_{NO}/v).

pressures. This indicates the range of CO partial pressures that can be used without compromising the hydrogenase activity.

- Hydrogenase inhibition by NO: The presence of NO at concentrations above 40 ppm led to a reversible inhibition of hydrogenase activity. The inhibition was non-competitive in nature, as discussed in Section 5.3.4.
- Initial cell-growth inhibition by NO: At concentrations above 80 ppm, NO inhibited initial cell-growth, i.e., the cells could not start growing in the presence of NO. However, when NO was introduced after the cells started growing, there was no inhibition.
- Product redistribution by NO: At all concentrations tested, NO increased the ethanol concentration by approximately 5-7 times and the acetic acid concentration by 1.1-1.5 times.

The rapid increase in the ethanol concentration following exposure to NO suggests that NO plays a role in the up-regulation of ethanol production. Since the onset of solventogenesis is often associated with the onset of sporulation (Durre and Hollergschwandner 2004), it is feasible that NO promotes solventogenesis and sporulation may eventually occur. Interestingly, the increase in ethanol concentration was a result also seen in previous studies with biomass-generated synthesis gas (Datar et al. 2004) indicating that NO may also be the cause of the product redistribution seen in the presence of synthesis gas. Thus, it appears that NO affects both the hydrogenase enzyme and the product re-distribution. Chapter 6 discusses the effects of NO on alcohol dehydrogenase, an enzyme utilized between acetyl CoA and ethanol (see Figure 5.1).

Though it is desirable for cells to produce high amounts of ethanol, the presence of NO in synthesis gas may not be entirely advantageous. As NO inhibits the hydrogenase activity, electrons for ethanol formation must come from CO rather than H_2, thus reducing the available carbon for product formation. This would reduce the carbon conversion efficiency of the process. Another problem that arises in the presence of NO is the initial growth inhibition. Removal of NO from the synthesis gas may therefore alleviate these problems and allow the H_2 to supply the required electrons. The reduction in NO could be done either by increasing the efficiency of the gasification system to eliminate any combustion that may be occurring (NO is produced during combustion but not gasification) (West et al. 2005) or by scavenging NO using sodium hypochlorite, potassium permanganate, or sodium hydroxide (Brogren et al. 1997; Chu et al. 2001; Sada et al. 1978). Nevertheless, this study shows that NO concentrations below 40 ppm have no effect on hydrogenase activity of *C. carboxidivorans* $P7^T$.

CHAPTER 6

METABOLIC REGULATION OF *C. CARBOXIDIVORANS* P7^T: EFFECTS ON ALCOHOL DEHYDROGENASE

6.1 Introduction

Clostridium carboxidivorans P7^T is a strictly anaerobic acetogen that uses the acetyl-CoA pathway for its metabolism. Chapter 2 outlines the acetyl-CoA pathway and describes the role of key enzymes. Acetogens typically display a "biphasic fermentation pattern" (Girbal et al. 1995b). During exponential growth, acetogens produce high amounts of acetate and butyrate (acetogenesis or acidogenesis); and when the growth slows down, they produce alcohols such as ethanol and butanol (solventogenesis). Acid production is favored during cell-growth as it leads to the generation of ATP, which provides cellular energy. When the organism has sufficient energy, the metabolism switches to solventogenesis. Several researchers have tried to predict and control the onset of solventogenesis. Factors like pH, ATP levels, acid concentration, sporulation, availability of reducing energy and iron-limitation among others have been found to influence alcohol production by clostridia (Adler and Crow 1987; Durre et al. 1995; Durre and Hollergschwandner 2004; Girbal et al. 1995a; Girbal et al. 1995b; Gottschal and Morris 1981; Guedon et al. 1999; Meyer and Papoutsakis 1989). These factors can be

used to regulate the metabolic pathway towards solventogenesis in order to increase ethanol yields during fermentation.

In the solventogenic branch of the pathway, acetyl CoA is first converted to acetaldehyde by the action of aldehyde dehydrogenase and acetaldehyde is then converted to ethanol by the action of alcohol dehydrogenase (ADH) as shown by equations 6.1 and 6.2.

$$Acetyl - CoA + NADH + H^+ \rightarrow Acetaldehyde + NAD^+ + CoA - SH \quad (6.1)$$

$$Acetaldehyde + NADH + H^+ \rightarrow Ethanol + NAD^+ \quad (6.2)$$

Therefore, the ethanol-forming branch of the pathway requires reducing energy in the form of NADH. However, the NAD+ formed in the above reactions then needs to be regenerated to NADH for the reactions to proceed. This is typically carried out with the help of reduced Ferredoxin (FdH_2) as shown in equation 6.3 (Rao and Mutharasan 1989).

$$NAD^+ + FdH_2 \Leftrightarrow NADH + Fd \quad (6.3)$$

This reaction is reversible, and depending on the culture conditions, either FdH_2 or NADH may form(Rao and Mutharasan 1987). Artificial electron carriers like neutral red (Girbal et al. 1995a; Girbal et al. 1995b), methyl viologen (Peguin 1994; Peguin and Soucaille 1995; Rao 1986), and benzyl viologen (Rao and Mutharasan 1987) can replace the natural electron carrier (Fd) and provide electrons to NAD^+, thereby reducing NAD^+ to NADH and regulating the pathway towards solventogenesis. Muthasaran et al. (1987) observed that the addition of a viologen dye to an acidogenic culture led to an immediate reduction of the dye, an increase in alcohol and decrease in acid production by a culture

of *C. acetobutylicum* (Rao and Mutharasan 1987). Girbal et al. (1995b) proposed that the increased alcohol production upon addition of neutral red was due to a simultaneous utilization of ferredoxin and the dye, which resulted in a pool of NADH.

Artificial electron carriers have only been studied in glucose-based media. The effects of adding electron carriers have not been assessed in the case of syngas fermentation. This chapter describes the effect of neutral red on product distribution and ADH activity in *C. carboxidivorans* $P7^T$ cultures grown on a CO/CO_2 gas mixture and synthetic syngas. In chapter 5, the effect of nitric oxide on product distribution was discussed. It was seen that nitric oxide caused an increase in ethanol production during syngas fermentation. This chapter also describes studies conducted to further the understanding of this effect, by monitoring ADH activities in the presence of NO.

6.2 Materials and Methods

6.2.1 Microbial Catalyst and Culture Medium

Clostridium carboxidivorans $P7^T$ was the microbial catalyst used for fermentation of syngas. The bacterium was grown under strictly anaerobic conditions in a medium containing (per liter) 30 ml mineral stock solution, 10 ml trace metal stock solution, 10 ml vitamin stock solution, 0.5 g yeast extract, 5 g morpholinoethanesulfonic acid (MES), and 10 ml of 4% cysteine-sulfide solution. Resazurin solution (0.1%) was added as a redox indicator. The composition of the mineral, vitamin and trace metal stock solutions was the same as that described in chapter 3.

6.2.2 Batch Studies

Batch experiments were conducted in 250-ml serum bottles with 100 ml of liquid media to assess the effects of neutral red on cell growth, pH and product formation. As there was no external pH control in the batch studies, a higher amount of MES buffer was used in batch, than in chemostat studies. The media was boiled and purged with nitrogen for 5 minutes to remove oxygen and then sterilized in an autoclave (Primus Sterilizer Co. Inc.) at 121°C for 20 minutes. The bottles were allowed to cool and the headspace was again purged with N_2 for approximately 1 minute. Cysteine sulfide (1 ml) was added to scavenge any remaining dissolved oxygen and the reactors were pressurized with a mixture of 80% CO and 20% CO_2 at 10 psig. Reactors were then inoculated with 1 ml inoculum and placed at 37°C in a shaker (Innova 2100, New Brunswick Scientific). After the cells started growing, neutral red (Sigma-Aldrich Inc., St. Louis, MO) was added to one set of reactors through a 0.2-µm sterile filter. Studies were carried out with 0.1 mM, 0.2 mM, 0.4 mM and 1 mM neutral red. In one study, 0.1 mM NADH (Sigma-Aldrich Inc., St. Louis, MO) was added to one set of reactors. This was done to determine whether the addition of NADH to the media would result in an increased ethanol production, as the cells require NADH in the solventogenic branch. All studies were performed in triplicate and had one set of controls with no neutral red or NADH. Cell-concentration, pH and products were measured at regular time intervals for all the reactors.

6.2.3 Semi-Batch Studies

Experiments to monitor ADH activity in the presence of neutral red and nitric oxide were conducted in 500-mlCytostir® cell culture flasks (Kontes/Kimble Glass Inc., Vineland, NJ) with two sampling arms. Each sampling arm contained a rubber stopper for inoculation, sampling, and gas sparging. One liter of media, excluding the cysteine-sulfide, was prepared and equally distributed into both reactors, following which the reactors were autoclaved at 121°C for 20 minutes. After cooling, the media was continuously purged with N_2 to provide an anaerobic environment. The reactors were then placed in a water bath maintained at 37°C. The water bath was a rectangular propylene tank fitted with a circulating thermostat unit (Model 1112, VWR International, West Chester, PA). The water bath was placed on magnetic stir plates to provide agitation. The water-bath level was always maintained such that the liquid level in the reactors was always below that of the water bath. Following the presence of an anaerobic environment, continuous gas sparging of the feed gases at 10 ml/min was initiated via the use of 18G luer needles for the inlet and outlet.

For the experiments with neutral red, Reactors A (control) and B were sparged with a gas mixture containing 20% CO, 15% CO_2, 5% H_2 and balance N_2 (Air Liquide, Houston, TX). After the cells started growing, 0.1 mM and 0.2 mM filter-sterilized neutral red was added to Reactor B in each study.

For the experiments with nitric oxide, Reactor A (control) was initially sparged with synthetic syngas containing 20% CO, 15% CO_2, 5% H_2 and balance N_2 (Air Liquide, Houston, TX). Reactor B was initially sparged with 20% CO, 15% CO_2, and 5% H_2 with 100 ppm of NO and balance N_2. Combinations of gas cylinders containing

CO, CO_2, H_2, N_2 and NO were mixed using mass flow controllers to obtain the appropriate concentrations. Cysteine-sulfide (5 ml) was then added to each reactor to scavenge any remaining dissolved oxygen. Finally, 5 ml of inoculum was added to each reactor. Since the presence of 100 ppm NO inhibited initial cell-growth, the gas sources were switched once the cell-concentration reached a steady state in Reactor A. In one study, both reactors were started on the same gas mixture (without NO) and then 100 ppm NO was added to Reactor B after the cell concentration stabilized.

For all the experiments described above, samples (1.5 ml) were taken periodically from each reactor to measure the OD, pH, and product concentrations. Samples for ADH activity (0.4-0.6 ml) were also obtained.

6.2.4 Alcohol Dehydrogenase Assays

Equation 6.2 indicates the reaction carried out by alcohol dehydrogenase. ADH activities were measured in both forward and reverse directions. Acetaldehyde was used as the substrate for the forward assay and ethanol was used for the reverse assay. In both cases, triton X-100 was used to permeabilize the cell membranes, as these assays were carried out with whole cell-broth. The forward assay buffer contained 0.4 ml 1M Tris-HCl, 0.5 ml 0.08 M dithiothreitol, 0.1 ml 5% v/v triton X-100, 0.12 ml 0.01 M NADH, 0.4 ml 0.1 M acetaldehyde and 1.5 ml degassed DI water (adapted from (Sridhar et al. 2000)). All chemicals were purchased from Sigma-Aldrich Inc., St. Louis, MO. The reverse assay buffer contained 0.4 ml 1M Tris-HCl, 0.2 ml 0.04 M benzyl viologen, 0.1ml 5% v/v triton X-100, 0.2 ml 0.04 M dithiothreitol, 0.2 ml of 0.04 mM ethanol and 3 ml degassed DI water.

All the above reagents, except for dithiothreitol and NADH, were prepared and stored in an anaerobic glove box (Coy Laboratory Products Inc., Grass Lake, MI). Dithiothreitol and NADH were freshly prepared each day as they are both unstable in water. Within the anaerobic chamber, the reagents were added in the above quantities to a 4.5-ml optical glass cuvette (Starna Cells Inc., Atascadero, CA) fitted with 10-mm screw caps (SCHOTT Corp., Yonkers, NY) and 13-mm butyl rubber stoppers (Bellco Glass Inc., Vineland, NJ). The cuvette was then removed from the chamber and purged with 100% N_2 for approximately one minute, using a 23 G long stainless steel needle as the inlet and a short 22 G needle as the outlet. The cuvette was placed in a 30°C receptacle of a spectrophotometer (Varian Inc., Palo Alto, CA). A gas-tight syringe was used to transport approximately 0.5 ml of anoxic broth from the reactor to the cuvette, after which the cuvette was shaken vigorously, placed in the spectrophotometer, and the absorbance (Abs) recorded every 0.5 seconds. For the forward assay, the wavelength was set to 340 nm and for the reverse assay it was set to 546 nm.

The concentration (C) of NAD^+ or reduced benzyl viologen was obtained from Beer's law: $C=Abs/(\varepsilon \cdot b)$, where b is the cuvette path length (1 cm) and ϵ is the extinction coefficient for NADH (6.22 $mM^{-1}cm^{-1}$ at 340 nm) in the forward assay and for benzyl viologen (7.55 $mM^{-1}cm^{-1}$ at 546 nm) in the reverse assay. The maximum rate of reaction (R) was calculated from the linear slope of the initial portion of the curve following the short lag phase ($R=\Delta C/\Delta t$). R was finally divided by the measured cell mass and converted into specific activity (U/mg) where U represents µmols of ethanol or acetaldehyde consumed per minute.

For the cell density, samples were collected in 4-ml cuvettes and the OD was measured at 660 nm using a UV-Vis spectrophotometer. The optical density (OD) is proportional to the cell density (~ 0.43 g/l per OD unit (Datar 2003)) as obtained from a standard calibration chart showing a linear range of cell density between 0 to 0.4 OD units. Samples with an OD greater than 0.4 units were diluted so that the OD was within the linear range of calibration. The cell density was the multiplied by the volume of broth injected to obtain the cell mass.

6.2.5 Product and Gas Analysis

Once the cell density and pH were measured, the samples from the reactors were centrifuged at 14000 rpm for 10 minutes. The cell-free supernatant was then analyzed for ethanol and acetic acid using a 6890 Gas Chromatograph (Agilent Technologies, Wilmington, DE), with a flame ionization detector and an 8-ft Porapak QS 80/100 column (Alltech, Deerfield, IL).

Gas samples were taken periodically to measure the CO, CO_2, H_2 and NO concentrations in the inlet and outlet gas streams. Two 6890 Gas Chromatographs (Agilent Technologies, Wilmington, DE), each with a TCD, were used to measure CO, CO_2 and H_2. A Chemiluminescence analyzer (Sievers) was used to measure the NO concentration.

6.3 Results and Discussion

6.3.1 Batch Studies –Effect of Neutral Red

Batch studies were conducted with 0.1, 0.2, 0.4 and 1mM neutral red and with 0.1mM NADH. All batch studies were in triplicate and are referred to as Set A (control), Set B (neutral red studies) and Set C (NADH studies), where each set consisted of three reactors. Figure 6.1 shows the cell concentration profile for the batch studies. The error bars shown in the figures indicate the standard error calculated from the standard deviation of the date from the three reactors in each set. Set A was a control, while 0.1 mM neutral red was added to Set B and 0.1 mM NADH was added to Set C on Day 1.6. The figure indicates that neither of the compounds had any effect on cell growth or pH. The amount of ethanol produced per cell mass is shown in Figure 6.2. All the reactors showed similar amounts of ethanol until Day 1.6 when NADH and neutral red were added to the respective reactors. On adding neutral red, the average value of ethanol increased from 0.05 g/g cells to about 0.2 g/g cells in Set A. The addition of NADH had no effect on ethanol production as Set A and Set C remained at 0.05 g/g cells. Figure 6.3 shows the acetic acid per cell mass. All sets of reactors had similar profiles, indicating that neutral red and NADH had no effect on acetic acid production by the cells.

Figures 6.4 and 6.5 show the cell concentration and product profiles in a batch study with 0.2 mM neutral red. The pH could not be recorded during this study due to a malfunction of the pH probe. Neutral red was added on Day 2.6. As shown in Figure 6.4, there was no effect of neutral red on cell-growth. The cell concentration reached an average steady concentration of 0.16 g/l in both sets of reactors. However, as shown in Figure 6.5, addition of neutral red caused the ethanol concentration to increase

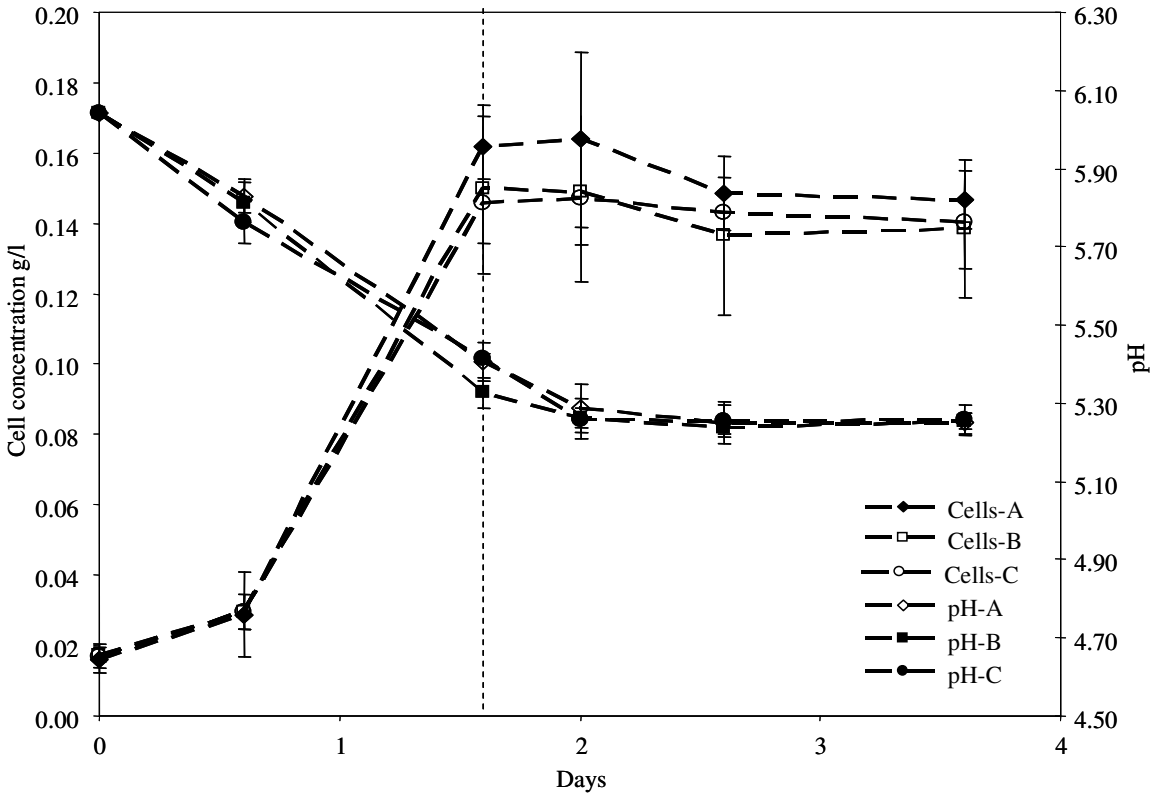

Figure 6.1 Cell concentration and pH profiles in the presence of 0.1mM neutral red (B) and 0.1mM NADH (C). Set A was the control with no neutral red or NADH. The error bars represent standard error (n=3).

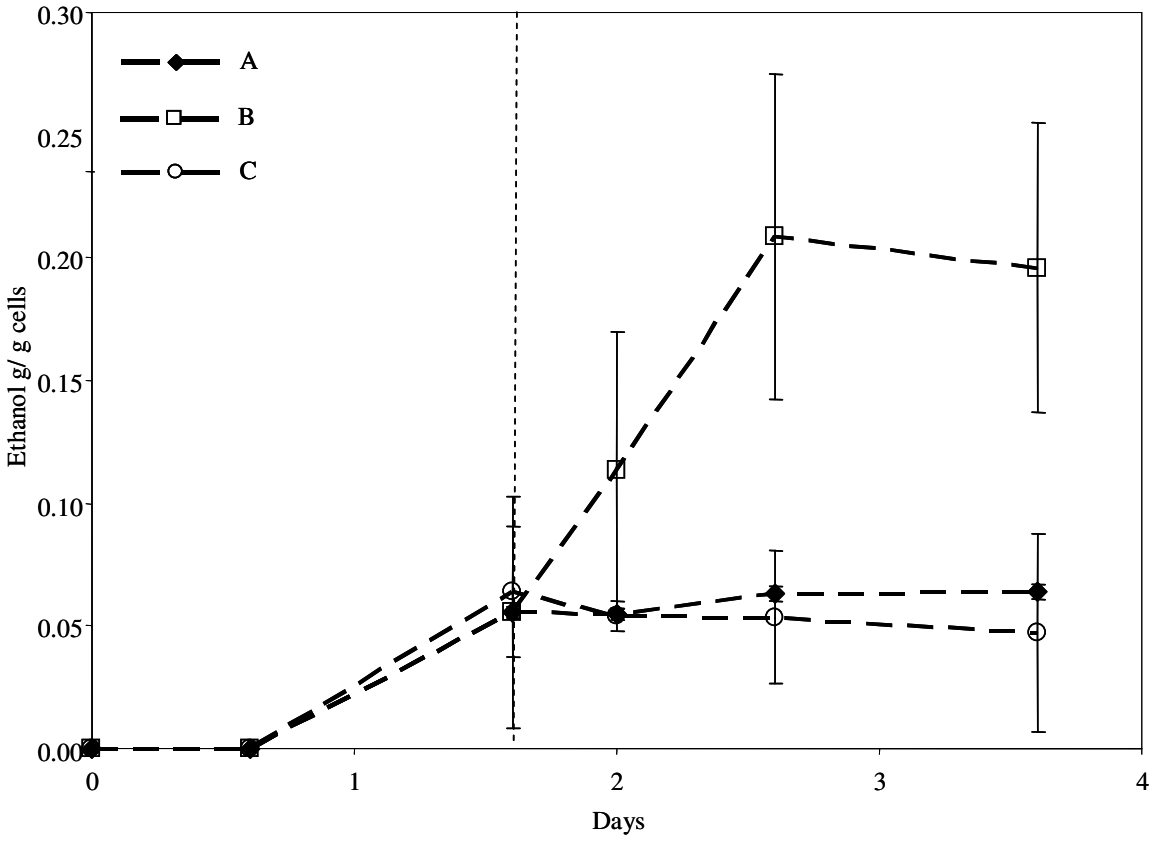

Figure 6.2 Ethanol per cell mass (g/g). Set A consisted of three control reactors. The vertical line represents the time at which 0.1 mM neutral red was added to Set B and 0.1 mM NADH was added to Set C. The error bars represents standard error (n=3).

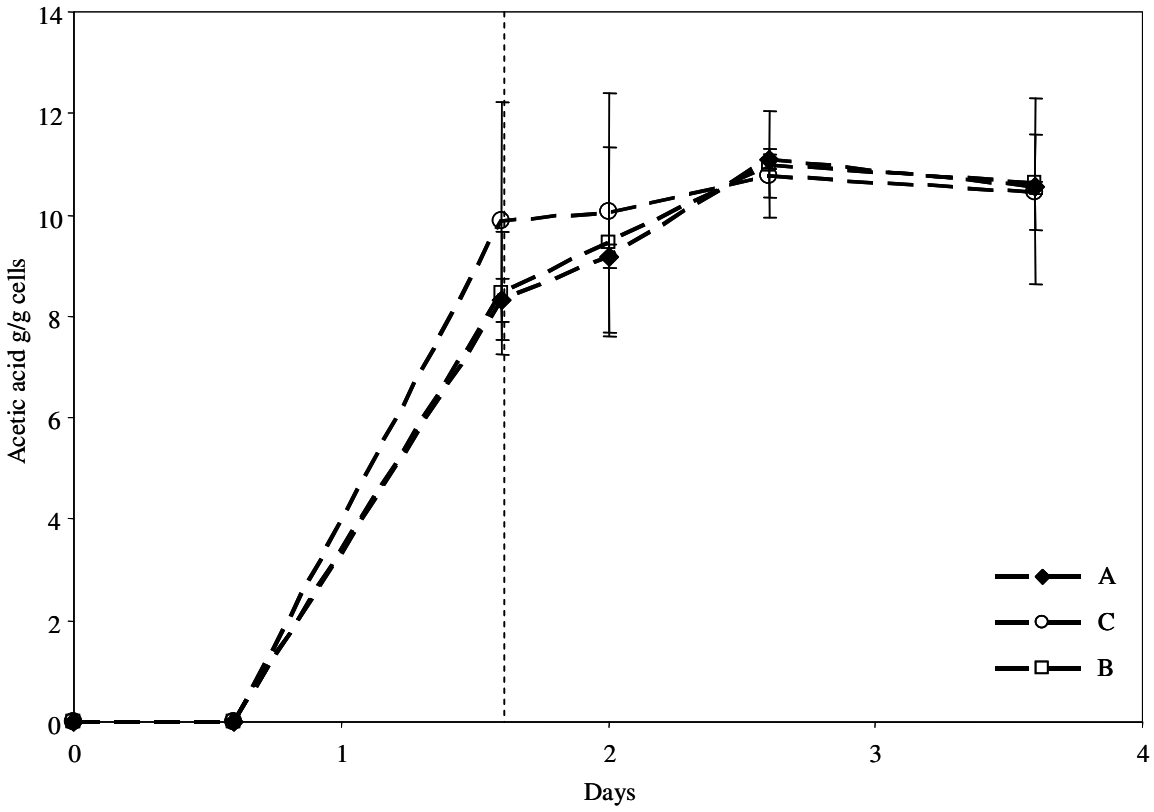

Figure 6.3 Acetic acid per cell mass (g/g). Set A consisted of three control reactors. The vertical line represents the time at which 0.1 mM neutral red was added to Set B and 0.1 mM NADH was added to Set C. The error bars represents standard error (n=3).

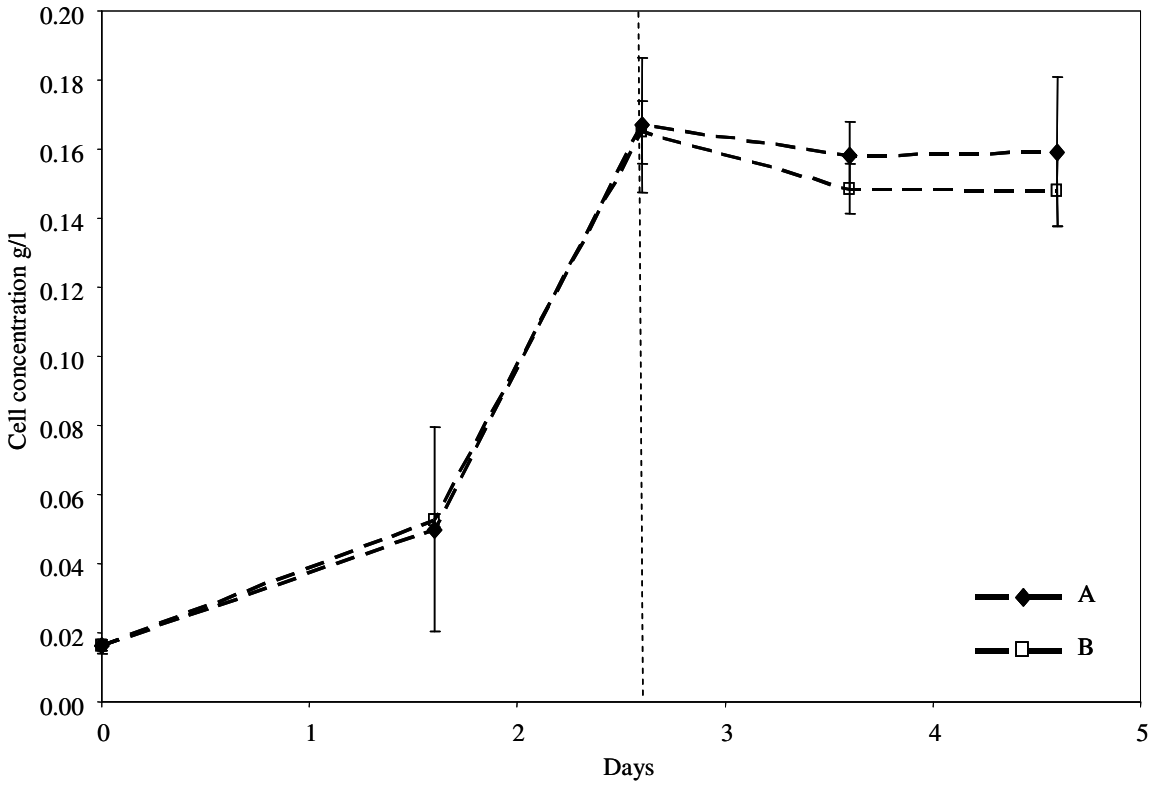

Figure 6.4 Effect of 0.2 mM neutral red on cell-growth. The error bars represent the standard error (n=3) and the vertical line represents the time at which neutral red was added to the reactors in Set B.

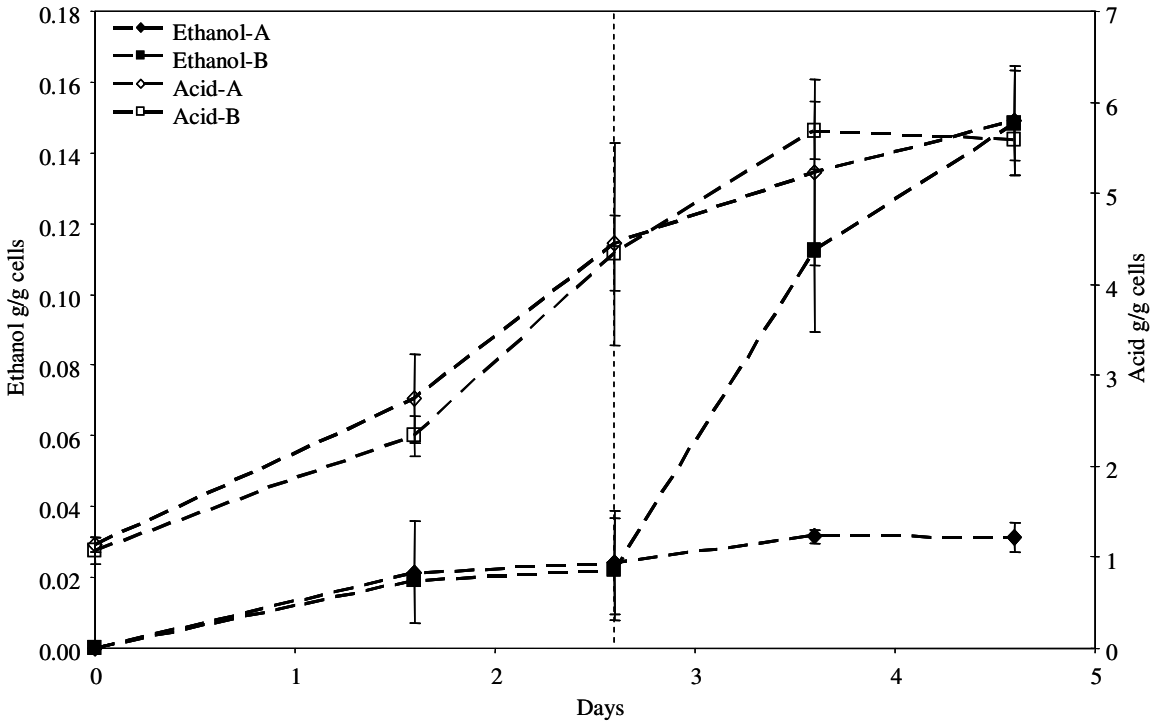

Figure 6.5 Ethanol and acetic acid per cell mass (g/g). The error bars represent the standard error (n=3). The vertical line represents the time at which neutral red was added to Set B.

in Set B from 0.02 g/g cells to about 0.15 g/ g cells. The ethanol in Set A with no neutral red remained at 0.02 g/g cells. As seen previously, there was no significant difference in the acetic acid concentrations between Sets A and B. In both sets of reactors, the acetic acid increased from 1 g/g cells to about 6 g/g cells on an average.

Figure 6.6 presents the cell concentration profile in the presence of 0.1 mM (Set B), 0.4 mM (Set C) and 1 mM (Set D) neutral red. Set A represents the control reactors with no neutral red. Neutral red was added to the reactors on day 1.6, as indicated by the vertical line. The profile indicates that neutral red had no effect on the cell concentration. Figure 6.7 shows the effect of neutral red on pH. Set A and Set B showed similar pH profiles, starting at an initial pH of about 6.0 and reaching a final pH of approximately 4.9 during the fermentation. However, in the presence of 0.4 mM and 1 mM neutral red, the final pH values were higher than the control at 5.1 and 5.3 respectively. Figures 6.8 and 6.9 show the ethanol and acetic acid profiles in the presence of neutral red. As seen in previous studies, the addition of neutral red increased the ethanol production. However, this study clearly indicated that with increasing amounts of neutral red, the ethanol produced per cell mass also increased. The final ethanol concentrations per cell mass at 0, 0.1, 0.4 and 1 mM neutral red were 0.39 g/g cells, 0.67 g/g cells, 0.96 g/g cells and 1.92 g/g cells, respectively. On the other hand, the acetic acid concentrations decreased with increasing amounts of neutral red. The final acid concentrations per cell mass at 0, 0.1, 0.4 and 1 mM neutral red were 11.8 g/g cells, 10.4 g/g cells, 7.2 g/g cells and 4.9 g/g cells respectively. This indicated that neutral red altered the electron flow from acid production towards ethanol production by *C. carboxidivorans* $P7^T$.

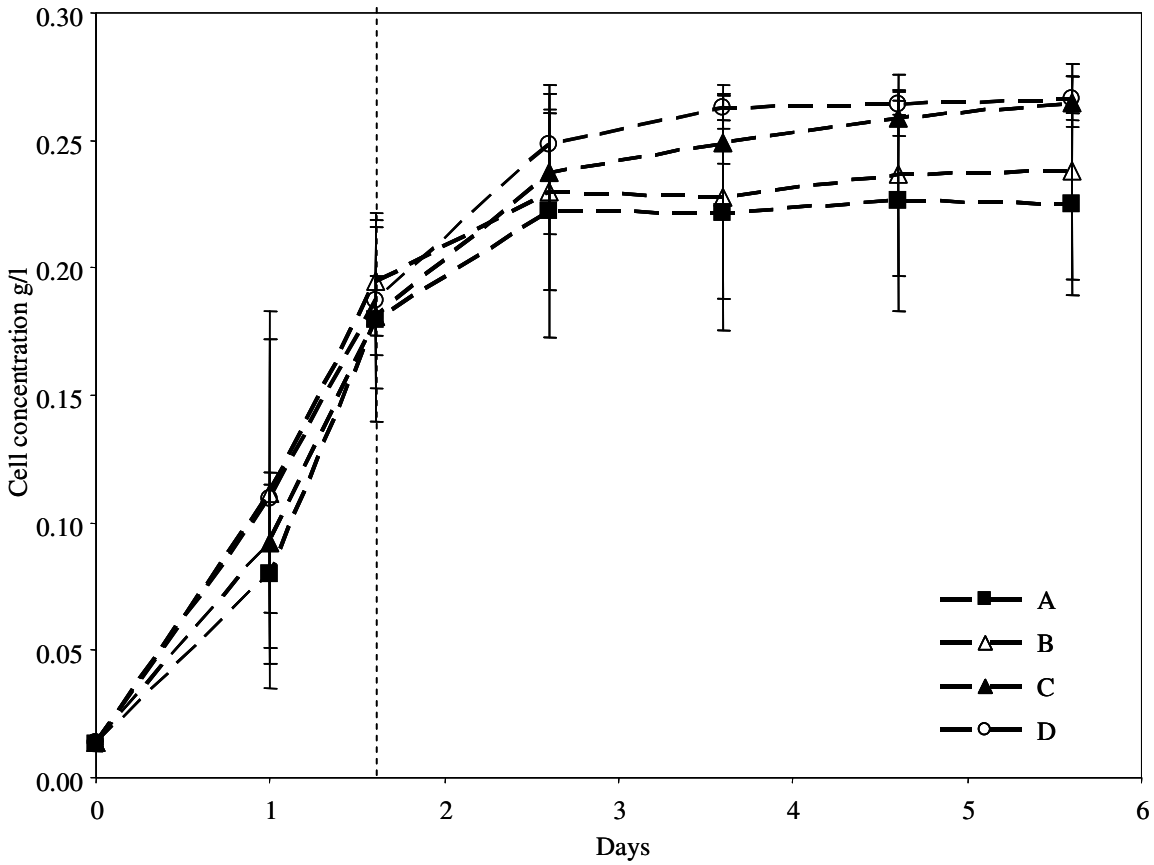

Figure 6.6 Effect of 0.1mM, 0.4mM and 1mM neutral red on cell concentration. The vertical line represents the time at which neutral red was added to Sets B, C and D. Set A was the control with no neutral red. The error bars represent the standard error (n=3).

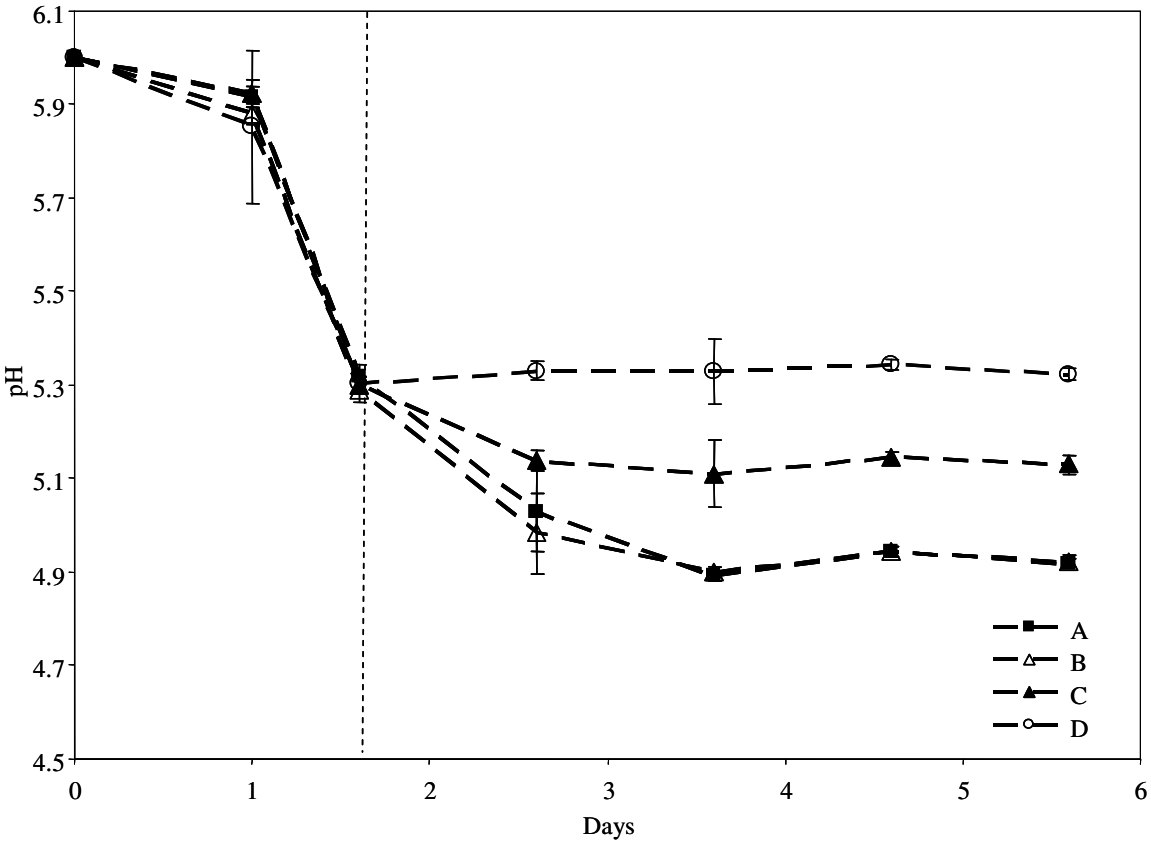

Figure 6.7 Effect of 0.1 mM (B), 0.4 mM(C) and 1 mM (D) neutral red on pH. Set A was a control with no neutral red. The vertical line represents the time at which neutral red was added. The error bars represent the standard error (n=3).

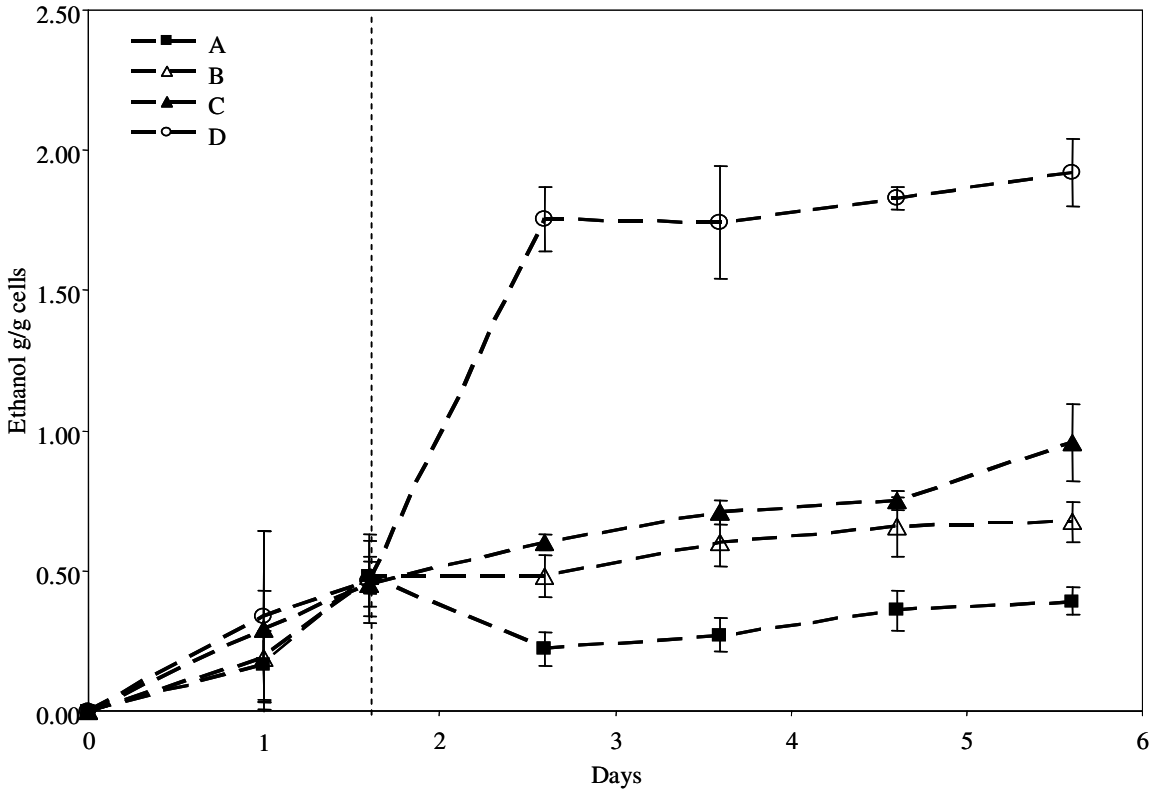

Figure 6.8 Effect of 0.1 mM (B), 0.4 mM(C) and 1 mM (D) neutral red on ethanol per cell mass (g/g). Set A was a control with no neutral red. The vertical line represents the time at which neutral red was added. The error bars represent the standard error (n=3).

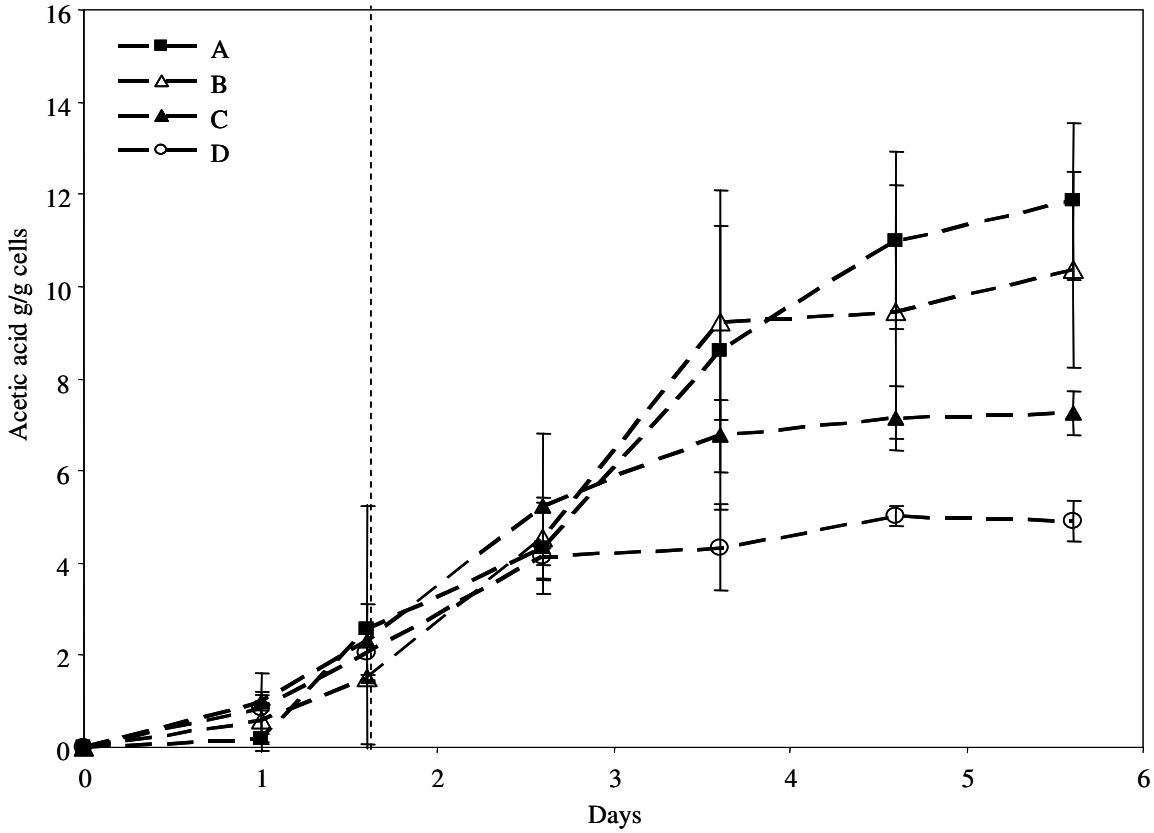

Figure 6.9 Effect of 0.1 mM (B), 0.4 mM(C) and 1 mM (D) neutral red on acetic acid per cell mass (g/g). Set A was a control with no neutral red. The vertical line represents the time at which neutral red was added. The error bars represent the standard error (n=3).

6.3.2 Semi-Batch Studies – Effect of Neutral Red

Semi-batch studies (batch liquid and continuous gas) were conducted to determine the effect of neutral red on ADH activity. In these studies, neutral red was added to Reactor B after the cells started growing. Reactor A was a control with no neutral red. Figure 6.10 shows the cell-concentration and pH profiles in the presence of 0.1mM neutral red in a 500-ml reactor. As shown in the figure, the cells in Reactor A experienced earlier growth and a higher final concentration than those in Reactor B. This difference in growth may not have been due to neutral red since it was not observed in any of the other studies. Neutral red was added to Reactor B on day 5.6, after which, the cell concentration increased from 0.1 g/l to 0.12 g/l, though the cell-concentration was still lower than that of Reactor A (0.16 g/l). Even though this difference in cell-growth may seem like an effect of adding neutral red, this effect was not observed in any of the other experiments indicating that this may have been an anomaly. Moreover, from the growth curve, the difference in cell-concentration can be observed even before the addition of neutral red. The pH profile followed the cell-growth profile in each reactor. The pH in Reactor A started dropping earlier than that in Reactor B. Reactor A reached a final pH of 5.35 and Reactor B reached a final pH of about 5.4.

Figure 6.11 shows the forward and reverse ADH activities during the fermentation. The forward activity is represented by ‘ADH f’ and the reverse activity is represented by ‘ADH r’ on the y-axes. The reverse ADH activity of Reactor A increased to a maximum of 1.88 U/mg on day 4.6 and then dropped to a final value of about 1.46 U/mg subsequently. As the reverse ADH activity dropped, the forward ADH activity increased in Reactor A, reaching a final value of 0.08 U/mg on day 9.6. In Reactor B, the

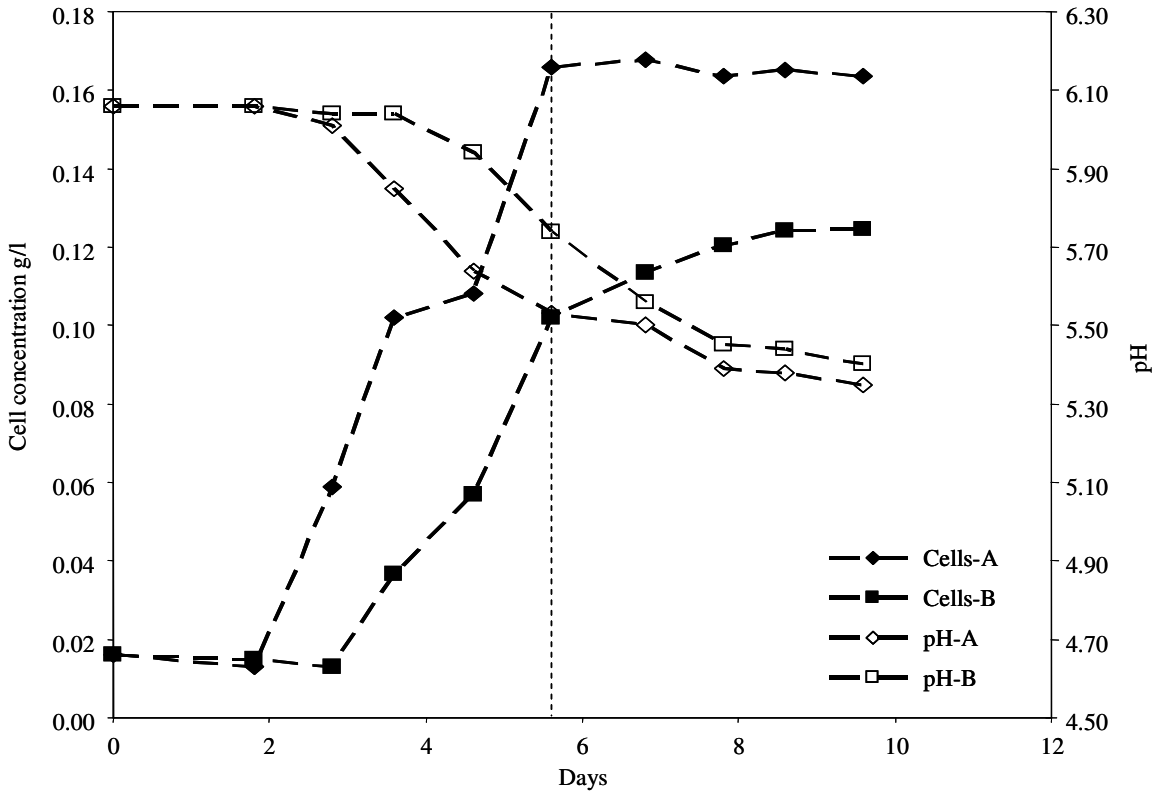

Figure 6.10 Semi-batch study with 0.1 mM neutral red-effect on cell concentration and pH. Reactor A was a control and neutral red was added to Reactor B on Day 5.6, as indicated by the vertical line.

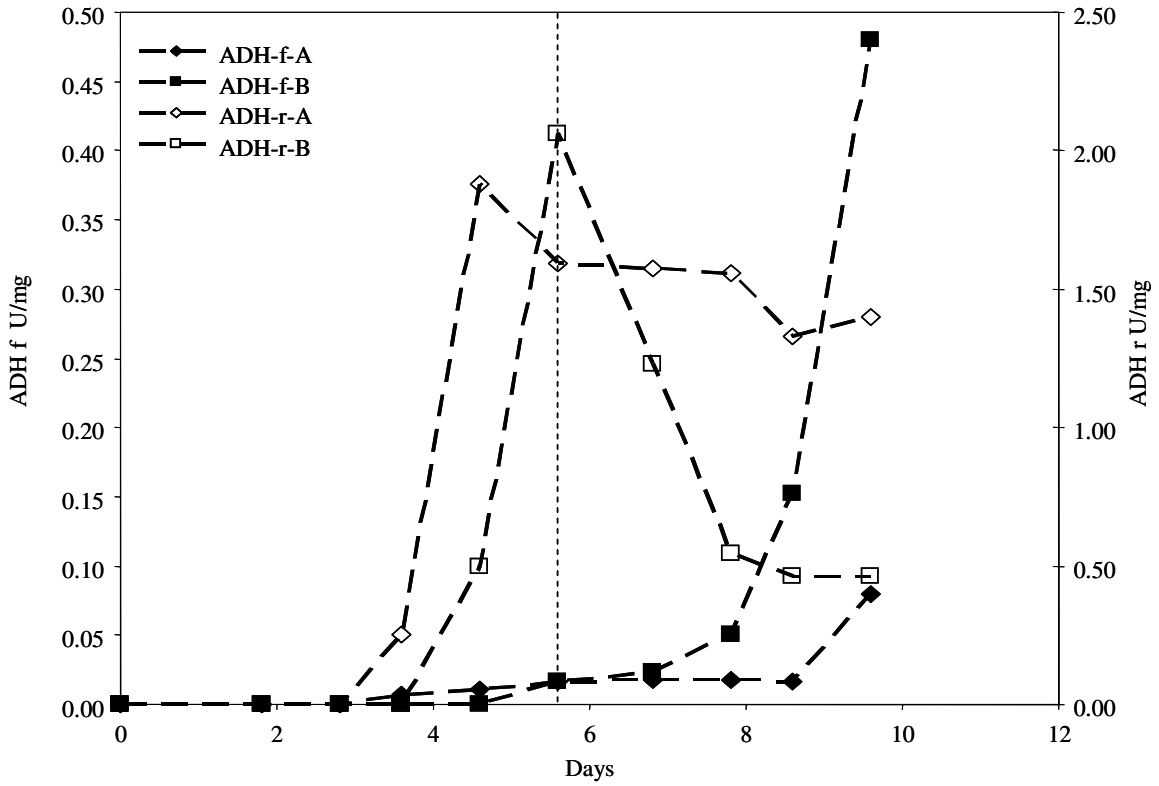

Figure 6.11 Effect of neutral red on ADH activities. The reactors are described in Figure 6.10. The vertical line represents the time at which neutral red was added to Reactor B.

reverse ADH activity increased to about 2 U/mg on day 5.6, at which point, neutral red was added to the reactor. The activity then dropped to about 0.46 U/mg in the next two days and remained at that level. On the other hand, the forward ADH activity started increasing a lot more than what was seen in Reactor A. The final activity in Reactor B reached approximately 0.48 U/mg. This indicated that neutral red caused the reverse ADH activity to decrease and forward ADH activity to increase. In both reactors, the forward ADH activity seemed to increase concurrently with the decrease in the reverse ADH activity. However, in the presence of neutral red, the change in the activities was more significant. This finding also agrees with the increase in ethanol concentration upon addition of neutral red as seen in Figure 6.12. The ethanol per cell mass in the presence of neutral red (Reactor B) increased to about 6.6 g/g cells, while that in Reactor A increased to about 3 g/g cells on day 9.6. The acetic acid concentrations increased to final values of about 7 and 6.7 g/g cells in reactors A and B, respectively. Figure 6.13 shows the cell-concentration and pH profiles in the presence of 0.2 mM neutral red. Neutral red was added on day 2.8, and as the figure shows, there was no effect of neutral red on cell-growth. The cell concentration in both reactors reached a maximum value of about 0.16 g/l and the pH dropped from 6.05 to about 5.08 in Reactor A and 5.19 in Reactor B. The ADH activities are shown in Figure 6.14. In both reactors, the reverse ADH activities increased to approximately 0.58 U/mg on day 3.8, after which the activities decreased in both reactors. In Reactor A, the activity dropped to about 0.25 U/mg, while in Reactor B (with neutral red), it decreased completely to zero. The forward ADH activities increased with the decrease in reverse activities reaching final values of 0.1 U/mg and 0.5 U/mg in reactors A and B respectively. This result was similar to that of the previous study

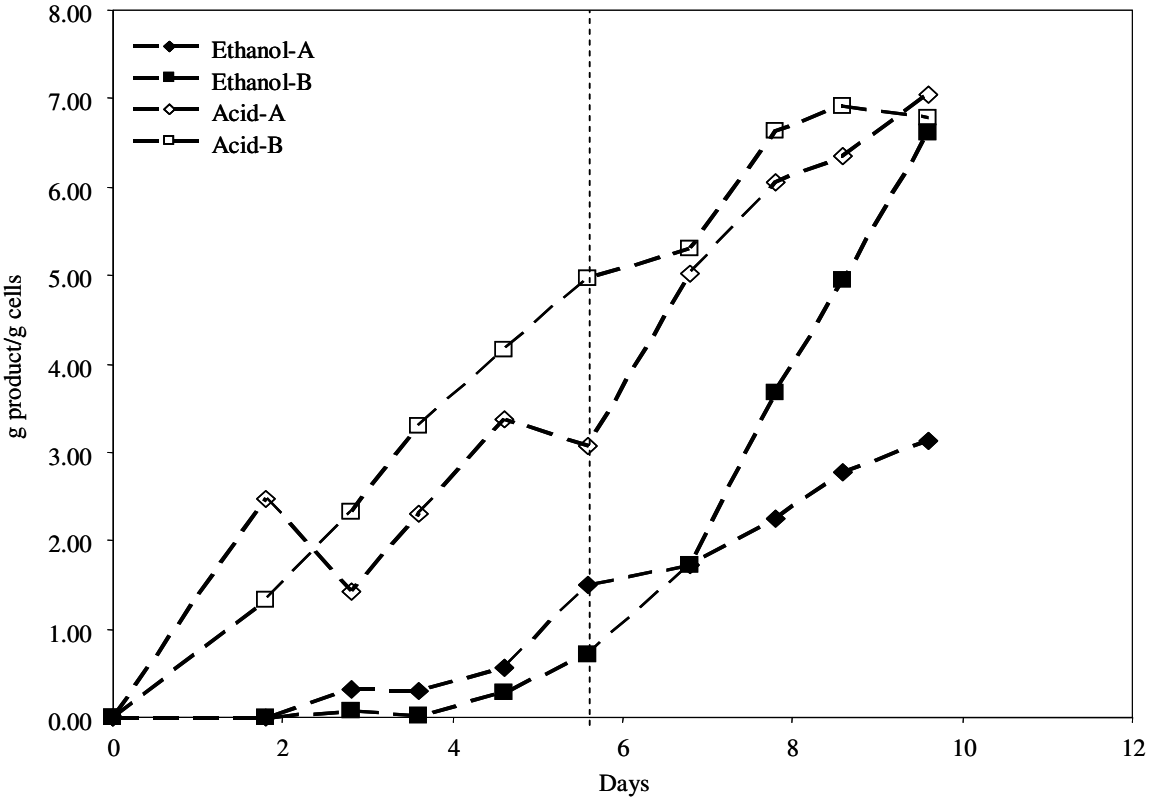

Figure 6.12 Effect of neutral red on products. The reactors are described in Figure 6.10. The vertical line represents the time at which neutral red was added to Reactor B.

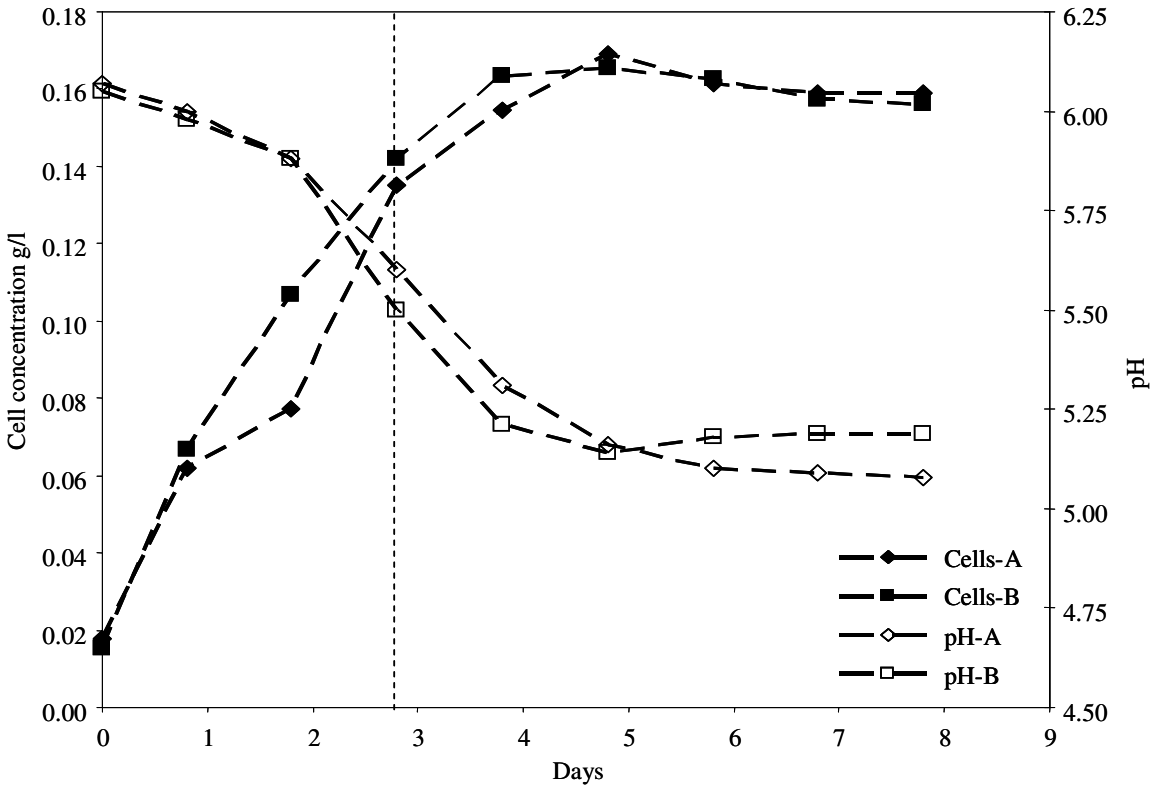

Figure 6.13 Semi-batch study with 0.2 mM neutral red-effect on cell concentration and pH. Reactor A was a control and neutral red was added to Reactor B on Day 2.8, as indicated by the vertical line.

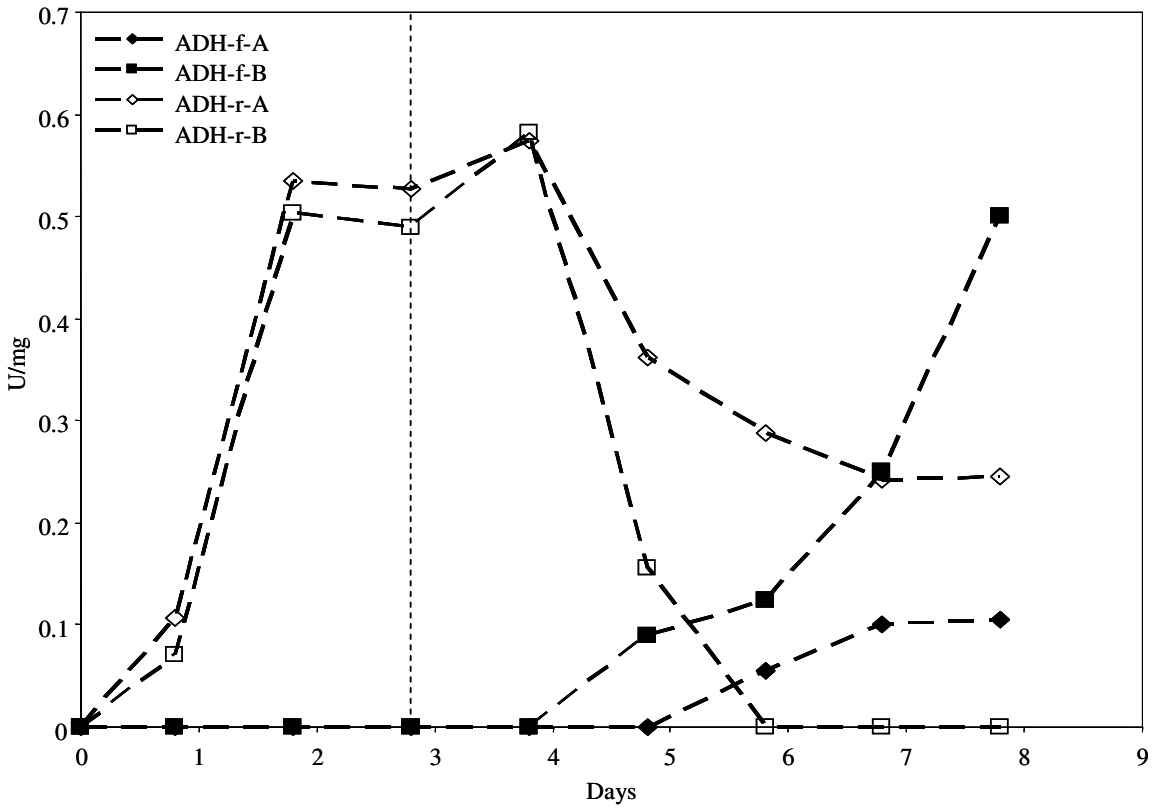

Figure 6.14 Effect of 0.2 mM neutral red on ADH activities. The reactors are described in Figure 6.13. The vertical line shows the time at which neutral red was added to Reactor B.

with 0.1 mM neutral red. As shown in Figure 6.15, on adding neutral red, the ethanol in Reactor B increased from 0.25 g/g cells to about 2.38 g/g cells while that in Reactor A reached a maximum of 0.94 g/g cells. The final acetic acid concentration in Reactor A was 19.4 g/g cells while in Reactor B, it was 18 g/g cells.

A similar study with 0.2 mM neutral red is shown in Figures 6.16, 6.17 and 6.18. The cell concentration and pH profiles are shown in Figure 6.16. The final cell-concentrations on day 5 were 0.163 g/l and 0.155 g/l in reactors A and B, respectively while the pH values were 5.24 and 5.3 respectively. Figure 6.17 shows the ADH activities during the study. As seen before, the reverse ADH activity in Reactor B decreased rapidly towards zero after the addition of neutral red. The activity in Reactor A decreased from its maximum value of 1.46 U/mg to about 0.6 U/mg. The forward ADH activity of the cells in Reactor A increased to about 0.04 U/mg while that in Reactor B increased to about 0.13 U/mg after the addition of neutral red. The product profiles were also similar to the previous results observed, as shown in Figure 6.18. After adding neutral red, the ethanol increased from 0.5 to 4.9 g/g ethanol in Reactor B while the ethanol in Reactor A increased from 0.49 to 1.8 g/g cells. The final acetic acid concentrations were 14g/g cells and 9.8 g/g cells in reactors A and B, respectively.

The studies described above showed that neutral red increased the ethanol concentration and decreased the acetic acid concentration. The enzyme assays showed that the forward ADH activity increased on addition of neutral red, which agrees with the result of increased ethanol formation.

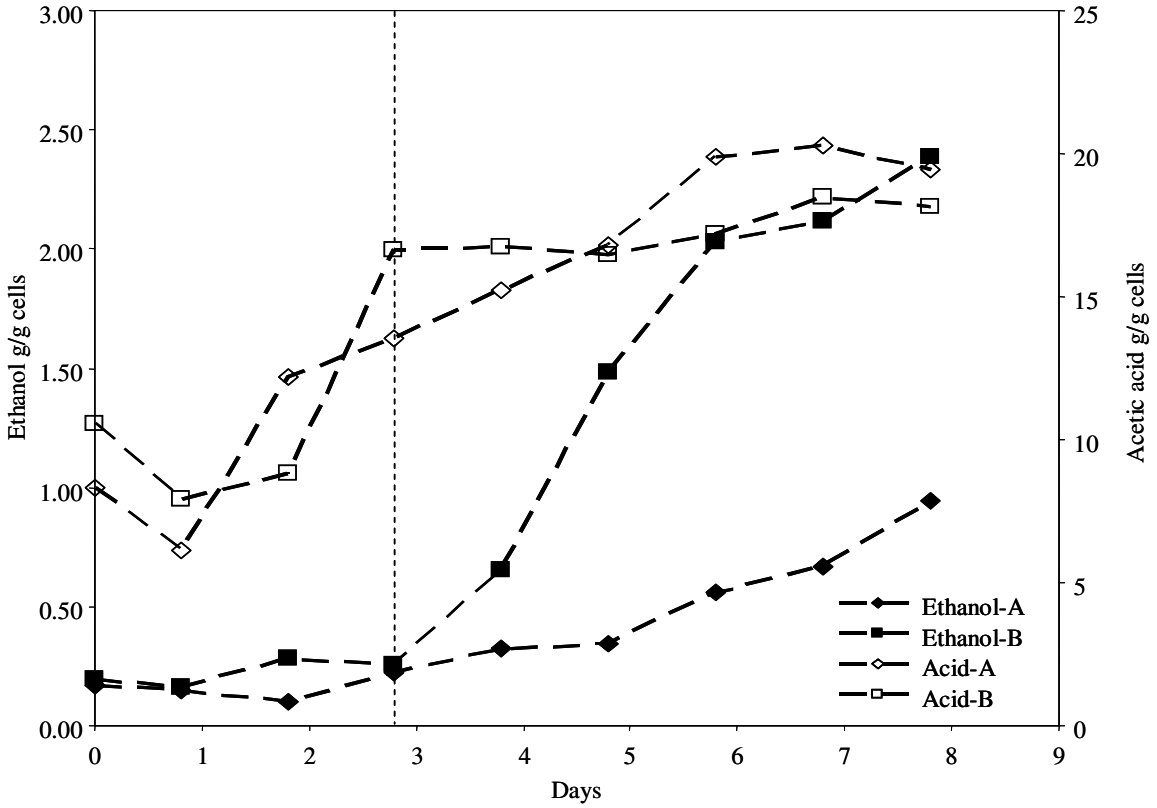

Figure 6.15 Effect of 0.2 mM neutral red on products. The reactors are described in Figure 6.13. The vertical line shows the time at which neutral red was added to Reactor B.

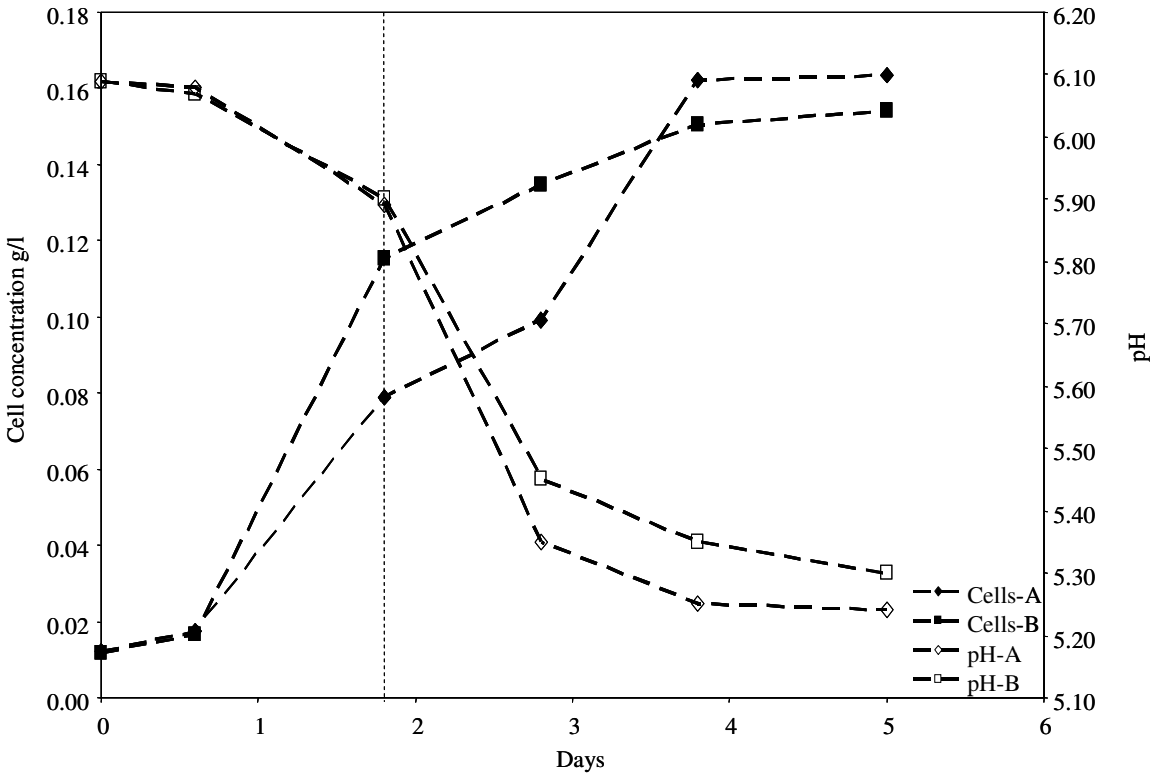

Figure 6.16 Semi-batch study with 0.2 mM neutral red-effect on cell concentration and pH. Reactor A was a control and neutral red was added to Reactor B on Day 1.8, as indicated by the vertical line.

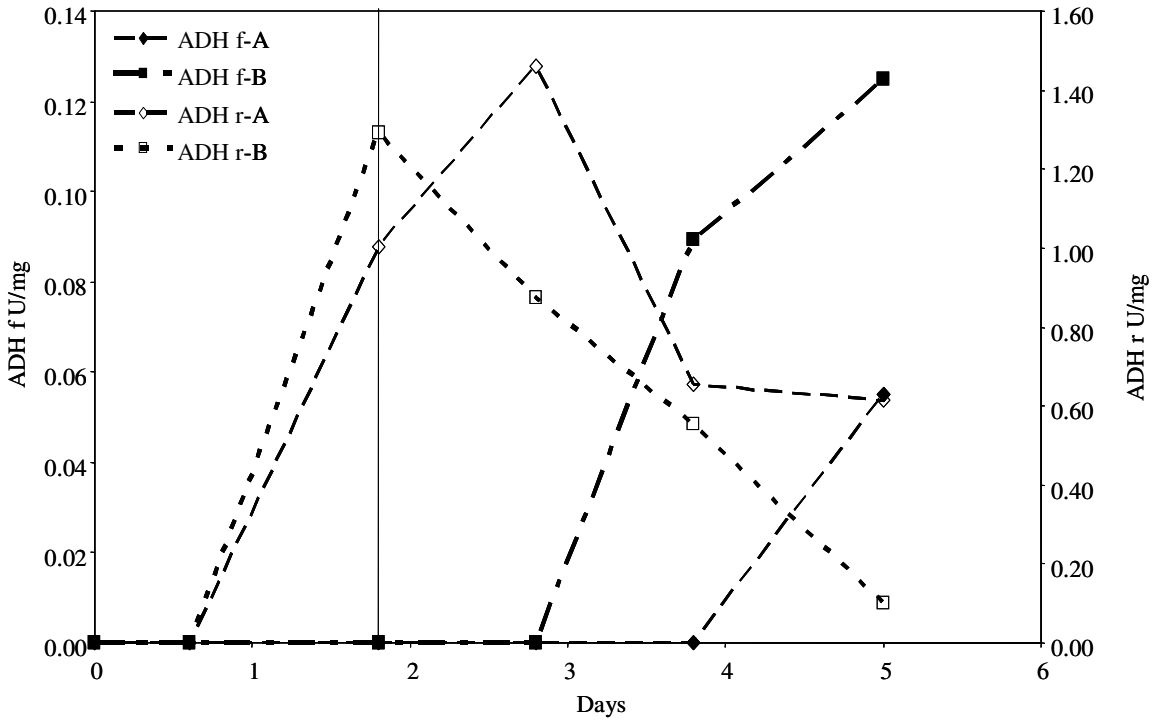

Figure 6.17 Effect of 0.2 mM neutral red on ADH activities. The reactors are described in Figure 6.16. The vertical line shows the time at which neutral red was added to Reactor B.

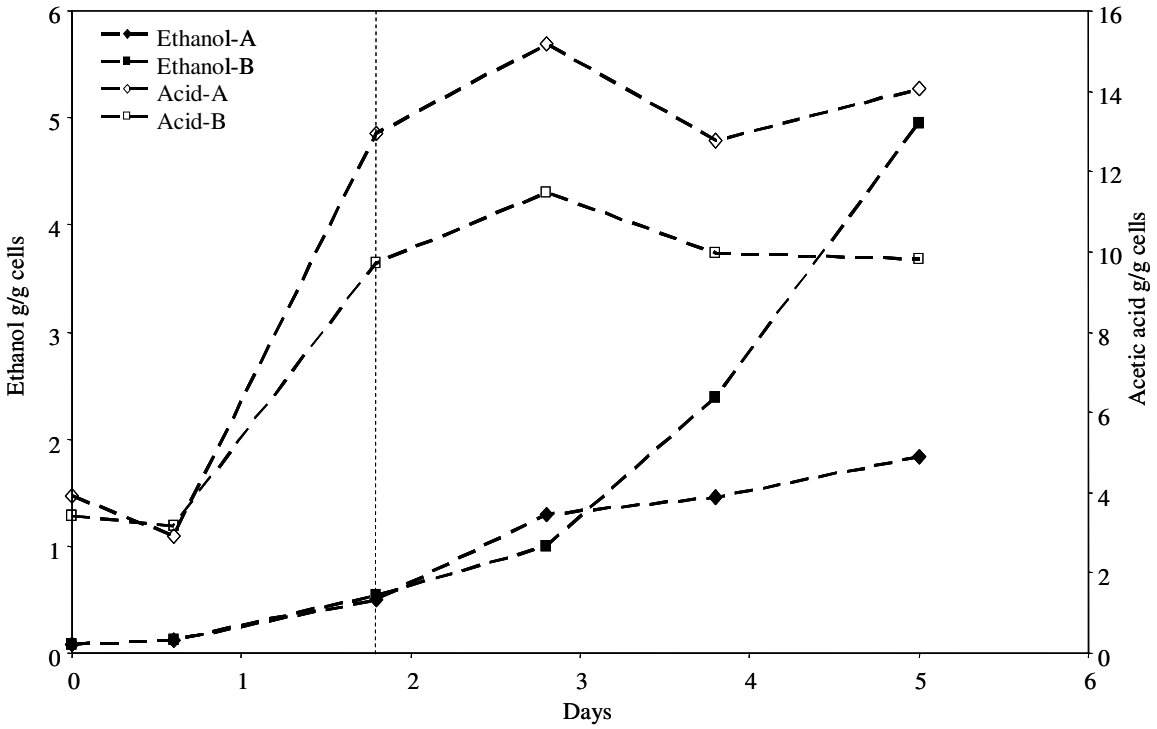

Figure 6.18 Effect of 0.2 mM neutral red on products. The reactors are described in Figure 6.16. The vertical line shows the time at which neutral red was added to Reactor B.

6.3.3 Semi-Batch Studies-Effect of Nitric Oxide

Chapter 5 describes the effects of NO on product distribution during syngas fermentation. It was observed that NO increased the ethanol production by the cells. Three studies were conducted to determine the effect of NO on ADH activities. NO at 100 ppm was tested in all the studies. Figure 6.19 describes the effect of NO on cell-growth and pH. Reactor A was initially exposed to synthetic syngas while Reactor B was exposed to synthetic syngas with 100 ppm NO. On day 4.8, the gases were switched such that Reactor A was now exposed to NO and Reactor B was not. As discussed in Chapter 5, the cells in Reactor B did not grow in the presence of NO, therefore, the pH remained at the initial value of 6.0, dropping slightly to 5.9 on day 7.8 when cell-growth commenced after removal of NO. In Reactor A, the cells grew and reached a concentration of 0.15 g/l, and increased to 0.17 g/l after introducing NO. The pH in this reactor decreased from 6.0 to about 5.3. Figure 6.20 shows the effect of NO on ADH activities. Both the forward and reverse activities in Reactor B remained negligible as there was almost no cell-growth. In Reactor A, the reverse activity increased to about 1.2 U/mg on Day 2.8 and then began to drop. However, instead of reaching a steady state as seen in the studies with neutral red, the activity continued to stop on switching to NO. On day 7.8, the reverse ADH activity was 0.3 U/mg. As the reverse activity began to drop after day 2.8, the forward activity increased to approximately 0.17 U/mg. On switching to NO, the activity started to increase again, reaching a value of 0.34 U/mg on Day 7.8. Figure 6.21 shows the product distribution. As seen in previous studies with NO, the ethanol per cell mass increased on switching to NO from 2 g/g cells to about 5 g/g cells.

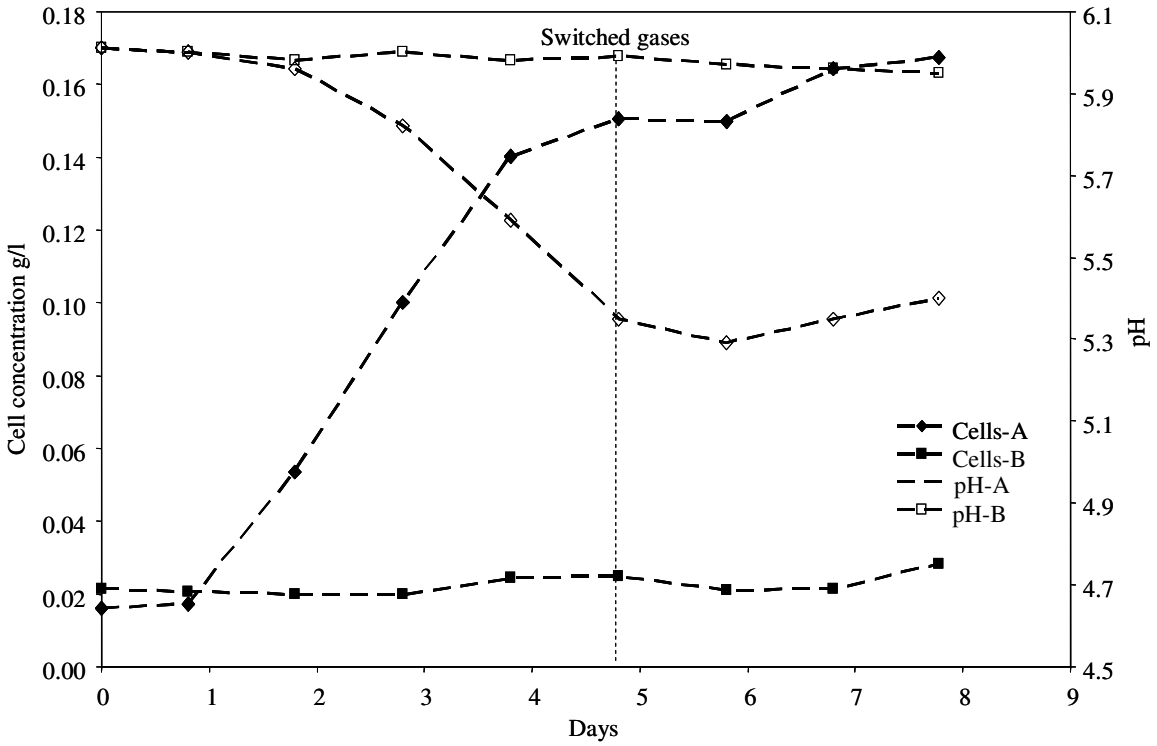

Figure 6.19 Cell concentration and pH profiles in the presence of 100 ppm NO. Reactor A was initially exposed to synthetic syngas and Reactor B was exposed to synthetic syngas containing 100 ppm NO. The vertical line indicates the time when the gas sources were switched.

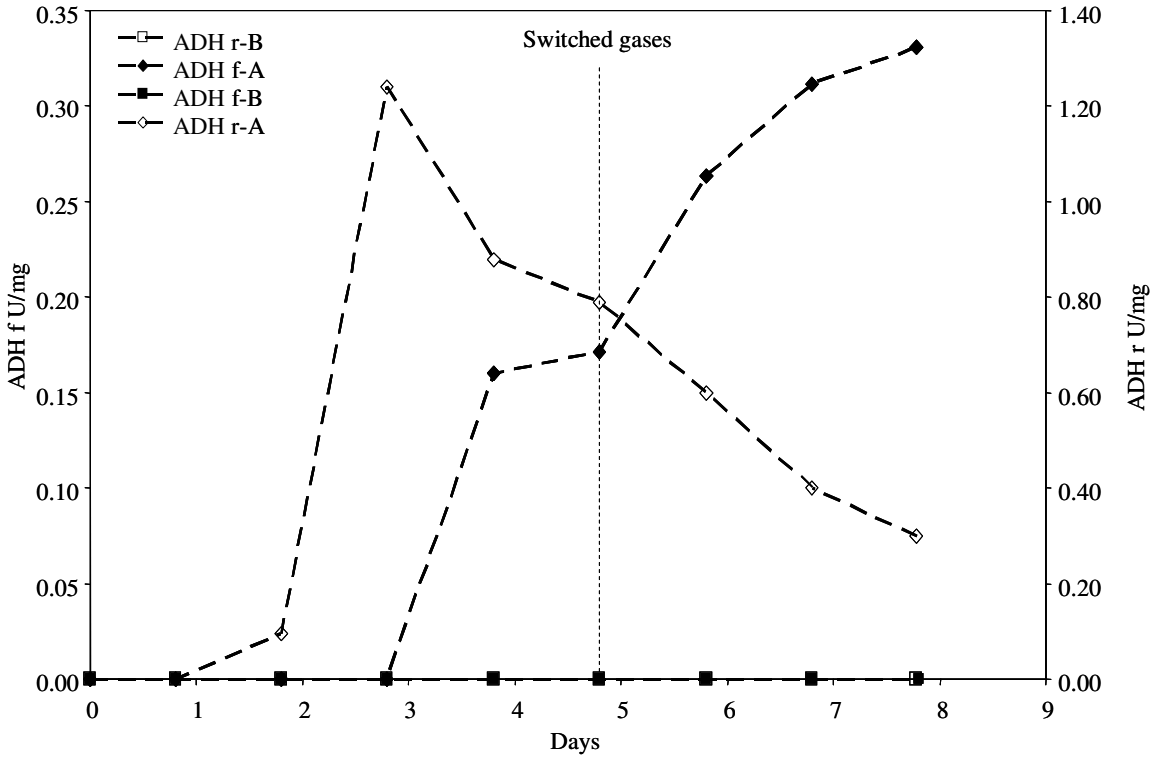

Figure 6.20 Effect of NO on ADH activities. The reactors are described in Figure 6.19. The vertical line indicates the switching of gases.

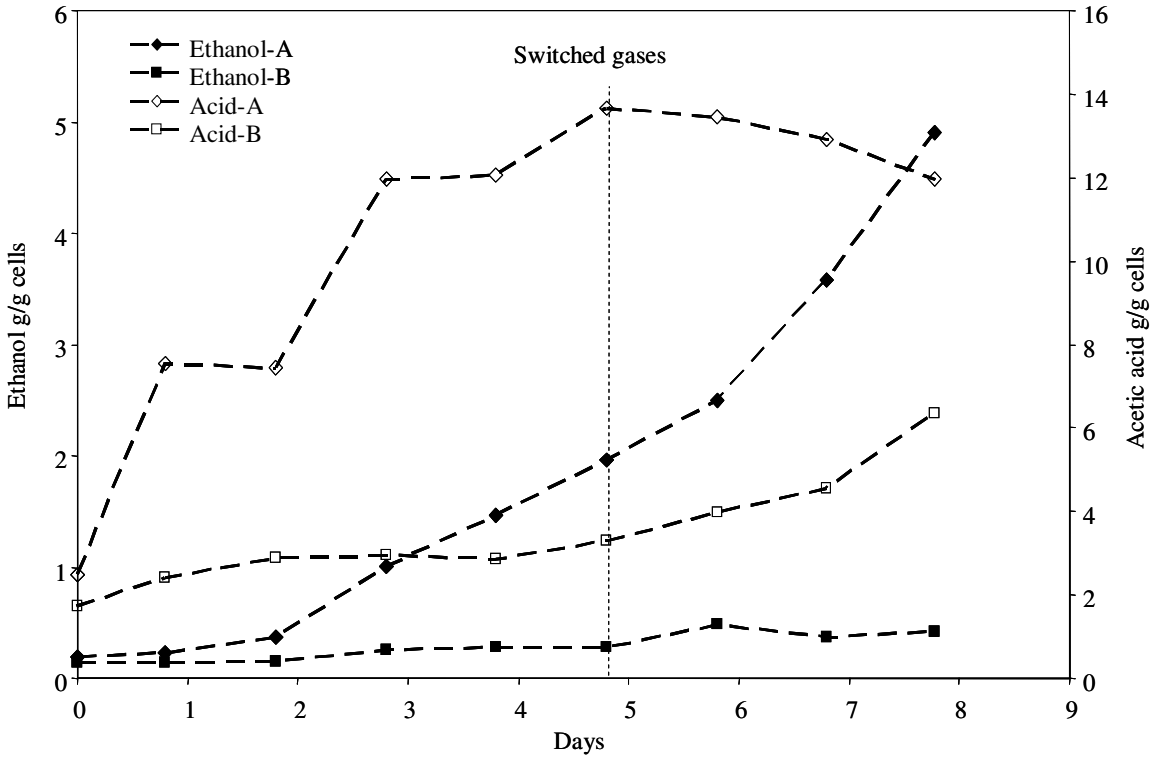

Figure 6.21 Effect of NO on product distribution. The reactors are described in Figure 6.19. The vertical line represents the time at which the gases were switched.

In Reactor B, the ethanol remained at 0.01 g/g cells throughout the study. In Reactor A, the acetic acid per cell mass increased to about 13 g/g cells. The acid per cell mass increased from 3 g/g cells to about 6.5 g/g cells when the cells started growing after removal of NO.

Another study was conducted with 100 ppm NO. Figure 6.22 shows the cell-concentration and pH profiles of the study. In Reactor A, the cell concentration increased to 0.10 g/l and on switching to NO on day 4.5, the concentration increased to about 0.12 g/l. In Reactor B, there was no initial cell-growth in the presence of NO, but when NO was removed, the cells started growing, reaching a concentration of approximately 0.10 g/l. The pH dropped from 6.0 to about 5.5 in both reactors during the course of the experiment. Figure 6.23 shows the effect of NO on ADH activities. The reverse activity in Reactor A increased to about 1.1 U/mg, but on switching to NO, the activity dropped to about 0.2 U/mg. In Reactor B, after NO was removed, the reverse activity increased to about 0.6 U/mg and then dropped slightly to 0.5 U/mg, and stayed nearly constant. The forward activity in Reactor A was very low at about 0.01 U/mg before the introduction of NO, but after the switch, the activity increased to about 0.07 U/mg. In Reactor B, after the NO was removed and the cells started growing, the forward activity increased to about 0.01 U/mg, similar to the activity in Reactor A in the absence of NO. The product profile is shown in Figure 6.24. As seen previously, introduction of NO increased the ethanol per cell mass in Reactor A. Ethanol increased from 0.2g/g cells to about 0.9 g/g cells and acetic acid increased from 4g/g cells to 6 g/g cells in Reactor A on introduction of NO. In Reactor B, after removal of NO, ethanol increased to about 0.25 g/g cells and acid increased to about 6.5 g/g cells.

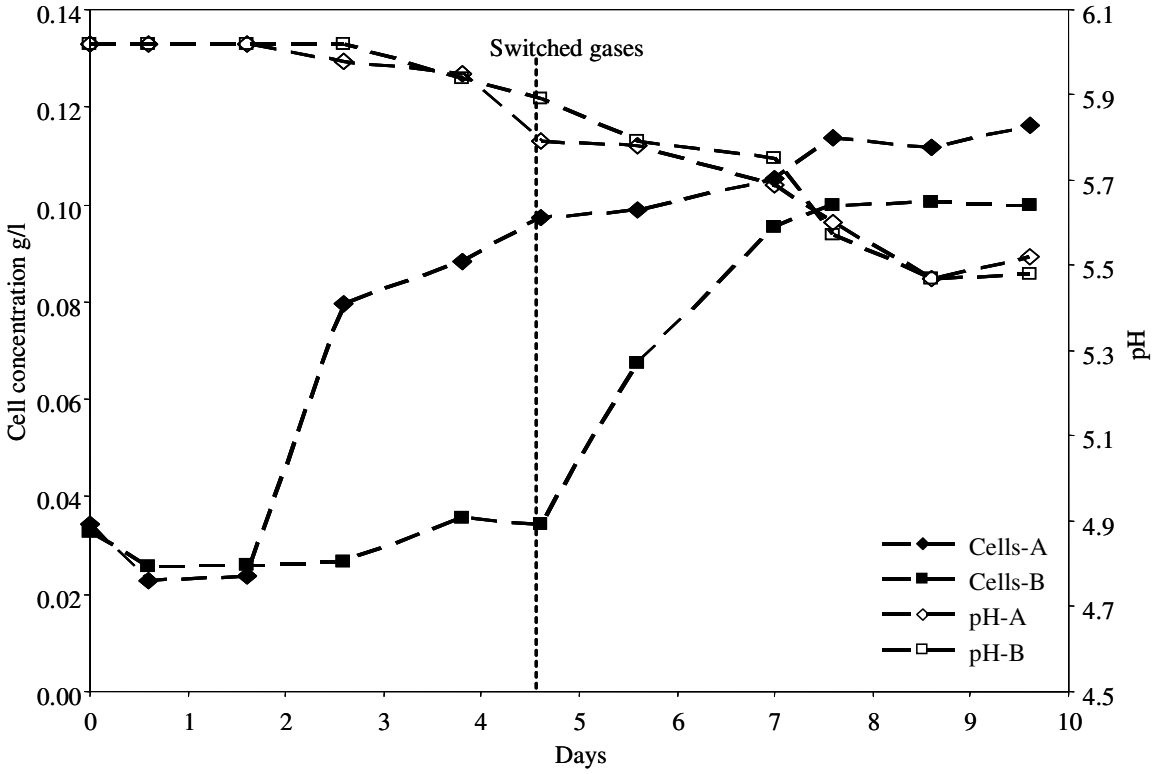

Figure 6.22 Cell concentration and pH profiles in the presence of 100 ppm NO. Reactor A was initially exposed to synthetic syngas and Reactor B was exposed to synthetic syngas containing 100 ppm NO. The vertical line indicates the time when the gas sources were switched.

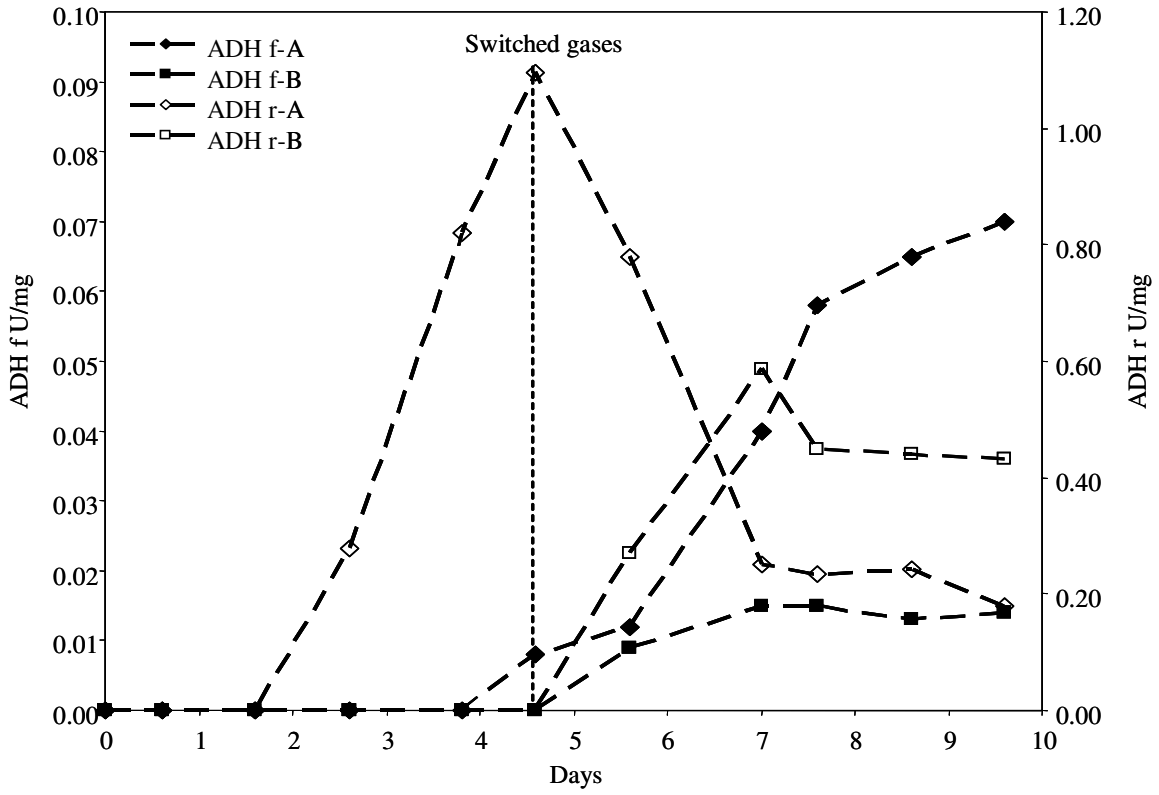

Figure 6.23 Effect of NO on ADH activities. The reactors are described in Figure 6.22. The vertical line indicates the switching of gases.

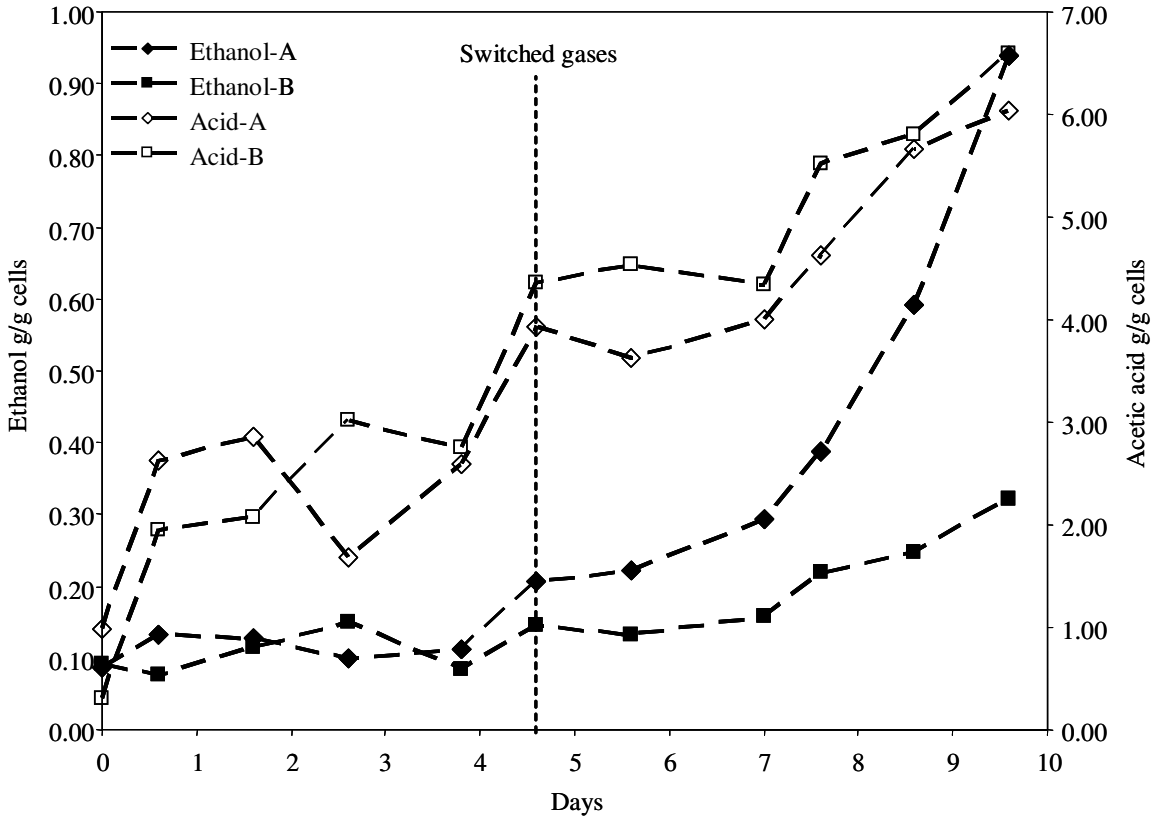

Figure 6.24 Effect of NO on ethanol and acetic acid produced per cell mass. The reactors are described in Figure 6.22. The vertical line indicates the switching of gases.

A third study was conducted with 100 ppm NO, but unlike the previous two studies, both reactors were started on synthetic syngas and NO was introduced to Reactor B on day 3.8. Reactor A remained on synthetic syngas without NO throughout the study. In both reactors, the cells concentration increased to about 0.13 g/l, as shown in Figure 6.25. The pH in Reactor A dropped to about 5.5 while that in Reactor B dropped to 5.7 at the end of the study. The ADH activities are shown in Figure 6.26. In both reactors, the reverse activity increased to about 1.4 U/mg. In Reactor A, the activity then dropped to about 1 U/mg. In Reactor B, on introducing NO, the activity decreased to nearly zero. Before the introduction of NO, the forward activities in both reactors increased to about 0.01 U/mg. In Reactor A, the activity remained nearly constant, increasing slightly to 0.02 U/mg on day 6. In Reactor B, after introducing NO, the forward activity increased significantly to about 0.18 U/mg. Figure 6.27 shows the product profiles. In Reactor A, the ethanol increased to about 2.3 g/g cells at the end of the study. In Reactor B, the ethanol increased to about 1.5 g/g cells and after introducing NO, it increased further to about 4.8 g/g cells. The acetic acid in Reactor A increased to approximately 14 g/g cells while in Reactor B, it only increased to 8 g/g cells.

The increase in ethanol due to NO was seen in previous studies. These studies showed that NO caused the forward activity of ADH to increase and the reverse activity to decrease.

6.4 Conclusions

Studies were conducted to determine whether an artificial electron carrier like neutral red can be used in syngas fermentation to regulate the metabolic pathway of.

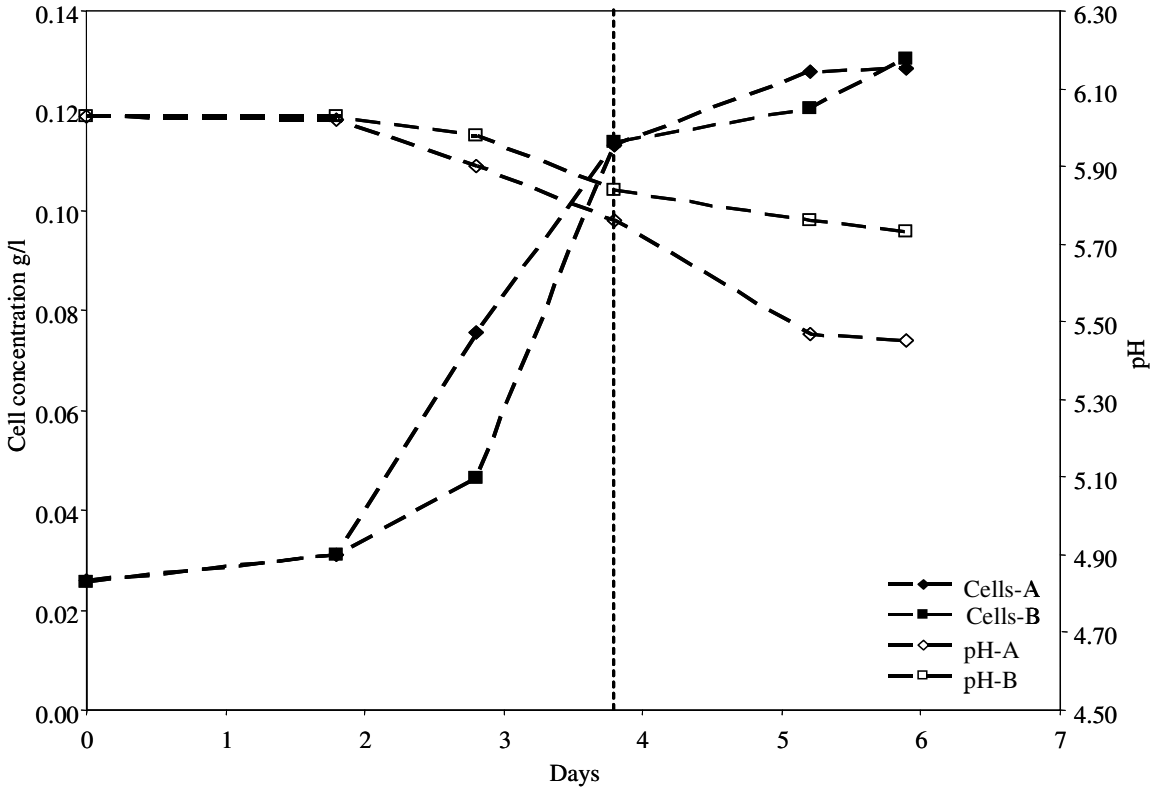

Figure 6.25 Cell concentration and pH profiles in the presence of 100 ppm NO. Both reactors were exposed to synthetic syngas initially. NO was introduced to Reactor B on Day 3.8 as indicated by the vertical line.

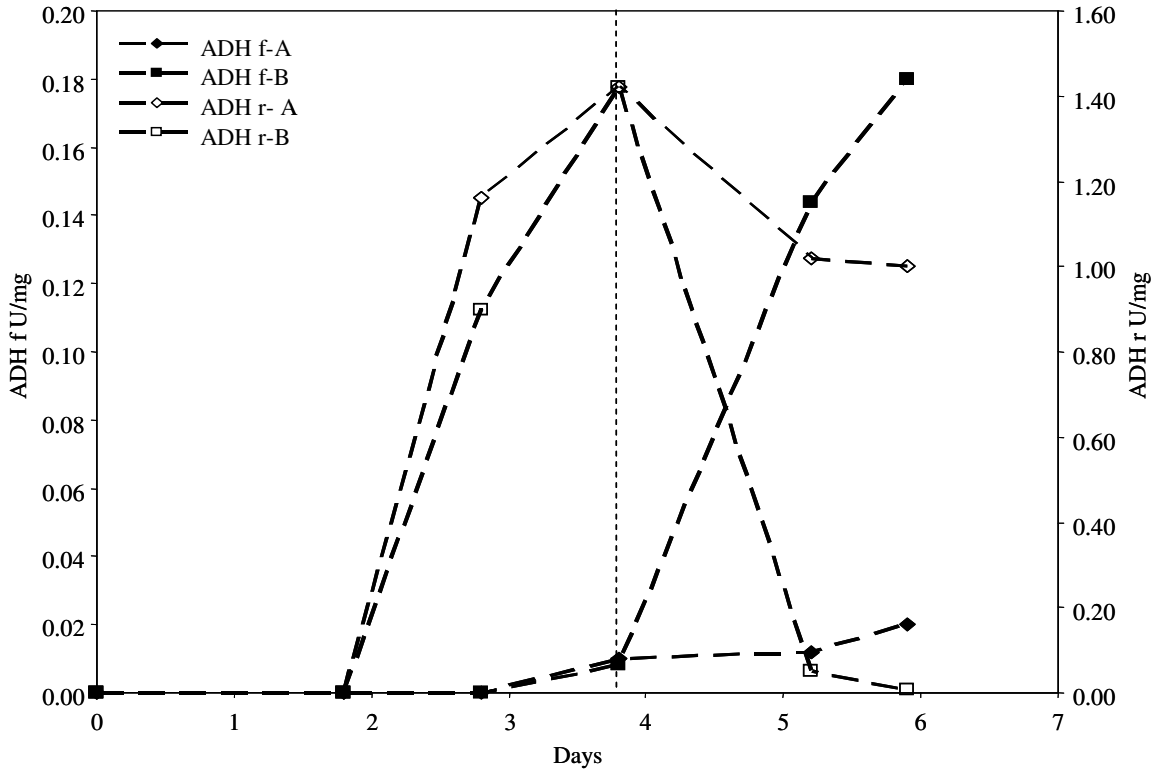

Figure 6.26 Effect of NO on ADH activities. The reactors are described in Figure 6.25. The vertical line represents the time of introduction of NO into Reactor B.

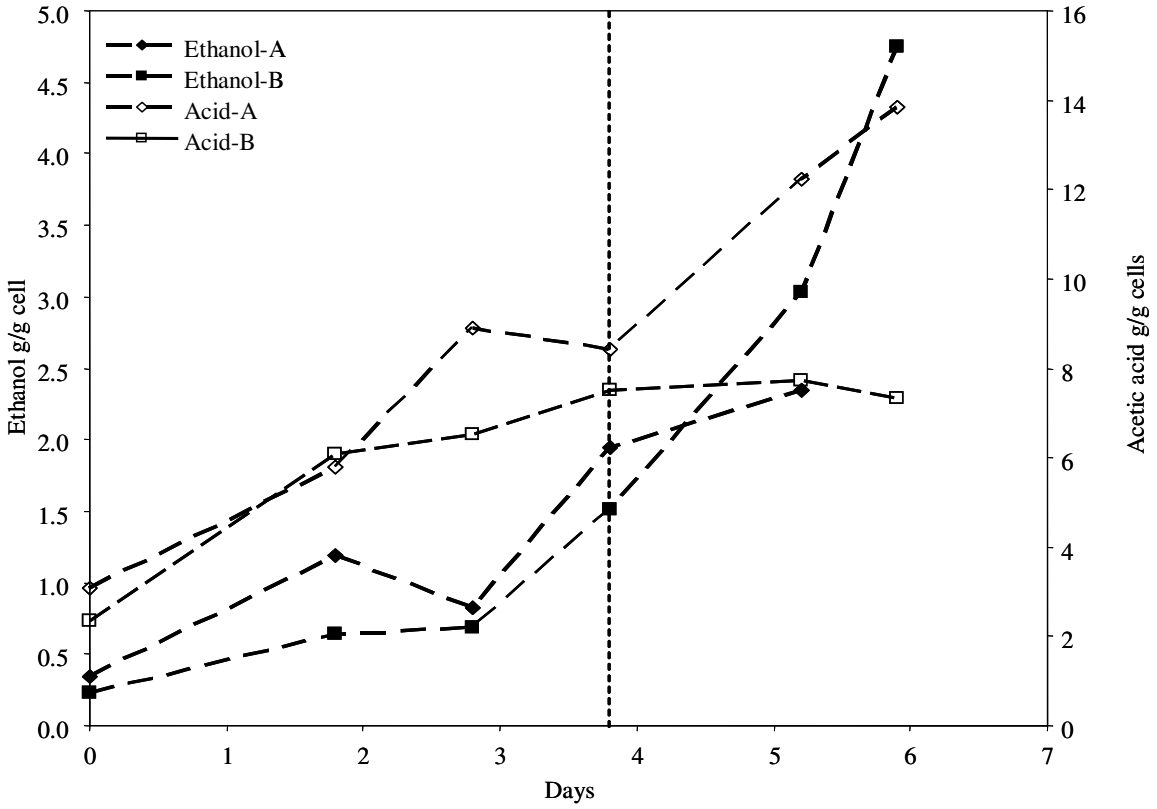

Figure 6.27 Effect of NO on ethanol and acetic acid produced per cell mass. The reactors are described in Figure 6.25. The vertical line represents the time of introduction of NO into Reactor B.

C. carboxidivorans $P7^T$ towards solventogenesis. Neutral red was found to have the following effects on the fermentation.

- An increase in ethanol concentration was observed at all the concentrations of neutral red studied. The more neutral red in the media, the higher the amount of ethanol produced per cell mass during fermentation.
- A decrease in acetic acid production was observed in the presence of neutral red. This effect was more pronounced at higher concentrations of neutral red (0.4 and 1 mM) compared to the lower concentrations like 0.1 and 0.2 mM studied.
- The addition of neutral red caused an increase in the forward ADH activity and a decrease in the reverse ADH activity during syngas fermentation. This could be a result of the regeneration of NADH, which regulates the electron and carbon flow towards ethanol production as described in the introduction to this chapter. This increased availability of NADH could increase the activity of the enzyme in the forward direction.

The studies described in Chapter 5 showed that NO increased the ethanol production by the microbial catalyst. This chapter investigated the effects of NO on ADH, the enzyme responsible for ethanol production. Results showed that nitric oxide had effects similar to neutral red on ADH. NO increased the forward ADH activity and decreased the ADH activity of the cells. The increase in ADH activity is directly connected to the increase in ethanol production in the presence of NO. However, the mechanism of this effect due to NO is not yet understood.

CHAPTER 7

CONCLUSIONS AND FUTURE WORK

7.1 Conclusions

The focus of this work was to investigate the effects of biomass-generated syngas on cell-growth, product distribution and enzyme activities of *Clostridium carboxidivorans* $P7^T$. Key issues like cell-dormancy, hydrogen uptake shutdown and low ethanol yields during syngas fermentation were addressed. The work reported in this dissertation is based on three main hypotheses: (1) Cell-dormancy of *C. carboxidivorans* $P7^T$ in the presence of biomass-syngas was caused by a solid or gaseous impurity of biomass-syngas; (2) Nitric oxide present in biomass-syngas causes an inhibition of hydrogenase activity in *C. carboxidivorans* $P7^T$, and (3) Artificial electron carriers can be used to regulate the metabolic pathway of *C. carboxidivorans* $P7^T$ towards alcohol production to increase ethanol yields. Each of these hypotheses were tested by various experiments that were described in this dissertation. A summary of the results obtained is presented below in three sections, corresponding to the hypothesis mentioned above.

1. Cell-dormancy

- Batch studies with ethane, acetylene and ethylene showed that cell-dormancy was not caused by these gases. Additional cleaning of biomass-syngas using a 0.025-µm filter prevented cell washout from the reactor indicating that a solid impurity was the cause of cell dormancy. Switching to the regular 0.2-µm filter once again led to cell washout, further confirming the effect of the 0.025-µm filter.
- Analysis of the 0.025-µm filter showed trapped particulates that appeared to be tars.
- Batch studies showed that tars caused cell-dormancy. The studies also showed that *C. carboxidivorans* $P7^T$ could adapt to the tars and start growing after an extended period of time.
- A product re-distribution was observed in the presence of tars, which was similar to the effect of biomass-syngas.
- Studies showed that cells can be prevented from washing out of the reactor in the presence of biomass-syngas using a cell-recycle system. An adaptation of cells was also observed such that the cells began to grown on biomass-syngas after 7-8 days in a chemostat with cell-recycle.

2. Hydrogenase inhibition

- Biomass-syngas was found to contain about 140-150 ppm nitric oxide. NO was found to inhibit hydrogenase.

- A kinetic analysis showed that the inhibition was reversible and non-competitive. The kinetic model indicated that the inhibition was non-linear and NO could be binding to multiple sites on the hydrogenase enzyme.
- Studies conducted at various concentrations of NO showed that below 40 ppm NO there was no inhibition and above 160 ppm, there was a complete inhibition of hydrogenase activity.
- NO was also found to affect product distribution during biomass-syngas fermentation. An increase in ethanol concentration was observed in the presence of NO.

3. Metabolic regulation of *C. carboxidivorans* $P7^T$

- Neutral red was found to have a positive effect on ethanol production by *C. carboxidivorans* $P7^T$. Studies showed an increase in ethanol and decrease in acetic acid production in the presence of neutral red.
- Externally added NADH had no effect on product distribution.
- An increase in the forward activity and decrease in reverse activity of alcohol dehydrogenase were observed in the presence of neutral red.
- Studies conducted with nitric oxide showed an increase in the forward activity and decrease in reverse activity of ADH.

7.2 Recommendations for Future Studies

This work provided an understanding of the effects of biomass-syngas and its impurities on the fermentation process. The results obtained from these studies also

pointed to other important areas that need to be addressed in order to make this process viable. Recommendations for future studies that can be carried out in such areas are outlined as follows:

- Further studies to determine the effect of dilution rates on product distribution may prove beneficial. As described in Chapter 4, and as shown in the literature (Qureshi et al. 2000), a high dilution rate causes an increased acid production and lower dilution rates favor alcohol production. Therefore, it is important to determine the optimal dilution rate in a chemostat with cell-recycle in order to optimize both cell density as well as ethanol production.
- Addition of neutral red increased the ethanol formation during syngas fermentation. Other electron carriers can be investigated to find a cost-effective means of regulating the metabolic pathway of the organism.
- Studies have reported the effect of pH on ethanol production (Grupe and Gottschalk 1992). The pH optima for acetogens like *C. carboxidivorans* $P7^T$ are different for growth and ethanol production. Therefore, studies involving a dual reactor set-up, operating at different pH values can be used to optimize cell-concentration in one and ethanol concentration in the other reactor.
- Another important factor governing cell-growth and ethanol production is yeast extract. Yeast extract is added to the culture media as it supports cell-growth. Preliminary studies showed that it is difficult to grow cells in the absence of yeast extract as it contains several nutrients, essential for cell-growth. However, studies have shown that yeast extract promotes growth and acetate formation at the expense of alcohol production (Klasson et al. 1992). Moreover, yeast extract is

one of the most expensive components of the media. Therefore, chemostat studies should be performed where the cells are grown initially with yeast extract, but then the yeast extract is phased out of the media so that the cells can then switch to ethanol formation.

- As nitric oxide above 40 ppm was found to inhibit hydrogenase and also increase ADH activity and ethanol production, it may be useful to conduct experiments in order to decrease the amount of nitric oxide in the syngas to below 40 ppm. This can be done using chemical scavengers or by improving the conditions in the gasifier.

REFERENCES

Abrini J, Naveau H, Nyns EJ. 1994. *Clostridium autoethanogenum*, Sp-Nov, an Anaerobic Bacterium That Produces Ethanol from Carbon-Monoxide. Archives of Microbiology 161(4):345-351.

Acosta F, Real F, Ruiz de Galarreta CM, Diaz R, Padilla D, Ellis AE. 2003. Toxicity of nitric oxide and peroxynitrite to *Photobacterium damselae* subsp. piscicida. Fish & Shellfish Immunology 15(3):241-248.

Adler HI, Crow W. 1987. A Technique for Predicting the Solvent-Producing Ability of *Clostridium acetobutylicum*. Applied and Environmental Microbiology 53(10):2496-2499.

Amartey SA, P.C. J. Leung, N. Baghaei-Yazdi. D. J. Leak, B. S. Hartley. 1999. Fermentation of a wheat straw acid hydrolysate by *Bacillus stearothermophilus* T-13 in continuous culture with partial cell recycle. Process Biochemistry 34(3):289-294.

Baker EG, Lyle K.M and Michael D.B. 1987. Steam Gasification of Biomass with Nickel Secondary Catalysts. Ind. Eng. Chem. Res. 26:1335-1339.

Bilgen S, Kaygusuz K, Sari A. 2004. Renewable energy for a clean and sustainable future. Energy Sources 26(12):1119-1129.

Blanchard CZ, Waldrop GL. 1998. Overexpression and Kinetic Characterization of the Carboxyltransferase Component of Acetyl-CoA Carboxylase. J. Biol. Chem. 273(30):19140-19145.

Bridgwater AV. 1994. Catalysis in thermal biomass conversion. Applied Catalysis A: General 116(1-2):5-47.

Brogren C, Karlsson HT, Bjerle I. 1997. Absorption of NO in an alkaline solution of KMnO4. Chemical Engineering & Technology 20(6):396-402.

Brown RC, Liu Q, Norton G. 2000. Catalytic effects observed during the co-gasification of coal and switchgrass. Biomass and Bioenergy 18(6):499-506.

Bull DN, Young MD. 1981. Enhanced Product Formation in Continuous Fermentations with Microbial Cell Recycle. Biotechnology and Bioengineering 23(2):373-389.

Byung Hong Kim PB, Rathin Datta and J.G. Zeikus. 1984. Control of Carbon and Electron Flow in *Clostridium acetobutylicum* Fermentations: Utilization of Carbon monoxide to Inhibit Hydrogen Production and to enhance butanol yields. Appl. Environ. Microbiol. 48(4):764-770.

Chang HN, Yoo I-K, Kim BS. 1994. High density cell culture by membrane-based cell recycle. Biotechnology Advances 12(3):467-487.

Chang IS, Kim BH, Kim DH, Lovitt RW, Sung HC. 1999. Formulation of defined media for carbon monoxide fermentation by *Eubacterium limosum* KIST612 and the growth characteristics of the bacterium. Journal of Bioscience and Bioengineering 88(6):682-685.

Chang IS, Kim BH, Lovitt RW, Bang JS. 2001. Effect of CO partial pressure on cell-recycled continuous CO fermentation by *Eubacterium limosum* KIST612. Process Biochemistry 37(4):411-421.

Chang IS, Kim DH, Kim BH, Shin PK, Sung HC, Lovitt RW. 1998. CO fermentation of *Eubacterium limosum* KIST612. Journal of Microbiology and Biotechnology 8(2):134-140.

Chu H, Chien TW, Li SY. 2001. Simultaneous absorption of SO2 and NO from flue gas with KMnO4/NaOH solutions. The Science of The Total Environment 275(1-3):127-135.

Clausen EC, Gaddy, J.L.; 1988. Concentrated sulfuric acid process for converting lignocellulosic materials to sugars. United States.

Datar RP. 2003. Anaerobic fermentation of biomass generated producer gas to ethanol [Ph.D Thesis]. Stillwater: Oklahoma State University. 229 p.

Datar RP, Shenkman RM, Cateni BG, Huhnke RL, Lewis RS. 2004. Fermentation of biomass-generated producer gas to ethanol. Biotechnology and Bioengineering 86(5):587-594.

Davis KM, E; Turko, IV; Murad, F. 2001. Novel effects of nitric oxide. Annual Review of Pharmacology and Toxicology 41:203-236.

Devi L, Ptasinski KJ, Janssen FJJG. 2003. A review of the primary measures for tar elimination in biomass gasification processes. Biomass and Bioenergy 24(2):125-140.

Diekert G, Wohlfarth G. 1994. Metabolism of Homoacetogens. Antonie Van Leeuwenhoek International Journal of General and Molecular Microbiology 66(1-3):209-221.

Drake HL. 1994a. Acetogenesis. New York: Chapman and Hall.

Drake HL. 1994b. Acetogenesis. New York: Chapman & Hall. xxi, 647 p. p.

Durre P, Fischer R-J, Kuhn A, Lorenz K, Schreiber W, Sturzenhofecker B, Ullmann S, Winzer K, Sauer U. 1995. Solventogenic enzymes of Clostridium acetobutylicum: catalytic properties, genetic organization, and transcriptional regulation. FEMS Microbiology Reviews 17(3):251-262.

Durre P, Hollergschwandner C. 2004. Initiation of endospore formation in *Clostridium acetobutylicum*. Anaerobe 10(2):69-74.

Engelen K, Zhang Y, Draelants DJ, Baron GV. 2003. A novel catalytic filter for tar removal from biomass gasification gas: Improvement of the catalytic activity in presence of H2S. Chemical Engineering Science 58(3-6):665-670.

Geller H. 2001. Strategies for reducing oil imports: Expanding oil production vs. Increasing vehicle efficiency. Washington D.C: ©American Council for an Energy-Efficient Economy. Report nr E011.

Girbal L, Croux C, Vasconcelos I, Soucaille P. 1995a. Regulation of metabolic shifts in *Clostridium acetobutylicum* ATCC 824. FEMS Microbiology Reviews 17(3):287-297.

Girbal L, Vasconcelos I, Saint-Amans S, Soucaille P. 1995b. How neutral red modified carbon and electron flow in *Clostridium acetobutylicum* grown in chemostat culture at neutral pH. FEMS Microbiology Reviews 16(2-3):151-162.

Gottschal JC, Morris JG. 1981. The Induction of Acetone and Butanol Production in Cultures of Clostridium-Acetobutylicum by Elevated Concentrations of Acetate and Butyrate. Fems Microbiology Letters 12(4):385-389.

Greene DL, Schafer, A. 2003. Reducing Greenhouse Gas Emissions from U.S Transportation. Pew Center on Global Climate Change.

Grube M, Gapes JR, Schuster KC. 2002. Application of quantitative IR spectral analysis of bacterial cells to acetone-butanol-ethanol fermentation monitoring. Analytica Chimica Acta 471(1):127-133.

Grupe H, Gottschalk G. 1992. Physiological Events in *Clostridium acetobutylicum* during the Shift from Acidogenesis to Solventogenesis in Continuous Culture and Presentation of a Model for Shift Induction. Appl. Environ. Microbiol. 58(12):3896-3902.

Guedon E, Payot S, Desvaux M, Petitdemange H. 1999. Carbon and Electron Flow in *Clostridium cellulolyticum* Grown in Chemostat Culture on Synthetic Medium. J. Bacteriol. 181(10):3262-3269.

He B-Q, Jian-Xin Wang, Hao J-M, Yan X-G, Xiao J-H. 2003. A study on emission characteristics of an EFI engine with ethanol blended gasoline fuels. Atmospheric Environment 37(7):949-957.

Hsieh W-D, Chen R-H, Wu T-L, Lin T-H. 2002. Engine performance and pollutant emission of an SI engine using ethanol-gasoline blended fuels. Atmospheric Environment 36(3):403-410.

Hurst KM. 2005. Effects of carbon monoxide and yeast extract on growth, hydrogenase activity, and product formation of Clostridium carboxidivorans P7T [M.S Thesis]. Stillwater: Oklahoma State University. 185 p.

Hyman MR AD. 1988. Reversible and irreversible effects of nitric oxide on the soluble hydrogenase from Alcaligenes eutrophus H16. Biochemical Journal 254:469-475.

Hyman MR AD. 1991. Kinetic analysis of the interaction of nitric oxide with the membrane-associated, nickel and iron-sulfur-containing hydrogenase from Azotobacter vinelandii. Biochim Biophys Acta 1076:165-172.

Kashket ER, Zhi-Yi Cao. 1995. Clostridial strain degeneration. FEMS Microbiology Reviews 17(3):307-315.

Kaylen M, Van Dyne, D.L., Choi, Y.S., Blase, M. 2000. Economic feasibility of producing ethanol from lignocellulosic feedstocks. Bioresource Technology 72:19-32.

Kim S, Dale BE. 2004. Global potential bioethanol production from wasted crops and crop residues. Biomass and Bioenergy 26(4):361-375.

Klasson KT, Ackerson MD, Clausen EC, Gaddy JL. 1992. Bioconversion of synthesis gas into liquid or gaseous fuels. Enzyme and Microbial Technology 14(8):602-608.

Kosaric N, Velikonja J. 1995. Liquid and Gaseous Fuels from Biotechnology - Challenge and Opportunities. Fems Microbiology Reviews 16(2-3):111-142.

Krasna AI. 1979. Hydrogenase: Properties and applications. Enzyme and Microbial Technology 1(3):165-172.

Krasna AI, Rittenberg, D. 1954. The inhibition of hydrogenase by nitric oxide. Proceedings of the National Academy of Sciences 40(4):225-227.

Kutzenok A, Aschner M. 1952. Degenerative Processes in a Strain of Clostridium Butylicum. Journal of Bacteriology 64(6):829-836.

Lashof DA, Ahuja DR. 1990. Relative contributions of greenhouse gas emissions to global warming. 344(6266):529-531.

Lemon BJ, Peters JW. 1999. Binding of exogenously added carbon monoxide at the active site of the iron-only hydrogenase (CpI) from Clostridium pasteurianum. Biochemistry 38(40):12969-12973.

Liou JS-C, Balkwill DL, Drake GR, Tanner RS. 2005. *Clostridium carboxidivorans* sp. nov., a solvent-producing clostridium isolated from an agricultural settling lagoon, and reclassification of the acetogen *Clostridium scatologenes* strain SL1 as *Clostridium drakei* sp. nov. Int J Syst Evol Microbiol 55(5):2085-2091.

Ljungdahl LG. 1986. The autotrophic pathway of acetate synthesis in acetogenic bacteria. Ann. Rev. Microbiology 40:415-450.

Long S, Jones, D.T., Woods, D.R. 1984. Initiation of solvent production, clostridial stage and endospore formation in *Clostridium acetobutylicum* P 262. Appl. Microbiol. Biotechnology 20:256-261.

Lorowitz WH, Bryant MP. 1984. *Peptostreptococcus productus* Strain That Grows Rapidly with Co as the Energy-Source. Applied and Environmental Microbiology 47(5):961-964.

Lynd LR. 1996. Overview and Evaluation of Fuel Ethanol from Cellulosic Biomass : Technology, Economics, the Environment, and Policy. Annual Review of Energy and the Environment 21(1):403-465.

Madigan MT, Martinko, J.M. and Parker, J. 2003. Brock Biology of Microorganisms. New Jersey: Prentice Hall. 1019 p.

McLaughlin SB, Walsh ME. 1998. Evaluating environmental consequences of producing herbaceous crops for bioenergy. Biomass and Bioenergy 14(4):317-324.

Meyer CL, Mclaughlin JK, Papoutsakis ET. 1985. The Effect of CO on Growth and Product Formation in Batch Cultures of *Clostridium acetobutylicum*. Biotechnology Letters 7(1):37-42.

Meyer CL, Papoutsakis ET. 1989. Increased Levels of Atp and Nadh Are Associated with Increased Solvent Production in Continuous Cultures of *Clostridium acetobutylicum*. Applied Microbiology and Biotechnology 30(5):450-459.

Meyer CL, Roos JW, Papoutsakis ET. 1986. Carbon-Monoxide Gasing Leads to Alcohol Production and Butyrate Uptake without Acetone Formation in Continuous Cultures of *Clostridium acetobutylicum*. Applied Microbiology and Biotechnology 24(2):159-167.

Misoph M, Drake HL. 1996. Effect of CO2 on the fermentation capacities of the acetogen *Peptostreptococcus productus* U-1. Journal of Bacteriology 178(11):3140-3145.

Nadim F, Zack P, Hoag GE, Liu S. 2001. United States experience with gasoline additives. Energy Policy 29(1):1-5.

Parekh SR, Cheryan M. 1994. Continuous production of acetate by *Clostridium thermoaceticum* in a cell-recycle membrane bioreactor. Enzyme and Microbial Technology 16(2):104-109.

Peguin S, G. Goma, P. Delorme, P. Soucaille. 1994. Metabolic flexibility of *Clostridium acetobutylicum* in response to methyl viologen addition. Appl. Microbiol. Biotechnology 42:611-616.

Peguin S, Soucaille P. 1995. Modulation of Carbon and Electron Flow in *Clostridium acetobutylicum* by Iron Limitation and Methyl Viologen Addition. Appl. Environ. Microbiol. 61(1):403-405.

Peters JW, Lanzilotta WN, Lemon BJ, Seefeldt LC. 1998. X-ray Crystal Structure of the Fe-Only Hydrogenase (CpI) from *Clostridium pasteurianum* to 1.8 Angstrom Resolution. Science 282(5395):1853-1858.

Qureshi N, Schripsema J, Lienhardt J, Blaschek HP. 2000. Continuous solvent production by *Clostridium beijerinckii* BA101 immobilized by adsorption onto brick. World Journal of Microbiology and Biotechnology 16(4):377-382.

Ragsdale S. 1991. Enzymology of the Acetyl-CoA Pathway of CO_2 Fixation. Critical Reviews in Biochemistry and Molecular Biology 26:261-300.

Rajagopalan S, P. Datar R, Lewis RS. 2002. Formation of ethanol from carbon monoxide via a new microbial catalyst. Biomass and Bioenergy 23(6):487-493.

Rao G, Mutharasan M. 1987. Altered Electron Flow in Continuous Cultures of *Clostridium acetobutylicum* Induced by Viologen Dyes. Appl. Environ. Microbiol. 53(6):1232-1235.

Rao G, Mutharasan R. 1989. Nadh Levels and Solventogenesis in Clostridium-Acetobutylicum - New Insights through Culture Fluorescence. Applied Microbiology and Biotechnology 30(1):59-66.

Rao G, Mutharasan, R. 1986. Alcohol Production by *Clostridium acetobutylicum* induced by methyl viologen. Biotechnology Letters 8(12):893-896.

Rasskazchikova TV, Kapustin VM, Karpov SA. 2004. Ethanol as High-Octane Additive to Automotive Gasolines. Production and Use in Russia and Abroad. Chemistry and Technology of Fuels and Oils 40(4):203-210.

Reed TB, Jantzen DE, Corcoran WP. 1980. Gasifiers for Biomass Feedback. Energy Engineering 77(3):24-31.

Renewable Fuels Association. 2005. Homegrown for the homeland : ethanol industry outlook 2005. Washington, DC: Renewable Fuels Association. 25 p. p.

Roberts DV. 1977. Enzyme kinetics. Cambridge Eng. ; New York: Cambridge University Press. x, 326 p. p.

Sada E, Kumazawa H, Kudo I, Kondo T. 1978. Absorption of NO in aqueous mixed solutions of NaClO2 and NaOH. Chemical Engineering Science 33(3):315-318.

Sander R. 1999. Compilation of Henry's Law Constants for Inorganic and Organic Species of Potential Importance in Environmental Chemistry. Mainz, Germany.

Sanderson MA, Reed RL, McLaughlin SB, Wullschleger SD, Conger BV, Parrish DJ, Wolf DD, Taliaferro C, Hopkins AA, Ocumpaugh WR. 1996a. Switchgrass as a sustainable bioenergy crop. Bioresource Technology 56(1):83-93.

Schlegel HG, Bowien B. 1989. Autotrophic bacteria. Madison, WI, Berlin ; New York: Science Tech Publishers, Springer-Verlag. xii, 528 p. p.

Schneider K SH. 1976. Purification and properties of soluble hydrogenase from *Alcaligenes eutrophus* H 16. Biochim Biophys Acta 452(1):66-80.

Seefeldt LC, Arp DJ. 1989. Oxygen Effects on the Nickel-Containing and Iron-Containing Hydrogenase from *Azotobacter vinelandii*. Biochemistry 28(4):1588-1596.

Shenkman RM. 2003. *C. carboxidovorans* culture advances and the effects of pH, temperature, and producer gas on key enzymes [M.S Thesis]. Stillwater: Oklahoma State University. 182 p.

Shuler ML, Kargi F. 1992. Bioprocess engineering : basic concepts. Englewood Cliffs, N.J.: Prentice Hall. xvi, 479 p. p.

Sridhar J, Eiteman MA, Wiegel JW. 2000. Elucidation of Enzymes in Fermentation Pathways Used by Clostridium thermosuccinogenes Growing on Inulin. Appl. Environ. Microbiol. 66(1):246-251.

Tibelius KH, Knowles R. 1984. Hydrogenase activity in *Azospirillum brasilense* is inhibited by nitrite, nitric oxide, carbon monoxide and acetylene. J. Bacteriol. 160(1):103-106.

van Reis R, Zydney A. 2001. Membrane separations in biotechnology. Current Opinion in Biotechnology 12(2):208-211.

Vasconcelos I, Girbal L, Soucaille P. 1994. Regulation of Carbon and Electron Flow in Clostridium-Acetobutylicum Grown in Chemostat Culture at Neutral Ph on Mixtures of Glucose and Glycerol. Journal of Bacteriology 176(5):1443-1450.

Vega JL, Clausen EC, Gaddy JL. 1990. Design of bioreactors for coal synthesis gas fermentations. Resources, Conservation and Recycling 3(2-3):149-160.

West DL, Montgomery FC, Armstrong TR. 2005. "NO-selective" NOx sensing elements for combustion exhausts. Sensors and Actuators B: Chemical 111-112:84-90.

Wheals AE, Basso LC, Alves DMG, Amorim HV. 1999. Fuel ethanol after 25 years. Trends in Biotechnology 17(12):482-487.

Wood HG, Ragsdale SW, Pezacka E. 1986a. The Acetyl-CoA Pathway - a Newly Discovered Pathway of Autotrophic Growth. Trends in Biochemical Sciences 11(1):14-18.

Wood HG, Ragsdale SW, Pezacka E. 1986b. The Acetyl-CoA Pathway of Autotrophic Growth. Fems Microbiology Reviews 39(4):345-362.

Wood HG, Ragsdale SW, Pezacka E. 1986c. A New Pathway of Autotrophic Growth Utilizing Carbon-Monoxide or Carbon-Dioxide and Hydrogen. Biochemistry International 12(3):421-440.

Worden RM, Bredwell MD, Grethlein AJ. 1997. Engineering issues in synthesis-gas fermentations. Fuels and Chemicals from Biomass 666:320-335.

Wyman CE. 1994. Ethanol from lignocellulosic biomass: Technology, economics, and opportunities. Bioresource Technology 50(1):3-15.

Wyman CE. 1999. BIOMASS ETHANOL: Technical Progress, Opportunities, and Commercial Challenges. Annual Review of Energy and the Environment 24(1):189-226.

Yacobucci BD, Womach, J. 2000. Fuel Ethanol: Background and Public Policy Issues.

Yuksel F, Yuksel B. 2004. The use of ethanol-gasoline blend as a fuel in an SI engine. Renewable Energy 29(7):1181-1191.

Zhang R, Brown RC, Suby A, Cummer K. 2004. Catalytic destruction of tar in biomass derived producer gas. Energy Conversion and Management 45(7-8):995-1014.

APPENDIX A

CHEMOSTAT EXPERIMENTS WITH BIOMASS-SYNGAS USING A 0.025-µm FILTER

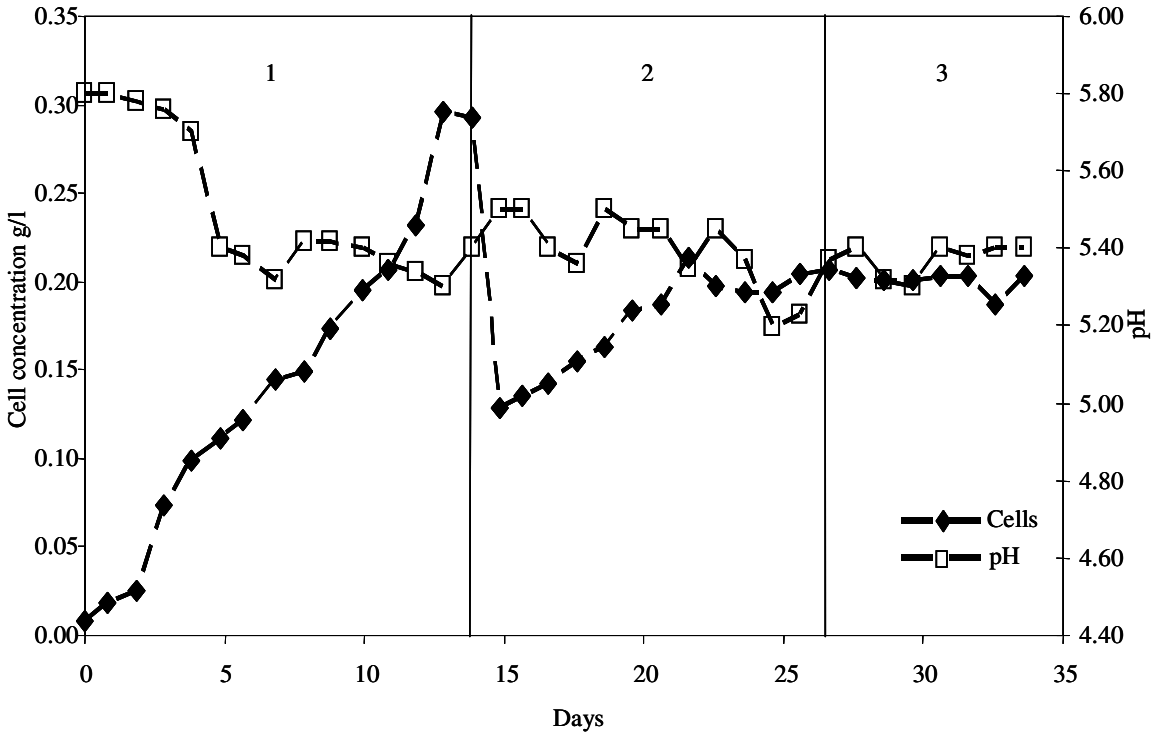

Figure A.1. Cell concentration and pH profile in a chemostat study. Stage 1 was a batch liquid mode with synthetic syngas. Stage 2 was a chemostat mode with synthetic syngas. In stage 3, biomass-syngas was introduced through a 0.025-µm filter in a chemostat mode. Cell washout occurred between day 13 and 14 due to high dilution rate ($D=0.02\ hr^{-1}$; growth rate, $\mu=0.005\ hr^{-1}$), after which dilution rate was adjusted according to the growth rate (µ).

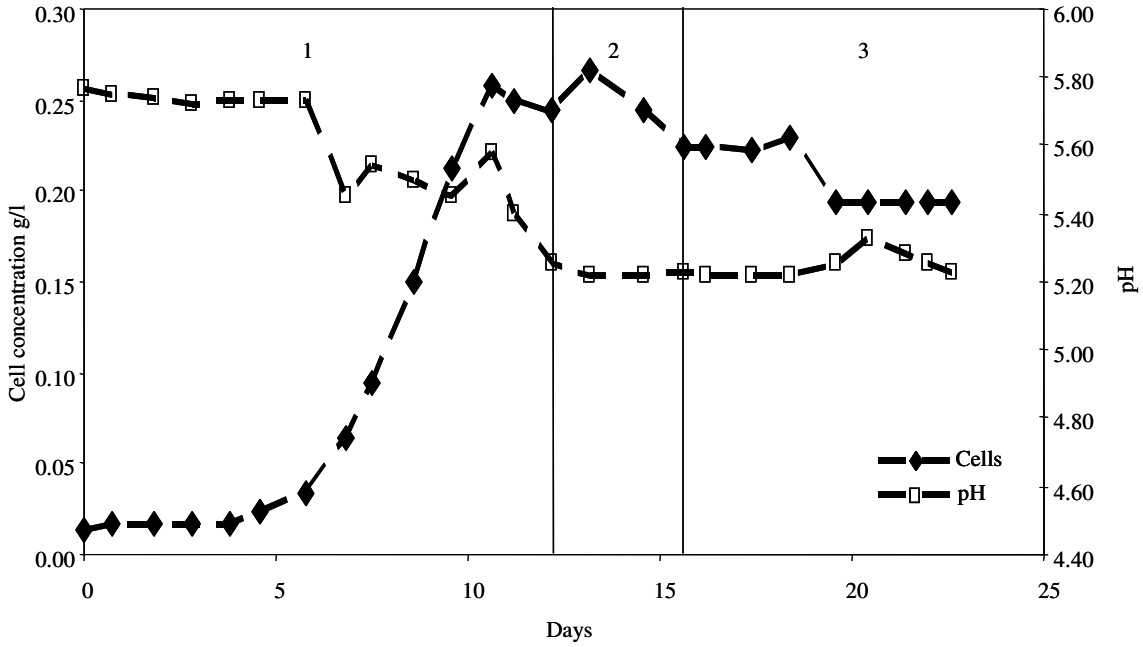

Figure A.2. Cell concentration and pH profile in a chemostat study. Stage 1 was a batch liquid mode with synthetic syngas. Stage 2 was a chemostat mode with synthetic syngas. In stage 3, biomass-syngas was introduced through a 0.025-µm filter in a chemostat mode. In this study, growth rate, μ=0.019 hr^{-1} and dilution rate, D was set to 0.018 hr^{-1}.

APPENDIX B

EXPERIMENTAL RAW DATA TABLES AND ERROR ANALYSIS

Days	C-1	C-2	C-3	Average	Error (2σ)
0	0.0139	0.0115	0.0114	0.0123	0.0028
1	0.0439	0.0413	0.0361	0.0404	0.0079
2	0.0683	0.0449	0.0499	0.0544	0.0246
3	0.1432	0.1203	0.1210	0.1282	0.0261
4	0.1565	0.1578	0.1514	0.1552	0.0068
5	0.1450	0.1481	0.1506	0.1479	0.0056
6	0.1415	0.1361	0.1372	0.1382	0.0057

Days	E-1	E-2	E-3	Average	Error (2σ)
0	0.0110	0.0107	0.0112	0.0110	0.0005
1	0.0400	0.0464	0.0396	0.0420	0.0077
2	0.0646	0.0462	0.0501	0.0536	0.0194
3	0.1277	0.1140	0.1204	0.1207	0.0138
4	0.1501	0.1552	0.1647	0.1567	0.0148
5	0.1359	0.1518	0.1479	0.1452	0.0166
6	0.1290	0.1398	0.1441	0.1376	0.0155

Table B.1. Raw data, average values and standard error values of cell concentration (g/l) for batch study with ethane. C-1, 2, 3 were controls and E-1, 2, 3 contained 0.35 % ethane. Results are discussed in Chapter 3, Section 3.3.1.

Days	C-1	C-2	C-3	Average	Error (2σ)
0	6.03	6.04	6.04	6.04	0.0115
1	6.00	5.97	5.96	5.98	0.0416
2	5.96	5.98	5.98	5.97	0.0231
3	5.82	5.89	5.85	5.85	0.0702
4	5.76	5.73	5.73	5.74	0.0346
5	5.72	5.70	5.71	5.71	0.0200
6	5.68	5.61	5.68	5.66	0.0808

Days	C-1	C-2	C-3	Average	Error (2σ)
0	6.03	6.03	6.02	6.03	0.0115
1	6.01	6.01	5.99	6.00	0.0231
2	6.00	6.02	5.98	6.00	0.0400
3	5.87	5.90	5.89	5.89	0.0306
4	5.72	5.78	5.80	5.77	0.0833
5	5.71	5.75	5.70	5.72	0.0529
6	5.65	5.69	5.63	5.66	0.0611

Table B.2. Raw data, average values and standard error values of pH for batch study with ethane. C-1, 2, 3 were controls and E-1, 2, 3 contained 0.35 % ethane. Results are discussed in Chapter 3, Section 3.3.1.

Days	C-4	C-5	C-6	Average	Error (2σ)
0	0.0099	0.0103	0.0108	0.0103	0.0009
1	0.0453	0.0384	0.0464	0.0433	0.0087
2	0.0916	0.0873	0.0559	0.0783	0.0390
3	0.1317	0.1273	0.0753	0.1114	0.0628
4	0.1351	0.1290	0.1281	0.1307	0.0076

Days	E-4	E-5	E-6	Average	Error (2σ)
0	0.0103	0.0099	0.0095	0.0099	0.0009
1	0.0442	0.0423	0.0412	0.0426	0.0031
2	0.0788	0.1054	0.1045	0.0962	0.0302
3	0.1389	0.1445	0.1466	0.1433	0.0080
4	0.1387	0.1408	0.1462	0.1419	0.0078

Table B.3. Raw data, average values and standard error values of cell concentration (g/l) for batch study with ethylene. C-1, 2, 3 were controls and E-1, 2, 3 contained 1.4 % ethylene. Results are discussed in Chapter 3, Section 3.3.1.

Days	C-4	C-5	C-6	Average	Error (2σ)
0	6.01	6.01	6.02	6.01	0.0115
1	5.98	5.97	5.97	5.97	0.0115
2	5.91	5.91	5.91	5.91	0.0000
3	5.88	5.87	5.89	5.88	0.0200
4	5.78	5.83	5.91	5.84	0.1311

Days	C-4	C-5	C-6	Average	Error (2σ)
0	6.01	6.00	6.00	6.00	0.0115
1	5.99	5.98	5.98	5.98	0.0115
2	5.98	5.91	5.91	5.93	0.0808
3	5.90	5.89	5.88	5.89	0.0200
4	5.80	5.75	5.72	5.76	0.0808

Table B.4. Raw data, average values and standard error values of pH for batch study with ethylene. C-1, 2, 3 were controls and E-1, 2, 3 contained 1.4 % ethylene. Results are discussed in Chapter 3, Section 3.3.1.

Days	C-7	C-8	C-9	Average	Error (2σ)
0	0.0107	0.0098	0.0100	0.0101	0.0009
1	0.0429	0.0604	0.0540	0.0524	0.0178
2	0.0774	0.0860	0.0800	0.0811	0.0088
3	0.1806	0.1724	0.1790	0.1773	0.0087
4	0.1862	0.2012	0.1750	0.1875	0.0263

Days	A-7	A-8	A-9	Average	Error (2σ)
0	0.0107	0.0099	0.0103	0.0103	0.0008
1	0.0404	0.0353	0.0456	0.0404	0.0103
2	0.1157	0.0861	0.0817	0.0945	0.0369
3	0.1754	0.1550	0.1574	0.1626	0.0223
4	0.1618	0.1668	0.1208	0.1498	0.0505

Table B.5. Raw data, average values and standard error values of cell concentration (g/l) for batch study with acetylene. C-1, 2, 3 were controls and E-1, 2, 3 contained 0.1 % acetylene. Results are discussed in Chapter 3, Section 3.3.1.

Days	C-7	C-8	C-9	Average	Error (2σ)
0	5.93	5.93	5.93	5.93	0.0000
1	5.76	5.79	5.78	5.78	0.0306
2	5.77	5.79	5.77	5.78	0.0231
3	5.67	5.69	5.67	5.68	0.0231
4	5.64	5.64	5.63	5.64	0.0115

Days	A-7	A-8	A-9	Average	Error (2σ)
0	5.92	5.93	5.93	5.93	0.0115
1	5.82	5.84	5.82	5.83	0.0231
2	5.82	5.84	5.84	5.83	0.0231
3	5.59	5.65	5.66	5.63	0.0757
4	5.60	5.65	5.65	5.63	0.0577

Table B.5. Raw data, average values and standard error values of pH for batch study with acetylene. C-1, 2, 3 were controls and E-1, 2, 3 contained 0.1 % acetylene. Results are discussed in Chapter 3, Section 3.3.1.

Days	C-10	C-11	C-12	Average	Error (2σ)
0.0	0.0153	0.0147	0.0181	0.0160	0.0036
0.6	0.0224	0.0297	0.0346	0.0289	0.0122
1.6	0.1582	0.1601	0.1667	0.1617	0.0089
2.0	0.1579	0.1553	0.1781	0.1638	0.0250
2.6	0.1462	0.1510	0.1477	0.1483	0.0049
3.6	0.1419	0.1481	0.1497	0.1466	0.0082

Days	N-10	N-11	N-12	Average	Error (2σ)
0.0	0.0169	0.0172	0.0162	0.0167	0.0010
0.6	0.0323	0.0286	0.0278	0.0296	0.0049
1.6	0.1519	0.1406	0.1450	0.1458	0.0114
2.0	0.1601	0.1430	0.1377	0.1469	0.0234
2.6	0.1457	0.1425	0.1407	0.1430	0.0051
3.6	0.1458	0.1422	0.1330	0.1403	0.0132

Days	NR-10	NR-11	NR-12	Average	Error (2σ)
0.0	0.0170	0.0189	0.0153	0.0171	0.0036
0.6	0.0316	0.0306	0.0268	0.0297	0.0051
1.6	0.1398	0.1630	0.1466	0.1498	0.0238
2.0	0.1430	0.1570	0.1462	0.1488	0.0147
2.6	0.1243	0.1388	0.1466	0.1366	0.0226
3.6	0.1278	0.1403	0.1470	0.1383	0.0195

Table B.6. Raw data, average values and standard error values of cell concentration (g/l) for batch study with 0.1 mM NADH (N-10, 11, 12) and 0.1 mM neutral red (NR-10, 11, 12). The controls were C-10, 11, 12, with no NADH or neutral red. Results are discussed in Chapter 6, Section 6.3.1.

Days	C-10	C-11	C-12	Average	Error (2σ)
0.0	6.04	6.04	6.04	6.04	0.0000
0.6	5.88	5.80	5.81	5.83	0.0872
1.6	5.46	5.36	5.40	5.41	0.1007
2.0	5.35	5.23	5.28	5.29	0.1206
2.6	5.31	5.23	5.21	5.25	0.1058
3.6	5.28	5.23	5.24	5.25	0.0529

Days	N-10	N-11	N-12	Average	Error (2σ)
0.0	6.04	6.04	6.04	6.04	0.0000
0.6	5.87	5.80	5.77	5.81	0.1026
1.6	5.37	5.31	5.30	5.33	0.0757
2.0	5.29	5.26	5.24	5.26	0.0503
2.6	5.23	5.26	5.23	5.24	0.0346
3.6	5.26	5.27	5.23	5.25	0.0416

Days	NR-10	NR-11	NR-12	Average	Error (2σ)
0.0	6.04	6.04	6.04	6.04	0.0000
0.6	5.79	5.80	5.70	5.76	0.1102
1.6	5.40	5.42	5.42	5.41	0.0231
2.0	5.32	5.23	5.23	5.26	0.1039
2.6	5.30	5.23	5.23	5.25	0.0808
3.6	5.30	5.22	5.25	5.26	0.0808

Table B.7. Raw data, average values and standard error values of pH for batch study with 0.1 mM NADH (N-10, 11, 12) and 0.1 mM neutral red (NR-10, 11, 12). The controls were C-10, 11, 12, with no NADH or neutral red. Results are discussed in Chapter 6, Section 6.3.1.

Days	C-10	C-11	C-12	Average	Error (2σ)
0.0	0.0000	0.0000	0.0000	0.0000	0.0000
0.6	0.0000	0.0000	0.0000	0.0000	0.0000
1.6	0.0506	0.0624	0.0540	0.0557	0.0122
2.0	0.0507	0.0579	0.0561	0.0549	0.0076
2.6	0.0616	0.0728	0.0542	0.0629	0.0188
3.6	0.0634	0.0743	0.0534	0.0637	0.0208

Days	N-10	N-11	N-12	Average	Error (2σ)
0.0	0.0000	0.0000	0.0000	0.0000	0.0000
0.6	0.0000	0.0000	0.0000	0.0000	0.0000
1.6	0.0790	0.0569	0.0552	0.0637	0.0266
2.0	0.0562	0.0560	0.0508	0.0543	0.0061
2.6	0.0686	0.0491	0.0427	0.0535	0.0270
3.6	0.0686	0.0281	0.0451	0.0473	0.0406

Days	NR-10	NR-11	NR-12	Average	Error (2σ)
0.0	0.0000	0.0000	0.0000	0.0000	0.0000
0.6	0.0000	0.0000	0.0000	0.0000	0.0000
1.6	0.0358	0.0491	0.0819	0.0556	0.0474
2.0	0.0839	0.1401	0.1162	0.1134	0.0564
2.6	0.2252	0.2305	0.1705	0.2088	0.0664
3.6	0.2035	0.2210	0.1632	0.1959	0.0592

Table B.8. Raw data, average values and standard error values of ethanol per cell mass (g/g) for batch study with 0.1 mM NADH (N-10, 11, 12) and 0.1 mM neutral red (NR-10, 11, 12). The controls were C-10, 11, 12, with no NADH or neutral red. Results are discussed in Chapter 6, Section 6.3.1.

Days	C-10	C-11	C-12	Average	Error (2σ)
0.0	0.0000	0.0000	0.0000	0.0000	0.0000
0.6	0.0000	0.0000	0.0000	0.0000	0.0000
1.6	7.4148	9.8918	7.6799	8.3289	2.7201
2.0	8.8476	9.6255	9.0711	9.1814	0.8011
2.6	10.5404	11.4822	11.2690	11.0972	0.9878
3.6	10.6061	10.9391	10.0947	10.5466	0.8507

Days	N-10	N-11	N-12	Average	Error (2σ)
0.0	0.0000	0.0000	0.0000	0.0000	0.0000
0.6	0.0000	0.0000	0.0000	0.0000	0.0000
1.6	8.5374	10.7564	10.3420	9.8786	2.3597
2.0	8.7803	10.2465	11.1160	10.0476	2.3611
2.6	10.5403	10.8247	10.9632	10.7760	0.4312
3.6	9.6288	10.3125	11.4362	10.4591	1.8252

Days	NR-10	NR-11	NR-12	Average	Error (2σ)
0.0	0.0000	0.0000	0.0000	0.0000	0.0000
0.6	0.0000	0.0000	0.0000	0.0000	0.0000
1.6	8.1191	9.1489	8.1044	8.4575	1.1977
2.0	9.1737	8.6986	10.5031	9.4585	1.8706
2.6	11.5113	10.9867	10.4716	10.9899	1.0397
3.6	10.5986	11.1217	10.1961	10.6388	0.9282

Table B.9. Raw data, average values and standard error values of acetic acid per cell mass (g/g) for batch study with 0.1mM NADH (N-10, 11, 12) and 0.1 mM neutral red (NR-10, 11, 12). The controls were C-10, 11, 12, with no NADH or neutral red. Results are discussed in Chapter 6, Section 6.3.1.

Days	C-13	C-14	C-15	Average	Error (2σ)
0.0	0.0156	0.0166	0.0167	0.0163	0.0012
1.6	0.0534	0.0336	0.0625	0.0499	0.0296
2.6	0.1753	0.1561	0.1695	0.1670	0.0197
3.6	0.1628	0.1532	0.1583	0.1581	0.0096
4.6	0.1717	0.1516	0.1544	0.1592	0.0218

Days	NR-13	NR-14	NR-15	Average	Error (2σ)
0.0	0.0151	0.0160	0.0173	0.0161	0.0022
1.6	0.0519	0.0521	0.0537	0.0525	0.0020
2.6	0.1614	0.1701	0.1634	0.1650	0.0090
3.6	0.1450	0.1522	0.1485	0.1486	0.0071
4.6	0.1425	0.1487	0.1530	0.1481	0.0105

Table B.10. Raw data, average values and standard error values of cell concentration (g/l) for batch study with 0.2 mM neutral red (NR-13, 14, 15). The controls were C-13, 14, 15, with no neutral red. Results are discussed in Chapter 6, Section 6.3.1.

Days	C-13	C-14	C-15	Average	Error (2σ)
0.0	0.0000	0.0000	0.0000	0.0000	0.0000
1.6	0.0187	0.0297	0.0160	0.0215	0.0146
2.6	0.0228	0.0320	0.0177	0.0242	0.0145
3.6	0.0307	0.0326	0.0316	0.0316	0.0019
4.6	0.0291	0.0330	0.0324	0.0315	0.0042

Days	NR-13	NR-14	NR-15	Average	Error (2σ)
0.0	0.0000	0.0000	0.0000	0.0000	0.0000
1.6	0.0193	0.0192	0.0186	0.0190	0.0007
2.6	0.0186	0.0176	0.0306	0.0223	0.0144
3.6	0.1241	0.1117	0.1010	0.1123	0.0231
4.6	0.1403	0.1546	0.1504	0.1484	0.0147

Table B.11. Raw data, average values and standard error values of ethanol per cell mass (g/g) for batch study with 0.2 mM neutral red (NR-13, 14, 15). The controls were C-13, 14, 15, with no neutral red. Results are discussed in Chapter 6, Section 6.3.1.

Days	C-13	C-14	C-15	Average	Error (2σ)
0.0	1.0891	1.1658	1.1448	1.1332	0.0793
1.6	2.7690	2.9739	2.4951	2.7460	0.4804
2.6	4.5519	4.9395	3.8396	4.4437	1.1157
3.6	4.6327	5.5104	5.5266	5.2232	1.0229
4.6	5.4877	5.8057	6.0893	5.7942	0.6019

Days	NR-13	NR-14	NR-15	Average	Error (2σ)
0.0	1.1163	1.1158	0.9835	1.0718	0.1531
1.6	2.2176	2.4389	2.3479	2.3348	0.2225
2.6	4.1382	4.3454	4.5459	4.3432	0.4077
3.6	5.5295	5.6907	5.8527	5.6910	0.3231
4.6	5.7315	5.5400	5.5116	5.5944	0.2393

Table B.12. Raw data, average values and standard error values of acetic acid per cell mass (g/g) for batch study with 0.2 mM neutral red (NR-13, 14, 15). The controls were C-13, 14, 15, with no neutral red. Results are discussed in Chapter 6, Section 6.3.1.

Days	C-16	C-17	C-18	Average	Error (2σ)
0.0	0.0129	0.0125	0.0142	0.0132	0.0018
1.0	0.0894	0.0903	0.0594	0.0797	0.0352
1.6	0.1828	0.1974	0.1582	0.1795	0.0395
2.6	0.2288	0.2430	0.1948	0.2222	0.0495
3.6	0.2249	0.2425	0.1969	0.2215	0.0460
4.6	0.2236	0.2494	0.2064	0.2265	0.0433
5.6	0.2193	0.2451	0.2107	0.2250	0.0358

Days	NR1-16	NR1-17	NR1-18	Average	Error (2σ)
0.0	0.0120	0.0133	0.0151	0.0135	0.0030
1.0	0.0916	0.0963	0.1462	0.1114	0.0605
1.6	0.1856	0.1924	0.2064	0.1948	0.0212
2.6	0.2227	0.2150	0.2516	0.2298	0.0385
3.6	0.2180	0.2146	0.2511	0.2279	0.0404
4.6	0.2322	0.2193	0.2580	0.2365	0.0394
5.6	0.2279	0.2236	0.2623	0.2379	0.0424

Table B.13. Raw data, average values and standard error values of cell concentration (g/l) for batch study with 0.1 mM, 0.4 mM and 1 mM neutral red. The controls (C-16, 17, 18) and 0.1 mM neutral red studies (NR1-16, 17, 18) are shown in this table. Table B.14 shows the rest of the data. Results are discussed in Chapter 6, Section 6.3.1.

Days	NR2-16	NR2-17	NR2-18	Average	Error (2σ)
0.0	0.0133	0.0138	0.0138	0.0136	0.0005
1.0	0.1011	0.0765	0.0998	0.0925	0.0276
1.6	0.1764	0.1770	0.1901	0.1811	0.0155
2.6	0.2335	0.2507	0.2279	0.2374	0.0238
3.6	0.2537	0.2494	0.2451	0.2494	0.0086
4.6	0.2554	0.2580	0.2623	0.2586	0.0070
5.6	0.2623	0.2709	0.2623	0.2652	0.0099

Days	NR3-16	NR3-17	NR3-18	Average	Error (2σ)
0.0	0.0142	0.0133	0.0133	0.0136	0.0010
1.0	0.0968	0.0800	0.1505	0.1091	0.0737
1.6	0.1845	0.1716	0.2055	0.1872	0.0343
2.6	0.2516	0.2408	0.2533	0.2485	0.0135
3.6	0.2584	0.2632	0.2670	0.2629	0.0086
4.6	0.2645	0.2666	0.2623	0.2645	0.0043
5.6	0.2666	0.2709	0.2623	0.2666	0.0086

Table B.14. Raw data, average values and standard error values of cell concentration (g/l) for batch study with 0.1 mM, 0.4 mM and 1 mM neutral red. Studies with 0.4 mM (NR2-16, 17, 18) and 1 mM neutral red (NR3-16, 17, 18) are shown in this table. Table B. 13 shows the rest of the data. Results are discussed in Chapter 6, Section 6.3.1.

Days	C-16	C-17	C-18	Average	Error (2σ)
0.0	6.00	6.00	6.00	6.00	0.0000
1.0	5.91	5.91	5.93	5.92	0.0231
1.6	5.32	5.32	5.32	5.32	0.0000
2.6	5.01	5.00	5.08	5.03	0.0872
3.6	4.89	4.90	4.89	4.89	0.0115
4.6	4.94	4.95	4.94	4.94	0.0115
5.6	4.91	4.92	4.92	4.92	0.0115

Days	NR1-16	NR1-17	NR1-18	Average	Error (2σ)
0.0	6.00	6.00	6.00	6.00	0.0000
1.0	5.92	5.92	5.80	5.88	0.1386
1.6	5.31	5.31	5.25	5.29	0.0693
2.6	4.98	4.99	4.98	4.98	0.0115
3.6	4.89	4.91	4.90	4.90	0.0200
4.6	4.95	4.94	4.94	4.94	0.0115
5.6	4.93	4.93	4.91	4.92	0.0231

Table B.15. Raw data, average values and standard error values of pH for batch study with 0.1 mM, 0.4 mM and 1 mM neutral red. The controls (C-16, 17, 18) and 0.1 mM neutral red studies (NR1-16, 17, 18) are shown in this table. Table B.16 shows the rest of the data. Results are discussed in Chapter 6, Section 6.3.1.

Days	NR2-16	NR2-17	NR2-18	Average	Error (2σ)
0.0	6.00	6.00	6.00	6.00	0.0000
1.0	5.92	5.94	5.91	5.92	0.0306
1.6	5.29	5.30	5.31	5.30	0.0200
2.6	5.13	5.15	5.14	5.14	0.0200
3.6	5.08	5.10	5.15	5.11	0.0721
4.6	5.14	5.15	5.15	5.15	0.0115
5.6	5.13	5.12	5.14	5.13	0.0200

Days	NR3-16	NR3-17	NR3-18	Average	Error (2σ)
0.0	6.00	6.00	6.00	6.00	0.0000
1.0	5.91	5.89	5.76	5.85	0.1629
1.6	5.31	5.32	5.28	5.30	0.0416
2.6	5.33	5.32	5.34	5.33	0.0200
3.6	5.29	5.35	5.35	5.33	0.0693
4.6	5.34	5.34	5.35	5.34	0.0115
5.6	5.32	5.33	5.32	5.32	0.0115

Table B.16. Raw data, average values and standard error values of pH for batch study with 0.1 mM, 0.4 mM and 1 mM neutral red. Studies with 0.4 mM (NR2-16, 17, 18) and 1 mM neutral red (NR3-16, 17, 18) are shown in this table. Table B. 15 shows the rest of the data. Results are discussed in Chapter 6, Section 6.3.1.

Days	C-16	C-17	C-18	Average	Error (2σ)
0.0	0.0000	0.0000	0.0000	0.0000	0.0000
1.0	0.2237	0.0997	0.1684	0.1639	0.1243
1.6	0.4378	0.4459	0.5688	0.4841	0.1468
2.6	0.2011	0.2058	0.2567	0.2212	0.0617
3.6	0.2935	0.2392	0.2844	0.2723	0.0582
4.6	0.3936	0.3208	0.3634	0.3592	0.0731
5.6	0.4104	0.3631	0.4034	0.3923	0.0510

Days	NR1-16	NR1-17	NR1-18	Average	Error (2σ)
0.0	0.0000	0.0000	0.0000	0.0000	0.0000
1.0	0.3275	0.1038	0.1368	0.1894	0.2416
1.6	0.4526	0.5198	0.4797	0.4840	0.0676
2.6	0.5073	0.4953	0.4373	0.4800	0.0749
3.6	0.6422	0.6059	0.5575	0.6018	0.0850
4.6	0.6891	0.6840	0.5969	0.6567	0.1036
5.6	0.6582	0.7156	0.6481	0.6740	0.0728

Table B.17. Raw data, average values and standard error values of ethanol per cell mass (g/g) for batch study with 0.1 mM, 0.4 mM and 1mM neutral red. The controls (C-16, 17, 18) and 0.1 mM neutral red studies (NR1-16, 17, 18) are shown in this table. Table B.18 shows the rest of the data. Results are discussed in Chapter 6, Section 6.3.1.

Days	NR2-16	NR2-17	NR2-18	Average	Error (2σ)
0.0	0.0000	0.0000	0.0000	0.0000	0.0000
1.0	0.3958	0.3920	0.0902	0.2927	0.3507
1.6	0.4989	0.4407	0.4209	0.4535	0.0811
2.6	0.5867	0.6103	0.6143	0.6038	0.0298
3.6	0.6937	0.7017	0.7344	0.7099	0.0431
4.6	0.7517	0.7364	0.7701	0.7527	0.0337
5.6	0.9531	0.8933	1.0294	0.9586	0.1364

Days	NR3-16	NR3-17	NR3-18	Average	Error (2σ)
0.0	0.0000	0.0000	0.0000	0.0000	0.0000
1.0	0.3101	0.5001	0.1993	0.3365	0.3043
1.6	0.4879	0.5187	0.3795	0.4620	0.1463
2.6	1.7531	1.8106	1.6978	1.7539	0.1128
3.6	1.8535	1.6568	1.7227	1.7443	0.2003
4.6	1.8340	1.8080	1.8490	1.8303	0.0416
5.6	1.9580	1.8494	1.9520	1.9198	0.1221

Table B.18. Raw data, average values and standard error values of ethanol per cell mass (g/g) for batch study with 0.1 mM, 0.4 mM and 1mM neutral red. Studies with 0.4 mM (NR2-16, 17, 18) and 1 mM neutral red (NR3-16, 17, 18) are shown in this table. Table B. 17 shows the rest of the data. Results are discussed in Chapter 6, Section 6.3.1.

Days	C-16	C-17	C-18	Average	Error (2σ)
0.0	0.0000	0.0000	0.0000	0.0000	0.0000
1.0	0.1119	0.2215	0.1684	0.1672	0.1096
1.6	1.7729	1.8240	4.1077	2.5682	2.6670
2.6	3.9955	4.0584	4.8770	4.3103	0.9836
3.6	7.1146	8.2467	10.5007	8.6207	3.4475
4.6	10.4651	10.4250	12.1124	11.0008	1.9257
5.6	11.8012	11.0159	12.7195	11.8455	1.7053

Days	NR1-16	NR1-17	NR1-18	Average	Error (2σ)
0.0	0.0000	0.0000	0.0000	0.0000	0.0000
1.0	0.4367	0.9344	0.3420	0.5710	0.6364
1.6	1.5357	1.4606	1.4535	1.4833	0.0910
2.6	4.7814	4.8047	4.0231	4.5364	0.8894
3.6	9.7702	9.8942	8.0121	9.2255	2.1053
4.6	9.1731	10.9439	8.2287	9.4486	2.7568
5.6	10.8381	11.0912	9.1498	10.3597	2.1108

Table B.19. Raw data, average values and standard error values of acetic acid per cell mass (g/g) for batch study with 0.1 mM, 0.4 mM and 1mM neutral red. The controls (C-16, 17, 18) and 0.1 mM neutral red studies (NR1-16, 17, 18) are shown in this table. Table B.20 shows the rest of the data. Results are discussed in Chapter 6, Section 6.3.1.

Days	NR2-16	NR2-17	NR2-18	Average	Error (2σ)
0.0	0.0000	0.0000	0.0000	0.0000	0.0000
1.0	0.8906	1.0452	1.0024	0.9794	0.1596
1.6	2.7667	2.1527	1.9888	2.3027	0.8201
2.6	6.1245	4.6033	4.9276	5.2185	1.6024
3.6	6.5826	7.2173	6.4831	6.7610	0.7966
4.6	7.0981	7.4922	6.7976	7.1293	0.6968
5.6	6.9767	7.3090	7.4419	7.2425	0.4791

Days	NR3-16	NR3-17	NR3-18	Average	Error (2σ)
0.0	0.0000	0.0000	0.0000	0.0000	0.0000
1.0	1.2610	0.7502	0.5316	0.8476	0.7487
1.6	2.0600	2.3314	1.7320	2.0411	0.6003
2.6	4.1662	4.1902	4.0234	4.1266	0.1804
3.6	4.5699	4.6474	3.7936	4.3369	0.9443
4.6	5.1087	5.0300	4.8913	5.0100	0.2201
5.6	5.1388	4.9096	4.7045	4.9176	0.4345

Table B.20. Raw data, average values and standard error values of acetic acid per cell mass (g/g) for batch study with 0.1 mM, 0.4 mM and 1mM neutral red. Studies with 0.4 mM (NR2-16, 17, 18) and 1 mM neutral red (NR3-16, 17, 18) are shown in this table. Table B. 19 shows the rest of the data. Results are discussed in Chapter 6, Section 6.3.1.

VITA

Asma Ahmed

Candidate for the Degree of

Doctor of Philosophy

Dissertation: EFFECTS OF BIOMASS-GENERATED SYNGAS ON CELL-GROWTH, PRODUCT DISTRIBUTION AND ENZYME ACTIVITIES OF *CLOSTRIDIUM CARBOXIDIVORANS P7*^{T}

Major Field: Chemical Engineering

Biographical:

Personal Data: Born in Hyderabad, India on September 18, 1981

Education: Graduated from Nasr School in May 1996, received Bachelor of Technology degree in Chemical Engineering from Osmania University, Hyderabad, India, in May 2002. Completed the requirements for the Doctor of Philosophy degree with a major in Chemical Engineering at Oklahoma State University in December 2006.

Experience: Employed at Oklahoma State University, Department of Chemical Engineering as Teaching Assistant during January-May 2003, Employed at Oklahoma State University, Department of Chemical Engineering as Doctoral Research Associate, 2002-2006.

Professional Memberships: American Institute of Chemical Engineers (AIChE), Society of Biological Engineers (SBE).

Name: Asma Ahmed Date of Degree: December, 2006

Institution: Oklahoma State University Location: Stillwater, Oklahoma

Title of Study: EFFECTS OF BIOMASS-GENERATED SYNGAS ON CELL-GROWTH, PRODUCT DISTRIBUTION AND ENZYME ACTIVITIES OF *CLOSTRIDIUM CARBOXIDIVORANS P7*^{T}

Pages in Study: 227 Candidate for the Degree of Doctor of Philosophy

Major Field: Chemical Engineering

Scope and Method of Study:

Previous results showed that biomass-generated syngas caused (1) cell-washout from a chemostat due to cell-dormancy, (2) cessation of hydrogen uptake due to hydrogenase inhibition and (3) product re-distribution in the microbial catalyst *Clostridium carboxidivorans* P7^T. The focus of this work was to investigate the factors responsible for these effects in order to overcome cell-dormancy and inhibition of hydrogen uptake for improving the fermentation process. Three goals were addressed in this work: (1) to overcome cell-dormancy due to biomass-syngas (2) to eliminate cessation of hydrogen consumption due to hydrogenase inhibition and (3) to increase ethanol production by regulating the metabolic pathway of the microbial catalyst.

Findings and Conclusions:

The studies conducted resulted in the following conclusions: (1) Additional cleaning of biomass-syngas using a 0.025-μm filter prevented cell-washout. (2) Cell-dormancy was caused by particulate contaminants (likely tars) of the biomass-syngas. (3) Cells could adapt to tar after prolonged exposure and start growing. (4) Tars caused an increase in ethanol and decrease in acetic acid production. (5) Use of a cell-recycle system prevented cell-washout, and allowed the cells to adapt to and grow on biomass-syngas (without additional cleaning). (6) Hydrogenase inhibition was caused by nitric oxide (7) A kinetic model was developed which indicated that nitric oxide inhibition was non-linear and non-competitive. (8) Nitric oxide also inhibited initial cell-growth and caused an increase in ethanol production. (9) Nitric oxide caused the alcohol dehydrogenase activity to increase. (10) Addition of neutral red, an artificial electron carrier, resulted in an increase in ethanol and decrease in acetic acid production. (11) Neutral red also caused an increase in alcohol dehydrogenase activity.

ADVISER'S APPROVAL: Dr. Randy S. Lewis